APPLICATIONS OF THE BOUNDARY INTEGRAL EQUATION METHODS TO SOLID MECHANICS(Dissertation_全文)

AUTHOR(S):

Nishimura, Naoshi

APPLICATIONS OF THE BOUNDARY INTEGRAL EQUATION METHODS TO SOLID MECHANICS

BY

NAOSHI NISHIMURA

APPLICATIONS OF THE BOUNDARY INTEGRAL EQUATION METHODS TO SOLID MECHANICS

February, 1988

BY

NAOSHI NISHIMURA

Contents

Chapter 0 Introduction 1

Chapter 1 Boundary Integral Equations 6
1.0 Introduction, 6
1.1 Green's formula and potentials in elastostatics, 6
1.2 Fundamental solutions, 8
1.3 Behaviour of potentials, 10
1.3.1 Surface integrals, 11
1.3.2 Volume integrals, 17
1.3.3 Elastic potentials, 20
1.4 Boundary value problems, 24
1.5 Boundary integral equation methods, 27
1.6 Concluding remarks, 30

Chapter 2 The simple layer potential method for three dimensional anisotropic elastostatics 35
2.0 Introduction, 35
2.1 Simple layer potential, 35
2.2 Limiting values of the simple layer potential on the plane of the element, 39
2.3 Special cases, 43
2.4 Numerical analysis, 49
2.5 Concluding remarks, 54

Chapter 3 Problems involving singularities 58
3.0 Introduction, 58
Part I
3.1 Elastoplastic crack analysis by double layer potential method, 60
3.1.1 Antiplane crack problems, 60
3.1.2 Double layer potential, 61
3.1.3 Galerkin's method in elastic crack analysis, 63
3.1.4 Double layer potential method for elastoplastic crack problems, 64
3.1.5 Numerical procedures, 66
3.1.6 Example, 68
Part II
3.2 Elastodynamic crack problems, 68
3.2.1 Formulation, 70
3.2.2 Numerical analysis, 73
3.2.3 Numerical results, 77
3.2.4 Remarks concerning the method of regularisation, 77
Part III

3.3 Simple layer potential method for domains having external corners, 87
3.3.1 Formulation, 87
3.3.2 Numerical procedure, 91
3.3.3 Examples, 95
3.4 Concluding remarks, 98

Chapter 4 Elastodynamics 102
4.0 Introduction, 102
Part I
4.1 Interior and exterior problems, 103
4.1.1 Formulation, 103
4.1.2 Special classes of the problem, 107
4.1.3 Fictitious eigenfrequencies, 110
4.1.4 Methods of avoiding fictitious eigenfrequencies, 114
4.1.5 Some preliminaries, 116
4.1.6 Elastodynamic counterpart of Jones's methods, 119
4.1.7 Remarks concerning Jones's methods, 121
4.1.8 Peripheral stress, 122
4.1.9 Numerical procedures, 123
4.1.10 Examples, 128
Part II
4.2 Half-plane problems, 147
4.2.1 Method of truncation, 149
4.2.2 Method of Green's function, 150
4.2.3 Numerical example, 156
4.3 Concluding remarks, 165
Appendix to Chapter 4
BIEM in incompressible elastostatics, 167

Chapter 5 Consolidation problems 173
5.0 Introduction, 173
Part I
5.1 Initial- boundary value problems for Biot's equations, 173
5.2 Green's formula, fundamental solution and integral representation of the solution, 177
5.3 Initial fields, 182
5.4 Initial behaviour of time dependent potentials on the boundary, 192
5.4.1 Surface-time integrals, 193
5.4.2 Volume-time integrals, 199
5.4.3 Volume integrals, 199
5.4.4 Potentials in consolidation, 200
5.5 Initial behaviour of pressure and fluid velocity on the boundary, 201
5.6 Boundary integral equations, 204
Part II
5.7 Numerical procedure, 209
5.7.1 Fundamental solutions, 209
5.7.2 Integral equations, 210
5.7.3 Numerical methods of integration, 212
5.8 Numerical examples, 217
5.8.1 Circular disc, 217

5.8.2 Circular hole in an infinite plane, 217
5.8.3 Loaded halfplane, 219
5.9 Concluding remarks, 222

Chapter 0 Introduction

The boundary integral equation method (BIEM) refers to the methods of numerical analysis based on certain boundary integral representations of solutions of partial differential equations. It is therefore a combination of new and old techniques; it is new in that it was made possible by the development of digital computing, and old because the basic idea of using integral representations of solutions dates back to the early 19th century. Because of this, we have a relatively incomplete knowledge about the numerical aspects of this method in contrast to a firmly established mathematical foundation (Kupradze et al.(1979)).

In view of this situation, researchers of applied mechanics tried to fill the gap between the theory and practice. They naturally endeavoured to investigate numerical aspects of the method, expecting that some of the apparent 'advantages' of this method would turn out to be significant. Some of these 'advantages' claimed from the earlier stage of investigation, and even now, are the following:

a) This method reduces the dimension of the problem by one. Namely, it converts problems of finding solutions in a domain to those of finding solutions on the boundary. We may therefore expect that this method will decrease the amount of computational load compared to conventional domain type methods such as FEM and FDM. Especially, it will be effective in three dimensional problems.

b) This method constructs the solutions by superposing exact solutions. Therefore the approximate solution thus obtained satisfy the field equations identically in linear problems. This suggests that we may obtain very accurate numerical results.

c) This method is applicable to problems for infinite domains.

d) Theoretically speaking, this method is applicable to any linear problems. We can also use this method for non-linear analysis at the cost of abandoning boundary-only property, or introducing volume potentials with unknown (sometimes known) densities. We may therefore say that this method is sufficiently general.

Two decades of investigation revealed that some of these 'advantages' were truly advantages while others were just illusory. Indeed, we have the following critical comments to each item of the 'advantages' listed above:

To a) concerning reduced dimensionality: Although the dimension of the problem decreases by one, this does not necessarily reduce the amount of computation. This is because

i) The BIE matrix is neither symmetric nor banded.

ii) The ratio of (boundary area)/(volume) can be very large for slender bodies. Hence the number of unknowns in BIEM cannot be too much different from that in FEM, etc., in such cases.

iii) We have to use more accurate numerical integration formulae in evaluating BIE matrix than in FEM, bearing in mind the singularity of kernels. This makes BIE matrix construction a fairly time consuming step in the BIEM algorithm. On the other hand, a relatively simple quadrature is sufficient for FEM.

iv) In general, boundaries have far more complex topological structures than domains. In fact, domains we consider in practice are always connected. However, it is rather exceptional that the boundary of a domain is connected. This makes the coding of BIEM complicated.

We therefore see that it is too optimistic to say that the boundary-only property is a favourable aspect of BIEM. As a matter of fact, Wendland(1981) concludes that BIEM and FEM have the same operation counts, indicating that the reduced dimensionality of BIEM does not contribute to enhance the computational efficiency. (We note that the discussion on operation counts by Bettess(1981), in favour of FEM, is inadequate because he considers matrix inversion as the dominating step in BIEM as well as in FEM, while in reality the most time consuming step in BIEM is matrix making. Mukherjee & Morjaria(1984) also raised an objection against Bettess from the point of view of accuracy.) However, it is true that BIEM decreases the effort required for data preparation. We may therefore say that BIEM is advantageous for three dimensional analysis only after considering human factors!

To b) concerning accuracy: It is true that BIEM can give very accurate numerical results if we use a carefully coded computer program. However, we have to remember that BIE uses singular solutions even for obtaining a regular field. Especially, when one uses numerical integration formulae, the obtained field is always given in terms of finite number of singular solutions regardless of whether or not the exact field is singular. This shows that the obtained approximate solution always possesses singularities, which implies that there are points where the error also has 'singularities' (i.e. error of ∞ % !).

To c) concerning applicability to infinite domains: We have no objection to this. Indeed, this is why we think BIEM is one of ideal numerical methods of solution for wave problems in infinite domains. As we shall see in Chapter 4, however, the application of BIEM to half-plane (-space) problems is by no means a simple matter.

To d) concerning generality: It is very difficult to obtain fundamental solutions in most equations. In fact, we will see that the determination of fundamental solution is not very easy even in linear equations with constant coefficient. Also, fundamental solutions are seldom available in linear equations with variable coefficients. In addition, it is dubious that the BIE formulations with volume integrals can have any effectiveness over FEM in non-linear problems.

Of course it is not the present author's intention to say that these items are not the advantages of BIEM. As a matter of fact, the

author believes that they are. However, the present author intends to emphasise that the investigations of BIEM are no more in the stage of developments where researchers could stay with those naive expectations; we have already found out in some applications that the simplest BIE formulations used in the incipient stage are not sophisticated enough to take advantage of the expected merits. Hence the present author believes that the researchers should pursue the refinement of this method. This is why this thesis deals with rather non-standard methods of BIE analysis exclusively.

Chapter 1 of this thesis gives the fundamentals of the potential theory and BIEM. This chapter investigates the behaviour of the potential functions in anisotropic elastostatics without using the explicit forms of fundamental solution. This method turns out to be simple as well as effective even in cases where the fundamental solutions are not available. We then describe some of possible BIE formulations and the numerical aspects of the resulting BIEM.

Chapter 2 discusses the simple layer potential method for general three dimensional elastostatics. We first propose a method of calculating the simple layer potential for a plane element of an arbitrary shape. The methods of Fourier transform and residue calculus are found to be useful to this end. We then obtain a formula which gives the required potential in the form of an integral having a regular integrand. After examining the accuracy of the new approach, we apply it to the stress analysis around a face of a tunnel in a transversely isotropic rock.

Chapter 3 investigates problems relevant to singularities. This chapter considers exclusively the problems of eliminating unfavourable singularities. Specifically, we discuss elastoplastic antiplane crack problems in the first part of this chapter. The double layer formulation, along with the Galerkin's method, is used to this end. We then employ an iterative method to determine the elastic-plastic boundary. The second part of this chapter deals with the double layer potential method in three dimensional elastodynamic crack problems. We use the regularisation technique to reduce the order of the singularity of the kernel functions. The last part of this chapter considers the simple layer potential method for domains having external corners. As will be seen, it is essential, for obtaining good results, to take into account the correct singular behaviour of the density function at corners. We do this by using an 'eigenfunction' expansion of the density function, together with a special technique to evaluate the resultant singular integrals.

Chapter 4 applies BIEM to elastdynamics in two parts. The first part describes its application to plane interior and exterior problems. We consider both transient and time-harmonic problems, reducing the former to the latter by using the method of Fourier transform, or so called frequency domain analysis. The time-harmonic problems are solved by using a direct BIEM. The obtained integral equation, however, is seen to lose the uniqueness of the solution for some frequencies even in exterior problems. We then discuss several methods, both analytical and numerical, to avoid this trouble. We also give some numerical results to demonstrate the effectiveness of the method. The second part of this chapter seeks the applicability of this technique to half-plane problems. We test a numerical method of truncating the boundaries of infinite length leaving only the finite

part of them for analysis. We then show the validity of this approximation by comparing the obtained numerical results with those computed by another BIEM using Green's function as the kernel.

Chapter 5 deals with the application of BIEM to consolidation problems using a direct formulation. The first part emphasises the usefulness of this method as a mathematical tool of investigating the behaviour of the solutions. We discuss the initial field and jump behaviour of the solution. In particular, we determine the structure of the singularity of the fluid velocity in the problems of instantaneous loading. The second part shows a method of numerical analysis based on the present formulation, together with numerical examples.

The author attempts, throughout this thesis, to lay stress on the theoretical aspects of various BIEMs rather than on numerical results. This is mainly due to the necessity in view of the present state of development of BIEM. The author would be happy if this thesis could be of any use for encouraging engineers to utilise BIEM in their practice.

Notation

We use conventional direct notation and cartesian indicial notation in the following chapters expect that we use $(\nabla u)_{ij}$ for $\partial_i u_j$.

Citation

We restrict our citation to those papers having direct connection with this thesis. The lists of references in this thesis are therefore by no means complete as a list of existing publications on BIEM.

Acknowledgement

The present author wishes to express his gratitude to Prof. S. Kobayashi for directing him to the research of BIEM. He also acknowledges Messrs. M. Kaneko, T. Kawakami, M. Kinoshita, T. Maruoka, K. Matsumoto, K. Mori and T. Shiraki for their contribution in numerical work, Mr. M. Sumiya for painstaking typing work, and Prof. T. Tamura for various comments especially on consolidation theory.

References

Bettess, P.(1981). Operation counts for boundary integral and finite element methods, *Int. J, Num. Meth. Eng.*, vol.17, pp 306-308.

Kupradze, V.D., Gegelia, T.G., Basheleishvili, M.O. & Burchuladze, T.V.(1979). *Three Dimensional Problems of the Mathematical*

Theory of Elasticity and Thermoelasticity, North-Holland.
Mukherjee, S. & Morjaria, M.(1984). On the efficiency and accuracy of the boundary element method and the finite element method, *Int. J. Num. Meth. Eng.*, vol.20, pp 515-522.
Wendland, W.L.(1981). Asymptotic convergence of boundary element methods. Lectures on the Numerical Solutions of Partial Differential Equations, Lecture notes # 20 (Ed. I. Babuska, T.-P. Liu, & J. Osborn), Univ. Maryland. Dept. Math.

Chapter 1 Boundary Integral Equations

1 . 0 Introduction

This chapter presents some fundamental aspects of the boundary integral equations using an example of anisotropic elastostatic boundary value problems. We first introduce some potential functions which naturally appear in the so called direct formulations. After a brief discussion on fundamental solutions, we proceed to the investigation of some properties of potential functions using Fourier transform. The obtained results then reduce the boundary value problem in question to some integral equations defined on the boundary of the domain. Rewriting the resulting formulations into forms convenient for numerical applications, we obtain the so called boundary integral equation method (BIEM). This chapter concludes with some additional remarks.

1 . 1 Green's formula and potentials in elastostatics

Let D be a domain in R^N (N=2 or 3), having a smooth boundary ∂D. We here try to find an integral representation of the solution u (displacement) of the equation of equilibrium

$$\mathrm{div}\ \tau + f = 0, \tag{1.1.1}$$

subject to certain boundary conditions, where f is the body force, and τ is the stress obtained by

$$\tau = C[\nabla u - \varepsilon_0], \tag{1.1.2*}$$

with C and ε_0 indicating the elasticity tensor and initial strain, respectively. Equations (1.1.1) and (1.1.2) yield the well-known equation of Navier

$$\mathrm{div}(C[\nabla u]) - \mathrm{div}(C[\varepsilon_0]) + f = 0. \tag{1.1.3}$$

We note, in passing, that the differentiation in (1.1.1) should be understood in the sense of distribution. This interpretation allows us to include jump conditions into (1.1.1). Indeed, let S be a surface of discontinuity of τ, such as the material boundaries, etc. Then (1.1.1) is equivalent to

$$\begin{aligned} &\mathrm{div}_c \tau + f = 0 \qquad \text{in } D\backslash S, \\ &[\tau n] = 0 \quad \text{on } S \ (n\text{:unit normal vector to } S), \end{aligned} \tag{1.1.4}$$

where div_C indicates the divergence in the classical sense, and

---

* $C[\varepsilon]_{ij}$ stands for $C_{ijkl}\,\varepsilon_{kl}$

$[\cdot] = \cdot^{+} - \cdot$ with superposed + indicating the limit from the side into which n points, and - the limit from the other side.

We next investigate the so-called Green formula. We multiply (1.1.3) by an arbitrary function v, and integrate the obtained expression over D, to have

$$0 = \int_D \{v \cdot (\mathrm{div}(C[\nabla u]) - \mathrm{div}(C[\varepsilon_0])) + v \cdot f\}\, dV$$

$$= \int_{\partial D} v \cdot (C[\nabla u - \varepsilon_0]n) dS - \int_D \{\nabla v \cdot (C[\nabla u - \varepsilon_0]) - v \cdot f\}\, dV$$

$$= \int_{\partial D} v \cdot (C[\nabla u - \varepsilon_0]n) dS - \int_{\partial D} (C[\nabla v]n) \cdot u dS$$

$$+ \int_D \{\mathrm{div}(C[\nabla v])u + \nabla v \cdot (C[\varepsilon_0]) + v \cdot f\}\, dV. \qquad (1.1.5)$$

We then substitute into $v(x)$ in (1.1.5) the fundamental solution $\Gamma(x,y)$ defined by

$$\triangle^*(\nabla_x)\Gamma(x,y) := \mathrm{div}_x(C[\nabla_x \Gamma(x,y)]) = -1\delta(x-y) \qquad (1.1.6)$$

to obtain

$$\tilde{u}(x) = \int_{\partial D} \Gamma(x,y)\, t(y) dS - \int (\mathrm{T}_y \Gamma(x,y))^{\mathrm{T}} u(y) dS$$

$$+ \int_D \Gamma(x,y) f(y) dV + \int_D \Gamma(x,y) \bar{\nabla}_y \cdot C[\varepsilon_0(y)] dV, \qquad (1.1.7)$$

or

$$\tilde{u}_i(x) = \int_{\partial D} \Gamma_{ij}(x,y)\, t_j(y) dS_y - \int_{\partial D} \partial_{l_y} \Gamma_{ik}(x,y) C_{kljm} n_m(y) u_j(y) dS_y$$

$$+ \int_D \Gamma_{ij}(x,y) f_j(y) dV_y + \int_D \partial_{k_y} \Gamma_{ij}(x,y) C_{jklm} (\varepsilon_0)_{lm} dV_y \qquad (1.1.8)$$

in the indicial notation, where 1 is the identity tensor, $\tilde{u}(x)$ is a field defined by

$$\tilde{u}(x) = \begin{cases} u(x) & x \in D \\ 0 & x \in R^N \backslash \bar{D}, \end{cases} \quad (\bar{D} = D \cup \partial D), \qquad (1.1.9)$$

T is the elastic traction operator defined by

$$T\boldsymbol{u} := C[\nabla \boldsymbol{u}]n, \tag{1.1.10}$$

and $\boldsymbol{t}$ is the traction vector defined by

$$\boldsymbol{t} = T\boldsymbol{u} - C[\varepsilon_0]n. \tag{1.1.11}$$

Also, the operator $\triangle^*$ in (1.1.6) is called the Navier operator. We thus obtain an integral representation for $\boldsymbol{u}$, i.e. (1.1.7), in terms of four potential functions. The first potential in (1.1.7), i.e.,

$$U(\boldsymbol{x}) := \int_{\partial D} \Gamma(\boldsymbol{x},\boldsymbol{y})\boldsymbol{\varphi}(\boldsymbol{y})dS_y \qquad (\boldsymbol{\varphi} = \boldsymbol{t}) \tag{1.1.12}$$

is called the simple layer potential with density $\boldsymbol{\varphi}$. The second potential

$$V(\boldsymbol{x}) := \int_{\partial D} (T_y\Gamma(\boldsymbol{x},\boldsymbol{y}))^T\boldsymbol{\varphi}(\boldsymbol{y})dS_y \qquad (\boldsymbol{\varphi} = \boldsymbol{u}) \tag{1.1.13}$$

is called the double layer potential with density $\boldsymbol{\varphi}$. For brevity, we shall write Γ_1 for the double layer kernel, i.e.,

$$\Gamma_1(\boldsymbol{x},\boldsymbol{y}) := \left(T_y\Gamma(\boldsymbol{x},\boldsymbol{y})\right)^T. \tag{1.1.14}$$

The third potential

$$W(\boldsymbol{x}) := \int_{\partial D} \Gamma(\boldsymbol{x},\boldsymbol{y})\boldsymbol{\varphi}(\boldsymbol{y})dV_y \qquad (\boldsymbol{\varphi} = \boldsymbol{f}) \tag{1.1.15}$$

is called the volume potential with density $\boldsymbol{\varphi}$. The fourth potential is essentially the derivative of $W(\boldsymbol{x})$.

In the following sections of this chapter, we discuss the behaviour of these potentials and their derivatives. To this end, we shall start with the investigation of fundamental solutions.

1 . 2 Fundamental solutions

Let the source point $\boldsymbol{y}$ be at the origin. It is then plain to see that the Fourier transform of $\Gamma(\boldsymbol{x},0)$ (see (1.1.6)) is written as

$$\hat{\Gamma}(\boldsymbol{x},0) = -\triangle^{*-1}(i\xi) \tag{1.2.1}$$

where ξ indicates the parameter of Fourier transform. The inverse transform is usually obtained by taking the finite part of divergent integral, i.e.,

$$\Gamma(x,0) = -\text{p.f.}\ \frac{1}{(2\pi)^N}\int_{R^N}\triangle^{*-1}(i\xi)e^{i\xi\cdot x}d\xi. \tag{1.2.2}$$

Example 1. 3D isotropy

We have

$$C_{ijkl} = \lambda\ \delta_{ij}\delta_{kl} + \mu(\delta_{ik}\delta_{jl} + \delta_{il}\delta_{jk}),$$

$$\triangle^*(\nabla) = \mu\triangle 1 + (\lambda + \mu)\nabla\otimes\nabla,$$

$$\triangle^{*-1}(i\xi) = \frac{1}{\mu}\{-|\xi|^2 1 - \frac{\lambda+\mu}{\lambda+2\mu}(i\xi)\otimes(i\xi)\}\frac{1}{|\xi|^4}\ , \tag{1.2.3a-c}$$

where λ and μ are Lame's constants. Since

$$\frac{\text{p.f.}}{(2\pi)^3}\int\frac{e^{i\xi\cdot x}}{|\xi|^4}d\xi = \frac{1}{(2\pi)^3}\text{p.f.}\int_0^\infty\left(\int_{S_3}\frac{e^{i|\xi||x|\cos(\xi\cdot x)}}{|\xi|^2}dS\right)d|\xi|$$

$$= \frac{\text{p.f.}}{(2\pi)^2}\int_0^\infty\frac{e^{i|\xi||x|} - e^{-i|\xi||x|}}{i|\xi|^3|x|}d|\xi|$$

$$= \frac{\text{p.f.}}{2i(2\pi)^2|x|}\int_{-\infty}^\infty\frac{e^{ir|x|} - e^{-ir|x|}}{r^3}dr$$

$$= \frac{1}{8\pi|x|}\left(-\frac{|x|^2}{2} - \frac{|x|^2}{2}\right) = -\frac{|x|}{8\pi}\ , \tag{1.2.4}$$

we use (1.2.1) and (1.2.2) to have

$$\Gamma(x,0) = \frac{1}{8\pi\mu}(1\triangle - \frac{\lambda + \mu}{\lambda + 2\mu}\nabla\nabla)|x|\ , \tag{1.2.5}$$

or

$$\Gamma(x,y) = \frac{1}{8\pi\mu}(1\triangle - \frac{\lambda + \mu}{\lambda + 2\mu}\nabla\nabla)|x - y|\ , \tag{1.2.6}$$

where S_3 stands for a unit sphere. This result is known as Kelvin's solution.

Example 2. 3D transverse isotropy

Let the x_1-x_2 plane be the plane of isotropy. We then have

$$\triangle^*_{\alpha\beta}(\nabla) = (C_{66}\partial_\gamma\partial_\gamma + C_{44}\partial_3\partial_3)\delta_{\alpha\beta} + (C_{11} - C_{66})\partial_\alpha\partial_\beta,$$

$$\triangle^*_{\alpha 3}(\nabla) = \triangle^*_{3\alpha}(\nabla) = (C_{13} + C_{44})\partial_\alpha\partial_3,$$

$$\triangle^*_{33}(\nabla) = C_{44}\partial_\gamma\partial_\gamma + C_{33}\partial_3\partial_3, \qquad (1.2.7a\text{-}c)$$

where C_{11}, C_{13}, C_{33}, C_{44}, and C_{66} are the elastic constants in Voigt's notation ($C_{11}=C_{1111}$, $C_{33}=C_{3333}$, $C_{13}=C_{1133}$, $C_{44}=C_{2323}$, $C_{66}=C_{1212}$), and Greek indices range from 1 to 2. Following the general procedure shown in (1.2.1) and (1.2.2), we have

$$\Gamma_{\alpha\beta}(\boldsymbol{x},\boldsymbol{y}) = \frac{1}{4\pi C_{66}}\left\{\frac{|X_3|}{\bar{R}_1\bar{R}_1^+}\delta_{\alpha\beta} + \frac{\kappa_1 X_\alpha X_\beta}{\bar{R}_1(\bar{R}_1^+)^2}\right\} + \sum_{i=2}^{3}\frac{K_i}{4\pi C_{44}}\left(\frac{\delta_{\alpha\beta}}{\bar{R}_i^+} - \frac{\kappa_i X_\alpha X_\beta}{\bar{R}_i(\bar{R}_i^+)^2}\right),$$

$$\Gamma_{\alpha 3}(\boldsymbol{x},\boldsymbol{y}) = \Gamma_{3\alpha}(\boldsymbol{x},\boldsymbol{y}) = \frac{\mathrm{sgn}(X_3)}{4\pi}\sum_{i=2}^{3}\frac{L_i X_\alpha}{C_{44}\bar{R}_i\bar{R}_i^+},$$

$$\Gamma_{33}(\boldsymbol{x},\boldsymbol{y}) = \frac{1}{4\pi}\sum_{i=2}^{3}\frac{M_i}{C_{44}\bar{R}_i}, \qquad (1.2.8a\text{-}c)$$

where

$$X = x - y,$$

$$K_2 = \frac{\kappa_2 C_{44} - C_{33}}{C_{11}(\kappa_2-\kappa_3)}, \quad L_2 = \frac{(C_{13}+C_{44})\kappa_2}{C_{11}(\kappa_2-\kappa_3)}, \quad M_2 = \frac{C_{11}\kappa_2 - C_{44}}{C_{11}(\kappa_2-\kappa_3)},$$

$$\bar{R}_i = \sqrt{(\kappa_i X_\alpha X_\alpha + X_3^2)}, \quad \bar{R}_i^+ = \bar{R}_i + |X_3|, \qquad (i= \quad 1,3) \qquad (1.2.9a\text{-}f)$$

$\kappa_1=C_{44}/C_{66}$, and $\kappa_{2,3}$ are the distinct roots of

$$\kappa^2 - \frac{C_{11}C_{33} - C_{13}^2 - 2C_{13}C_{44}}{C_{11}C_{44}}\kappa + \frac{C_{33}}{C_{11}} = 0. \qquad (1.2.10)$$

Also, L_3, K_3 and M_3 are defined by interchanging κ_2 and κ_3 in the definitions of L_2, K_2, and M_2. This result is seen to coincide with the result of Kröner (1953) within a scalar factor which is missing in his paper. See Kobayashi & Nishimura (1980) for the detail.

1 . 3 Behaviour of potentials

We now discuss the behaviour of potentials introduced in 1.1 . The

conventional methods of investigating these potentials usually rely on the explicit form of the fundamental solution. This approach, however, is both restrictive and laborious because the explicit form of fundamental solution is not always available, and, even if it is, the form is usually very complicated. We therefore attempt to deviate from the standard approach and develop a new method which uses only the Fourier transform of the fundamental solution; as we have seen in (1.2.1), the Fourier transform of the fundamental solution is usually very easy to obtain.

To begin with we introduce the notion of (m,n) homogeneity of a function $f(\boldsymbol{x})$ $(\boldsymbol{x}\in R^N,\ N=2,3)$: A function is (m,n) homogeneous if

$$f(\lambda\boldsymbol{x}) = \lambda^m |\lambda|^n f(\boldsymbol{x}) \qquad \text{for} \quad \lambda\in R. \tag{1.3.1}$$

We are particularly interested in functions having $(n, 0)$ homogeneous Fourier transforms $(n = -2, -1, 0)$ because we have (1.1.12-15) and (1.2.1). Such functions are known to be either functions with logarithmic singularities at the origin for $(N = 2, n = -2)$, or $(-n,-N)$ homogeneous functions for $-N < n < 0$, or linear combinations of $\delta(\boldsymbol{x})$ (Dirac's delta) and v.p. (Cauchy's principal value) of $(0,-N)$-homogeneous functions for $n = 0$ (Mizohata(1965)).

We now consider a domain D in R^N $(N= 2$ or $3)$ whose boundary ∂D is very smooth near $\boldsymbol{x}_0\in\partial D$. Our problem is to determine the behaviour of the potentials of the forms

$$\int_{\partial D} F(\boldsymbol{x}-\boldsymbol{y})\varphi(\boldsymbol{y})\mathrm{d}S_y, \quad \int_D F(\boldsymbol{x}-\boldsymbol{y})\varphi(\boldsymbol{y})\mathrm{d}S_y, \tag{1.3.2a,b}$$

near $\boldsymbol{x}_0$, where $F(\cdot)$ is a kernel having $(n,0)$ homogeneous Fourier transform $(n = -2, -1, 0)$, and φ is a smooth density function. Since the comments below (1.3.1) show that F is an ordinary function away from $\boldsymbol{x}_0$, we may introduce a ball $B_\rho(\boldsymbol{x}_0)$ which has a radius of $\rho>0$ and is centred at $\boldsymbol{x}_0$, and concentrate our attention on the contribution to (1.3.2) from within $B_\rho(\boldsymbol{x}_0)$. The assumed smoothness of ∂D then enables us to approximate $\partial D\cap B_\rho(\boldsymbol{x}_0)$ and $D\cap B_\rho(\boldsymbol{x}_0)$ by a circular plane segment S and a half ball B shown in Fig.1.3.1. Hence we are led to the investigation of the limits of the forms

$$\lim_{\boldsymbol{x}\to\boldsymbol{x}_0}\int_S F(\boldsymbol{x}-\boldsymbol{y})\varphi(\boldsymbol{y})\mathrm{d}S_y, \quad \lim_{\boldsymbol{x}\to\boldsymbol{x}_0}\int_B F(\boldsymbol{x}-\boldsymbol{y})\varphi(\boldsymbol{y})\mathrm{d}S_y, \tag{1.3.3a,b}$$

where the approach of $\boldsymbol{x}$ to $\boldsymbol{x}_0$ is along the unit outward normal vector to S at $\boldsymbol{x}_0$, denoted by $\boldsymbol{n}$. In the sequel we shall compute these limits by using a cartesian frame whose Nth axis is in the direction of $\boldsymbol{n}$ and whose origin is at $\boldsymbol{x}_0$.

1 . 3 . 1 Surface integrals

We consider the following integral

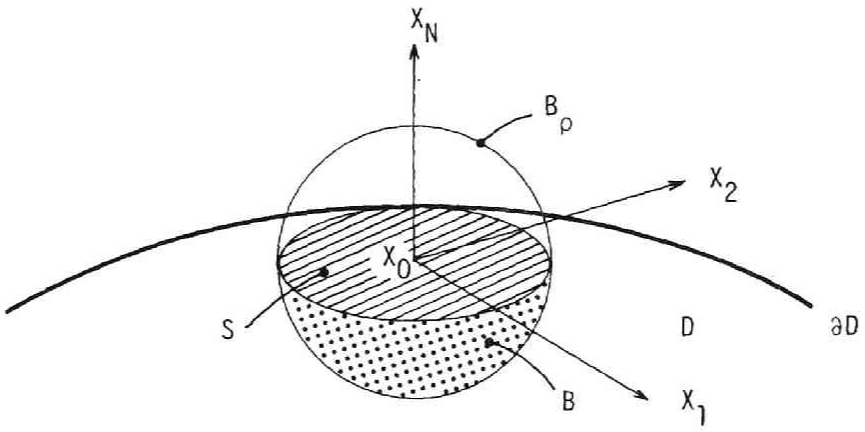

Fig.1.3.1 Notation.

$$\int_S F(x-y)\varphi(y)dS_y. \tag{1.3.1.1}$$

Obviously, one may replace the domain of integration by R^{N-1} with the extension $\varphi(y)=0$ for $y\in R^{N-1}\setminus S$. We have the following results for different n:

i) $n = -2$. Since the kernels have estimates of the form

$$|F(x_\alpha,x_N)| \leqq \frac{C}{(|x_\alpha|^2 + x_N^2)^{(N-2)/2}} \leqq \frac{C}{|x_\alpha|^{N-2}}$$

$$(N = 3)^* \tag{1.3.1.2}$$

or

$$|F(x_\alpha,x_N)| \leqq C_1+C_2\left|\log\sqrt{(|x_\alpha|^2+x_N^2)}\right|$$

$$\leqq C_1+C_2|\log|x_\alpha||\quad (N = 2) \tag{1.3.1.3}$$

near the origin (see the comments below (1.3.1)), we have

$$\lim_{x\to x_0}\int_S F(x_\alpha-y_\alpha,x_N)\varphi(y)dS_y = \int_S F(x_0-y)\varphi(y)dS_y \tag{1.3.1.4}$$

for a sufficiently smooth $\varphi(y)$.

ii) $n = -1$. We use the notion of partial Fourier (inverse) transform of $\hat{F}(\xi_\alpha,\xi_N)$ with respect to ξ_N, which is denoted by $\hat{F}(\xi_\alpha|x_N)$, and is defined by

$$\hat{F}(\xi_\alpha|x_N) = \frac{1}{2\pi}\lim_{\varepsilon\downarrow 0}\int_{-\infty}^{\infty} e^{i\xi_N x_N-\varepsilon\xi_N^2}\hat{F}(\xi_\alpha,\xi_N)d\xi_N\ . \tag{1.3.1.5}$$

The required limit is calculated in terms of $\hat{F}(\xi_\alpha|x_N)$ as

$$\lim_{x\to x_0}\int_S F(x-y)\varphi(y)dy = \frac{1}{(2\pi)^{N-1}}\lim_{x_N\to 0}\int_{R^{N-1}}\hat{F}(\xi_\alpha|x_N)\hat{\varphi}(\xi_\alpha)d\xi_1.....d\xi_{N-1}\ ,$$

(Note $x_0 = (0,.....,0)$ by definition.) (1.3.1.6)

where $\hat{\varphi}(\xi_\alpha)$ is the Fourier transform of $\varphi(y_\alpha)$ on S. Into the right hand side of (1.3.1.5) we substitute an expansion

---

$*$ Greek indices run from 1 to $N-1$

$$\hat{F}(\xi_\alpha,\xi_N) = \xi_N^n \hat{F}(\frac{\xi_\alpha}{\xi_N},1) = \xi_N^n \hat{F}(0,1) + \xi_N^{n-1}\xi_\alpha \frac{\partial}{\partial \xi_\alpha}\hat{F}(0,1)$$

$$+ \frac{1}{2}\xi_N^{n-2}\xi_\alpha\xi_\beta \frac{\partial^2}{\partial\xi_\alpha\partial\xi_\beta}\hat{F}(0,1) + \cdots\cdots \qquad (1.3.1.7)$$

which is valid for a large ξ_N. Subsequent use of Lebesgue's theorem converts the limit in (1.3.1.5) into

$$\lim_{\varepsilon\downarrow 0}\Big[\int_{|\xi_N|<\delta}\hat{F}(\xi)e^{i\xi_N x_N-\varepsilon\xi_N^2}d\xi_N + \int_{|\xi_N|>\delta}(\hat{F}(\xi) - \frac{\hat{F}(0,1)}{\xi_N})e^{i\xi_N x_N-\varepsilon\xi_N^2}d\xi_N$$

$$+ \hat{F}(0,1)\int_{|\xi_N|>\delta}\frac{e^{i\xi_N x_N-\varepsilon\xi_N^2}}{\xi_N}d\xi_N\Big]$$

$$= \int_{|\xi_N|<\delta}\hat{F}(\xi)e^{i\xi_N x_N}d\xi_N + \int_{|\xi_N|>\delta}(\hat{F}(\xi) - \frac{\hat{F}(0,1)}{\xi_N})e^{i\xi_N x_N}d\xi_N$$

$$+ \hat{F}(0,1)\lim_{\varepsilon\downarrow 0}\int_{|\xi_N|>\delta}\frac{e^{i\xi_N x_N-\varepsilon\xi_N^2}}{\xi_N}d\xi_N \qquad (1.3.1.8)$$

for a $\delta > 0$ and $|\xi_\alpha| \neq 0$. The last term is equal to

$$\begin{bmatrix}\pi i\\ 0\\ -\pi i\end{bmatrix} - i\ \mathrm{sgn}\ x_N\int_{-\delta|x_N|}^{\delta|x_N|}\frac{\sin\xi}{\xi}d\xi \qquad \text{for} \quad \begin{bmatrix}x_N>0\\ x_N=0\\ x_N<0\end{bmatrix}. \qquad (1.3.1.9)$$

Therefore, by letting $\delta\downarrow 0$ in (1.3.1.8-9) we have

$$\hat{F}(\xi_\alpha|x_N) = \frac{i}{2}\begin{bmatrix}1\\ 0\\ -1\end{bmatrix}\hat{F}(0,1)$$

$$+ \frac{1}{2\pi}\ \mathrm{v.p.}\int_{-\infty}^{\infty}(\hat{F}(\xi) - \frac{\hat{F}(0,1)}{\xi_N})e^{i\xi_N x_N}d\xi_N \qquad (1.3.1.10)$$

according as $x_N > 0$ (upper), $x_N = 0$ (middle), or $x_N < 0$ (lower), where v.p. indicates the integral in the sense of Cauchy's principal value. Note that the function (of ξ_α) defined by

$$\hat{F}(\xi_\alpha|0) = \frac{1}{2\pi}\lim_{\varepsilon\downarrow 0}\int_{-\infty}^{\infty}\hat{F}(\xi_\alpha,\xi_N)e^{-\varepsilon\xi_N^2}d\xi_N \qquad (1.3.1.11)$$

is $(n,1)$ homogeneous for $n = -1, 0$. In particular, for the present case of $(-1,1)$ homogeneity, we have

$$\int_{S_{N-1}} \hat{F}(\xi_\alpha \mid 0)\,dS = 0 \tag{1.3.1.12}$$

from the symmetry. This shows that $\mathfrak{F}_{\xi_\alpha}^{-1}(\hat{F}(\xi_\alpha \mid 0))(x_\alpha)^*$, as an $N-1$ dimensional distribution, is expressed as a principal value of a $(1,-N)$ homogeneous function (Mizohata(1965)). In addition, $\mathfrak{F}_{\xi_\alpha}^{-1}(\hat{F}(\xi_\alpha \mid 0))(x_\alpha)$ coincides with $F(x_\alpha,0)$ — a $(1,-N)$ homogeneous function— away from the origin. Hence we conclude

$$\lim_{x\to x_0} \int_S F(x-y)\varphi(y)\,dS = \pm\frac{i}{2}\,\hat{F}(n)\varphi(x_0) + \text{v.p.}\int_S F(x_0-y)\varphi(y)\,dS. \tag{1.3.1.13}$$

The upper (lower) sign is for the approach from the positive (negative) side, with 'positive side' indicating $x_N>0$. This convention will be used throughout this chapter.

iii) $n = 0$. Without loss of generality we may assume

$$\hat{F}(0,1) = 0. \tag{1.3.1.14}$$

Actually, if this is not to be the case we may modify the definition of $\hat{F}(\xi)$ by subtracting $\hat{F}(0,1)$ from $\hat{F}(\xi)$. This process changes F in (1.3.1.1) by $-\hat{F}(0,1)\delta(x-y)$, but this term vanishes for $x \notin \partial D$ and $y \in \partial D$, thus keeping (1.3.1.1) unchanged. With this assumption, we use (1.3.1.5) and an expansion (1.3.1.7) for $\hat{F}$ to obtain

$$2\pi\hat{F}(\xi_\alpha \mid x_N) = \xi_\alpha \frac{\partial}{\partial \xi_\alpha}\hat{F}(0,1)\begin{bmatrix} \pi i \\ 0 \\ -\pi i \end{bmatrix}$$

$$+ \text{v.p.}\int_{-\infty}^{\infty}\left(\hat{F}(\xi) - \frac{\xi_\alpha}{\xi_N}\frac{\partial}{\partial \xi_\alpha}\hat{F}(0,1)\right)e^{i\xi_N x_N}d\xi_N \quad , \tag{1.3.1.15}$$

and hence

$$\lim_{x_N\to 0}\hat{F}(\xi_\alpha \mid x_N) = \pm\frac{i}{2}\xi_\alpha\frac{\partial}{\partial \xi_\alpha}\hat{F}(0,1) + \hat{F}(\xi_\alpha \mid 0) \quad , \tag{1.3.1.16}$$

where we have used the same notation as has been used in ii).

We now proceed to the interpretation of $\mathfrak{F}_{\xi_\alpha}^{1}(\hat{F}(\xi_\alpha \mid 0))$, or the Fourier inverse transform of the second term in (1.3.1.16). To this end we note that

$$\hat{F}(\xi_\alpha \mid 0) = \frac{1}{2\pi}\lim_{\varepsilon\downarrow 0}\int_{-\infty}^{\infty}\hat{F}(\xi_\alpha,\xi_N)e^{-\varepsilon\xi_N^2}d\xi_N \tag{1.3.1.17}$$

$*$ $\mathfrak{F}_{\xi_\alpha}^{1}$ denotes the Fourier inverse transform. ($\xi_\alpha \to x_\alpha$)

is a well-defined $(0,1)$-homogeneous function of ξ_α. Its Fourier inverse transform with respect to ξ_α is equal to the restriction to $x_N=0$ of $F(x_\alpha,x_N)$ for a nonzero x_α; a $(0,N)$-homogeneous function of x_α. From these observations, we can show that $\mathcal{F}^{-1}_{\xi_\alpha}\hat{F}(\xi_\alpha\,|\,0)$ (as an N-1 dimensional distribution) is to be understood as a finite part (p.f.) defined by

$$\text{p.f.}\int_{R^{N-1}}F(x_\alpha,0)\varphi(x_\alpha)dx_\alpha = \lim_{\varepsilon\downarrow 0}\Big[\int_{R^{N-1}\setminus B_\varepsilon(0)}F(x_\alpha,0)\varphi(x_\alpha)dx_\alpha - \frac{\varphi(0)}{\varepsilon}\int_{S_{N-1}}F(x_\alpha,0)dS\Big], \quad (1.3.1.18)$$

where S_{N-1} is an N-1 dimensional unit sphere. To see this, we start with an observation that p.f.$F(x_\alpha,0)$ and $\mathcal{F}^{-1}_{\xi_\alpha}(\hat{F}(\xi_\alpha\,|\,0))$ coincide on R^{N-1} except at the origin. We therefore have

$$\mathcal{F}^{-1}_{\xi_\alpha}(\hat{F}(\xi_\alpha\,|\,0)) = \sum_{|\alpha|\le M}C^\alpha D^\alpha\delta(x) + \text{p.f.}F(x_\alpha), \quad (1.3.1.19)$$

where C^α is a certain constant,

$$D^\alpha := \partial_{x_1}^{\alpha_1}\,\partial_{x_2}^{\alpha_1}\,\cdots\cdots\,\partial_{x_{N-1}}^{\alpha_{N-1}},$$

$$\alpha = (\alpha_1,\alpha_2,\cdots\cdots,\alpha_{N-1}) \quad (1.3.1.20a,b)$$

and

$$|\alpha| := \sum_i|\alpha_i|. \quad (1.3.1.21)$$

Indeed a distribution having a point support is known to have the form given in the first term of (1.3.1.19) (Mizohata(1965)). In addition, we see

$$\mathcal{F}_{x_\alpha}\text{p.f.}\big(F(x_\alpha,0)\big)(\lambda\xi_\alpha) = \lim_{\varepsilon\downarrow 0}\Big[\int_{R^{N-1}\setminus B_\varepsilon(0)}F(x_\alpha,0)e^{-i\lambda\xi_\alpha\cdot x_\alpha}dx_\alpha - \frac{1}{\varepsilon}\int_{S_{N-1}}F(x_\alpha,0)dS\Big]$$

$$= \lim_{|\lambda|\varepsilon\downarrow 0}\Big[\int_{R^{N-1}\setminus B_{|\lambda|\varepsilon}}F(y_\alpha,0)e^{-i\xi y_\alpha}dy_\alpha - \frac{1}{|\lambda|\varepsilon}\int_{S_{N-1}}F(x_0,0)dS\Big]\,|\lambda|$$

$$= |\lambda| \mathcal{F}_{x_\alpha}(\text{p.f.}F(x_\alpha,0)) \ , \qquad (\lambda x_\alpha = y_\alpha) \tag{1.3.1.22}$$

which shows that

$$\mathcal{F}_{x_\alpha}(\text{p.f.}F(x_\alpha,0)) \tag{1.3.1.23}$$

is (0,1)-homogeneous. On the other hand $\mathcal{F}_{x_\alpha}(D^\alpha\delta(\boldsymbol{x}))(|\alpha| = 1)$ is (1,0)-homogeneous. Hence we conclude $C^{\forall\alpha} = 0$, which proves our statement. We thus have

$$\lim_{x\to x_0}\int_S F(\boldsymbol{x}-\boldsymbol{y})\varphi(\boldsymbol{y})dS = \pm\frac{1}{2}\frac{\partial}{\partial\xi_\alpha}\hat{F}(0,1)\frac{\partial}{\partial x_\alpha}\varphi(\boldsymbol{x}_0)$$

$$+ \ \text{p.f.}\int_S F(\boldsymbol{x}_0-\boldsymbol{y})\varphi(\boldsymbol{y})dS. \tag{1.3.1.24}$$

1 . 3 . 2 Volume integrals

We next investigate limits of the form

$$\lim_{x\to x_0}\int_B F(\boldsymbol{x}-\boldsymbol{y})\varphi(\boldsymbol{y})d\boldsymbol{y} \ , \tag{1.3.2.1}$$

where $F(\boldsymbol{x})$ is the same function as in 1.3.1, and $\varphi(\boldsymbol{y})$ is a smooth density function. As in 1.3.1 we replace the domain of integration by R^N with the help of an extension $\varphi(\boldsymbol{y})=0$ for $\boldsymbol{y}\in R^N\backslash B$. We then have the following results for different n:

i) $n = -2, -1$. We easily see

$$\lim_{x\to x_0}\int_B F(\boldsymbol{x}-\boldsymbol{y})\varphi(\boldsymbol{y})d\boldsymbol{y} = \int_B F(\boldsymbol{x}_0-\boldsymbol{y})\varphi(\boldsymbol{y})d\boldsymbol{y} \ . \tag{1.3.2.2}$$

ii) $n = 0$. We decompose $\hat{F}(\boldsymbol{\xi})$ into

$$\hat{F}(\boldsymbol{\xi}) = C_F + \hat{F}\grave{}(\boldsymbol{\xi}), \tag{1.3.2.3}$$

where

$$C_F = \frac{1}{|S_N|}\int_{S_N}\hat{F}(\xi)dS, \qquad \hat{F}\grave{}(\boldsymbol{\xi}) = \hat{F}(\boldsymbol{\xi}) - C_F \ . \tag{1.3.2.4a,b}$$

The inverse transform of C_F is $C_F\delta(\boldsymbol{x})$. Also we know that $\mathcal{F}_\xi^{-1}\hat{F}\grave{}(\boldsymbol{\xi})$ is equal to v.p.$\grave{F}(\boldsymbol{x})$ where $\grave{F}(\boldsymbol{x})$ is a $(0,-N)$-homogeneous function. Hence

we see that the Fourier 'integral'

$$\mathcal{F}_{\xi}^{-1}\{\hat{F}(\xi)\hat{\varphi}(\xi)\} \tag{1.3.2.5}$$

has an expression

$$C_F\varphi(x) + \text{v.p.}\int_D F(x-y)\varphi(y)dV_y \tag{1.3.2.6}$$

for $x\in D$, and

$$\int_D F(x-y)\varphi(y)dV_y \tag{1.3.2.7}$$

for $x\in D^c\backslash\partial D$, where C_F is given in (1.3.2.4a). In these formulae we have dropped $\tilde{}$ because $F = \tilde{F}$ in the classical sense.

In order to further investigate $\tilde{F}(x)$, we use the partial Fourier transform in the following manner:

$$\int_B \tilde{F}(x-y)\varphi(y)dy = \mathcal{F}_{\xi_\alpha}^{-1}\Big(\int_{-\rho}^{0}\hat{F}\tilde{}(\xi_\alpha \mid x_N-y_N)\hat{\varphi}(\xi_\alpha \mid y_N)dy_N\Big)(x_\alpha),$$

$$(x_N\neq 0) \tag{1.3.2.8}$$

where

$$\hat{\varphi}(\xi_\alpha \mid y_N) = \int_{(y_\alpha, y_N)\in B} e^{-i\xi_\alpha y_\alpha}\varphi(y_\alpha, y_N)dy_\alpha. \tag{1.3.2.9}$$

Into $\hat{F}\tilde{}(\cdot \mid \cdot)$ in (1.3.2.8) we substitute an analogue of (1.3.1.15) given by

$$2\pi\hat{F}\tilde{}(\xi_\alpha \mid x_N) = \sqrt{\pi}\lim_{\varepsilon\downarrow 0}\frac{e^{-x_N^2/4\varepsilon}}{\varepsilon^{1/2}}\hat{F}\tilde{}(0,1) + \xi_\alpha\frac{\partial}{\partial\xi_\alpha}\hat{F}\tilde{}(0,1)\begin{bmatrix}\pi i\\ 0\\ -\pi i\end{bmatrix}$$

$$+ \text{v.p.}\int_{-\infty}^{\infty}\Big(\hat{F}\tilde{}(\xi) - \hat{F}\tilde{}(0,1) - \frac{\xi_\alpha}{\xi_N}\frac{\partial}{\partial\xi_\alpha}\hat{F}\tilde{}(0,1)\Big)e^{i\xi_N x_N}d\xi_N \quad , \tag{1.3.2.10}$$

which differs from (1.3.1.15) because $\hat{F}\tilde{}(0,1) \neq 0$ in general. Use of (1.3.2.10),

$$\frac{1}{2\pi}\lim_{\varepsilon\downarrow 0}\sqrt{\pi}\int_{-\rho}^{0}\frac{e^{-(x_N-y_N)^2/4\varepsilon}}{(\varepsilon)^{1/2}}\hat{\varphi}(\xi_\alpha \mid y_N)dy_N$$

$$= \begin{bmatrix} 0 \\ \hat{\varphi}(\xi_\alpha \mid 0)/2 \\ \hat{\varphi}(\xi_\alpha \mid x_N) \end{bmatrix} \text{ for } \begin{bmatrix} x_N>0 \\ x_N=0 \\ x_N<0 \end{bmatrix} , \tag{1.3.2.11}$$

and

$$\mathcal{F}_{\xi_\alpha}^{-1}\Big(\int_{-\rho}^{0} \hat{F}(\xi_\alpha \mid x_N-y_N)\hat{\varphi}(\xi_\alpha \mid y_N)\mathrm{d}y_N\Big)(x_\alpha)$$

$$= \mathcal{F}_{\xi}^{-1}(\hat{F}(\xi)\hat{\varphi}(\xi))(x) \tag{1.3.2.12}$$

then transforms (1.3.2.8) into

$$\lim_{x\to x_0} \int_B \check{F}(x-y)\varphi(y)\mathrm{d}y = \mp\frac{\hat{F}(0,1)}{2}\varphi(x_0) + \mathcal{F}_{\xi}^{-1}(\hat{F}(\xi)\hat{\varphi}(\xi))(x_0),$$

$$(x_0=(0,0,\ldots\ldots 0)) , \tag{1.3.2.13}$$

where $\hat{\varphi}(\xi)$ is the Fourier transform of $\varphi(x)$ on B. Hence we are left with the interpretation of the last term in (1.3.2.13). To this end we note the following relations which follow from the symmetry and (1.3.2.4):

$$\int_{S_N^+} \check{F}(x)\mathrm{d}S = \int_{S_N^-} \check{F}(x)\mathrm{d}S = 0 , \tag{1.3.2.14}$$

where $S_N^{+,-} = S_N \cap \{x_N>,<0\}$ (+,- and >,< are to be taken in the same order). Since

$$\mathcal{F}_{\xi}^{-1}(\hat{F}(\xi)\hat{\varphi}(\xi))(x_0) = \lim_{\varepsilon\downarrow 0} \int_{R^N\setminus B_\varepsilon(x_0)} \check{F}(x_0-y)\varphi(y)\mathrm{d}V_y$$

$$= \text{v.p.} \int_B \check{F}(x_0-y)\varphi(y)\mathrm{d}V_y , \tag{1.3.2.15}$$

we obtain

$$\lim_{x\to x_0} \mathcal{F}^{-1}(\hat{F}(\xi)\hat{\varphi}(\xi))(x) = \lim_{x\to x_0} \Big\{\begin{bmatrix} 0 \\ C_F \end{bmatrix}\varphi(x) + \text{v.p.}\int_B F(x-y)\varphi(y)\mathrm{d}V_y\Big\}$$

$$= \Big(\frac{C_F}{2} \mp \frac{\hat{F}(n)}{2}\Big)\varphi(x_0) + \text{v.p.}^{-}\int_B F(x_0-y)\varphi(y)\mathrm{d}V_y , \tag{1.3.2.16}$$

where

$$\text{v.p.}^{-}\int_B \cdot\, dV = \lim_{\varepsilon \downarrow 0} \int_{B\setminus B_\varepsilon(x_0)} \cdot\, dV. \tag{1.3.2.17}$$

Note that the special principal-value integral, denoted by v.p. and defined above, is convergent due to (1.3.2.14). Actually, this is why (1.3.2.15) holds. We also have

$$\lim_{x\to x_0} \text{v.p.}\int_B F(x-y)\varphi(y)dV = \pm\left(\frac{C_F}{2} - \hat{F}(n)\right)\varphi(x_0)$$

$$+ \text{v.p.}^{-}\int_B F(x_0-y)\varphi(y)dV_y \ . \tag{1.3.2.18}$$

1 . 3 . 3 Elastic potentials

We now apply the foregoing analysis to elastic potentials. Since $-\triangle^{*-1}(i\xi)$ is a (-2,0)-homogeneous function, we have the following results.

a) Simple layer potential

We have $F = \Gamma$ and $\hat{F}(\xi) = \triangle^{*-1}(\xi)$ by definition (see (1.2.1)). The comments below (1.3.1) (or (1.3.1.4)) readily give

$$\lim_{x\to x_0} \int_{\partial D} \Gamma(x-y)\varphi(y)dS = \int_{\partial D} \Gamma(x_0-y)\varphi(y)dS. \tag{1.3.3.1}$$

As to the derivatives of this potential, we shall start with an identity

$$\lim_{x\to x_0} \nabla\int_{\partial D} \Gamma(x-y)\varphi(y)dS = \lim_{x\to x_0} \Big[\int_{\partial D\cap B_\varepsilon(x_0)} \nabla\Gamma(x-y)\varphi(y)dS$$

$$+ \int_{\partial D\setminus(\partial D\cap B_\varepsilon(x_0))} \nabla\Gamma(x-y)\varphi(y)dS\Big]. \tag{1.3.3.2}$$

After approximating $\partial D\cap B_\varepsilon(x_0)$ by a small plane segment, we apply (1.3.1.13) to the first integral on the right hand side of (1.3.3.2), where $\varepsilon>0$ is a sufficiently small number. This, together with an observation that the second integral has no singularity, yields

$$\lim_{x\to x_0} \nabla\int_{\partial D} \Gamma(x-y)\varphi(y)dS$$

$$= \lim_{x\to x_0} \int_{\partial D} \mathfrak{F}_{\xi}^{-1}(i\xi\otimes\triangle^{*-1}(\xi))(x-y)\varphi(y)dS$$

$$= \mp\frac{n}{2}\otimes\triangle^{*-1}(n)\varphi(x_0) + \text{v.p.}\int_{\partial D}\nabla_x\Gamma(x_0-y)\varphi(y)dS. \qquad (1.3.3.3)$$

In particular, we have a well-known formula (Kupradze et al.(1979))

$$\lim_{x\to x_0} T_x\int_{\partial D}\Gamma(x-y)\varphi(y)dS = \mp\frac{1}{2}\varphi(x_0) + \text{v.p.}\int_{\partial D}T_x\Gamma(x-y)\varphi(y)dS, \qquad (1.3.3.4)$$

since $C_{ipjq}n_pn_q = \triangle_{ij}^{*}(n)$.

b) Double layer potential

We now apply the same reasoning as we have used in a) to obtain various limits relevant to double layer potentials. To begin with, we note from (1.1.10) and (1.1.14) that the Fourier transform of the double layer kernel can locally be written as

$$-i\triangle_{ip}^{*-1}(\xi)\xi_qC_{pqrj}n_r, \qquad (1.3.3.5)$$

since n is locally constant. This observation, together with (1.3.1.13), yields (Kupradze et al.(1979))

$$\lim_{x\to x_0}\int_{\partial D}\Gamma_{\text{l}}(x,y)\ \varphi(y)dS$$

$$= \pm\frac{\varphi(x_0)}{2} + \text{v.p.}\int_{\partial D}\Gamma_{\text{l}}\ \varphi(y)dS\ . \qquad (1.3.3.6)$$

Also, we have

$$\lim_{x\to x_0}\partial_i\int_{\partial D}\Gamma_{\text{l}\,jk}\varphi_k(y)dS$$

$$= \pm\frac{1}{2}\frac{\partial}{\partial\xi_\alpha}(\xi_i\triangle_{jp}^{*-1}(\xi)\xi_qC_{pqrk})\,|_{\xi=n}n_r\frac{\partial}{\partial x_\alpha}\varphi_k(x_0)$$

$$+ \text{p.f.}\int_{\partial D}\partial_i\Gamma_{\text{l}\ jk}\varphi_k(y)dS$$

$$= \pm\frac{1}{2}\{\delta_{i\alpha}\frac{\partial}{\partial x_\alpha}\varphi_j(x_0) - n_i\triangle_{jr}^{*-1}(n)C_{rpaq}n_p\frac{\partial}{\partial x_\alpha}\varphi_q(x_0)\}$$

$$+ \text{ p.f.}\int_{\partial D} \partial_i \Gamma_{l\ jk} \varphi_k(\boldsymbol{y}) dS, \tag{1.3.3.7}$$

where we have used (1.3.1.24). In particular, we obtain

$$\lim_{x \to x_0} T_x \int_{\partial D} \Gamma_l(\boldsymbol{x},\boldsymbol{y})\ \boldsymbol{\varphi}(\boldsymbol{y}) dS$$

$$= \text{p.f.}\int_{\partial D} T_x \Gamma_l(\boldsymbol{x},\boldsymbol{y})\ \boldsymbol{\varphi}(\boldsymbol{y}) dS \tag{1.3.3.8}$$

since

$$n_k C_{ijkl}\left(\delta_{ia}\frac{\partial}{\partial x_\alpha}\varphi_j - n_i \triangle^{*-1}_{jr}(\boldsymbol{n}) C_{rpaq} n_p \frac{\partial}{\partial x_\alpha}\varphi_q\right) = 0\ . \tag{1.3.3.9}$$

Equation (1.3.3.8) is often called the generalised Lyapunov-Tauber theorem. (Kupradze et al.(1979))

We finally remark that the present derivation of (1.3.3.7) is not rigorous from a purely mathematical point of view because it does not take into consideration the possible effect of the curvature of ∂D. However, it is not difficult to see that the result is correct. Indeed, one starts with a well-known formula (e.g. Sladek & Sladek(1982))

$$\partial_k \int_{\partial D} \Gamma_{l\ ij}\ \varphi_j\ dS = e_{pqk} \int_{\partial D} \Gamma_{il,m}\ C_{lmqj}\ e_{pab}\ n_a\ \varphi_{j,b}\ dS, \tag{1.3.3.10}$$

and then use (1.3.1.13) to obtain (1.3.3.7), where e_{ijk} is the permutation symbol.

c) Volume potential

From (1.3.2.2) one readily sees

$$\nabla \int_D \Gamma(\boldsymbol{x},\boldsymbol{y})\boldsymbol{\varphi}(\boldsymbol{y}) dV = \int_D \nabla\Gamma(\boldsymbol{x},\boldsymbol{y})\boldsymbol{\varphi}(\boldsymbol{y}) dV\ , \tag{1.3.3.11}$$

where x is a point in R^N. We also have (see (1.3.2.6) and (1.3.2.7))

$$\nabla\nabla\int_D \Gamma(\boldsymbol{x},\boldsymbol{y})\varphi(\boldsymbol{y}) dV$$

$$= C_\Gamma \tilde{\boldsymbol{\varphi}}(\boldsymbol{x}) + \text{v.p.}\int \nabla\nabla\Gamma(\boldsymbol{x},\boldsymbol{y})\boldsymbol{\varphi}(\boldsymbol{y}) dV \qquad \boldsymbol{x} \in \partial D, \tag{1.3.3.12}$$

where

$$C_{\Gamma ijkl} = -\frac{1}{|S_N|}\int_{S_N}\xi_i\xi_j\triangle^{*-1}_{kl}(\xi)dS \qquad (\text{see } (1.3.2.4a)). \tag{1.3.3.13}$$

In particular, we obtain

$$\left(\triangle^*\int_D\Gamma(x,y)\varphi(y)dV\right)_i = C_{iprq}\partial_p\partial_q\left(\int_D\Gamma(x,y)\varphi(y)dV\right)_r$$

$$= \begin{cases} -\varphi_i(x) & x\in D \\ 0 & x\in R^N\setminus\overline{D} \end{cases}. \tag{1.3.3.14}$$

This well-known result is usually called the Poisson formula (Kupradze et al.(1979)).

The second derivative

$$\nabla\nabla\int_D\Gamma(x,y)\varphi(y)dV \tag{1.3.3.15}$$

jumps as the point x crosses ∂D. Actually, we see from (1.3.2.16) that

$$\lim_{x\to x_0}\nabla\nabla\int_D\Gamma(x,y)\varphi(y)dV = \frac{1}{2}\left(C_\Gamma \pm n\otimes n\otimes\triangle^{*-1}(n)\right)\varphi(x_0)$$

$$+ \text{v.p.}^-\int_D\nabla\nabla\Gamma(x,y)\varphi(y)dV \tag{1.3.3.16}$$

holds. Also, from (1.3.2.18), we have

$$\lim_{x\to x_0}\text{v.p.}\int_D\nabla\nabla\Gamma(x,y)\varphi(y)dV = \pm\frac{1}{2}(C_\Gamma + n\otimes n\otimes\triangle^{*-1}(n))\varphi(x_0)$$

$$+ \text{v.p.}^-\int_D\nabla\nabla\Gamma(x,y)\varphi(y)dV \quad . \tag{1.3.3.17}$$

Note that these results are consistent with the Poisson formula since

$$-C_{ijkl}C_{\Gamma jklm} = \frac{1}{|S_N|}\int_{S_N}C_{ijkl}n_jn_k\triangle^{*-1}_{lm}(\xi)dS = \delta_{im}. \tag{1.3.3.18}$$

We finally remark that the potentials of the form

$$\int \Gamma_{ij,k_y}(\boldsymbol{x}-\boldsymbol{y})\varphi_{jk}(\boldsymbol{y})\mathrm{d}V \tag{1.3.3.19}$$

can be viewed as

$$-\partial_{k_x}\int \Gamma_{ij}(\boldsymbol{x}-\boldsymbol{y})\varphi_{jk}(\boldsymbol{y})\mathrm{d}V \ , \tag{1.3.3.20}$$

which is exactly the derivative of a volume potential. Therefore, we can apply the foregoing analysis for volume potentials to the potential of this type, which plays an essential role in BIEM for elastoplasticity (e.g. Nishimura(1979))

d) Application

It is easy to see that (1.1.7), (1.3.3.3), (1.3.3.7), (1.3.3.16) and (1.3.3.11) yield the following identity on ∂D (Nishimura & Kobayashi(1987))

$$\tau_{pq} := C_{pqij}\ (\partial_i u_j - \varepsilon_{0\ ij}) = 2\Big(\mathrm{v.p.}\int_{\partial D} C_{pqij}\ \partial_i\Gamma_{jk}\ t_k\ dS$$

$$-\ \mathrm{p.f.}\int_{\partial D} C_{pqij}\ \partial_i\Gamma_{l\ jk}\ u_k\ dS + \mathrm{v.p.}\int_{\partial D} C_{pqij}\ \partial_i\Gamma_{jk,l_y}\ C_{klmn}\ \varepsilon_{0\ mn}\ dV$$

$$+\int_{\partial D} C_{pqij}\ \partial_i\Gamma_{jk}\ f_k\ dV\Big) - (C_{pqij}C_{\Gamma ijk}C_{klmn} + C_{pqmn})\ \varepsilon_{0\ mn} \ , \tag{1.3.3.21}$$

where τ_{pq} stands for the stress on the boundary. Cruse & VanBuren (1971) obtained this formula for the isotropic case by using a direct calculation. Equation (1.3.3.21) generalises their result to the anisotropic cases.

1 . 4 Boundary value problems

The boundary value problems of elastostatics consist in finding a displacement field $\boldsymbol{u}$ in D which satisfies the equation of equilibrium

$$\triangle^*(\nabla)\boldsymbol{u} - \mathrm{div}\big(C[\varepsilon_0]\big) + \boldsymbol{f} = \boldsymbol{0} \qquad \text{in } D, \tag{1.4.1}$$

subject to boundary conditions

$$\boldsymbol{u}(\boldsymbol{x}) = \boldsymbol{u}_0(\boldsymbol{x}) \qquad\qquad \boldsymbol{x}\in\partial D_u \ ,$$

$$\boldsymbol{t}(\boldsymbol{x}) = \mathrm{T}\boldsymbol{u}(\boldsymbol{x}) - \big(C[\varepsilon_0]\big)\boldsymbol{n} = \boldsymbol{t}_0(\boldsymbol{x}) \qquad \boldsymbol{x}\in\partial D_s \ ,$$

$$(\partial D_u \cap \partial D_s = \phi \ , \ \overline{\partial D_u \cup \partial D_s} = \partial D), \qquad (1.4.2a,b)$$

where u_0 and t_0 are the given values of boundary displacement and traction, respectively.

We can most naturally obtain an integral representation of the solution u by using Green's formula as in (1.1.7). Since the form in (1.1.7) satisfies the field equation (1.4.1) automatically, we are left with the imposition of the boundary conditions. This can be accomplished in several ways, although we here discuss two out of them.

The method of Kupradze's functional equation determines the unspecified values of u (on ∂D_s) and t (on ∂D_u) in a way that the expression

$$\int_{\partial D} \Gamma(x,y)\, t(y) \mathrm{d}S_y \ - \ \int_{\partial D} \Gamma_1(x,y) u(y) \mathrm{d}S$$

$$+ \ \int_D \Gamma(x,y) f(y) \mathrm{d}V \ + \ \int_D \Gamma(x,y) \bar{\nabla} \cdot \big(C[\varepsilon_0] \big) \mathrm{d}V \qquad (1.4.3)$$

vanishes in $R^N \backslash \bar{D}$. It can be shown, from (1.1.7), (1.1.9) and the results in 1.3, that (1.4.3) vanishes identically in $R^N \backslash \bar{D}$ only with the exact values of u and t on ∂D. In numerical analysis, however, we usually set (1.4.3) to be zero at several points in $R^N \backslash \bar{D}$.

Another method, which we shall call for convenience the (direct) method of integral equation, takes the limit of the expression (1.4.3) as $x \to \partial D$ from $R^N \backslash \bar{D}$, and then put it equal to zero. This process uses (1.3.3.1), (1.3.3.6) and (1.3.3.11) to yield

$$0 = \int_{\partial D} \Gamma(x_0,y)\, t(y) \mathrm{d}S \ - \ \frac{u(x_0)}{2} \ - \ \mathrm{v.p.} \int_{\partial D} \Gamma_1(x_0,y) u(y) \mathrm{d}S$$

$$+ \ \int_D \Gamma(x_0,y) f(y) \mathrm{d}V \ + \ \int_D \Gamma(x_0,y) \bar{\nabla} \cdot \big(C[\varepsilon_0] \big) \mathrm{d}V, \quad (x_0 \in \partial D) \qquad (1.4.4)$$

from which we obtain an integral equation for unspecified halves of u and t as we introduce into (1.4.4) the boundary data u_0 and t_0 given in (1.4.2).

It is readily seen that the above two methods are equivalent as far as the uniqueness of the solution of displacement boundary value problems for $R^N \backslash \bar{D}$ holds true. Hence in 3D elastostatics these methods are equivalent.

In some cases, it is convenient to replace the two surface potentials in (1.4.4) by one. To discuss this, we assume that $f = \varepsilon_0 = 0$ for simplicity. Also, we assume D to be bounded, and denote the unit outward normal vector to ∂D by n. These assumptions, however, apply only in the rest of this section.

The simple layer potential method uses the integral representation

$$u(x) = \int_{\partial D} \Gamma(x,y)\varphi(y)dS_y, \tag{1.4.5}$$

where φ is the unknown simple layer density.

The double layer potential method uses the integral representation

$$u(x) = \int_{\partial D} \Gamma_1(x,y)\psi(y)dS_y, \tag{1.4.6}$$

where ψ is the unknown double layer density.

The former (latter) is useful mainly in traction (displacement) boundary value problems. Actually, the simple layer potential method uses the integral equation (see (1.3.3.4) and (1.4.5))

$$t_0(x) = \mp\frac{\varphi(x)}{2} + \text{v.p.}\int_{\partial D} T_x\Gamma(x,y)\varphi(y)dS_y, \qquad x\in\partial D \tag{1.4.7}$$

where the upper (lower) sign is for exterior (interior) problems. (By 'exterior problems' we mean boundary value problems for an unbounded domain $R^N\setminus\bar{D}$.) The double layer potential method leads to the integral equation (see (1.3.3.6) and (1.4.6))

$$u_0(x) = \pm\frac{\psi(x)}{2} + \text{v.p.}\int_{\partial D} \Gamma_1(x,y)\psi(y)dS_y \qquad x\in\partial D \tag{1.4.8}$$

for the unknown density ψ. Solving these equations for φ and ψ, and substituting the obtained solution in the corresponding integral representation, we can calculate the displacement field. In the sequel, we call those methods of solution which use some integral representations but are not based on the Green's formula as indirect methods. The simple and double layer potential methods provide typical examples of indirect methods.

As methods of solution, the indirect methods are older than the direct methods. In fact, the indirect methods had been used as tools for investigating mathematical problems such as the existence of the solution, analyticity, etc. It is, therefore, not surprising that the equivalence (or non-equivalence) of the direct and indirect methods has long been known to mathematicians. See Lamb(1932) for example. We here list the solvability conditions for each indirect integral equation. The proof, which we shall omit, can easily be obtained by using Fredholm's theorems, which are known to be valid for our singular integral equations (Kupradze(1965), Kupradze et al.(1979)).

a) Equation (1.4.7) for exterior problems is always solvable.

b) Equation (1.4.7) for interior problems is solvable iff (if and only if)

$$\int_{\partial D} t_0 dS = 0, \quad \int_{\partial D} x \times t_0 dS = 0 \ . \tag{1.4.9a,b}$$

The solution is determined to within a linear combination of 6 (N=3) or 3 (N=2) functions.

c) Equation (1.4.8) for exterior problems is solvable iff the boundary traction to be obtained satisfies (1.4.9). The density is determined to within a 'rigid motion'.

d) Equation (1.4.8) for interior problems is always solvable.

We may interpret these results as indications of equivalence of the indirect methods to the direct methods, with an exception of double layer formulation for exterior displacement boundary value problems. The last non-equivalence, as a mater of fact, can also be resolved by modifying the kernel function in a manner to be discussed in Chapter 4 within a different context. We here omit the detail since this topic is purely of theoretical interest.

1 . 5 Boundary integral equation methods

The boundary integral equation method refers to those numerical methods of solution of partial differential equations which utilise integral representations of the solutions and resultant integral equations. We here outline the method by using the example of elastostatics assuming that the body force and the initial strain (see (1.1.1-2)) are absent.

We consider direct formulations for mixed boundary value problems. To this end, we introduce a set of collocation points x_I (I=1,.....,M) on ∂D , and shape functions $\Omega_I(\boldsymbol{x})$ ($\boldsymbol{x} \in \partial D$) such that

$$\Omega_I(x_J) = \begin{cases} 1 & I=J \\ 0 & I \neq J. \end{cases} \tag{1.5.1}$$

The integral equation in (1.4.4) is then discretised as

$$\sum_J \int_{\partial D} \Gamma(x_I, y) \Omega_J(y) dS_y t_J - \frac{u_I}{2} - \sum_J \text{v.p.} \int_{\partial D} (T_y \Gamma(x_I, y))^T \Omega_J(y) dS_y u_J$$

$$= 0, \tag{1.5.2}$$

where $u_J = u(x_J)$ and $t_J = t(x_J)$. Substituting from (1.4.2) the known values of u and t into (1.5.2), we obtain a system of algebraic equations for unknown u_I's and t_I's whose coefficient matrix can be calculated by using numerical quadrature. After solving this system of equations, we obtain displacement in D by

$$u(x) = \sum \int_{\partial D} \Gamma(x,y) \Omega_I(y) dS \ t_I - \sum \int_{\partial D} \Gamma_I(x,y) \Omega_I(y) dS \ u_I \quad , \tag{1.5.3}$$

and its gradients by differentiating (1.5.3) directly.

This boundary integral equation method in its most fundamental, but rather primitive form, is the one proposed initially. Subsequent developments, however, have found various modified versions of BIEM. We shall discuss some of these modifications in the rest of this section.

a) Use of isoparametric element, etc.

Lachat & Watson(1976) were the first to introduce isoparametric elements for the discretisation of integral equations. However, the earlier attempts at using piecewise constant plane (line) elements can be interpreted as the use of superparametric elements. It is therefore not clear who was the first to introduce the notion of FEM to BIEM.

b) Choice of shape functions

There can be various BIE formulations according as the choice of shape functions. The early researches of BIEM started with piecewise constant element (Rizzo(1967)). Gradually, researchers have come to use higher order elements, e.g., Cruse(1974), Lachat & Watson(1976) and Rizzo & Shippy(1977). Also, there are some attempts at using spline functions, e.g., Hansen(1976), Wendland(1981), and even Hermitian polynomials (Watson(1982)).

In the present author's opinion, we have to choose the shape function on the following basis

i) The order of shape functions should be sufficiently high that the boundary value of the numerical solution is a good approximation of the exact solution.

We are therefore advised not to use piecewise constant approximation for stress analyses using double layer potentials. It is because the boundary stresses of double layer potential depend explicitly on the derivatives of the double layer density (see (1.3.3.7)), and because we cannot approximate the derivatives of densities by using piecewise constant element. To examplify this, we first note the relation

$$\tau_{ij} = C_{ijkl}\partial_k\Big[\int_{\partial D}\Gamma_{lm}t_m dS - \int_{\partial D}\Gamma_{l\ lm}u_m dS\Big] \quad \text{in } D, \tag{1.5.4}$$

which holds when $f = \varepsilon_0 = 0$. Also, we have (1.3.3.21), which holds on ∂D as we have seen. Cruse(1972) reported that his piecewise constant direct (therefore it includes the double layer potential) BIEM computed stresses near the boundary more accurately with (1.3.3.21) (with integrals taken in an ordinary manner) than with the correct formula (1.5.4). This means that the relative error of his results with (1.5.4) was as large as 100%. This inaccuracy could have been resolved by the use of at least piecewise linear shape functions for the double layer density. In passing it is interesting to note that the limit to ∂D of (1.5.4) does not coincide with (1.3.3.21) when one uses approximations to u and t on ∂D.

In simple layer potential methods, however, the boundary stress does not depend on the derivatives of the density so that the piecewise constant approximation is acceptable if the boundary is smooth (Kobayashi & Nishimura(1979)).

ii) The shape functions should be sufficiently smooth that they do not introduce unfavourable singularities into solutions.

Piecewise linear simple layer formulation, for example, gives rise to a logarithmic singularity in stress at inter-element nodes. This formulation, therefore, is still insufficient for a very fine resolution of stresses everywhere in D (Kobayashi, et al.(1984)). A possible remedy for this inaccuracy problem is the use of Spline functions. Experience tells, however, that the piecewise linear simple layer formulation is not that bad from a practical point of view (Kobayashi & Nishimura(1979)).

Some authors propose boundary elements with relaxed conditions of continuity (Patterson & Sheikh(1981)). From our point of view, however, such attempts are pointless. Indeed a numerical comparison by Manolis & Banerjee(1986) confirms our view.

iii) The shape functions should be able to simulate the singular nature of the solution.

The solution can have singularities on the boundary where (1) the given data have singularities, (2) the type of boundary condition changes, (3) the boundary forms a corner. Related problems will be discussed in Chapter 3.

c) Collocation, Galerkin or least square method.

Most engineers use collocation method for discretising integral equations. Kobayashi & Nishimura(1979), Lean, et.al.(1979) and Wendland(1981), however, tried Galerkin's method. Kobayashi & Nishimura(1979) used the least square method also. Arnold & Wendland(1982) concluded that the collocation is superior to Galerkin when the solution does not have singularities. Nishimura(1979) showed, however, that Galerkin's method is preferable in some crack analyses (which necessarily involve singularities) using double layer potential with piecewise linear shape functions. Nedelec(1980) also proposed a Galerkin method in order to reduce the order of singularity in formulations using differentiated double layer potential. We finally remark that the so-called Galerkin - collocation method of Wendland(1981) is essentially Galerkin.

d) Evaluation of integrals

Few integrals involved in BIEM algorithm can be evaluated analytically. Therefore, we usually have to resort to numerical integration formulae. We, however, have to be careful in doing this because some integrands include singularities.

In general, we can remove the singularity of integrands in integrable integrals by using appropriate coordinate transformations. For example, an integral of the form

$$\int_B \frac{f(x_1,x_2)}{|x|}dx_1dx_2 \quad (|f| < \infty \ \text{ in } B,\ B := \{x,\ |x| \leqq 1\}) \qquad (1.5.5)$$

is reduced to

$$\oint d\theta \int_0^1 f(x_1,x_2)dr \qquad (1.5.6)$$

by using the polar coordinate (r,θ) centred at the origin. For the evaluation of principal-value integrals, however, we cannot apply this technique. It is because any coordinate transformation would convert one singular integral into another. The most popular technique for evaluating singular integrals in direct method is that of Lachat & Watson(1976). This technique calculates the non-integral terms plus singular integrals in (1.5.2) in a way that (1.5.2) is satisfied identically by some known solutions, such as rigid translations. This technique is effective, and is useful also in problems for domains having corners. However, this technique works only in direct methods, since exact solutions of indirect integral equations are seldom available. In some cases the use of Kutt's numerical integration formulae for finite part may be effective (Kutt(1975)). However, Kutt's formulae are not as versatile as the standard Gaussian integration formulae because of the limited tabulation. In addition Kutt's formulae are likely to cause numerical trouble because they may include negative weights or even integration points outside of the integration limits. In the present author's opinion, an analytical integration is the most suitable technique for indirect methods. It is because one of the biggest advantages of indirect methods over direct methods is the simplicity; an indirect method would not be worthwhile if it requires an equally, or more, elaborate numerical procedure as does a direct method. Probably this is why researchers do not try to use such sophisticated techniques as isoparametric elements, Hermitian elements, etc., in indirect methods.

From various versions of BIEM algorithm, of which we have seen just a few, one has to choose the most suitable one for his/her purpose.

1 . 6 Concluding remarks

a) We have so far restricted our attention to anisotropic elastostatic problems. However, the BIE method can be applied, in principle, to any problems governed by linear differential operators, as we shall see.

Let L be a linear differential operator of order n defined in a domain D in R^N, and u be a function defined in D. Since integration by part gives

$$\int_D v\, Lu \ dV = \int_{\partial D}(\ldots\ldots) + \int_D L^* v\ u\ dV$$

$$((\ldots\ldots);n \text{ surface integrals},\ L^* : \text{formal adjoint of } L) \qquad (1.6.1)$$

for any smooth functions u and v, we have

$$\tilde{u}(x) = \int_{\partial D}(\ldots\ldots)+\int_D \Gamma\, Lu\ dV, \qquad x \notin \partial D,$$

$$(\ (\ldots\ldots);n \text{ surface potentials}) \qquad (1.6.2)$$

where Γ is a fundamental solution of L^* ($L^*\Gamma = \delta$). This well-known procedure shows how one can formulate BIEM's for arbitrary linear differential equations.

b) It is customary to use the explicit form of the fundamental solutions for the discussion of the behaviour of potentials. We here used another method, developed by the present author (Nishimura & Kobayashi(1987)), using only the Fourier transform of the fundamental solutions. This technique is useful for those problems in which the fundamental solutions are not available. One may think that it would be of no use to calculate limiting formulae of potentials involving kernels which cannot be written down explicitly. This is not true. Indeed, our method paves the way for the use of numerical fundamental solutions. In addition, the conventional method of investigating the behaviour of various potentials is much more laborious than the present method.

c) There is some confusion of terminology in BIEM community. For example, what Patterson & Sheikh(1981) call their method of 'regular' integral equations is identical with Kupradze's functional equation method. Some authors call the simple layer potential methods as fictitious force method (Clouch & Starfield(1983)) or ever 'the' indirect method (Brebbia & Walker(1980)).

d) There are many indirect methods in addition to the two mentioned here. We can find as many as 32 different indirect formulations for plane elastostatics in the paper by Heise(1978).

e) The availability of a fundamental solution is crucial for the success of BIEM in particular problems. We can find a list of fundamental solutions for differential operators with constant coefficients in the paper by Ortner(1980). It is often very difficult to obtain fundamental solutions for equations having variable coefficients. Clements(1980) and Clements & Rogers(1983) were able to formulate BIEM for a Laplace type equation having variable coefficients. Hirose (Niwa & Hirose(1983)) pointed out that a fundamental solution is available for a special class of Helmholz type equations with variable coefficients.

f) We have restricted our considerations to the problems for domains having smooth boundaries. For corner points x_0 of ∂D, the limiting formulae derived in 1.3 need some modifications. For example, the

limiting formula (1.3.3.6) for double layer potential is replaced by

$$\lim_{x \to x_0} \int_{\partial D} \Gamma_{\mathrm{I}}(x,y)\varphi(y)\mathrm{d}S$$

$$= \begin{bmatrix} C^e\varphi(x_0) \\ C^i\varphi(x_0) \end{bmatrix} + \int_{\partial D} \Gamma_{\mathrm{I}}(x_0,y)\ \varphi(y)\mathrm{d}S_y, \qquad (1.6.3)$$

where C^e (C^i) is the non-integral term of the exterior (interior) limit of double layer potential. C^e (C^i) is equal to 1/2 (-1/2) when ∂D is smooth near x_0. C^e and C^i are related by

$$C^e - C^i = 1 \quad (1:\text{unit tensor}). \qquad (1.6.4)$$

Hartmann(1982) tried to calculate $C^{e,i}$ for some particular geometries. However, the determination of these tensors are not of practical importance since the method of Lachat & Watson(1976) calculates these tensors (plus certain singular integrals) automatically.

The present author is not able to extend the method of Fourier transform developed here to the cases of cornered geometry at present.

g) The method of Fourier transform discussed in this chapter seems to have connection with the theory of symbols (Mikhlin(1965)) and hence with pseudo-differential operators (Kumano-go (1974)).

h) The content of this chapter is taken mainly from Nishimura & Kobayashi(1987).

References

Arnold, D.N., & Wendland, W.L.(1982). Collocation versus Galerkin procedures for boundary integral methods, *Proc. 4th Int. Seminar BEM*, pp 18-33, Springer.

Brebbia, C.A. & Walker, S.(1980). *Boundary Elements Techniques in Engineering*, Butterworths.

Clements, D.L.(1980). A boundary integral equation method for the numerical solution of second order elliptic equation with variable coefficients, *J. Aust. Math. Soc.(B)*, vol.22, pp 218-28.

Clements, D.L. & Rogers, C.(1983). A boundary integral equation for the solution of a class of problems in anisotropic inhomogeneous thermostatics and elastostatics, *Q. Appl. Math.*, vol.41, pp 99-105.

Clouch, S.L. & Starfield, A.M.(1983). *Boundary Element Methods in Solid Mechanics*, George Allen & Unwin.

Cruse, T.A.(1972). Application of the boundary-integral equation solution method in solid mechanics, *Variational Methods in Engineering* (Eds. C.A. Brebbia & H. Tottenham), II, pp 9/1-9/29, Southampton Univ. Press.

Cruse, T.A.(1974). An improved boundary-integral equation method for three dimensional elastic stress analysis, *Computers and Structures*, vol.4, pp 741-54.

Cruse, T.A. & VanBuren, W.(1971). Three-dimesional elastic stress analysis of a fracture specimen with an edge crack, *Int. J. Fracture Mech.*, vol.7, pp 1-15.

Hansen, E.B.(1976). Numerical solution of integro-differential and singular integral equations for plane bending problems, *J. Elasticity*, vol.6, pp 39-56.

Hartmann, F.(1982). Elastic potentials on piecewise smooth surfaces, *J. Elasticity*, vol.12, pp 31-50.

Heise, U.(1978). Application of singularity method for the formulation of plane elastostatical boundary value problems as integral equations, *Acta Mech.*, vol.31 pp 33-69.

Kobayashi, S. & Nishimura, N.(1979). Some considerations on the improvement of integral equation method, *Proc. Japan Soc. Civil Eng.*, vol.291, pp 15-25 (in Japanese).

Kobayashi, S. & Nishimura, N.(1980). Green's tensors for elastic half-spaces ___ An application of boundary integral equation method, *Mem. Fac. Eng. Kyoto Univ.*, vol.42, pp 228-41.

Kobayashi, S., Nishimura, N. & Kawakami, T.(1984). Simple layer potential method for domains having external corners, *Appl. Math. Modelling*. vol.8, pp 61-65.

Kröner, E.(1953). Das Fundamentalintegral der anisotropen elastischen Differentialgleichungen, *Z. Physik*, vol.136, pp 402-10.

Kumano-go, H.(1974). *Pseudo-Differential Operators*, Iwanami (in Japanese).

Kupradze, V.D.(1965). *Potential Methods in the Theory of Elasticity* (tr. H. Gotfreund), Israel Program for Scientific Translations.

Kupradze, V.D., Gegelia, T.G., Basheleishvili, M.O. & Burchuladze, T.V.(1979). *Three-Dimensional Problems of the Mathematical Theory of Elasticity and Thermoelasticity*, North-Holland.

Kutt, H.R.(1975). The numerical evaluation of principal value integrals by finite part integration, *Num. Math.*, vol.24, pp 205-210.

Lachat, J.C. & Watson, J.O.(1976). Effective numerical treatment of boundary integral equations, *Int. J. Num. Meth. Eng.*, vol.10, pp 991-1005.

Lamb, H.(1932). *Hydrodynamics*, Cambridge Univ. Press.

Lean, M.H., Friedman, M. & Wexler, A.(1979). Application of boundary element method in electrical engineering problems, In : *Developments in Boundary Element Methods - I* (Eds. P.K. Banerjee & R. Butterfield), pp 207-250, Appl. Sci. Publ.

Manolis, G.D, & Banerjee, P.K.(1986). Conforming versus non-conforming boundary elements in three-dimensional elastostatics, *Int. J. Num. Meth. Eng.*, vol.23, pp 1885-1904.

Mikhlin, S.G.(1965). *Multidimensional Singular Integrals and Integral Equations*, (tr. W.J.A.Whyte), Pergamon.

Mizohata, S.(1965). *Theory of Partial Differential Equations*, Iwanami (in Japanese).

Nédélec, J.C.(1980). Formulations variationnelles de quelques equations intégrales faisant intervenir des parties finis, *Proc. 2nd Int. Symp. Innovative Num. Anal. Appl. Eng. Sci.*, pp 517-524, The Univ. Press of Virginia.

Nishimura, N.(1979). Elastoplastic analysis by the integral equation method, *M. Eng. Thesis, Kyoto Univ.* (in Japanese).

Nishimura, N. & Kobayashi, S.(1987). On the behaviour of elastic potentials, *Mem. Fac. Eng. Kyoto Univ.*, vol.49, pp 294-307.

Niwa, Y. & Hirose, S.(1983). An analysis of wave propagation in a inhomogeneous ground, Preprint for J.S.C.E. Kansai convention, I-78. (in Japanese).

Ortner, N.(1980). Regularisierte Faltung von Distributionen. Teil 2 : Eine Tabelle von Fundamentallösungen, *ZAMP*, vol.31, pp 155-73.

Patterson, C. & Sheikh, M.A.(1981). Non-conforming boundary elements for stress analysis, *Proc. 3rd Int. Seminar BEM*, pp 137-52, Springer.

Rizzo, F.J.(1967). An integral equation approach to boundary value problems of classical elastostatics, *Q. Appl. Math.*, vol.25, pp 85-93.

Rizzo, F.J. & Shippy, D.J.(1977). An advanced boundary integral equation method for three-dimensional thermoelasticity, *Int. J. Num. Meth. Eng.*, vol.11, pp 1753-68.

Sladek, V. & Sladek, J.(1982). Three dimensional crack analysis for an anisotropic body, *Appl. Math. Model.*, vol.6, pp 374-380.

Wendland, W.L.(1981). On the asymptotic convergence of boundary integral methods, *Proc. 3rd Int. Seminar BEM*, pp 412-430, Springer.

Watson, J.O.(1982). Hermitian boundary elements for plane problems of fracture mechanics, *Res Mech.*, vol.4, pp 23-42.

Chapter 2 The Simple Layer Potential Method for Three Dimensional Anisotropic Elastostatics

2 . 0 Introduction

This chapter discusses some applications of BIEM to three dimensional anisotropic elastostatics ——— a typical case of elliptic problems.

Since the publication of Rizzo's paper (Rizzo(1967)), many researchers have attempted to apply BIEM to elastostatics. Most of these investigations, however, have restricted themselves to the direct methods for isotropic materials. This trend is understandable considering the difficulty of obtaining the fundamental solutions in problems such as anisotropic elasticity, inhomogeneous cases, etc. In 3D anisotropic elastostatics, for example, it is not impossible to evaluate the fundamental solutions numerically (Wilson & Cruse(1978)). However a BIEM using this numerical fundamental solution is made practicable only after constructing a huge table of fundamental solutions, which is quite prohibitive. Hence one either has to be satisfied with a limited applicability of BIEM, or has to deviate from the conventional BIEM approach. This chapter constitutes one of the attempts along the latter line.

We develop in this chapter a 3D elastostatic simple layer potential method which does not use explicit expressions for the fundamental solutions. As a matter of fact, a closed form for the fundamental solution for 3D elastostatics is not available except in isotropic and transversely isotropic cases. Our method, however, is applicable to any class of anisotropy. We choose the simple layer potential method because we can use the simplest piecewise constant elements with this formulation (Kobayashi & Nishimura(1979)), and because it utilises only one potential function, in contrast to two in direct formulations; this reduces the computational load considerably. Besides, there is no ambiguity in using the simple layer potential method because it is known to be equivalent to the direct method (chapter 1).

We consider, in the sequel, a plane piecewise constant element for the sake of simplicity. We calculate the simple layer potential for this element rather than the fundamental solution itself by using the Fourier transform and residue calculus. The final expression is given in terms of integrals having finite limits of integration. The obtained formula is convenient for the numerical purpose because its integrand has no singularity. We next test the accuracy of our new formula by considering the special cases of isotropy and transverse isotropy, in which cases the fundamental solutions are available. After confirming the accuracy of the present formulation, we apply the new method to the three dimensional stress analysis of a tunnel in an anisotropic rock.

2 . 1 Simple layer potential

Let E be a plane segment of an arbitrary shape. Inspired by the theory of Mura(1982), we try to calculate the simple layer potential

with density φ, i.e.,

$$u(x) = \int_E \Gamma(x,x_0)\varphi(x_0)dS_{x_0} \tag{2.1.1}$$

by using the Fourier transform.
To start with we use (1.2.1) to have

$$u(x) = -\frac{1}{(2\pi)^3}\int_{R^3} d\xi\ \triangle^{*-1}(i\xi)\int_E e^{i\xi\cdot(x-x_0)}\varphi(x_0)dS_{x_0}$$

$$= -\frac{1}{(2\pi)^3}\int_{S_3} dS\int_0^\infty d|\xi|\ \triangle^{*-1}(i\bar{\xi})\int_E e^{i|\xi|\bar{\xi}\cdot(x-x_0)}\varphi(x_0)dS_y$$

$$= -\frac{1}{8\pi^2}\int_{S_3}\triangle^{*-1}(i\bar{\xi})dS_{\bar{\xi}}\int_E\delta(\bar{\xi}\cdot(x-x_0))\varphi(x_0)dS_{x_0}\ , \tag{2.1.2}$$

where $\bar{\xi} = \xi/|\xi|$, and S_3 is the unit sphere. Writing ξ instead of $\bar{\xi}$, we have

$$u(x) = \frac{1}{8\pi^2}\int_{S_3}\triangle^{*-1}(\xi)dS_\xi\int_E\delta(\xi\cdot(x-x_0))\varphi(x_0)dS_{x_0}\ , \tag{2.1.3}$$

$$\nabla u(x) = \frac{1}{8\pi^2}\int_{S_3}\xi\otimes\triangle^{*-1}(\xi)dS_\xi\int_E\delta'(\xi\cdot(x-x_0))\varphi(x_0)dS_{x_0}\ . \tag{2.1.4}$$

Now we take the unit vectors m, n and $m^\perp$ as in Fig.2.1.1. These vectors give

$$\xi = \zeta n + \sqrt{1-\zeta^2}\,m \quad (-1\leqq\zeta\leqq 1) \tag{2.1.5}$$

and

$$x - x_0 = hn - ym - zm^\perp\ , \tag{2.1.6}$$

where ζ, h, y and z are numbers. Using (2.1.5) and (2.1.6) we have

$$\int_E\delta(\xi\cdot(x-x_0))\varphi(x_0)dS_{x_0} = \int\delta(\zeta h - \sqrt{1-\zeta^2}\,y)w(y,m)dy$$

$$= \frac{w(\zeta h/\sqrt{1-\zeta^2},m)}{(1-\zeta^2)^{1/2}}\ , \tag{2.1.7}$$

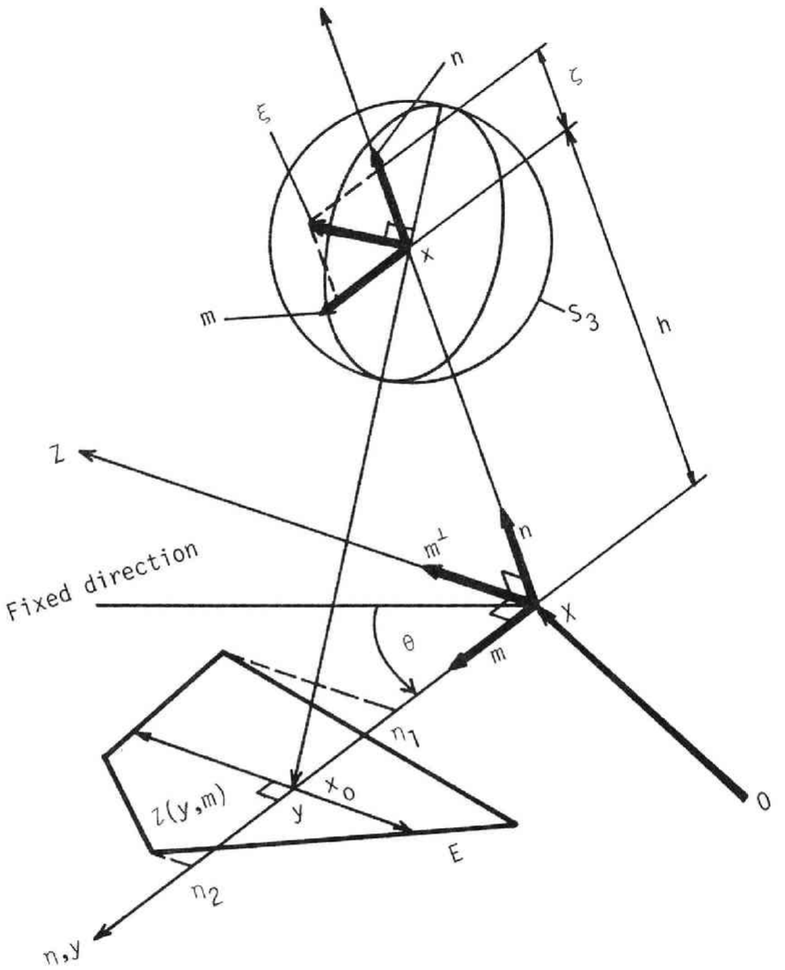

Fig.2.1.1 Notation.

where

$$w(y,\boldsymbol{m}) = \int_{l(y,\boldsymbol{m})} \varphi(y\boldsymbol{m} + z\boldsymbol{m}^{\perp} + X)\mathrm{d}z,$$

$$X = \boldsymbol{x} - h\boldsymbol{n}\ , \qquad (2.1.8a,b)$$

and $l(y,\boldsymbol{m})$ is the cross section of E on which $\boldsymbol{m}\cdot(\boldsymbol{x}_0-\boldsymbol{x}) = y$ holds. Therefore (2.1.3), (2.1.5) and (2.1.7) yield

$$u(\boldsymbol{x}) = \frac{1}{8\pi^2}\int_0^{2\pi}\mathrm{d}\theta\int_{-1}^{1}\frac{\triangle^{*-1}\left(\zeta\boldsymbol{n} + \sqrt{1-\zeta^2}\boldsymbol{m}(\theta)\right)\ w\left(\zeta h/\sqrt{1-\zeta^2},\boldsymbol{m}(\theta)\right)}{(1-\zeta^2)^{1/2}}\mathrm{d}\zeta$$

$$= \frac{|h|}{8\pi^2}\int_0^{2\pi}\mathrm{d}\theta\int_{\eta_1}^{\eta_2}\triangle^{*-1}(\eta\boldsymbol{n} + h\boldsymbol{m}(\theta))\ w(\eta,\boldsymbol{m}(\theta))\mathrm{d}\eta$$

$$= \frac{|h|}{4\pi^2}\int_0^{\pi}\mathrm{d}\theta\int_{\eta_1}^{\eta_2}\triangle^{*-1}\left(\eta\boldsymbol{n} + h\boldsymbol{m}(\theta)\right)\ w(\eta,\boldsymbol{m}(\theta))\mathrm{d}\eta\ , \qquad (2.1.9)$$

where we have used a substitution $\eta = \zeta h/\sqrt{1-\zeta^2}$, and the relations $w(-\eta,\boldsymbol{m}(\theta+\pi)) = w(\eta,\boldsymbol{m}(\theta))$ and

$$\triangle^{*-1}(-\eta\boldsymbol{n} - h\boldsymbol{m}) = \triangle^{*-1}(\eta\boldsymbol{n} + h\boldsymbol{m}). \qquad (2.1.10)$$

In order to simplify (2.1.9), we introduce the Cauchy integral W defined by

$$W(z,\theta) = \frac{1}{2\pi i}\int_{\eta_1}^{\eta_2}\frac{w(\eta,\boldsymbol{m}(\theta))}{\eta-z}\mathrm{d}\eta. \qquad (2.1.11)$$

Since $W^{+}(z,\theta) - W^{-}(z,\theta) = w(\eta,\boldsymbol{m}(\theta))$, we use (2.1.9) and (2.1.11) to have

$$u(\boldsymbol{x}) = \frac{\mathrm{sgn}(h)}{4\pi^2}\int_0^{\pi}\mathrm{d}\theta\oint_C\triangle^{*-1}(\chi\boldsymbol{n} + \boldsymbol{m})W(h\chi,\theta)\mathrm{d}\chi, \qquad (2.1.12)$$

where C is a contour surrounding the segment $[\eta_1/|h|\ ,\ \eta_2/|h|]$, and the contour integration in (2.1.12) is carried out clockwise. Consequently, we use a residue calculus in (2.1.12), together with the relations

$$\triangle^{*-1}(\chi\boldsymbol{n} + \boldsymbol{m}) \sim O(\chi^{-2}),\ W(h\chi) \sim O(\chi^{-1}), \qquad (2.1.13)$$

valid for a large χ, to obtain

$$\boldsymbol{u}(\boldsymbol{x}) = \frac{i\ \mathrm{sgn}(h)}{2\pi}\int_0^{\pi} d\theta \sum_{\alpha} \mathrm{Res}\,[\triangle^{*-1}(\chi\boldsymbol{n}+\boldsymbol{m})]_{\chi=\chi_\alpha}\ W(h\chi_\alpha,\theta)$$

$$= -\frac{\mathrm{sgn}(h)}{\pi}\int_0^{\pi} d\theta \sum_{\alpha}^{\cap} \mathrm{Im}\{\mathrm{Res}\,[\triangle^{*-1}(\chi\boldsymbol{n}+\boldsymbol{m})]_{\chi=\chi_\alpha}\ W(h\chi_\alpha,\theta)\}, \quad (2.1.14)$$

where χ_α (α=1,6) are the roots (tentatively assumed to be distinct) of the equation

$$\det \triangle^*(\chi\boldsymbol{n}+\boldsymbol{m}) = 0 \quad , \quad (2.1.15)$$

and the $\sum$ with $\cap$ indicates the sum over χ_α's such that Im $\chi_\alpha > 0$. It is known that χ_α's are never real (Mura(1982)).

Analogously, we have

$$\nabla\boldsymbol{u}(\boldsymbol{x}) = -\frac{\mathrm{sgn}(h)}{\pi}\int_0^{\pi} d\theta \sum_{\alpha}^{\cap} \mathrm{Im}\{\mathrm{Res}\{(\chi\boldsymbol{n}+\boldsymbol{m})\otimes\triangle^{*-1}(\chi\boldsymbol{n}+\boldsymbol{m})\}_{\chi=\chi_\alpha}$$

$$\cdot W^{\mathrm{P}}(h\chi_\alpha,\theta)\}, \quad (2.1.16)$$

where $W^{\mathrm{P}}(z,\theta)$ denotes the Cauchy integral defined by

$$W^{\mathrm{P}}(z,\theta) = \frac{1}{2\pi i}\int_{\eta_2}^{\eta_1} \frac{(d/d\eta)w(\eta,\boldsymbol{m}(\theta))}{\eta - z} d\eta, \quad (2.1.17)$$

which is equal to

$$\frac{d}{dz}W(z,\theta) \quad (2.1.18)$$

when $w(\eta_1,\boldsymbol{m}(\theta)) = w(\eta_2,\boldsymbol{m}(\theta)) = 0$.

2 . 2 Limiting values of the simple layer potential on the plane of the element

In this section we compute the limits of (2.1.14) and (2.1.16) as h approaches 0, assuming that φ = const (= 1) over the element. In this case, $w(\eta,\boldsymbol{m}(\theta))$, defined in (2.1.8a), reduces to the width of the element E at (η,θ).

Before calculating these limits, we shall prepare the following formulae :

$$\sum_{\alpha}^{\cap} \mathrm{Re}\ \mathrm{Res}\,[\triangle^{*-1}(\chi\boldsymbol{n}+\boldsymbol{m})]_{\chi=\chi_\alpha} = 0 \quad (2.2.1)$$

and

$$\sum_{\alpha}^{\cap} \text{Re Res}\,[(\chi \boldsymbol{n} + \boldsymbol{m}) \otimes \triangle^{*-1}(\chi \boldsymbol{n} + \boldsymbol{m})]_{\chi=\chi_\alpha} = \boldsymbol{n} \otimes \triangle^{*-1}(\boldsymbol{n})/2. \tag{2.2.2}$$

These results are proved with the help of

$$\sum_{\alpha}^{\cap} \text{Re Res}\,[\triangle^{*-1}(\chi \boldsymbol{n} + \boldsymbol{m})]_{\chi=\chi_\alpha} = \frac{1}{4\pi i} \oint_{C_0} \triangle^{*-1}(\chi \boldsymbol{n} + \boldsymbol{m}) d\chi$$

$$\sim \frac{\triangle^{*-1}(\boldsymbol{n})}{4\pi i} \oint_{C_0} \frac{d\chi}{\chi^2} \tag{2.2.3}$$

and

$$\sum_{\alpha}^{\cap} \text{Re Res}\,[(\chi \boldsymbol{n} + \boldsymbol{m}) \otimes \triangle^{*-1}(\chi \boldsymbol{n} + \boldsymbol{m})]_{\chi=\chi_\alpha}$$

$$= \frac{1}{4\pi i} \oint_{C_0} (\chi \boldsymbol{n} + \boldsymbol{m}) \otimes \triangle^{*-1}(\chi \boldsymbol{n} + \boldsymbol{m}) d\chi \sim \frac{\boldsymbol{n} \otimes \triangle^{*-1}(\boldsymbol{n})}{4\pi i} \oint_{C_0} \frac{d\chi}{\chi}\ , \tag{2.2.4}$$

where C_0 denotes a sufficiently large circle, and the integration is carried out counter clockwise. Equations (2.2.3) and (2.2.4) follow from the (-2,0) homogeneity of $\triangle^{*-1}$ (see (1.3.1)). We then compute the contour integrals in (2.2.3) and (2.2.4) to obtain (2.2.2) and (2.2.3).

We now proceed to the calculation of the aforementioned limits. To start with, we use the Plemelj formula (Muskhelishvili(1953)) to have

$$\lim_{h \to 0} W(h\chi, \theta) = \frac{\text{sgn}(h) w(0, \boldsymbol{m}(\theta))}{2} + \frac{1}{2\pi i}\ \text{v.p.} \int_{\eta_1}^{\eta_2} \frac{w(\eta, \boldsymbol{m}(\theta))}{\eta}\ d\eta, \tag{2.2.5}$$

where v.p. stands for Cauchy's principal value. We then introduce (2.2.5) into (2.1.14), followed by the use of (2.2.1), to obtain

$$u(x) = -\frac{1}{2\pi} \int_0^{\pi} d\theta \sum_{\alpha}^{\cap} \text{Im Res}\,[\triangle^{*-1}(\chi \boldsymbol{n} + \boldsymbol{m})]_{\chi=\chi_\alpha}\ w(0, \boldsymbol{m}).$$

$$x \in E \tag{2.2.6}$$

In this formula $u(x)$ refers to the limit of u as the observation point tends to a point x on S. In the same manner we obtain the analogous limit for ∇u in the following form:

$\nabla u(x)$

$$= -\frac{\mathrm{sgn}(h)}{\pi}\int_0^{\pi} d\theta \Bigg\{ \sum_{\alpha}^{\cap} \mathrm{Re}\ \mathrm{Res}\left[(\chi \boldsymbol{n}+\boldsymbol{m}) \otimes \triangle^{*-1} (\chi \boldsymbol{n}+\boldsymbol{m}) \right]_{\chi=\chi_\alpha}$$

$$\cdot \left(-\frac{1}{2\pi} \mathrm{v.p.} \int_{\eta_1}^{\eta_2} \frac{w'(\eta, \boldsymbol{m})}{\eta} d\eta \right)$$

$$+ \sum_{\alpha}^{\cap} \mathrm{Im}\ \mathrm{Res}\left[(\chi \boldsymbol{n}+\boldsymbol{m}) \otimes \triangle^{*-1} (\chi \boldsymbol{n}+\boldsymbol{m}) \right]_{\chi=\chi_\alpha} \frac{\mathrm{sgn}(h) w'(0, \boldsymbol{m})}{2} \Bigg\}. \qquad (2.2.7)$$

The first integral in (2.2.7) allows a further simplification. Indeed, we use the notation shown in Fig.2.2.1 to have

$$\int_0^{\pi} d\theta\ \mathrm{v.p.} \int_{\eta_1}^{\eta_2} \frac{w'(\eta, \boldsymbol{m})}{\eta} d\eta$$

$$= \frac{1}{2} \int_0^{2\pi} d\theta\ \mathrm{v.p.} \int \left(\cot(\varphi-\theta) \frac{r'(\varphi)}{r(\varphi)} - 1 \right) d\varphi^*$$

$$= \frac{1}{2} \int d\varphi\ \mathrm{v.p.} \int_0^{2\pi} \left(\cot(\varphi-\theta) \frac{r'(\varphi)}{r(\varphi)} - 1 \right) d\theta = \begin{cases} -2\pi^2 & \text{on the element} \\ 0 & \text{otherwise.} \end{cases} \qquad (2.2.8)$$

In the step leading to the third line in (2.2.8) we have transferred the principal value integration from φ to θ. The validity of this process is seen by noting that the v.p. integral in (2.2.8) is defined as the limit as $\varepsilon \to 0$ of the ordinary integral carried out on the shaded region in Fig.2.2.2. Consequently, we combine (2.2.2), (2.2.7) and (2.2.8) to obtain

$$\nabla \boldsymbol{u}(\boldsymbol{x}) = -\frac{\mathrm{sgn}(h)}{2}\ \boldsymbol{n} \otimes \triangle^{*-1}(\boldsymbol{n}) \begin{bmatrix} 1 \\ 0 \end{bmatrix}$$

$$-\frac{1}{2\pi} \int_0^{\pi} \sum_{\alpha}^{\cap} \mathrm{Im}\ \mathrm{Res}\left[(\chi \boldsymbol{n}+\boldsymbol{m}) \otimes \triangle^{*-1} (\chi \boldsymbol{n}+\boldsymbol{m}) \right]_{\chi=\chi_\alpha} w'(0, \boldsymbol{m}) d\theta, \qquad (2.2.9)$$

where $[1,0]^{\mathrm{T}}$ indicates 1 on the element and 0 otherwise.

$*$ The integration with respect to φ in (2.2.8) stands for

$$\int_0^{2\pi} f(r(\varphi), \theta) d\varphi \quad \text{for } x \text{ on } E$$

and

$$\int_{\varphi_1}^{\varphi_2} f(r_1(\varphi), \theta) d\varphi + \int_{\varphi_1}^{\varphi_2} f(r_2(\varphi), \theta) d\varphi \quad \text{otherwise,}$$

where $f(.,.)$ denotes a certain function.

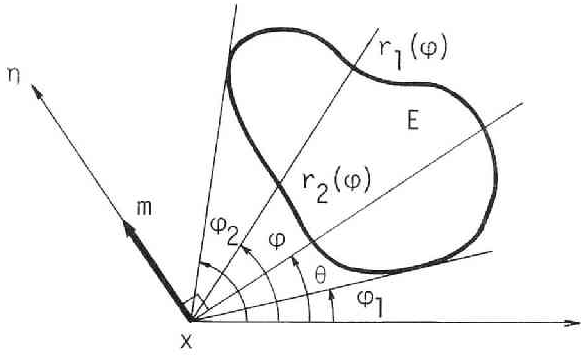

Fig.2.2.1 Notation.

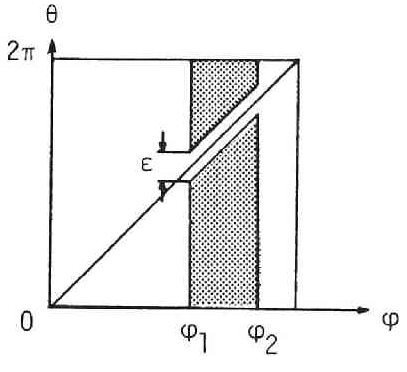

Fig.2.2.2 Domain of integration.

2 . 3 Special cases

a) Multiple root

It may happen that (2.1.15) has multiple roots. In such cases (2.1.14) and (2.1.16) must be modified. For example, we have

$$\boldsymbol{u}(\boldsymbol{x}) = -\frac{\mathrm{sgn}(h)}{\pi}\int_0^{\pi} d\theta \Big[\mathrm{Im}\{\mathrm{Res}_{-1}[\triangle^{*-1}(\chi\boldsymbol{n}+\boldsymbol{m})]_{\chi_1} W(h\chi_1,\theta)\} + \mathrm{Im}\{\mathrm{Res}_{-1}[\triangle^{*-1}(\chi\boldsymbol{n}+\boldsymbol{m})]_{\chi_2} W(h\chi_1,\theta)\} + h\mathrm{Im}\{\mathrm{Res}_{-2}[\triangle^{*-1}(\chi\boldsymbol{n}+\boldsymbol{m})]_{\chi_2} W'(h\chi_1,\theta)\}\Big] \tag{2.3.1}$$

if χ_1 is a single root and χ_2 is a double root, and

$$\boldsymbol{u}(\boldsymbol{x}) = -\frac{\mathrm{sgn}(h)}{\pi}\int_0^{\pi} d\theta \Big[\mathrm{Im}\{\mathrm{Res}_{-1}[\triangle^{*-1}(\chi\boldsymbol{n}+\boldsymbol{m})]_{\chi_1} W(h\chi_1,\theta)\} + h\mathrm{Im}\{\mathrm{Res}_{-2}[\triangle^{*-1}(\chi\boldsymbol{n}+\boldsymbol{m})]_{\chi_1} W'(h\chi_1,\theta)\} + h^2\mathrm{Im}\{\mathrm{Res}_{-3}[\triangle^{*-1}(\chi\boldsymbol{n}+\boldsymbol{m})]_{\chi_1} \frac{W''(h\chi_1,\theta)}{2}\}\Big] \tag{2.3.2}$$

if χ_1 is a triple root. In these formulae $\mathrm{Res}_{-n}[\,]_{\chi_\alpha}$ indicates the coefficient of the $1/(\chi-\chi_\alpha)^n$ term in the Laurent series of the expression in $[\,]$. $\nabla\boldsymbol{u}$ also admits an analogous expression.

It is to be noted that (2.3.1) and (2.3.2) tell that the limiting formulae in (2.2.6) and (2.2.9) remain valid if 'Res' is interpreted as 'Res_{-1}'.

b) Isotropy

We here check (2.1.14) by comparing its prediction in the isotropic case with the result for the same quantity obtained by the direct integration of the fundamental solution in (1.2.5).

The inverse of the Navier tensor for isotropic elastostatics shown in (1.2.3c) is rewritten as

$$\triangle^{*-1}(\chi\boldsymbol{n}+\boldsymbol{m}) = \frac{1(\chi^2+1)-(\lambda+\mu)/(\lambda+2\mu)(\boldsymbol{n}\otimes\boldsymbol{n}\chi^2+(\boldsymbol{n}\otimes\boldsymbol{m}+\boldsymbol{m}\otimes\boldsymbol{n})\chi+\boldsymbol{m}\otimes\boldsymbol{m})}{\mu(\chi^2+1)^2}, \tag{2.3.3}$$

with χ_α's being i (This i is a double root. Since the numerator and

denominator share a factor, we have only 2 roots.). Using (2.3.3) and (2.3.1) with some modifications, we have

$$u(x) = \frac{\mathrm{sgn}(h)}{8\pi\mu}\int_0^{2\pi} d\theta \Big[1\{2\mathrm{Re}W(hi,\theta)\}$$

$$- \frac{\lambda+\mu}{\lambda+2\mu}\{ n\otimes n\{\mathrm{Re}W(hi,\theta) - h\ \mathrm{Im}W'(hi,\theta)\}$$

$$+ (n\otimes m+m\otimes n)h\ \mathrm{Re}W'(hi,\theta)$$

$$+ m\otimes m\{\mathrm{Re}W(hi,\theta) + h\ \mathrm{Im}W'(hi,\theta)\}\}\Big] . \qquad (2.3.4)$$

The integrals with respect to θ in (2.3.4) are then transformed into those with respect to φ (Fig.2.3.1), with the help of the following formulae:

$$\int_0^{2\pi} \mathrm{Re}W(hi,\theta)d\theta = \int (\mathrm{sgn}(h)\sqrt{r^2+h^2} - h)d\varphi ,$$

$$\int_0^{2\pi} \mathrm{Im}W'(hi,\theta)d\theta = -\int (\mathrm{sgn}(h)\frac{h}{(r^2+h^2)^{1/2}} - 1)d\varphi ,$$

$$\int_0^{2\pi} m\ \mathrm{Re}W'(hi,\theta)d\theta = \mathrm{sgn}(h)\int l\ [\log\{\sqrt{r^2+h^2} + r\}$$

$$- \frac{r}{(r^2+h^2)^{1/2}}]\ d\varphi ,$$

$$\int_0^{2\pi} m\otimes m\{\mathrm{Re}W(hi,\theta) + h\ \mathrm{Im}W'(hi,\theta)\}d\theta$$

$$= \int\Big[\{\mathrm{sgn}(h)\sqrt{r^2+h^2}-h\}\ k\otimes k$$

$$- \{\mathrm{sgn}(h)\frac{h^2}{(r^2+h^2)^{1/2}} - h\}\ l\otimes l\Big]d\varphi, \qquad (2.3.5a\text{-}d)$$

where k and l are unit vectors on the plane of the element E which have the directions shown in Fig.2.3.1. To see (2.3.5a), for example, we use (2.1.11) to have

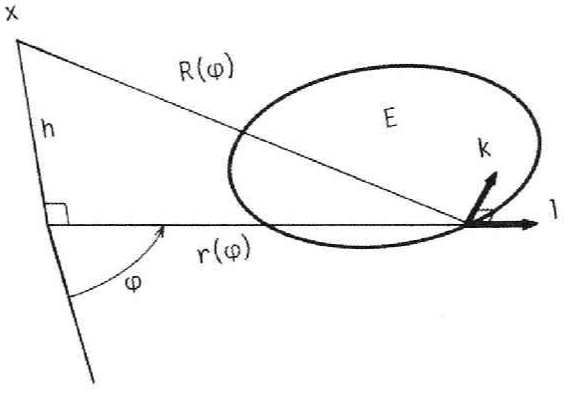

Fig.2.3.1 Notation.

$$\int_0^{2\pi} \mathrm{Re}W(hi,\theta)\mathrm{d}\theta$$

$$= \int_0^{2\pi} \mathrm{d}\theta \ \mathrm{Re} \ \frac{1}{2\pi i}\int \frac{w(t,\boldsymbol{m})}{t-hi}\mathrm{d}t$$

$$= \int_0^{2\pi} \mathrm{d}\theta \ \mathrm{Re} \ \int \frac{r(\varphi)\cos(\varphi-\theta)\left(r'(\varphi)\sin(\varphi-\theta)+r(\varphi)\cos(\varphi-\theta)\right)}{2\pi i\left(r(\varphi)\sin(\varphi-\theta)-hi\right)}\mathrm{d}\varphi$$

$$= \int_0^{2\pi} \mathrm{d}\theta \int \mathrm{d}\varphi \frac{hr(\varphi)\cos(\varphi-\theta)\left(r'(\varphi)\sin(\varphi-\theta)+r(\varphi)\cos(\varphi-\theta)\right)}{2\pi\left(r^2(\varphi)\sin^2(\varphi-\theta)+h^2\right)}, \qquad (2.3.6)$$

where we have substituted $r(\varphi)\sin(\varphi-\theta)$ for t. The limits of integration for φ in (2.3.6) are as have been stated in the previous foot note. We then change the variable of integration from θ to $u = \sin(\varphi-\theta)$, to rewrite the integral in (2.3.6) into

$$\frac{h}{\pi}\int \mathrm{d}\varphi \int_{-1}^{1} \frac{r^2(\varphi)\sqrt{1-u^2}}{r^2(\varphi)u^2 + h^2}\mathrm{d}u \ , \qquad (2.3.7)$$

which is equal to

$$\int (\mathrm{sgn}(h)\sqrt{r^2(\varphi)+h^2} - h)\mathrm{d}\varphi. \qquad (2.3.8)$$

We thus obtain (2.3.5a). We can also prove other formulae in (2.3.5) by using similar calculations. Finally we combine (2.3.4) and (2.3.5) to obtain

$$u(x) = \frac{1}{8\pi\mu}\int \left\{(2R-2|h|)\mathbf{1} - \frac{\lambda+\mu}{\lambda+2\mu}\left[(R-|h|)\mathbf{1}\right.\right.$$

$$- \left(R + \frac{h^2}{R} - 2|h|\right)\boldsymbol{l}\otimes\boldsymbol{l} + \left(\log(R+r) - \frac{r}{R}\right)(\boldsymbol{l}\otimes\boldsymbol{n} + \boldsymbol{n}\otimes\boldsymbol{l})$$

$$\left.\left. + \left(\frac{h^2}{R} - |h|\right)\boldsymbol{n}\otimes\boldsymbol{n}\right]\right\}\mathrm{d}\varphi, \qquad (2.3.9)$$

where $R = \sqrt{r^2+h^2}$.

We now show that a direct integration yields the same result. To do this we use (1.2.5) to have

$$\int_E \Gamma(x,x_0)\mathrm{d}S_{x_0} = \frac{1}{8\pi\mu}\int \left(1\triangle - \frac{\lambda+\mu}{\lambda+2\mu}\nabla\nabla\right)|x-x_0|\,\mathrm{d}S_{x_0}$$

$$= \frac{1}{8\pi\mu}\int\int\left[1\frac{2}{|x-x_0|} - \frac{\lambda+\mu}{\lambda+2\mu}\left(\frac{1}{|x-x_0|} - \frac{(x-x_0)\otimes(x-x_0)}{|x-x_0|^3}\right)\right] r\mathrm{d}r\mathrm{d}\varphi$$

$$= \frac{1}{8\pi\mu}\int\int\left[1\frac{2}{R} - \frac{\lambda+\mu}{\lambda+2\mu}\left(\frac{1}{R} - \frac{r^2 l\otimes l - rh(l\otimes n+n\otimes l)+h^2 n\otimes n}{R^3}\right)\right] R\mathrm{d}R\mathrm{d}\varphi .$$

$$(\ |x-x_0|=R, \ r^2=R^2-h^2, \ x-x_0=-rl+hn \ ) \qquad (2.3.10)$$

The use of

$$\int_{|h|}^{R}\mathrm{d}R = R - |h| \ , \qquad \int_{|h|}^{R}\frac{r^2}{R^2}\mathrm{d}R = R + \frac{h^2}{R} - 2|h| \ ,$$

$$\int_{|h|}^{R}\frac{r}{R^2}\mathrm{d}R = \log(R+r) - \frac{r}{R} - \log h, \quad \int_{|h|}^{R}\frac{\mathrm{d}R}{R^2} = -\left(\frac{1}{R} - \frac{1}{|h|}\right),$$

$$\int l\,\mathrm{d}\varphi=0, \qquad (2.3.11a\text{-}e)$$

then shows that (2.3.10) is equal to (2.3.9).

c) Transverse isotropy

The roots of (2.1.15) can be obtained analytically in the transversely isotropic case. These are the solutions of the equations

$$\chi^2(1-(1-\kappa_i)n_3^2) - 2\chi(1-\kappa_i)m_3n_3 + 1-(1-\kappa_i)m_3^2 = 0 \ ,$$

$$i=1,3 \ , \qquad (2.3.12)$$

where $\kappa_1=C_{44}/C_{66}$ and $\kappa_{2,3}$ are the roots of the equation

$$\kappa^2 - \frac{C_{11}C_{33}-C_{13}^2-2C_{13}C_{44}}{C_{11}C_{44}}\kappa + \frac{C_{33}}{C_{11}} = 0 \ . \qquad (2.3.13)$$

Equation (2.3.12) has a double root when $\sqrt{C_{11}C_{33}} = C_{13} + 2C_{44}$, and a triple root i when $m_3 = n_3 = 0$.

d) Quadrilateral element

Let E have a quadrilateral shape shown in Fig.2.3.2. The Cauchy integrals W and W^p then assume the following forms*

$$W(z) = \frac{1}{2\pi i}\left[\frac{w_2}{\eta_2-\eta_1}(z-\eta_1)\log\frac{z-\eta_2}{z-\eta_1} + \left\{\frac{w_3-w_2}{\eta_3-\eta_2}(z-\eta_2) + w_2\right\}\log\frac{z-\eta_3}{z-\eta_2}\right.$$

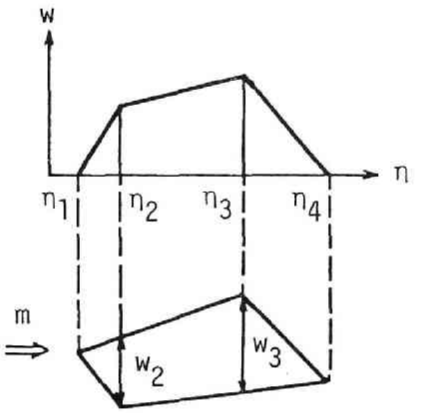

Fig.2.3.2 Quadrilateral element.

$$+\left\{\frac{-w_3}{\eta_4-\eta_3}(z-\eta_3)+w_3\right\}\log\frac{z-\eta_4}{z-\eta_3}\Bigg], \tag{2.3.14}$$

$$W^P(z)=\frac{1}{2\pi i}\Bigg[\frac{w_2}{\eta_2-\eta_1}\log\frac{z-\eta_2}{z-\eta_1}+\frac{w_3-w_2}{\eta_3-\eta_2}\log\frac{z-\eta_3}{z-\eta_2}$$

$$-\frac{w_3}{\eta_4-\eta_3}\log\frac{z-\eta_4}{z-\eta_3}\Bigg]\ . \tag{2.3.15}$$

The branch for $\log\{(z-\eta_\alpha)/(z-\eta_\beta)\}$ is the one which is single valued on the plane cut along $[\eta_\beta,\eta_\alpha]$ and $O(1/z)$ as $|z|\to\infty$. We note that these formulae require some modifications when one of the sides of the element is perpendicular to the η axis. For example, the first term in (2.3.15) is replaced by $-w_2/(z-\eta_2)$ when $\eta_1\to\eta_2$.

We substitute (2.3.14) and (2.3.15) into (2.1.14) and (2.1.16) to compute the simple layer potential and its gradient at the points away from the plane of the element E. For the points lying on the plane of the element, however, it is convenient to use (2.2.6) and (2.2.9). The integrands of these formulae show no singularity except when x lies on the continuation of one of the side lines, where w jumps, say, from 0 to r_1-r_2 (Fig.2.3.3) and w' behaves like Dirac's delta. Since

$$\frac{dw}{d\eta}=\frac{1}{r_1}\frac{dr_1}{d\theta}-\frac{1}{r_2}\frac{dr_2}{d\theta}=\frac{d}{d\theta}\log\left(\frac{r_1}{r_2}\right), \tag{2.3.16}$$

the contribution of this discontinuity to the integral in (2.2.9) is

$$-\frac{1}{2\pi}\sum_{\alpha}^{\cap}\mathrm{Im}\ \mathrm{Res}\left[\left(\chi\boldsymbol{n}+\boldsymbol{m}(\theta)\right)\otimes\triangle^{*-1}\left(\chi\boldsymbol{n}+\boldsymbol{m}(\theta)\right)\right]_{\chi=\chi_\alpha}\log\left(\frac{r_1}{r_2}\right)\ . \tag{2.3.17}$$

2 . 4 Numerical analysis

Equations (2.1.14), (2.1.16), (2.2.6) and (2.2.9) can be used to calculate the influence coefficient defined in (2.1.1). Some favourable aspects of the present formulation are

a) We do not have to compute singular integrals. Hence the numerical integration is not difficult.

b) Residue analysis is required just once for all for one particular set of $\boldsymbol{n}$ and $\boldsymbol{m}$'s for each element.

c) Cancellation is not likely to take place.

---

* Dependence on θ is suppressed here .

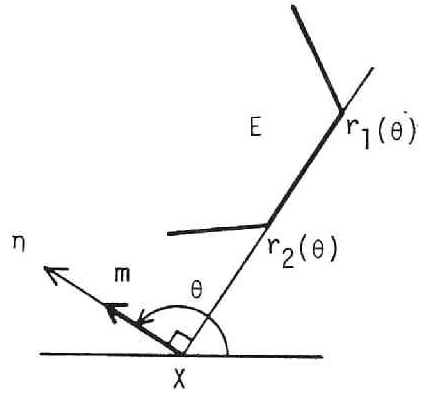

Fig.2.3.3 A special case.

d) It is applicable to any anisotropic material, even if the fundamental solution is not known. The roots of (2.1.15) for the general case, may be obtained by using any existing algorithms for solving algebraic equations (Iri(1981) for example).

We now discuss the computational aspects of our method by using numerical examples. We restrict our attention to the cases of isotropy and transverse isotropy, where the fundamental solutions are available (see (1.2.5) and (1.2.8)). We use 20 point trapezoidal rule for the numerical integrations with respect to θ in (2.1.14), (2.1.16), (2.2.6), and (2.2.9). We compute χ_α's and the residues $\mathrm{Res}\,[\triangle^{*-1}(\chi \boldsymbol{n}+\boldsymbol{m})]_{\chi=\chi_\alpha}$ just once for the 20 $\boldsymbol{m}(\theta)$'s corresponding to the integration 'points' θ_i $(1 \leqq i \leqq 20)$ for each element, and store them in core. One may thus improve the computational efficiency.

Table 2.4.1 compares the values of

$$u_{ij} = \int_E \Gamma_{ij}(\boldsymbol{x},\boldsymbol{y})\mathrm{d}S_y, \qquad \tau_{ijk} = C_{ijmn}\int_E \partial_m \Gamma_{nk}(\boldsymbol{x},\boldsymbol{y})\mathrm{d}S_y \qquad (2.4.1a,b)$$

calculated by several methods, at $\boldsymbol{x} = (0,0,0.1a)$ for isotropic and almost isotropic cases, where E is a square which lies in the plane of isotropy ($y_3 = 0$) (see Fig.2.4.1). We specified the elasticity as $C_{11} = 20C_0$, $C_{13} = 20C_0$, $C_{33} = 80C_0$, $C_{44} = 30C_0$ and $C_{66} = 30C_0$ (in Voigt's notation) in the isotropic case where C_0 is a certain constant having the dimension of stress. The almost isotropic case also uses the same values for C_{ij} except for $C_{33} = 80.8C_0$. 'Closed form' in this table indicates the results obtained by the method of Fukui (Niwa et al.(1979)) ——— a method which integrates the isotropic fundamental solutions analytically over planar elements. Also, 'direct integration' refers to the results obtained by integrating Kröner's fundamental solution (Kröner(1953)) for transversely isotropic elastostatics (We here used the modified form given in Kobayashi & Nishimura(1980), or in (1.2.8), in order to avoid possible cancellation.) by using 100 or 900 point trapezoidal rule. This table shows that the present method gives sufficiently accurate numerical results. It is also remarkable that the conventional numerical integration technique using trapezoidal rule is very inefficient for obtaining stresses near the element. The CPU time for 100 (900) point formula was about 3.8(30) times that of the proposed method.

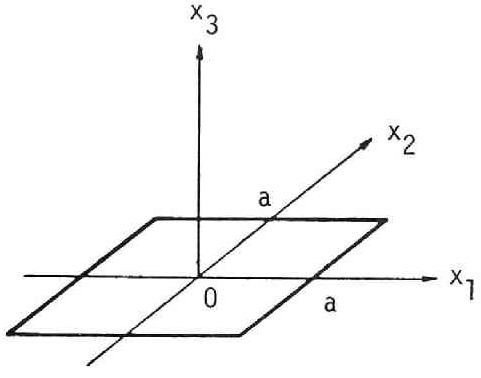

Fig.2.4.1 Square element.

Table 2.4.1 Simple layer potential for (almost) isotropic case
[$*10^{-1}$ u: a/C_0]

	Isotropic		Almost Isotropic		
	Closed form	Present Method	Direct integration		Present Method
			100 points	900 points	
u_{11}	0.1420	0.1420	0.1419	0.1420	0.1420
u_{33}	0.1224	0.1224	0.1207	0.1217	0.1217
τ_{131}	-4.413	-4.414	-4.308	-4.416	-4.415
τ_{113}	-0.9990	-0.9863	-1.350	-0.9933	-0.9765
τ_{333}	-4.830	-4.884	-3.153	-4.818	-4.884

Table 2.4.2 gives the numerical results at $x = (0,0,0^+)$ for (almost) isotropic materials having the same elasticity as in the preceding example. We see that the present method is reliable also for calculating limiting values on the element.

Table 2.4.2 Limiting values on the element for (almost) isotropic case [$*10^{-1}$, u: a/C_0]

	Isotropic		Almost isotropic
	Closed form	Present meth.	Present meth.
u_{11}	0.1578	0.1583	0.1583
u_{33}	0.1286	0.1282	0.1282
τ_{131}	-5.000	-5.001	-5.001
τ_{113}	-1.250	-1.238	-1.238
τ_{333}	-5.000	-4.999	-4.999

Table 2.4.3 compares the field quantities at $x = (0,0,0.1a)$ for a fully anisotropic case ($C_{11}=80C_0$, $C_{13}=10C_0$, $C_{33}=40C_0$, $C_{44}=15C_0$, $C_{66}=30C_0$) obtained by several methods. This table also indicates the high accuracy and efficiency of the present method when the field point is near the element.

Table 2.4.3 Simple layer potential for an anisotropic case [$*10^{-1}$, u: a/C_0]

	Direct integration				Present Method
Int.points	100	400	900	2500	
u_{11}	0.1881	0.1880	0.1880	0.1879	0.1880
u_{33}	0.2300	0.2320	0.2321	0.2321	0.2322
τ_{131}	-4.193	-4.194	-4.176	-4.173	-4.171
τ_{113}	-1.190	-0.9351	-0.8907	-0.8840	-0.8733
τ_{333}	-3.182	-4.548	-4.773	-4.805	-4.864

We next applied the present method to the analysis of stresses around the face of a tunnel in an infinite anisotropic rock. To this end we solved the discretised version of (1.4.7) obtained by using piecewise constant boundary elements, together with the method of integration discussed in this chaper. The cross section of the tunnel is assumed to be a circle having a radius of a. The initial stress is specified as a hydrostatic pressure having a magnitude of p^0. The material constants are set as $C_{11}=80p^0$, $C_{13}=10p^0$, $C_{33}=40p^0$, $C_{44}=15p^0$, and $C_{66}=30p^0$ with the plane of isotropy (x_1-x_2 plane) being tilted from the axis of the tunnel by 40° (see Fig.2.4.2). In the numerical analysis we took into consideration the part of the side wall of length $10a$ from the face, neglecting the influence from the rest of the tunnel. From the point of view of efficiency, it is preferable to use the conventional method of integration when the element and the collocation points are far apart (see 2.5 c)). In the present example we have used the proposed method only when a element includes the collocation point. The obtained displacement and stress in the x_2-x_3 plane are shown in Fig.2.4.2.

2 . 5 Concluding remarks

a) We developed a method of evaluating simple layer potential over plane elements for three dimensional anisotropic elastostatics. We could confirm the applicability of the proposed method through several numerical examples of isotropic and transversely isotropic cases. In principle we can apply this method to any classes of anisotropy although we have tested only two cases out of them.

b) Some authors tried to use numerical fundamental solutions in order to extend the applicability of BIEM, e.g. Vogel & Rizzo(1973) and Wilson & Cruse(1978). Since these methods 'tabulate' numerical fundamental solutions, however, they necessarily require a huge computer. These methods therefore may not be very practical for engineering purposes, although they are very general. In addition, these direct formulations may increase the numerical work compared with indirect methods since the former involve two potential functions in contract to one in the latter.

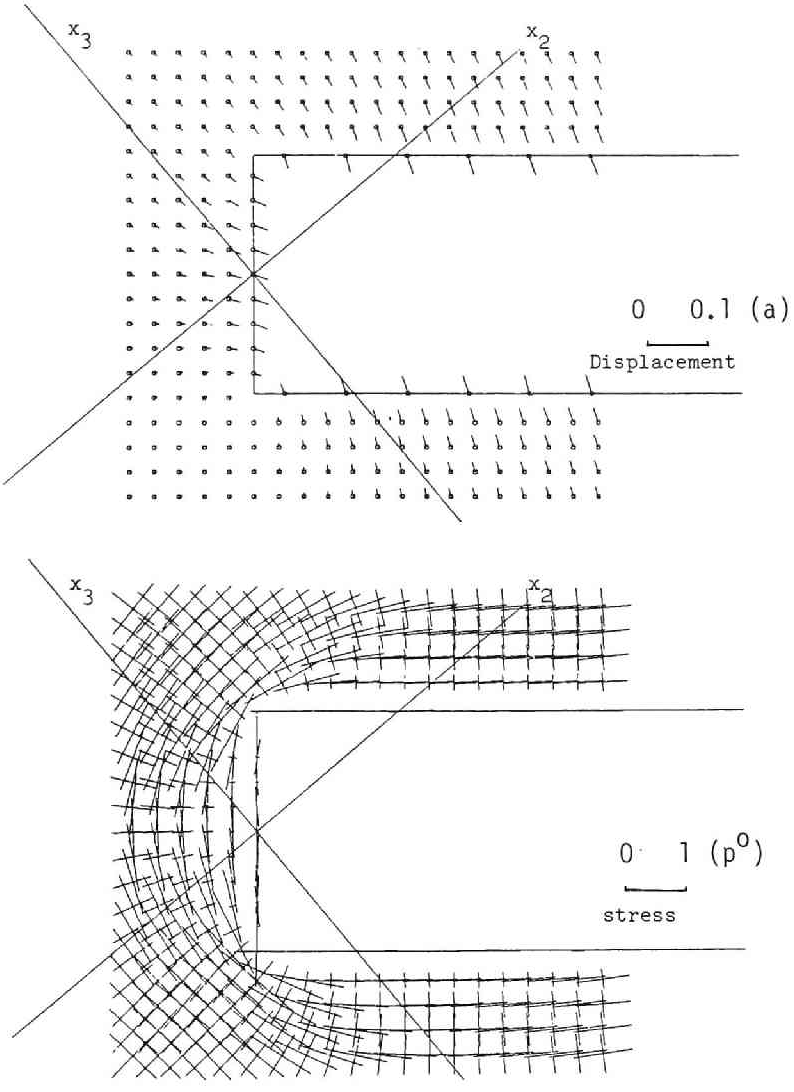

Fig.2.4.2 Displacement and principal stress near the face of the tunnel.

c) As we have seen, our method is particularly effective for evaluating potentials near the boundary element. This is why our method is useful also in the transeversely isotropic case where the fundamental solution is known. From the point of view of efficiency, however, it is desirable to use conventional integration method when the field point is far away from the element, provided the fundamental solution is available.

d) We did not take into consideration the well known singularity of the simple layer density at corners in the sample analysis of tunnel. One may obtain more accurate results by considering the effect of this singularity. For related topics, see chapter 3 where we shall discuss the singularities of this type in the context of acoustics.

e) Maruoka(1982) applied the present method to the calculation of stresses and displacements around a face of tunnel under various stress conditions. Interested reader is referred to his thesis. Nishimura & Kobayashi(1983) also discuss the same topics.

f) The content of this chapter is taken from Nishimura & Kobayashi(1983).

References

Iri, M.(1981). *Numerical Analysis*, Asakura (in Japanese).

Kobayashi, S. & Nishimura, N.(1979). Some considerations on the improvement of integral equation method, *Proc. Japan Soc. Civil Eng.*, vol.291, pp 15-26 (in Japanese).

Kobayashi, S. & Nishimura, N.(1980). Green's tensors for elastic half-spaces ---- An application of boundary integral equation method, *Mem. Fac. Eng. Kyoto Univ.*, vol.42, pp 228-241.

Kröner, E.(1953). Das Fundamentalintegral der anisotropen elastischen Differetialgreichungen, *Z.Physik*, vol.136, pp 402-410.

Maruoka, T.(1982). Analysis of three dimensional anisotropic elastic solids by the integral equation method, *M. Eng. thesis, Kyoto Univ.* (in Japanese).

Mura, T.(1982). *Micromechanics of Defects in Solids*, Nijhoff.

Muskhelishvili, N.I.(1953). *Singular Integral Equations*, (tr. J.R.M. Radok), Noordhoff.

Nishimura, N. & Kobayashi, S.(1983). A boundary integral equation formulation for three dimensional anisotropic elastostatics, *Proc.5th Int. Conf. BEM* (Eds. C.A. Brebbia, T. Futagami & M. Tanaka), Springer, pp 345-354.

Niwa, Y., Kobayashi, S. & Fukui, T.(1979). Stresses and displacements around an advancing face of a tunnel In : *Proc. 4th Int. Congr. Rock Mech.*, Int. Soc. Rock Mech., A.A. Balkema, Montreux, pp 703-710.

Rizzo, F.J.(1967). An integral equation approach to boundary value problems of classical elastostatics, *Q. Appl. Math.*, vol.25, pp

85-93.
Vogel, S.M. & Rizzo, F.J.(1973). An integral equation formulation of three dimensional anisotropic elastostatic boundary value problems, *J. Elasticity*, vol.3, pp 203-216.
Wilson, R.B. & Cruse, T.A.(1978). Efficient implementation of anisotropic three dimensional boundary-integral equation stress analysis, *Int. J. Num. Meth. Eng.*, vol.12, pp 1383-1397.

Chapter 3 Problems Involving Singularities

3 . 0 Introduction

This chapter investigates typical problems involving singularities, i.e., crack problems and simple layer potential methods for domains having corners.

BIEM is sometimes said to be an advantageous method for solving problems involving high stress concentration, singularities, etc. This is presumably because it constructs the solutions by superposing singular solutions. (One cannot expect that FEM, which usually approximates solutions by polynomials, is capable of coping with steep gradients of field quantities.) In fact, a meticulous coding provides a highly accurate numerical BIE implementation (e.g. Watson(1982)). However, a careless job usually ends up with unsatisfactory results polluted by unfavourable singularities.

Consider, for example, the double layer potential for two dimensional Laplace's equation. One may think of using an isoparametric boundary element having a linear shape function. To do this, it is convenient to calculate the double layer potential with a piecewise linear density φ:

$$W(\boldsymbol{x}) = \frac{1}{2\pi}\int_{Y_1-Y_0-Y_2}\frac{\partial}{\partial n_y}\log\frac{1}{|\boldsymbol{x}-\boldsymbol{y}|}\varphi(\boldsymbol{y})\mathrm{d}S_y \tag{3.0.1}$$

where we have used the notation given in Fig.3.0.1 ($\varphi(y_0)=1$). It is not difficult to show that

$$W(\boldsymbol{x}) = \sum_{l=1}^{2}\frac{1}{2\pi l_l}\left[(\boldsymbol{x}_l\cdot\boldsymbol{t}_l)\theta_l + (\boldsymbol{x}_l\cdot\boldsymbol{n}_l)\log|\boldsymbol{x}_0|/|\boldsymbol{x}_l|\right], \tag{3.0.2}$$

and

$$\nabla W(\boldsymbol{x}) = \sum_{l=1}^{2}\frac{1}{2\pi l_l}\left(\boldsymbol{t}_l\theta_l + \boldsymbol{n}_l\log|\boldsymbol{x}_0|/|\boldsymbol{x}_l|\right) \tag{3.0.3}$$

hold (See Fig.3.0.1 for notation). Equation (3.0.2) clearly shows that ∇W has a logarithmic singularity at Y_0, Y_1 and Y_2. This singularity tells us that the piecewise linear isoparametric boundary element may not be adequate for modelling a smooth boundary when one uses formulations including the double layer potential. In fact, the exact solution does not have singularity on the boundary provided the data are smooth, whereas the approximate solution always has singular gradients at nodes. Therefore, the resultant approximate solution cannot be very accurate on the whole boundary. Besides, it is impossible to combine this boundary element with the nodal collocation when one wishes to solve Neumann problem via double layer potential method, because (3.0.3) diverges at nodal points.

Also in the simple layer potential method, one encounters difficulty caused by the singularity when the boundary ∂D has

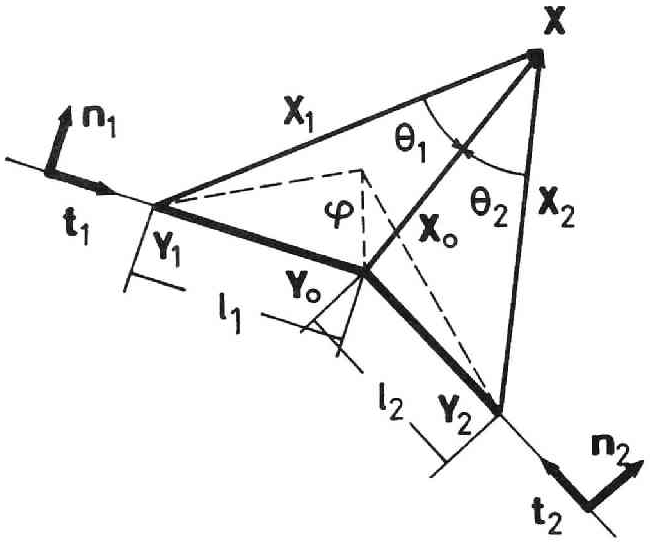

Fig.3.0.1 Double layer potential with piecewise linear density.

corners. Specifically when ∂D has external corners, we may expect that the solution of the boundary value problem itself is regular there. However, the simple layer density is usually singular (e.g. Hartmann(1982)). In fact, we shall see that only those densities having correct singularities there can make the solution regular. This implies that a careless choice of shape functions leads to a poor numerical resolution.

This chapter deals with methods of avoiding such unfavourable singularities; one might therefore more properly have entitled this chapter as the Methods of 'Avoiding' Singularities. The first part of this chapter discusses an elastic - perfectly plastic mode III crack analysis using double layer potential method. It may be conceivable that the double layer potential provides an ideal tool of analysing crack problems since this potential is physically a displacement discontinuity. However, we cannot use directly the simplest piecewise linear isoparametric element in this application since this element has logarithmically singular gradients at nodes whereas the exact displacement in elastic region has finite gradients because the stress is finite in elastic - perfectly plastic material. Two methods of avoiding this trouble occurs to us, i.e., the use of smoother elements and the formulation of the problem in a certain variational sense. In Part I of this chapter we choose the latter, using a Galerkin formulation. The second part of this chapter, on the other hand, utilises the former approach. Specifically, we consider double layer potential methods in 3D elastodynamic crack problems. We shall discuss the use of the method of regularisation of a hypersingular kernel and C^1 boundary elements. The last part of this chapter deals with the singularity of the simple layer density function for domains having external corners in the context of plane acoustics. We take into analysis the effect of singular density by using 'eigenfunctions' of the problem. We introduce an auxiliary contour to evaluate the resulting singular integrals.

Part I

3 . 1 Elastoplastic crack analysis by double layer potential method

In this section we discuss a method of elastoplastic crack analysis using the double layer potential and Galerkin's method. For the sake of simplicity we assume the domain D to be the whole plane R^2. The reader may find no difficulty in extending the content of this section to general cases.

3 . 1 . 1 Antiplane crack problems

Although we can find many elastoplastic analyses for cracked bodies in literature, our present knowledge of the singularity at the tip of elastoplastic cracks is still incomplete except in some simple cases. We therefore restrict our attention to antiplane shear deformation of an isotropic perfectly elastoplastic cracked body with the Mises yield criterion; the singularity of the solution is well-understood in this

case.

Let the crack S be a slit having n as the unit normal vector. Then the following results are available (Rice(1968)):

a) The antiplane displacement $w(x_1,x_2)$ satisfies $\triangle w = 0$ in D_e and $\partial w/\partial n^{\pm} = 0$ on the crack surface, where D_e is the elastic zone, and (x_1,x_2) is the cartesian coordinate whose origin is at a tip of S and whose x_1 axis is tangent to S there, respectively.

b) $w(x_1,x_2)$ in D_p is a function of θ (denoted by $u(\theta)$) satisfying

$$\frac{\partial w}{\partial \theta} = \frac{du}{d\theta} = \gamma_y Q(\theta), \tag{3.1.1.1}$$

where D_p is the plastic zone, $\gamma_y = \tau_y/\mu$, τ_y is the yield stress in shear, μ is the shear modulus and $Q(\theta)$ is the distance from the tip to the elastic-plastic boundary ∂D_{ep} (See Fig.3.1.1.1.), respectively.

c) $\boldsymbol{\tau} = \tau_{13}\boldsymbol{i}_1 + \tau_{23}\boldsymbol{i}_2$ in D_p is written as

$$\boldsymbol{\tau} = \tau_y(-\boldsymbol{i}_1\sin\theta + \boldsymbol{i}_2\cos\theta), \tag{3.1.1.2}$$

where $\boldsymbol{i}_J$ $(J=1,2)$ are the unit base vectors shown in Fig.3.1.1.1. Therefore, the traction on ∂D_{ep} can be written as

$$t := t_3 = \boldsymbol{\tau}\cdot\boldsymbol{n}_{ep} = -\frac{\tau_y Q'}{(Q^2+Q'^2)^{1/2}}, \qquad (Q' = \frac{d}{d\theta}Q(\theta)) \tag{3.1.1.3}$$

where $\boldsymbol{n}_{ep}$ is the unit normal vector to ∂D_{ep} directed towards D_e.

3 . 1 . 2 Double layer potential

We now state the fundamentals concerning the double layer potential.

The (classical) double layer potential

$$W(\boldsymbol{x}) = \frac{1}{2\pi}\int_S \frac{\partial}{\partial n_y}(\log\frac{1}{R})\varphi(\boldsymbol{y})dS_y, \qquad (R = |\boldsymbol{x}-\boldsymbol{y}|) \tag{3.1.2.1}$$

is known to satisfy the Laplace equation in $R^2\backslash\partial D$, and the jump condition

$$W^{\pm}(\boldsymbol{x}) = \pm\frac{\varphi(\boldsymbol{x})}{2} + \frac{1}{2\pi}\int_S \frac{\partial}{\partial n_y}(\log\frac{1}{R})\varphi(\boldsymbol{y})dS_y, \quad \boldsymbol{x}\in S \tag{3.1.2.2}$$

Also, we can show that the following identity holds:

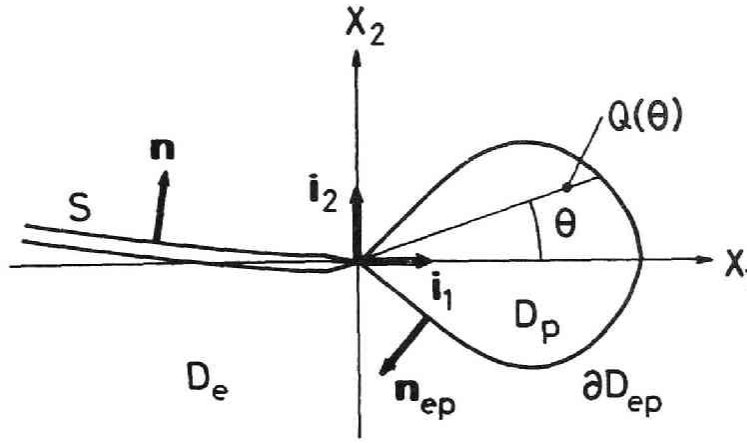

Fig.3.1.1.1 Antiplane deformation of crack.

$$(\nabla W)^{\pm}(x) = \pm\frac{1}{2}\frac{\partial\varphi}{\partial s}(x)c$$

$$+ \text{p.f.}\frac{1}{2\pi}\int_S \nabla_x \frac{\partial}{\partial n_y}(\log\frac{1}{R})\varphi(y)dS_y \ , \quad x \in S \tag{3.1.2.3}$$

where s and c indicate the arc length of S and a unit tangent vector to S in the direction of increasing s, and p.f. denotes the finite part of the integral, respectively. In particular, we have

$$(\frac{\partial W}{\partial n})^{+}(x) = (\frac{\partial W}{\partial n})^{-}(x)$$

$$= \text{p.f.}\frac{1}{2\pi}\int_S \frac{\partial}{\partial n_x}\frac{\partial}{\partial n_y}(\log\frac{1}{R})\varphi(y)dS_y . \quad x \in S \tag{3.1.2.4}$$

One may prove these results by using the method of Fourier transform discussed in Chapter 1.

3 . 1 . 3 Galerkin's method in elastic crack analysis

We first consider the problem of finding the antiplane elastic deformation $w(x)$ which satisfies the Laplace equation and the traction boundary condition of the form

$$(\frac{\partial w}{\partial n})^{+} = (\frac{\partial w}{\partial n})^{-} = t \qquad \text{on } S, \tag{3.1.3.1}$$

where t is the given traction. Both the direct method and indirect method using the double layer potential lead to

$$w(x) = \int_S \frac{\partial}{\partial n_y}\Gamma(x,y)\varphi(y)dS_y \ , \qquad \Gamma = \frac{1}{2\pi}\log\frac{1}{|x-y|} \ , \tag{3.1.3.2a,b}$$

where φ indicates the double layer density. It is clear, from (3.1.2.2), that the density φ can be identified with the gap of the displacement on S, or $\varphi = [w] := w^{+} - w^{-}$.

The Galerkin solution $\sum_\alpha \Omega_\alpha\varphi_\alpha$ (Ω_α: shape function) of the 'integral' equation

$$t(x) = \text{p.f.}\int_S \frac{\partial}{\partial n_x}\frac{\partial}{\partial n_y}\Gamma(x,y)\varphi(y)dS_y \tag{3.1.3.3}$$

is obtained by solving

$$\int_S \Omega_\alpha (t - \sum_\beta \text{p.f.} \int_S \frac{\partial}{\partial n_x} \frac{\partial}{\partial n_y} \Gamma \Omega_\beta dS_y \varphi_\beta) dS_x = 0 \ . \qquad (3.1.3.4)$$

for φ_α.

In the sequel, we shall see that the Galerkin solution also makes the potential energy

$$\Pi(w) = \frac{1}{2} \int_D \nabla w \cdot \nabla w dV + \int_S t [w] \, dS \qquad (3.1.3.5)$$

minimum among the solutions which can be written as

$$w = \sum_\alpha \int_S \frac{\partial}{\partial n_y} \Gamma \Omega_\alpha dS \ \varphi_\alpha = \sum_\alpha w_\alpha \varphi_\alpha , \quad w_\alpha := \int_S \frac{\partial}{\partial n_y} \Gamma \Omega_\alpha dS \ . \qquad (3.1.3.6a,b)$$

To see this we substitute (3.1.3.6a) into (3.1.3.5) assuming that $\nabla w \cdot \nabla w$ is integrable in R^2. This assumption rules out the piecewise constant shape functions since ∇w would then have $1/r$ singularities at the ends of elements. Since $\triangle w = 0$ in D, we have

$$\Pi(w) = -\frac{1}{2} \int_S \{ [w \frac{\partial w}{\partial n}] - t [w] \} \, dS, \qquad w = \sum_\alpha w_\alpha \varphi_\alpha \ . \qquad (3.1.3.7a,b)$$

We then differentiate (3.1.3.7a) with respect to φ_β, use Green's formula, (3.1.2.2) and (3.1.2.4), and then put the resulting expression equal to zero to obtain

$$0 = -\frac{1}{2} \sum_\alpha \int_S [w_\alpha \frac{\partial w_\beta}{\partial n} + w_\beta \frac{\partial w_\alpha}{\partial n}] \varphi_\alpha dS + \int_S t [w_\beta] \, dS$$

$$= -\sum_\alpha \int_S [w_\beta \frac{\partial w_\alpha}{\partial n}] \varphi_\alpha dS + \int_S t [w_\beta] \, dS$$

$$= -\sum_\alpha \int_S \Omega_\beta \frac{\partial w_\alpha^+}{\partial n} \varphi_\alpha dS + \int_S t \Omega_\beta dS \ , \qquad (3.1.3.8)$$

which is exactly the Galerkin equation given in (3.1.3.4). We thus conclude that the Galerkin solution in elastic crack problems gives the best approximation in the sense of energy.

3.1.4 Double layer potential method for elastoplastic crack problems

In the problems of antiplane shear, the stress field in D_p at each crack tip is already known (see (3.1.1.2)). Therefore, what are left to be determined are the location of the elastic-plastic boundary and

the field quantities in the elastic domains. We here try to find w in D_e in the following form:

$$w = w_0 + \int_S \frac{\partial}{\partial n_y}\Gamma\varphi dS + \sum_{I=1}^{n_{tip}} \int_{\partial D_{ep}^I} \frac{\partial}{\partial n_y}\Gamma\psi_I dS \ , \qquad (3.1.4.1)$$

where w_0 is a far field which satisfies

$$\triangle w_0 = 0 \qquad \text{in } D, \qquad (3.1.4.2)$$

φ and ψ_I are unknown densities, ∂D_{ep}^I is the elastic-plastic boundary associated with D_p^I $(1 \leqq I \leqq n_{tip})$, n_{tip} is the number of tips and D_p^I is the plastic domain at the I-th tip, respectively. Our problem then reduces to a problem of finding φ, ψ_I and ∂D_{ep}^I which satisfy

$$(\frac{\partial w}{\partial n})^+ = (\frac{\partial w}{\partial n})^- = \frac{\partial w_0}{\partial n} + \text{p.f.}\int_S \frac{\partial}{\partial n_x}\frac{\partial}{\partial n_y}\Gamma\varphi dS$$

$$+ \sum_I \int_{\partial D_{ep}^I} \frac{\partial}{\partial n_x}\frac{\partial}{\partial n_y}\Gamma\psi_I dS = 0 \qquad \text{on } S,$$

$$(\frac{\partial w}{\partial n})^+ = \frac{\partial w_0}{\partial n} + \int_S \frac{\partial}{\partial n_x}\frac{\partial}{\partial n_y}\Gamma\varphi dS + \sum_J \text{p.f.}\int_{\partial D_{ep}^J} \frac{\partial}{\partial n_x}\frac{\partial}{\partial n_y}\Gamma\psi_J dS$$

$$= -\frac{\tau_y Q'}{(Q^2 + Q'^2)^{1/2}} \qquad \text{on } \partial D_{ep}^I \ , \qquad (3.1.4.3a,b)$$

and

$$\frac{\partial}{\partial\theta}w^+ = \gamma_y Q(\theta) \qquad \text{on} \quad \partial D_{ep}^I \ , \qquad (3.1.4.4)$$

where we have used the notation employed in 3.1.1.

We notice that the traction on ∂D_{ep}^I (see (3.1.1.3)) satisfies

$$-\tau_y \int_{\partial D_{ep}^I} \frac{Q'}{(Q^2 + Q'^2)^{1/2}} dS = -\tau_y \int_{-\pi/2}^{\pi/2} Q' d\theta = 0 \ . \qquad (3.1.4.5)$$

This guarantees that w certainly admits an expression given in (3.1.4.1). Indeed, the simple layer potential on each ∂D_{ep}^I in the direct potential representation

$$w = w_0 + \int_S \frac{\partial}{\partial n_y}\Gamma\varphi dS + \sum_{I=1}^{n_{tip}} \int_{\partial D_{ep}^I} (\frac{\partial}{\partial n_y}\Gamma w - \Gamma\frac{\partial w}{\partial n}) dS \text{ in } D_e \qquad (3.1.4.6)$$

is known to possess a double layer representation with a continuous density if (3.1.4.5) is satisfied (Kupradze et al.(1979)). However, ψ_I in (3.1.4.3) are not determined uniquely; they are determined to within an additive constant, as can be inferred from the above discussion. It also follows that ψ_I is discontinuous at the tip x_I, the amount of discontinuity there being

$$\psi_I^+(x_I) - \psi_I^-(x_I) = \varphi(x_I) , \quad 1 \leqq I \leqq n_{tip} , \tag{3.1.4.7}$$

in the notation given in Fig.3.1.4.1. Therefore one may arbitrarily put

$$\psi_I^+(x_I) = \varphi(x_I) \quad \text{and} \quad \psi_I^-(x_I) = 0 . \tag{3.1.4.8a,b}$$

We will formulate an iterative method of solution for this problem in the next section.

3 . 1 . 5 Numerical procedures

In this section we discuss an iterative numerical method of solution for our problem. We take one particular crack tip for explanation (Fig.3.1.5.1).

Our method goes as follows:

a) Assume an initial shape of ∂D_{ep}.

b) Model S and ∂D_{ep} by using line segments. Locate the nodes on ∂D_{ep} in an equal spacing of azimuth angle θ as shown in Fig.3.1.5.1.

We can then use the piecewise linear elements discussed in 3.0 as shown in Fig.3.1.5.1(b)(see (3.1.4.8)). In the example of this figure, the unknowns are ...., φ^{n-1} , $\varphi^n(=\psi^1)$, ψ^2,...., ψ^{m-1} and ψ^m.

c) Solve (3.1.4.3) by using the Galerkin method.
This decision is made on the following grounds:

i) As has been discussed in 3.1.3, the Galerkin method in elastic cases gives the best approximation in the sense of energy. This suggests a good accuracy of this method also in elastoplasticity.

ii) We intend to use the piecewise linear element discussed in 3.0. This approximation, however, introduce a logarithmic singularity in ∇w at the nodal points (see (3.0.1)-(3.0.3)), which makes collocation difficult to apply.

In applying Galerkin's method, we have to evaluate integrals of the following form:

$$\int N_\beta dS_x \frac{\partial}{\partial n_x} \int \frac{\partial}{\partial n_y} \Gamma N_\alpha dS_y . \tag{3.1.5.1}$$

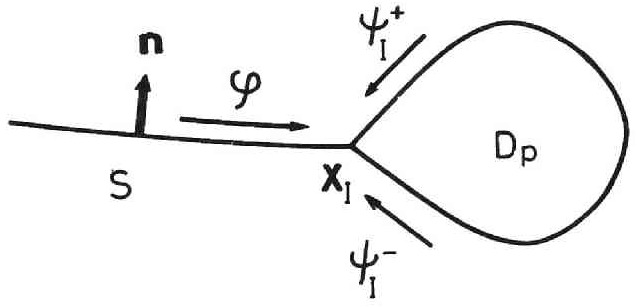

Fig.3.1.4.1 Limiting values of densities at a crack tip.

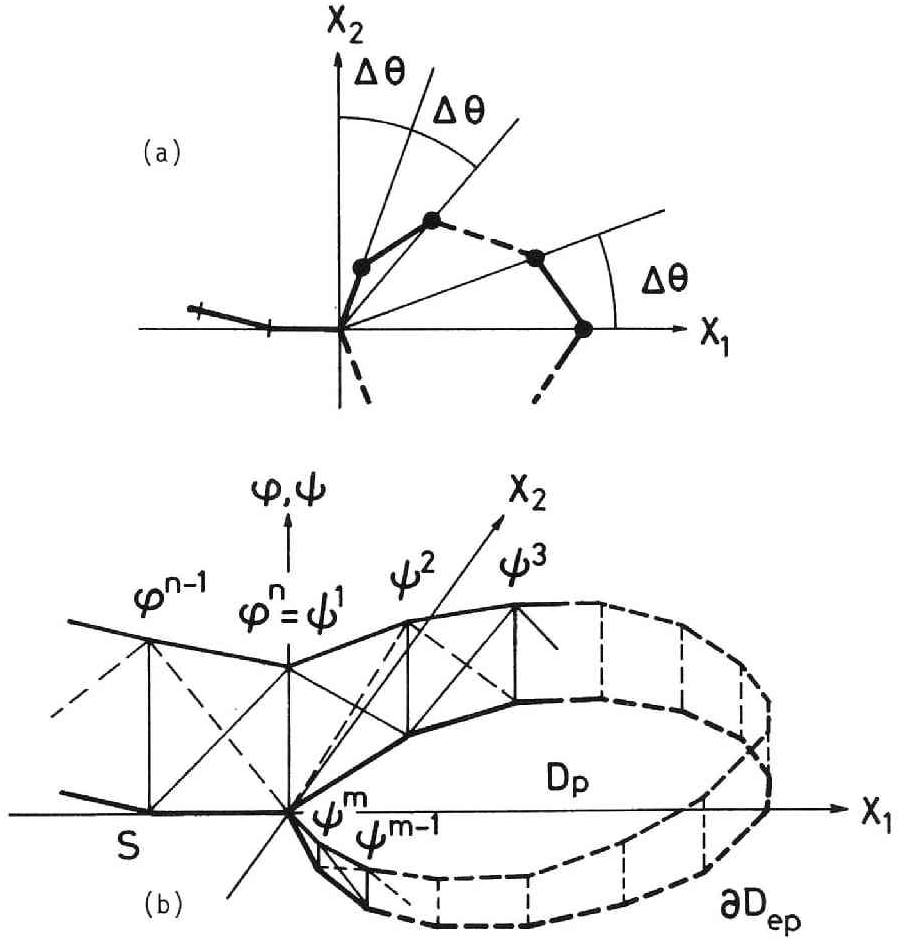

Fig.3.1.5.1 Use of boundary elements in elastoplastic crack analysis.

Here we have evaluated the inner integral analytically (see (3.0.2)) and the outer integral by using a special 8 point Gaussian integration formula which takes into consideration the logarithmic singularity of the integrand. For the evaluation of Q' on the right hand side of (3.1.4.3b) we have used the central difference formula.

d) Calculate w on ∂D_{ep} by (3.1.4.1) and then update $Q(\theta)$ by

$$Q_{new}(\theta) \longleftarrow Q_{old}(\theta) + \zeta\left(\frac{1}{\gamma_y}\frac{\partial w}{\partial \theta} - Q_{old}(\theta)\right) , \qquad (3.1.5.2)$$

where ζ $(0 < \zeta \leqq 1)$ is a constant (see (3.1.1.1)). Using the new $Q(\theta)$, we calculate the new configuration of ∂D_{ep}.

Again we have used the central difference formula to evaluate $\partial w/\partial \theta$. Also, we have chosen $\zeta = 0.3$.

e) Repeat this process until a convergence condition is met.

We have terminated the computation when the increment of Q becomes less than 1 percent of Q everywhere on ∂D_{ep}.

3 . 1 . 6 Example

We solved the problem of a straight crack of length $2a$ subject to a uniform remote shear τ_2^∞ (Fig.3.1.6.1). One may also view this crack as emanating from the traction free boundary $x_1 = 0$ of a half-plane $x_1 \geqq 0$ because of the symmetry. This problem was solved by Hult and McClintock(1956) analytically.

We solved this problem for the cases of $\tau_2^\infty/\tau_y = 1/3$, $1/2$ and $2/3$, by using the mesh shown in Fig.3.1.6.1. We took advantage of the symmetry of the problem and applied our method to the right half of the crack. The initial configuration of ∂D_{ep} is assumed to be a circle having a diameter of $a/100$. Fig.3.1.6.1 compares the plastic domain calculated by the present method (shown by symbols) with the analytical results. The agreement is satisfactory. 16 iterations have led to convergence when $\tau_2^\infty/\tau_y = 2/3$, requiring about 0.5 sec of CPU time per step.

This analysis was carried out by using FACOM M382 of the Data Processing Centre of Kyoto University.

Part II

3 . 2 Elastodynamic crack problems

In part II we discuss a BIEM for elastodynamic crack problems. Our main interests here are the regularisation of a hypersingular kernel and the use of C^1 base functions. (We here prefer the word 'base functions' to 'shape functions' due to a reason which we shall describe later.)

As will be discussed in Chapter 4 there are two approaches in elastodynamics, i.e., the time domain method and the frequency domain

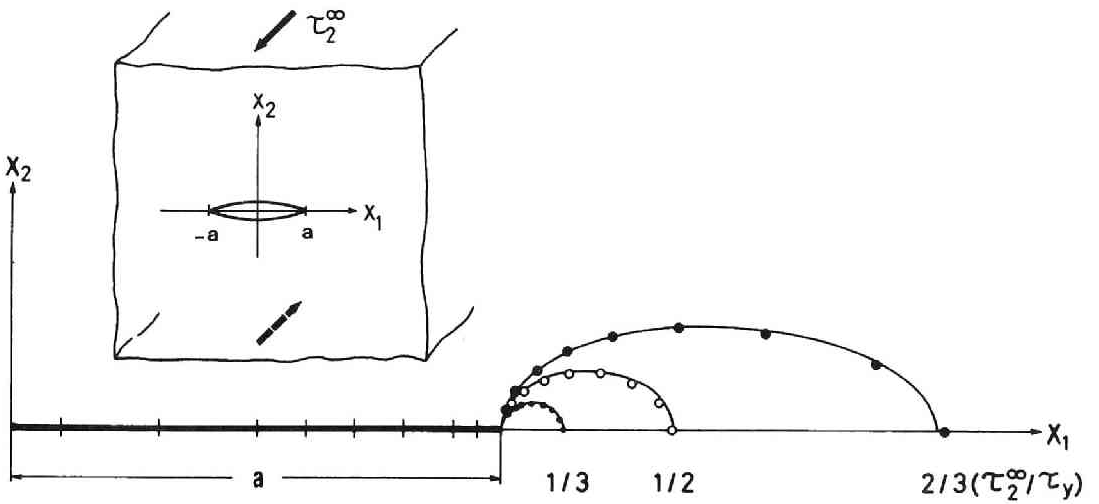

Fig.3.1.6.1 Plastic domains near the crack tip.
Lines: exact, Symbols: BIE.

method. We here use the latter. One may, however, think that we are considering a steady state with an $e^{-i\omega t}$ time dependence.

3 . 2 . 1 Formulation

Let S be a piece of smooth curved surface in R^3 bounded by a piecewise smooth edge ∂S. Also let $\boldsymbol{n}$ be the unit normal vector to S, which points into a side of S called the 'positive side'. Our problem is to find a solution $\boldsymbol{u}$ which satisfies the equations

$$\triangle^*\boldsymbol{u} + \rho\omega^2\boldsymbol{u} = 0 \qquad \text{in } R^3\backslash S, \quad (\triangle^*\boldsymbol{u} := \text{div } C[\nabla\boldsymbol{u}])$$

$$T\boldsymbol{u}^{\pm} = 0 \qquad \text{on } S, \quad (T\boldsymbol{u} := C[\nabla\boldsymbol{u}]\boldsymbol{n})$$

$$\lim_{x\to x_0} \left(\boldsymbol{u}^+(\boldsymbol{x}) - \boldsymbol{u}^-(\boldsymbol{x})\right) = 0, \quad \boldsymbol{x}\in S, \quad x_0\in\partial S, \qquad (3.2.1.1a\text{-}c)$$

and radiation condition (Kupradze et al.(1979) or (4.1.1.13)) for $\boldsymbol{u}-\boldsymbol{u}_I$, where $\triangle^*$, T, C, ρ, ω, and $\boldsymbol{u}_I$ stand for the Navier operator, elastic traction operator, elasticity tensor, density, frequency, and the incident field which satisfies (3.2.1.1a) in R^3, respectively. Also, we have used a superposed + (-) to indicate a limit from the positive (negative) side of S. The solution to this problem has a double layer representation given as

$$\boldsymbol{u}(\boldsymbol{x}) = \int_S \Gamma_I(\boldsymbol{x},\boldsymbol{y})\boldsymbol{\varphi}(\boldsymbol{y})\, dS + \boldsymbol{u}_I(\boldsymbol{x}), \qquad \boldsymbol{x}\notin S \qquad (3.2.1.2)$$

where Γ_I is the double layer kernel defined in (1.1.14). The fundamental solution for the isotropic case is written as (Kupradze et al.(1979))

$$\Gamma(\boldsymbol{x},\boldsymbol{y}) = \mathbf{1}\, F(R) + \nabla\otimes\nabla G(R), \quad (R := |\boldsymbol{x}-\boldsymbol{y}|) \qquad (3.2.1.3)$$

where

$$F(R) = \frac{e^{ik_TR}}{4\pi\mu R}, \qquad G(R) = \frac{1}{4\pi\mu k_T^2}\left(\frac{e^{ik_TR}}{R} - \frac{e^{ik_LR}}{R}\right),$$

$$k_T = \frac{\omega}{(\mu/\rho)^{1/2}}, \qquad k_L = \frac{\omega}{\left((\lambda+2\mu)/\rho\right)^{1/2}}, \qquad (3.2.1.4a\text{-}d)$$

and λ and μ are Lame's constants, respectively. Also, C takes the form shown in (1.2.3a). For a smooth $\boldsymbol{\varphi}$, (3.2.1.1b),(3.2.1.2) and (1.3.3.8) yield an 'integral' equation

$$-T\boldsymbol{u}_I(\boldsymbol{x}) = \text{p.f.}\int_S T\Gamma_I(\boldsymbol{x},\boldsymbol{y})\boldsymbol{\varphi}(\boldsymbol{y})\, dS, \qquad \boldsymbol{x}\in S \qquad (3.2.1.5)$$

where p.f. designates the finite part of a divergent integral.

As one sees easily, the integrand in (3.2.1.5) is hypersingular, making (3.2.1.5) not suitable as a tool of numerical analysis. In isotropic cases, however, we can reduce the order of the singularity of $T\Gamma_{l}$ by using the integration by part. To see this we assume $x \notin S$. As has been shown by several authors (Weaver(1977) in statics and Sladek & Sladek (1984) in dynamics) we have

$$-\int_S \Gamma_{ij,kp} C_{jklm} n_l \varphi_m \, dS = \rho\omega^2 \int_S \Gamma_{im} n_p \varphi_m \, dS$$

$$+ \, e_{lpu} C_{jklm} \int_S \Gamma_{ij,k} e_{tsu} n_t \varphi_{m,s} \, dS, \qquad (3.2.1.6)$$

where e_{ijk} is the permutation symbol and the differentiation in (3.2.1.6) is with respect to the integration variable y. Since this expression still includes an integral convergent in the sense of Cauchy's principal value as $x \to \partial D$, we shall attempt to use the integration by part once again to reduce the singularity of the kernel further. To do this we note that the second integral on the RHS of (3.2.1.6) is written as

$$e_{lpu} C_{jklm} \left[\int_S \Gamma_{ij,q} n_q n_k e_{tsu} n_t \varphi_{m,s} \, dS \right.$$

$$\left. + \int_S \Gamma_{ij,r} e_{qrw} n_q e_{vkw} n_v e_{tsu} n_t \varphi_{m,s} \, dS \right], \qquad (3.2.1.7)$$

where we have used

$$\partial_i = n_i n_j \partial_j + e_{tik} n_t e_{sjk} n_s \partial_j . \qquad (3.2.1.8)$$

The second term in (3.2.1.7) obviously allows a regularisation with the help of Stokes's theorem. The first term in (3.2.1.7), on the other hand, is written as

$$\int_S n_k \frac{(\boldsymbol{n} \cdot \bar{\boldsymbol{x}})}{R} \left\{ \delta_{ij} F' + (\delta_{ij} + 2 n_i n_j) \left(\frac{1}{R} G' \right)' \right.$$

$$\left. + \, \bar{x}_i \bar{x}_j \left(\frac{1}{R} \left(\frac{1}{R} G' \right)' \right)' \right\} e_{tsu} n_t \varphi_{m,s} \, dS$$

$$- \, \text{p.f.} \int_S \frac{1}{R} G' e_{qrw} n_q \partial_r \{ (n_i e_{pjw} n_p + n_j e_{piw} n_p) n_k e_{tsu} n_t \varphi_{m,s} \} dS, \qquad (3.2.1.9)$$

where $\bar{\boldsymbol{x}} = \boldsymbol{y} - \boldsymbol{x}$ and $R = |\bar{\boldsymbol{x}}|$. In the derivation of (3.2.1.9) we have

used

$$n_l \partial_l \partial_i \partial_j G$$

$$= \frac{\boldsymbol{n}\cdot\bar{\boldsymbol{x}}}{R}\{(\delta_{ij} + 2n_i n_j)(\frac{1}{R}G')' + \bar{x}_i\bar{x}_j(\frac{1}{R}(\frac{1}{R}G')')'\}$$

$$+ (n_i e_{pjw} n_p + n_j e_{piw} n_p) e_{qrw} n_q \frac{\partial}{\partial y_r}\left(\frac{1}{R}G'\right). \qquad (3.2.1.10)$$

The p.f. symbol in (3.2.1.9) is due to the singularity of φ on ∂S. ($\varphi \sim \delta^{1/2}$ where δ is the distance from ∂S.) Finally we combine (3.2.1.6), (3.2.1.7) and (3.2.1.9) to obtain

$$\partial_p \int_S \Gamma_{l\ im}\varphi_m \, dS = \rho\omega^2 \int_S \Gamma_{im} n_p \varphi_m dS$$

$$+ e_{lpu} C_{jklm}\left[\int_S n_k \frac{\boldsymbol{n}\cdot\bar{\boldsymbol{x}}}{R}\left\{\delta_{ij}F' + (\delta_{ij} + 2n_i n_j)(\frac{1}{R}G')'\right.\right.$$

$$\left.\left. + \bar{x}_i\bar{x}_j(\frac{1}{R}(\frac{1}{R}G')')'\right\} e_{tsu} n_t \varphi_{m,s} dS\right.$$

$$- \text{p.f.}\int_S \left\{\frac{1}{R}G' e_{qrw} n_q \ \partial_r\{(n_i e_{njw} n_n + n_j e_{niw} n_n) n_k e_{tsu} n_t \varphi_{m,s}\}\right.$$

$$\left. + \Gamma_{ij} e_{qrw} n_q \partial_r (e_{vkw} n_v e_{tsu} n_t \varphi_{m,s})\right\} dS\Big]. \qquad (3.2.1.11)$$

Notice that all the integrals in (3.2.1.11), except for the 'p.f.' introduced by the near tip singularity of φ, converge in the ordinary sense for any φ having C^1 continuity on S. This convergence is partly due to the smoothness of S. Hence we are justified to use (3.2.1.11) as the basis of our BIEM because there is an easy way of evaluating the p.f integrals in (3.2.1.11), as we shall see.

Obviously, from the $(\boldsymbol{n}\cdot\bar{\boldsymbol{x}})$ term in (3.2.1.11) results a non-integral term as x tends to S. However, (1.3.3.8) guarantees that this discontinuity term vanishes as one multiplies it by $C_{ipab}n_b$. One may alternatively show this by a direct calculation using (3.2.1.11), but we shall omit the detail. Finally, we note, in the flat crack case, that the 2nd integral in the RHS of (3.2.1.11) vanishes as x tends to S. In addition, one shows that the in plane and out of plane components of (3.2.1.11) decouple as one multiplies (3.2.1.11) by $C_{ipab}n_b$ to obtain an integral equation.

3 . 2 . 2 Numerical analysis

We first decide to use collocation method, which is believed to be efficient in engineering applications. This choice in our formulation, however, requires the use of C^1 base functions. Indeed, piecewise constant base functions for φ would pollute the solution by introducing $1/\delta$ singularities in (3.2.1.11), where δ is the distance between x and a point where φ is discontinuous. Actually, the second derivatives of φ in (3.2.1.11) would behave like the 1st derivatives of Dirac's delta, which would pick up singularities from the kernel functions. Still worse is a piecewise linear approximation, in which case (3.2.1.11) would diverge logarithmically at points where the slope of the base functions are discontinuous. This means that a nodal collocation with piecewise linear base functions breaks down. Hence we are left with the use of C^1 base functions with which (3.2.1.11) is seen to remain bounded on S.

This restriction of C^1 continuity is not very stringent in a special case where one can find a smooth mapping from S onto a square, say $|x_1|<a$, $|x_2|<a$, $x_3=0$. Indeed, one first generates B-spline functions of x_1 and x_2 independently in the following manner:

1) Introduce a parameter t such that $s = a\sin(\pi t/2a)$ $(|t|<a)$ where s is either x_1 or x_2.

2) Divide the interval $(-a, a)$ for t into subintervals of equal length $\triangle t$ by using nodes $(-a =)\ t_0 < t_1 < \ldots < t_{n+1}\ (= a)$.

3) Define 3rd order spline functions $\sigma_i(t)$ $(i = 1,2,\ldots,n)$ by $\sigma_i(t) = f(|t-t_i|/\triangle t)$ $(i = 1,..,n)$ with exceptions $\sigma_1(t) = g(|t-t_1|/\triangle t)$ for $t_0<t<t_1$ and $\sigma_n(t) = g(|t-t_n|/\triangle t)$ for $t_n<t<t_{n+1}$ where (see Fig.3.2.2.1)

$$f(\eta) = \begin{cases} 1 - (3/2)\eta^2 + (3/4)\eta^3 & 0\leqq\eta<1, \\ (1/4)(2 - \eta)^3 & 1\leqq\eta<2, \\ 0 & \text{otherwise}, \end{cases} \qquad (3.2.2.1)$$

$$g(\eta) = (3/2)(1 - \eta) - (1/2)(1 - \eta)^3 \quad 0\leqq\eta<1. \qquad (3.2.2.2)$$

With the spline functions of x_1 and x_2 thus defined, we can now proceed to construct a system of base functions on the square by multiplying the x_1 and x_2 spline functions. Finally one determines the base functions $\Omega_i(x)$ on S by using the pull back of the base functions on the square which we have just defined.

Now assume

$$\varphi = \sum\varphi_i\Omega_i(x), \qquad (3.2.2.3)$$

where φ_i are numbers. We substitute (3.2.2.3) into (3.2.1.11) to discretise (3.2.1.5), and solve the resulting numerical matrix for φ_i to determine φ with the help of (3.2.2.3). Note that $\varphi \sim (a \pm s)^{1/2}$ holds near edges due to the relation between s and t. Hence one easily

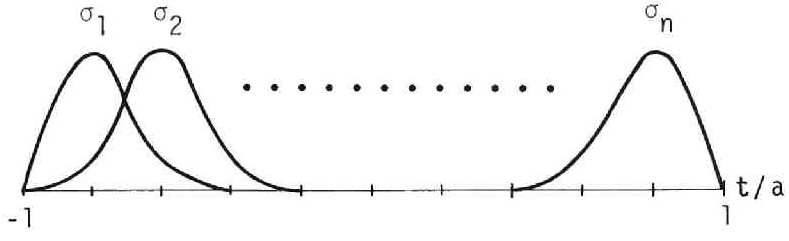

Fig.3.2.2.1 Spline functions.

obtains stress intensity factors by computing the coefficients of square root singular terms in φ. At corner points, however, this method renders φ non singular. The exact solution, on the other hand, is known to be weakly singular there with an exponent ($> 1/2$) dependent on Poisson's ratio (Takakuda(1985)). This neglecting of the corner singularity, however, does not have a significant effect on the overall accuracy of the numerical solution as we shall see through examples.

Another practically important special case which allows a simple implementation is the case where there exists a smooth mapping from S onto a disc. By the same reasoning as before we are justified to restrict our attention to the case of a penny shaped crack having a radius of a. Our scheme for this case goes as follows:

1) Introduce (t, θ) coordinate system by which the natural polar coordinate on the crack, denoted by (r, θ), is expressed as $(r,\theta) = (a \sin(\pi t/2a), \theta)$. We also define $(\xi_1, \xi_2) = (t \cos\theta, t \sin\theta)$.

2) Divide the interval $(0, a)$ for t into subintervals of equal length $\triangle t$ by introducing nodes $(0 =)\ t_0 < t_1 < \ldots < t_{n+1}\ (= a)$. Also divide $(0, 2\pi)$ for θ into subintervals of equal length $(0 =)\ \theta_0 < \theta_1 < \ldots < \theta_m\ (= 2\pi)$. For nodes (t_i, θ_j) $(2 \leqq i \leqq n,\ 1 \leqq j \leqq m)$ we use 'product' base functions similar to those used before. This determines $(n-1)m$ base functions $\Omega_i(x)$.

3) In the domain defined by (t,θ), $t \leqq t_1$, $0 \leqq \theta < 2\pi$, we take points ξ^i $(1 \leqq i \leqq k)$ arbitrarily. Draw circles of arbitrary (but not too large) radius $2r_i$ centred at ξ^i. Define 'bell shaped' base functions associated with ξ^i by $\Omega_{(n-1)m+i}(x) = f(|\xi - \xi^i|/r_i)$. A standard choice for r_i is $\triangle t$.

4) Use the base functions defined in 2) and 3) (see Fig.3.2.2.2), assume (3.2.2.3) for φ, and then discretise (3.2.1.5) with the help of (3.2.1.11).

We remark that φ_i in (3.2.2.3) does not have a clear physical meaning since our Ω_i does not satisfy relations similar to (1.5.1). This is why we prefer the name 'base functions' for our Ω_i. Finally we discuss the evaluation of the remaining p.f. integral in (3.2.1.11) taking the second special case as an example. We shall start with a formula

$$\text{p.f.}\int_0^{2\pi}\int_0^a \left(\frac{\partial}{\partial r}\right)^2 \Omega(r,\theta)\ H(r,\theta)\, r dr d\theta$$

$$= \int_0^{2\pi}\int_0^a \left(\frac{\partial}{\partial r}\right)^2 \Omega(r,\theta)\left(rH(r,\theta) - aH(a,\theta)\right) dr d\theta, \qquad (3.2.2.4)$$

where Ω stands for one of the base functions having singularities on ∂S $((\partial/\partial r)^2\Omega \sim (a-r)^{-3/2})$, and H is a function regular at $r=a$. In deriving (3.2.2.4) we have used the fact that Ω vanishes except in a region near the tip. With (3.2.2.4) we can compute the p.f. integrals

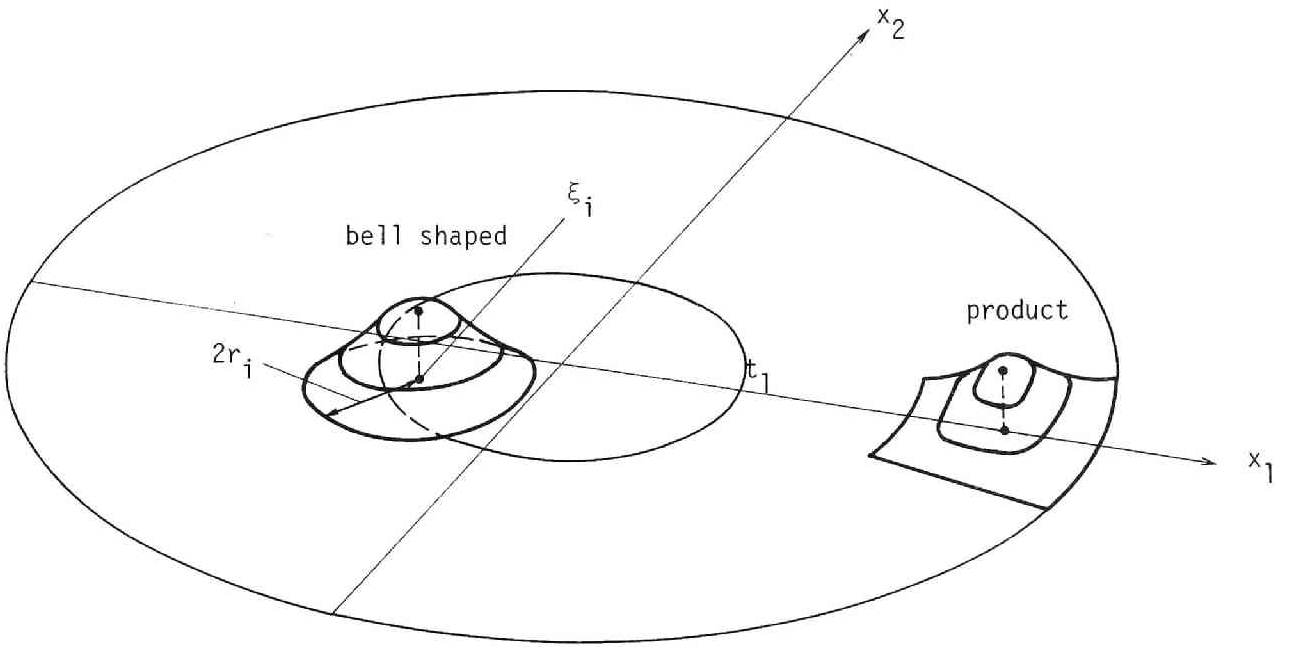

Fig.3.2.2.2 Base functions for penny shaped crack.

in (3.2.1.11) numerically since they take the form of the LHS of (3.2.2.4), and the RHS of (3.2.2.4) converges in the ordinary sense. For evaluating an integral having an integrable but weakly singular integrand, we use a change of coordinate used by Lachat & Watson(1976) and Watson(1982), together with the Gaussian integration.

3 . 2 . 3 Numerical results

This section shows some numerical results obtained by the present formulation. In the figures to follow, the lines indicate solutions from references and symbols stand for BIEM solutions.

1) Square crack

We consider a square crack having side length of $2a$ subject to a plane P wave of normal incidence. The stress magnitude of the incident wave is p_0. This problem has been investigated by Itou(1980). Our analysis has used a mesh having 225 nodes. Poisson's ratio is set equal to 0.2. Fig.3.2.3.1 shows the stress intensity factor along an edge of the crack. Fig.3.2.3.2 plots the stress intensity factor at the middle of an edge vs wave number. These figures show that the accuracy of the present formulation is satisfactory.

2) Penny shaped crack

We next consider a penny shaped crack having a radius of a subject to the same incident wave as in the previous example. Among the existing investigations for this problem in literature the result by Mal(1970) seems to be reliable. Our analysis employed a 177 degree of freedom mesh (in (t,θ) plane) shown in Fig.3.2.3.3. Poisson's ratio is 1/4. Fig.3.2.3.4 gives the magnitude of the crack opening displacement vs r. Fig.3.2.3.5 displays the stress intensity factors. This example also confirms the applicability of the present method.

3 . 2 . 4 Remarks concerning the method of regularisation

The formulation developed so far is closely related to the variational formulation by Nedelec(1986). In this section, we shall attempt to simplify his idea and apply the simplified version to the collocation formulation discussed in 3.2.1. In particular, we shall discuss the regularisation in the anisotropic cases.

To begin with, we consider the static case. We readily see that there exists a stress function Φ_{pqrs} which satisfies

$$C_{abik}\frac{\partial}{\partial x_k}\frac{\partial}{\partial y_l}\Gamma_{ij}(\boldsymbol{x}-\boldsymbol{y})C_{cdjl}$$

$$= e_{aip}e_{bjq}e_{ckr}e_{dls}\frac{\partial}{\partial x_i}\frac{\partial}{\partial x_j}\frac{\partial}{\partial y_k}\frac{\partial}{\partial y_l}\Phi_{pqrs}(\boldsymbol{x}-\boldsymbol{y}) + D_{abcd}\delta(\boldsymbol{x}-\boldsymbol{y}), \qquad (3.2.4.1)$$

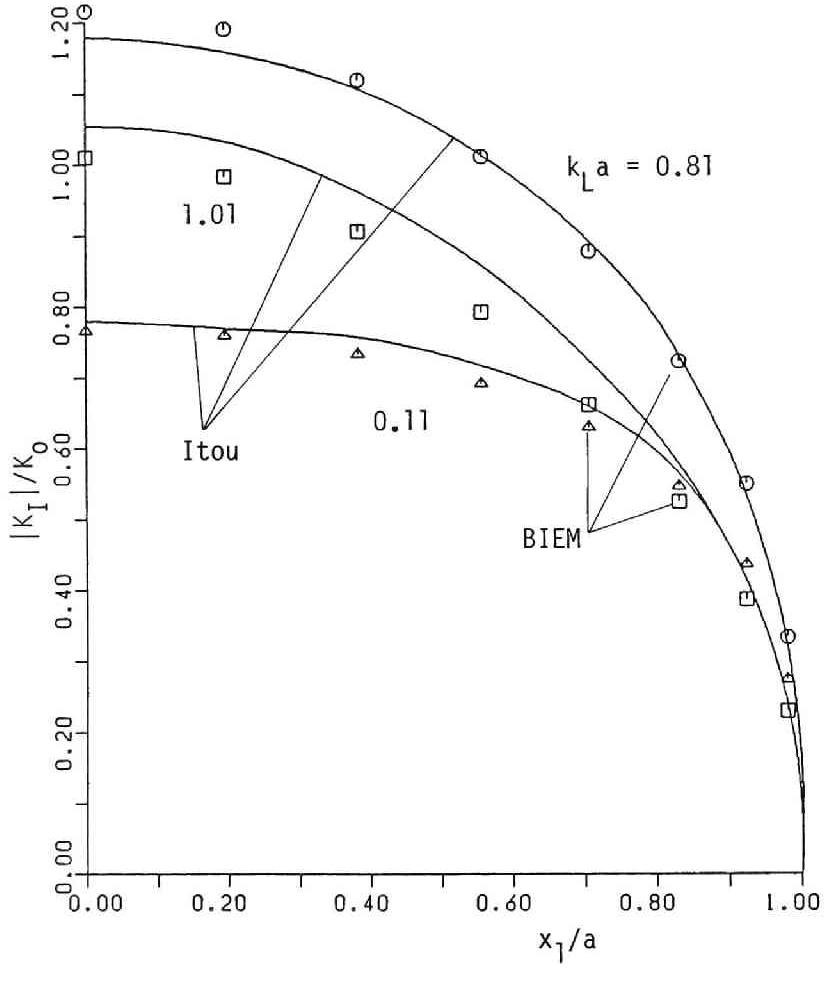

Fig.3.2.3.1 Stress intensity factor along an edge.
K_0: 2D static stress intensity factor.

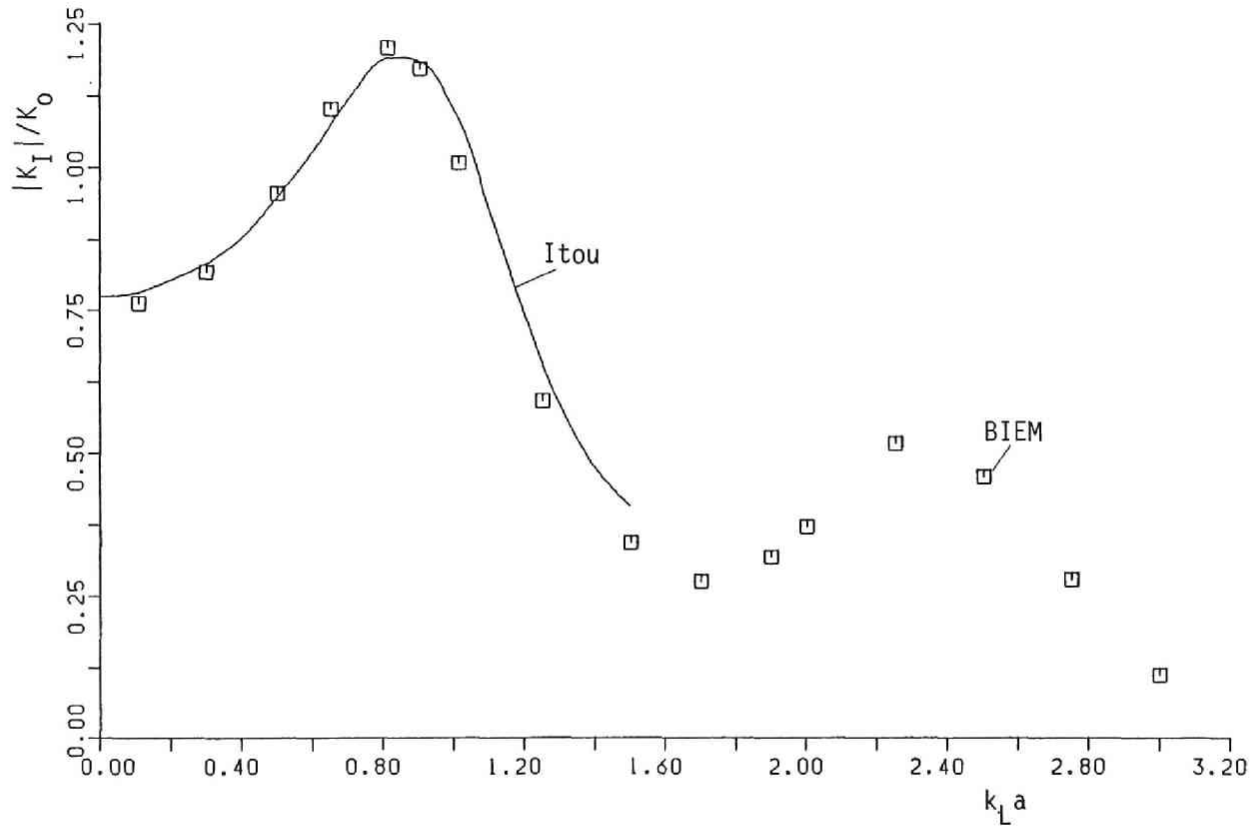

Fig.3.2.3.2 Stress intensity factor at the middle on an edge vs $k_L a$.
K_0: 2D static stress intensity factor.

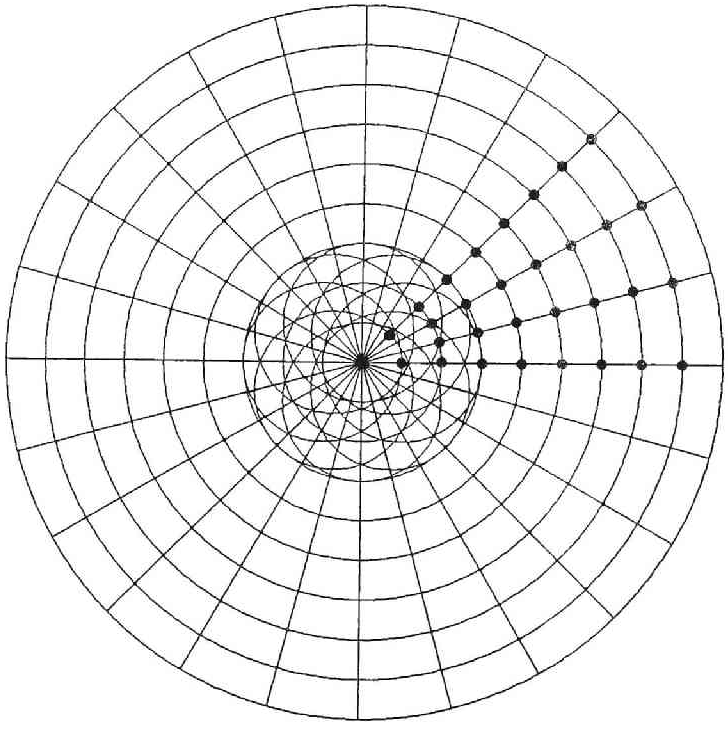

Fig.3.2.3.3 Mesh in (t,θ) plane. • : nodes.

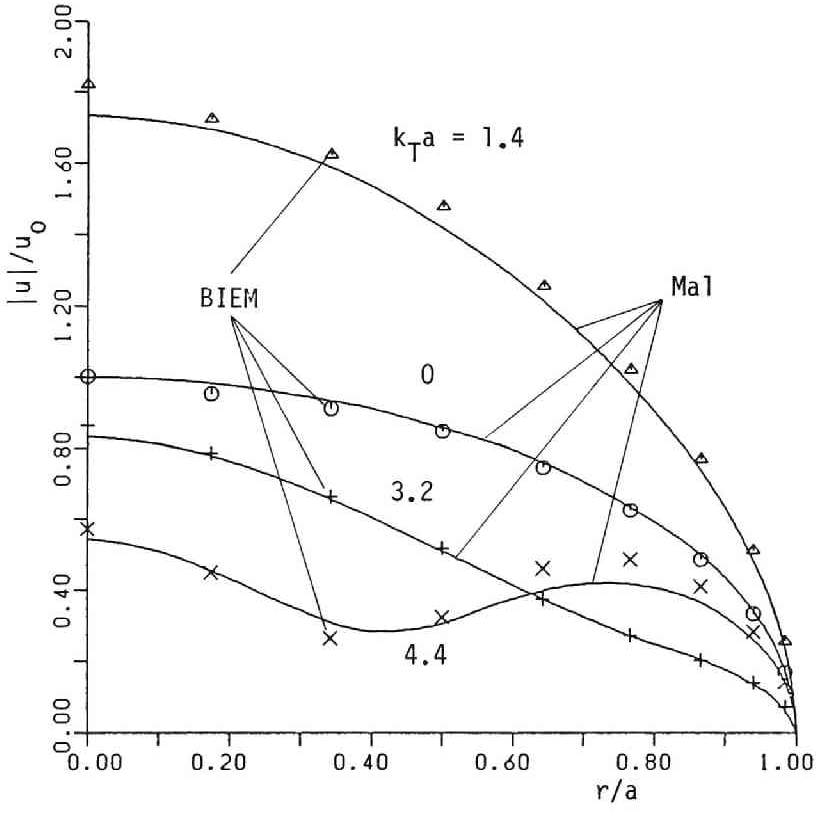

Fig.3.2.3.4 Magnitude of displacement.
u_0 : static displacement at the centre.

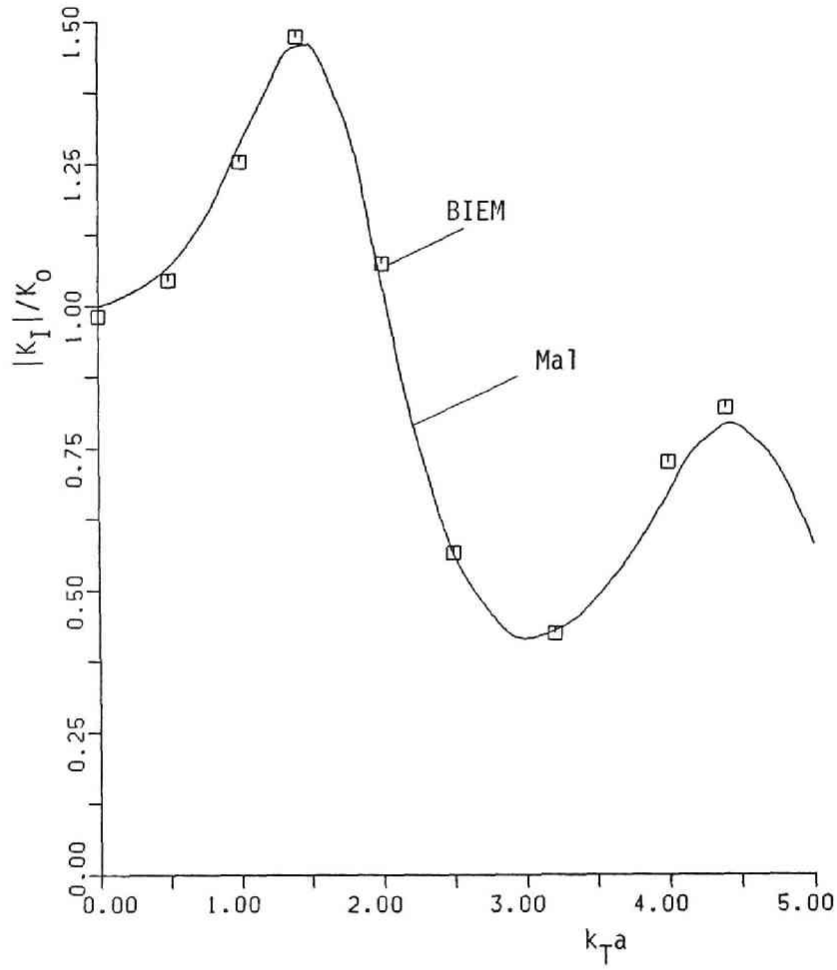

Fig.3.2.3.5 Stress intensity factor vs $k_T a$.
K_0 : static stress intensity factor.

where Γ_{ij} is the fundamental solution and D_{abcd} is a constant. Also, we may rewrite the 3D result in (3.2.4.1) into its 2D counterpart by suppressing p, q, r and s. We then use (3.2.4.1) to compute the traction of the double layer potential as follows:

$$\int_S n_b(\boldsymbol{x}) C_{abik} \frac{\partial}{\partial x_k} \frac{\partial}{\partial y_l} \Gamma_{ij}(\boldsymbol{x}-\boldsymbol{y}) C_{cdjl} n_c(\boldsymbol{y}) \varphi_d(\boldsymbol{y}) dS$$

$$= - \int_S n_b(\boldsymbol{x}) e_{aip} e_{bjq} e_{dls} \frac{\partial}{\partial x_i} \frac{\partial}{\partial x_j} \frac{\partial}{\partial y_l} \Phi_{pqrs}(n_c e_{ckr} \varphi_{d,k}) dS$$

$$= - \int_S \left(n_b(\boldsymbol{x}) - n_b(\boldsymbol{y}) \right) e_{aip} e_{bjq} e_{dls} \frac{\partial}{\partial x_i} \frac{\partial}{\partial x_j} \frac{\partial}{\partial y_l} \Phi_{pqrs}(n_c e_{ckr} \varphi_{d,k}) dS$$

$$- \text{p.f.} \int_S e_{aip} e_{dls} \frac{\partial}{\partial x_i} \frac{\partial}{\partial y_l} \Phi_{pqrs} n_b e_{bjq} \frac{\partial}{\partial y_j} (n_c e_{ckr} \varphi_{d,k}) dS, \qquad (3.2.4.2)$$

where $x \notin S$, and the normal vector $\boldsymbol{n}(x)$ is arbitrary as far as it approaches to the positive normal vector to S as x tends to a point on S. As in (3.2.1.11) the p.f. symbol is due to the singularity of $\nabla\nabla\varphi$ on ∂S. The limit of (3.2.4.2) as $x \to S$ takes exactly the same form as (3.2.4.2) because all the kernels in (3.2.4.2) are integrable. Hence we see that the regularisation of (3.2.1.5) is straightforward once one gets the stress function Φ in (3.2.4.1).

We now proceed to the computation of Φ. This calculation is made easier with the help of the Fourier transform. In 3D isotropic case the Fourier transform of

$$- C_{abik} \frac{\partial}{\partial x_k} \frac{\partial}{\partial x_l} \Gamma_{ij}(\boldsymbol{x}) C_{cdjl} \qquad (3.2.4.3)$$

is written as

$$\frac{1}{(\lambda+2\mu) |\boldsymbol{\xi}|^4} \{ \lambda^2 |\boldsymbol{\xi}|^4 \delta_{ab}\delta_{cd} + 2\lambda\mu |\boldsymbol{\xi}|^2 (\xi_a\xi_b\delta_{cd} + \xi_c\xi_d\delta_{ab})$$

$$+ \mu(\lambda+2\mu) |\boldsymbol{\xi}|^2 (\delta_{ac}\xi_b\xi_d + \delta_{bd}\xi_a\xi_c + \delta_{ad}\xi_b\xi_c + \delta_{bc}\xi_a\xi_d)$$

$$- 4\mu(\lambda+\mu)\xi_a\xi_b\xi_c\xi_d \}, \qquad (3.2.4.4)$$

where $\boldsymbol{\xi}$ is the parameter of the Fourier transform. But (3.2.4.4) is equal to

$$\frac{1}{(\lambda+2\mu) |\boldsymbol{\xi}|^4} \{ (2\lambda\mu e_{aim} e_{bjm} e_{ckn} e_{dln}$$

$$+ \mu(\lambda+2\mu)(e_{aim}e_{cjm}e_{bkn}e_{dln} + e_{aim}e_{djm}e_{bkn}e_{cln})\}\xi_i\xi_j\xi_k\xi_l \qquad (3.2.4.5)$$

modulo a constant tensor. Hence we use (3.2.4.1) and (3.2.4.5) to have

$$\Phi_{stuv} = -\frac{\mu}{8\pi(\lambda+2\mu)}\{2\lambda\delta_{st}\delta_{uv} + (\lambda+2\mu)(\delta_{su}\delta_{tv} + \delta_{sv}\delta_{tu})\}$$

$$\cdot |x-y| . \qquad (3.2.4.6)$$

We now consider the dynamic case. Since the elastodynamic counterpart of (3.2.4.4) differs from (3.2.4.4) by a function of order $1/|\xi|^2$ as $|\xi| \to \infty$, we generally have

$$C_{abik}\frac{\partial}{\partial x_k}\frac{\partial}{\partial y_l}\Gamma_{ij}(x-y)C_{cdjl}$$

$$= e_{aip}e_{bjq}e_{ckr}e_{dls}\frac{\partial}{\partial x_i}\frac{\partial}{\partial x_j}\frac{\partial}{\partial y_k}\frac{\partial}{\partial y_l}\Phi^*_{pqrs}(x-y) + \Psi^*_{abcd}(x-y)$$

$$+ D^*_{abcd}\delta(x-y) , \qquad (3.2.4.7)$$

where Φ^* is a function of order $|x-y|$ as $|x-y| \sim 0$, and Ψ^* is a function locally integrable in R^3. Of course, Γ_{ij} in (3.2.4.7) indicates the elastodynamic fundamental solution. The functions Φ^* and Ψ^* in (3.2.4.7) are not determined uniquely. For example one may use the elastostatic Φ for Φ^*, or alternatively use the following:

$$C_{abik}\frac{\partial}{\partial x_k}\frac{\partial}{\partial y_l}\Gamma_{ij}(x-y)C_{cdjl}$$

$$\sim \frac{1}{4\pi(\lambda+\mu)}\left\{\mu k_T^2\{\lambda\delta_{ab}\delta_{cd} + \mu(\delta_{ac}\delta_{bd} + \delta_{ad}\delta_{bc})\}\left(\frac{k_T^2}{k_L^2}\frac{e^{ik_TR}}{R} - \frac{k_L^2}{k_T^2}\frac{e^{ik_LR}}{R}\right)\right.$$

$$- \{\lambda^2\delta_{ab}\delta_{cd}\delta_{st} + 2\lambda\mu(\delta_{ab}\delta_{cs}\delta_{dt} + \delta_{cd}\delta_{as}\delta_{bt})$$

$$\left. + \mu^2(\delta_{ac}\delta_{bs}\delta_{dt} + \delta_{ad}\delta_{bs}\delta_{ct} + \delta_{bd}\delta_{as}\delta_{ct} + \delta_{bc}\delta_{as}\delta_{dt})\}\right.$$

$$\frac{\partial}{\partial x_s}\frac{\partial}{\partial y_t}\left(\frac{e^{ik_TR}}{R} - \frac{e^{ik_LR}}{R}\right)$$

$$- \frac{\mu}{k_T^2}\{2\lambda\delta_{pq}\delta_{rs} + (\lambda+2\mu)(\delta_{pr}\delta_{qs} + \delta_{ps}\delta_{qr})\}$$

$$e_{aip}e_{bjq}e_{ckr}e_{dls}\frac{\partial}{\partial x_i}\frac{\partial}{\partial x_j}\frac{\partial}{\partial y_k}\frac{\partial}{\partial y_l}\left(\frac{e^{ik_s R}}{R} - \frac{e^{ik_c R}}{R}\right)\Big\}, \qquad (3.2.4.8)$$

where $R=|x-y|$, and $\sim$ indicates an equality modulo Dirac's delta. The first 4 lines on the RHS of (3.2.4.8) are identified as Ψ^*_{abcd}. It is now a simple matter to regularise the traction of the elastodynamic double layer potential. Indeed, we have

$$\int_S n_b(x)C_{abik}\frac{\partial}{\partial x_k}\frac{\partial}{\partial y_l}\Gamma_{ij}(x-y)C_{cdjl}n_c(y)\varphi_d(y)dS$$

$$= -\int_S \big(n_b(x) - n_b(y)\big)e_{aip}e_{bjq}e_{dls}\frac{\partial}{\partial x_i}\frac{\partial}{\partial x_j}\frac{\partial}{\partial y_l}\Phi^*_{pqrs}(n_c e_{ckr}\varphi_{d,k})dS$$

$$- \text{p.f.}\int_S e_{aip}e_{dls}\frac{\partial}{\partial x_i}\frac{\partial}{\partial y_l}\Phi^*_{pqrs}n_b e_{bjq}\frac{\partial}{\partial y_j}(n_c e_{ckr}\varphi_{d,k})dS$$

$$+ \int_S n_b(x)\Psi^*_{abcd}n_c(y)\varphi_d dS. \qquad (3.2.4.9)$$

Equation (3.2.4.8) is similar (but not identical) to the expression used by Nedelec(1986), whose calculation is less intuitive.

The same idea applied to 2D yields

$$\mathfrak{F}\Big(-C_{abik}\frac{\partial}{\partial x_k}\frac{\partial}{\partial x_l}\Gamma_{ij}C_{jlcd}\Big)$$

$$= -\frac{e_{ai}e_{bj}e_{ck}e_{dl}\xi_i\xi_j\xi_k\xi_l}{2J_0}\ \det C \qquad (3.2.4.10)$$

for the static case and

$$\mathfrak{F}\Big(-C_{abik}\frac{\partial}{\partial x_k}\frac{\partial}{\partial x_l}\Gamma_{ij}C_{jlcd}\Big)$$

$$= \Big[-\frac{1}{2}e_{ai}e_{bj}e_{ck}e_{dl}\xi_i\xi_j\xi_k\xi_l\det C$$

$$+ \rho\omega^2(C_{abcd}C_{ijil} - C_{ijab}C_{ilcd})\xi_j\xi_l - \rho^2\omega^4 C_{abcd}\Big]/J \qquad (3.2.4.11)$$

for the dynamic case, where

$$J_0 = \frac{1}{2} C_{ijkl}\xi_j\xi_l C_{pqrs}\xi_q\xi_s e_{ip}e_{kr},$$

$$J = J_0 - \rho\omega^2 C_{ijil}\xi_j\xi_l + \rho^2\omega^4,$$

$$\det C = 2(C_{1111}C_{2222}C_{1212} + 2C_{1122}C_{1222}C_{1112}$$

$$- C_{1112}^2 C_{2222} - C_{1122}^2 C_{1212} - C_{1222}^2 C_{1111}). \qquad (3.2.4.12a\text{-}c)$$

Equations (3.2.4.10) and (3.2.4.11) are valid for the fully anisotropic case. The Fourier inversion of (3.2.4.10) for the static case can be carried out explicitly if the material is orthotropic. The dynamic counterpart, however, is possible only in the time domain.

Finally we remark that the Nedelec type formulation is indispensable in the anisotropic case, but it regularises the traction only. The formulation in 3.2.1-3, on the other hand, is restricted to isotropic case, but regularises all the stress components on S.

3 . 3 Simple layer potential method for domains having external corners

In this section we develop a simple layer potential method for Neumann problem for 2D Helmholtz's equation for domains having external corners. Our method solves those problems in which the solutions are analytic at the corners. As has been pointed out, however, the density function will then have singularity at the corners. We here incorporate into the analysis the effect of this singularity by using 'eigenfunctions'. Also, we solve some sample problems to test our approach.

We finally remark that our method can easily be extended to other problems of interest such as Laplace's equation, elasticity, etc.

3 . 3 . 1 Formulation

Let D be a domain in R^2 having a piecewise smooth boundary ∂D. Also, let the corners of ∂D, denoted by x_c^i,* $1 \leqq i \leqq n_c$ (n_c : number of corners), be external, or the vertex angle α^i (Fig.3.3.1.1) be less than π.

We shall now find a scalar field $u(\boldsymbol{x})$ in D which satisfies the Helmholtz equation

$$(\triangle + k^2)u(\boldsymbol{x}) = 0 , \qquad \boldsymbol{x} \in D \tag{3.3.1.1}$$

and the Neumann boundary condition

$$\frac{\partial u}{\partial n}(\boldsymbol{x}) = f(\boldsymbol{x}) , \qquad \boldsymbol{x} \in \partial D \tag{3.3.1.2}$$

where k is a constant named wave number, $\boldsymbol{n}$ is an external unit normal vector to ∂D, and f is a given function on ∂D. We assume that $f(\boldsymbol{x})$ is sufficiently smooth except at corners, and that $f(\boldsymbol{x})$ has definite limiting values from both sides on ∂D at the corners. We further assume that u is analytic there. This assumption is not a too stringent restriction since many solutions of practical interest indeed satisfy this.

We now seek a solution of this problem in the form of simple layer potential, i.e.,

$$u(\boldsymbol{x}) = \int_{\partial D} \Gamma(\boldsymbol{x},\boldsymbol{y})\varphi(\boldsymbol{y})\mathrm{d}S_y , \tag{3.3.1.3}$$

where φ is the simple layer density and Γ is the fundamental solution

---

* In the rest of this chapter we use superscripts exclusively as the indices for the corner points. However, we sometimes omit the superscripts in order to simplify the notation.

$$\Gamma(x,y) = \frac{i}{4} H_0^{(1)}(k|x-y|) , \qquad (3.3.1.4)$$

with $H_0^{(1)}$ being the Hankel function of the first kind and zeroth order. Equations (3.3.1.2) and (3.3.1.3) yield an integral equation

$$f(x) = \frac{\varphi(x)}{2} + \int_{\partial D} \frac{\partial}{\partial n_x}\Gamma(x,y)\varphi(y)dS_y , \quad x \in \partial D \setminus \cup_i \{x_c^i\} \qquad (3.3.1.5)$$

for x which is not on the corner.

We are now interested in the behaviour of φ near x_c.* To investigate this, we first assume that we already know the exact solution φ. Then the function $v(x)$ defined by

$$v(x) = \int_{\partial D} \Gamma(x,y)\varphi(y)dS_y , \qquad x \in R^2$$

satisfies

$$v(x) = u(x) , \qquad x \in D \qquad (3.3.1.7)$$

by assumption. It is necessary for us to know the structure of $v(x)$ in $U \cap D_e$ for the ensuing considerations, where D_e is a domain exterior to D, and U is a small neighborhood of x_c. To study this, we remember that $u(x)$ allows an analytical continuation to $U \cap D_e$ as has been assumed. Also, we know that $v(x)$ is continuous in R^2. We therefore see that $v(x)$ can be written as

$$v(x) = u^*(x) - w(x) , \quad x \in U \cap D_e \qquad (3.3.1.8)$$

where u^* is the continuation of u, and w is a function satisfying

$$(\triangle + k^2)w(x) = 0 , \qquad x \in U \cap D_e \qquad (3.3.1.9)$$

and

$$w^+(x) = 0. \qquad x \in \partial D \cap U \qquad (3.3.1.10)$$

From (3.3.1.7) and (3.3.1.8), and a well-known property on the jump of the normal derivative of the simple layer potential, we get

$$\varphi(x) = \frac{\partial v^-}{\partial n}(x) - \frac{\partial v^+}{\partial n}(x) = \frac{\partial w^+}{\partial n}(x) , \quad x \in \partial D \cap U \setminus \{x_c\} \qquad (3.3.1.11)$$

where we have used

---

* See the previous foot note.

$$\frac{\partial u^{*+}}{\partial n}(x) = \frac{\partial u^{-}}{\partial n}(x) \ . \qquad x \in \partial D \cap U \tag{3.3.1.12}$$

Our next step is to obtain an explicit formula for w. To this end, we introduce the following set of 'eigenfunctions'

$$\psi_j(x) = J_{j\pi/\beta}(kr)\sin\frac{j\pi\theta}{\beta} \ , \qquad \beta = 2\pi - \alpha \ ,$$

$$j = 1,2,\ldots\ldots, \tag{3.3.1.13}$$

which satisfy the Helmholtz equation and the boundary conditions

$$\psi_j|_{\theta=0} = \psi_j|_{\theta=\beta} = 0 \ , \qquad j = 1,2,\ldots\ldots, \tag{3.3.1.14}$$

where $J_{\cdot}(\ \cdot\ )$ is the Bessel function, θ is the angle measured from one of the tangents at x_c, and $r = |x - x_c|$, respectively (Fig.3.3.1.1). We may therefore infer, from (3.3.1.10), that $w(x)$ has an expansion

$$w(x) = \sum_{j=1}^{\infty} A_j \psi_j(x) \tag{3.3.1.15}$$

in the immediate vicinity of x_c, where A_j's are complex constants. Equation (3.3.1.15), together with (3.3.1.11), yields

$$\varphi(x) = A_1 \frac{\partial}{\partial n}\psi_1(x) + \sum_{j=2}^{\infty} A_j \frac{\partial}{\partial n}\psi_j(x) \ . \tag{3.3.1.16}$$

We note that the first term in (3.3.1.16) is estimated as

$$\frac{\partial}{\partial n}\psi_1^{+} = O(r^{-(1-\pi/\beta)}) \qquad (0 < 1 - \frac{\pi}{\beta} < \frac{1}{2}) \quad \text{as } r \to 0 \ , \tag{3.3.1.17}$$

thus giving rise to a singularity in $\varphi(x)$. Also, we see that the second term in the same equation is of order

$$O(r^{(2\pi/\beta-1)}) \qquad (0 < \frac{2\pi}{\beta} - 1 < 1) \tag{3.3.1.18}$$

as $r \to 0$. We thus conclude that φ admits the following decomposition:

$$\varphi(x) = \sum_{i=1}^{n_c} C^i \varphi_S^i(x) + \varphi_R(x) \ . \qquad (C^i : \text{const.}) \tag{3.3.1.19}$$

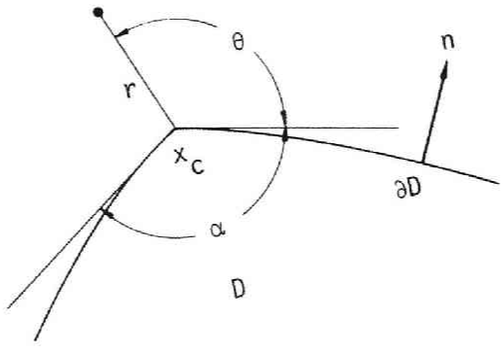

Fig.3.3.1.1 Corner; notation.

In (3.3.1.19), $\varphi_S^i(x)$ denotes a function which has the same singularity as $\partial\psi^i/\partial n(x)$ at x_c^i and whose support is in a neighborhood U^i of x_c^i. Also, $\varphi_R(x)$ indicates a function which vanishes at the corners, the order of magnitude there being as given in (3.3.1.18).

We here have localised the function $\varphi_S^i(x)$ to U^i in order to avoid possible trouble caused by the multi-valuedness of $\partial\psi^i/\partial n(x)$ when D is multiply connected. This modification for $\partial\psi^i/\partial n$ also helps us to simplify the structure of numerical equations to be solved.

Finally, we have

$$g(x_c) = \lim_{x(\in D)\to x_c} \int_{\partial D} \frac{\partial}{\partial N_x}\Gamma(x,y)\varphi(y)\mathrm{d}S_y \qquad (3.3.1.20)$$

as an 'integral' equation at corners, where N is an arbitrary unit vector. The quantity g on the left hand side of (3.3.1.20) stands for

$$g(x_c) := \frac{\partial u}{\partial N}(x_c) = N\cdot(\nu_l f_l(x_c) + \nu_r f_r(x_c)) \ , \qquad (3.3.1.21)$$

where the suffix l (r) indicates the limiting value at x_c from the left (right) side of ∂D (Fig.3.3.1.2), and ν_l and ν_r denote the vectors reciprocal to n_l and n_r ($\nu_l\cdot n_r = \nu_r\cdot n_l = 0$, $\nu_l\cdot n_l = \nu_r\cdot n_r = 1$), respectively.

3 . 3 . 2 Numerical procedure

In this section we outline our numerical procedure for the formulation given in the previous section.

We first model ∂D by using appropriate boundary elements. Of course, we have to make sure that all the corners x_c^i coincide with one of nodal points of boundary elements. It is desirable that the modelled boundary does not have corners other than x_c^i (see 3.4). We then discretise φ_R, rather than φ, by using shape functions associated with boundary elements. We use piecewise polynomial shape functions of order greater than 1 (i.e. at least piecewise linear) for φ_R. This choice makes it possible to put φ_R=0 at x_c^i. Because of this constraint, the number of unknowns arising from φ_R is $n_n - n_c$, where n_n is the number of nodal points. However, we have n_c more unknowns C^i in (3.3.1.19) in addition to φ_R. Hence the total number of unknowns amounts to n_n.

In order to determine these unknowns, we solve the discretised version of integral equations obtained from (3.3.1.5) and (3.3.1.20) by using the collocation. As usual, we use the nodal points as collocation points. Keeping in mind the decomposition of φ in (3.3.1.19), we obtain

$$t(x_i) = \frac{\varphi_R(x_i)}{2} + \sum_j \int_{\partial D} \frac{\partial}{\partial n_x}\Gamma(x_i,y)\Omega_j(y)\mathrm{d}S_y\varphi_R(x_j)$$

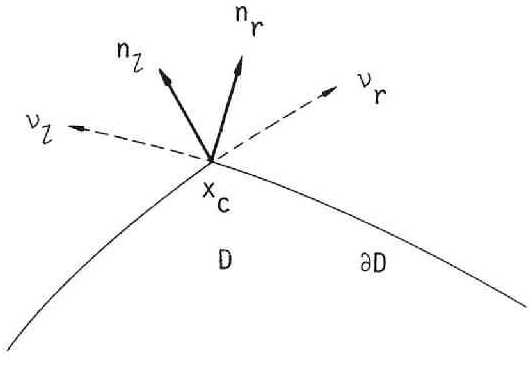

Fig.3.3.1.2 Normals at the corner.

$$+ \sum_k \int_{\partial D} \frac{\partial}{\partial n_x} \Gamma(\boldsymbol{x}_i, \boldsymbol{y}) \varphi_S^k(\boldsymbol{y}) \mathrm{d}S_y \; C^k \quad , \tag{3.3.2.1}$$

and

$$g(\boldsymbol{x}_c^i) = \sum_j \int_{\partial D} \frac{\partial}{\partial N_x} \Gamma(\boldsymbol{x}_c^i, \boldsymbol{y}) \Omega_j(\boldsymbol{y}) \mathrm{d}S_y \varphi_R(\boldsymbol{x}_j)$$

$$+ \lim_{x \to x_c^i} \sum_k \int_{\partial D} \frac{\partial}{\partial N_x} \Gamma(\boldsymbol{x}, \boldsymbol{y}) \varphi_S^k(\boldsymbol{y}) \mathrm{d}S_y \; C^k \quad , \tag{3.3.2.2}$$

provided $\varphi_S^i(\boldsymbol{x})$'s are chosen such that $\varphi_S^i(\boldsymbol{x}_j) = 0$ for any i and j, where $\boldsymbol{x}_j$'s are non-corner nodal points, and Ω_j's are shape functions corresponding to $\boldsymbol{x}_j$, respectively. We readily see that the integrals in (3.3.2.1) and (3.3.2.2) involving Ω_j can be evaluated by using any standard quadrature formula, since the integrands have no singularity.

Before discussing other integrals, we shall describe our choice for $\varphi_S(\boldsymbol{x})$. Let $\boldsymbol{x}_i$ and $\boldsymbol{x}_j$ be two non-corner nodal points adjacent to $\boldsymbol{x}_c$. We put (see Fig.3.3.2.1)

$$\varphi_S(\boldsymbol{x})$$

$$= \begin{cases} \partial\psi_1/\partial n(\boldsymbol{x}) - \Omega_i(\boldsymbol{x}) \partial\psi_1/\partial n(\boldsymbol{x}_i) - \Omega_j(\boldsymbol{x}) \partial\psi_1/\partial n(\boldsymbol{x}_j), \\ \qquad\qquad \boldsymbol{x} \in \{\boldsymbol{x}_i - \boldsymbol{x}_c - \boldsymbol{x}_j\} \\ 0, \qquad\qquad \boldsymbol{x} \in \partial D \setminus \{\boldsymbol{x}_i - \boldsymbol{x}_c - \boldsymbol{x}_j\} \end{cases} \tag{3.3.2.3}$$

where $\{\boldsymbol{x}_i - \boldsymbol{x}_c - \boldsymbol{x}_j\}$ indicates the portion of boundary between $\boldsymbol{x}_i$ and $\boldsymbol{x}_j$ via $\boldsymbol{x}_c$. This choice (essentially due to Watson(1982)) is easily seen to satisfy the requirements for $\varphi_S(\boldsymbol{x})$ stated in the preceding section. Having determined $\varphi_S(\boldsymbol{x})$, we can calculate those integrals in (3.3.2.1) and (3.3.2.2) involving φ_S by introducing an auxiliary contour, as we shall see. We take the second integral in (3.3.2.2) for example. We readily see from (3.3.2.3) that this integral is written as

$$\lim_{x(\in D) \to x_c} \int_{\Gamma_2} \frac{\partial}{\partial N_x} \Gamma(\boldsymbol{x}, \boldsymbol{y}) \; \frac{\partial \psi_1}{\partial n}(\boldsymbol{y}) \mathrm{d}S_y$$

$$+ \left[\begin{array}{l} \text{Integrals whose integrands} \\ \text{do not have singularities} \end{array} \right], \tag{3.3.2.4}$$

where Γ_2 is the part of ∂D shown in Fig.3.3.2.2. To evaluate the first integral we note the relation

$$0 = \frac{\partial}{\partial N_x} \int_{\Gamma_1 + \Gamma_2} \left(\Gamma(\boldsymbol{x}, \boldsymbol{y}) \frac{\partial \psi_1}{\partial n}(\boldsymbol{y}) - \frac{\partial \Gamma}{\partial n_y}(\boldsymbol{x}, \boldsymbol{y}) \psi_1(\boldsymbol{y}) \right) \mathrm{d}S_y \quad , \quad \boldsymbol{x} \in D \tag{3.3.2.5}$$

where Γ_1 is an auxiliary contour in D_e (Fig.3.3.2.2). From the above

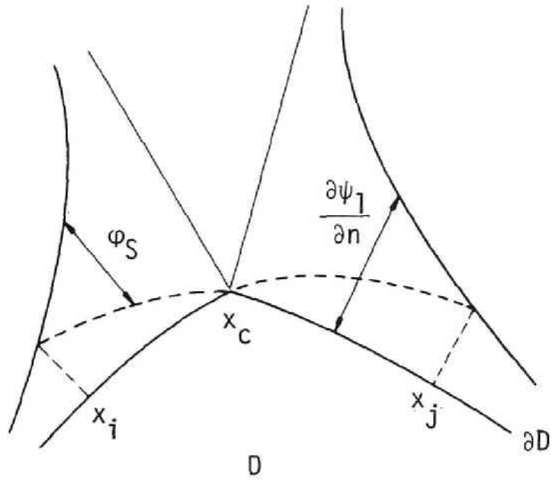

Fig.3.3.2.1 Singular function at the corner.

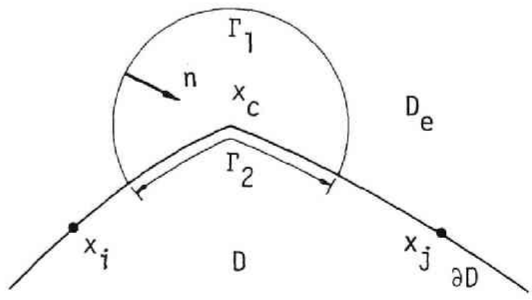

Fig.3.3.2.2 Auxiliary contour.

formula follows

$$\lim_{x(\in D)\to x_c} \int_{\Gamma_2} \frac{\partial}{\partial N_x}\Gamma(x,y)\ \frac{\partial \psi_1}{\partial n}(y)\mathrm{d}S_y$$

$$= -\ \{ \int_{\Gamma_1} \frac{\partial}{\partial N_x}\Gamma(x_c,y)\ \frac{\partial \psi_1}{\partial n}(y)\mathrm{d}S_y - \int_{\Gamma_1} \frac{\partial}{\partial N_x}\ \frac{\partial}{\partial n_y}\Gamma(x_c,y)\ \psi_1(y)\mathrm{d}S_y\}$$

$$+ \int_{\Gamma_2} \frac{\partial}{\partial N_x}\ \frac{\partial}{\partial n_y}\Gamma(x_c,y)\ \psi_1(y)\mathrm{d}S_y\ . \qquad (3.3.2.6)$$

Since $\psi_1 \sim O(r^{1+\pi/\beta})$ near x_c as long as the curvature of ∂D is finite, the last integral on the right hand side of the above expression is integrable; the order of magnitude at x_c of the integrand is $O(r^{-(1-\pi/\beta)})$ with $0 < 1-\pi/\beta < 1/2$. We can therefore calculate this integral numerically by introducing a new variable of integration s behaving as $s \sim r^{\pi/\beta}$ near x_c (Watson(1982)). In particular, this integral vanishes when Γ_2 is piecewise linear because we would then have $\psi_1(x) = 0$ on Γ_2. The numerical computation of other two integrals on the right hand side of the above formula is not difficult. The remaining integral in (3.3.2.1) can also be estimated either by coordinate transformation or by introducing an auxiliary contour.

We can thus evaluate all the integrals needed for numerical analyses accurately.

3 . 3 . 3 Examples

We tested the formulation proposed above through a simple example. We chose a square having sides of length $2a$ as the domain D (Fig.3.3.3.1). As the Neumann data, we gave

$$f(x) = \frac{\partial}{\partial n}J_0(k|x|)\ , \qquad (3.3.3.1)$$

where we took the origin of the coordinate at the centre of D. Of course the exact solution to this problem is

$$u(x) = J_0(k|x|)\ . \qquad (3.3.3.2)$$

We used piecewise linear isoparametric boundary elements of equal length with 8 point Gaussian integration formula. The vector N (see (3.3.1.20)) for each corner is taken in the direction bisecting the adjacent normals.

Fig.3.3.3.2 compares the BIE solutions (symbols) for u on one of the sides (Due to the symmetry of the problem the solutions on all the sides are identical.) with analytical solutions (lines). Figs. 3.3.3.2(a) and (b) show the results of analyses for ka = 1, 2, 3, 4 obtained by using 40 elements, and ka = 1, 2 with 16 elements (It

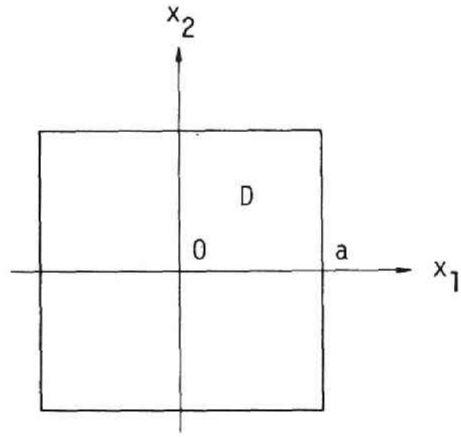

Fig.3.3.3.1 Domain for a sample problem.

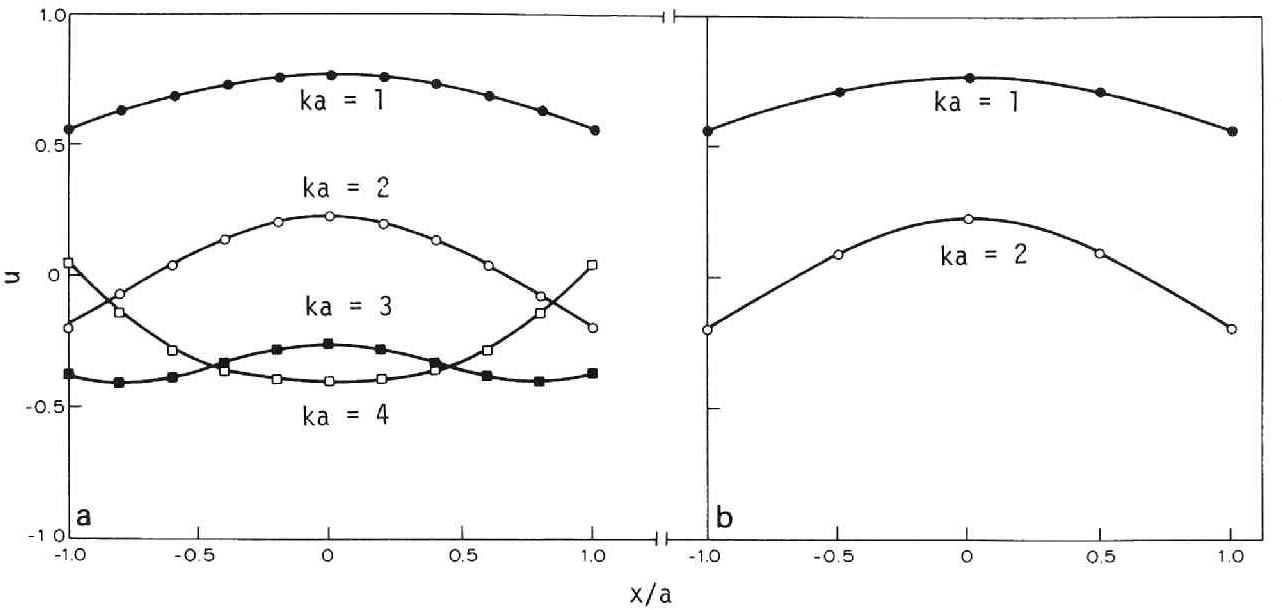

Fig.3.3.3.2 u on a side of square. symbols: BIE, lines: exact
(a) 40 elements, (b) 16 elements.

would be meaningless to attempt at analyses for larger k by using 16 element model.), respectively. These results show the good accuracy of the present method. We used FACOM M382 of the Data Processing Centre of Kyoto University for the computation.

3 . 4 Concluding remarks

a) As has been stated in Chapter 1, Arnold & Wendland(1982) concludes that the collocation method is more effective than Galerkin's method for BIEM in problems without having singularities. The results in 3.1, however, show that Galerkin's method is convenient for crack problems. Nedelec(1986) also concluded to this effect. Besides, Nishimura(1979) found that a collocation method using the conventional double layer potential formulation can sometimes be led to a numerical instability in elastic crack problems. Weaver(1977), however, used successfully a collocation BIEM with an analogue of (3.2.1.6) in 3D elastostatic crack problems. The same conclusion was obtained by Takakuda et al.(1985), who used a elastostatic version of (3.2.1.5), by Polch et al.(1987) who proposed a modification of Weaver's method, and by the present author as we have seen in 3.2 (see Kaneko(1987) for more numerical results). We therefore have two choice in crack analysis: use Galerkin method with a relatively simple base functions (C^0 is admissible) or use collocation with C^1 base functions. Obviously the former is easier to implement in problems including cracks of arbitrary shapes. However, the double integration in the Galerkin scheme requires more CPU time than the collocation, even after counting the symmetry of the resulting matrix. Actually Nedelec estimates the CPU time of the Galerkin's method to be about 10% more than that of collocation (Nedelec(1986)). On the other hand the requirement of C^1 continuity for base functions makes the collocation method extremely complicated in 3D problems.

In 2D cases the collocation method is considered to be preferable because it is not difficult to generate C^1 base functions in this case. As discussed in 3.1, however, a Galerkin method is still worthwhile in 2D when the double integrals included in the expressions for the coefficient matrix allow a fast numerical evaluation. In 3D the present author prefers the collocation because one seldom has to consider a 3D crack having a complicated geometry in engineering practice. If one really needs to analyse a crack with a complicated geometry, Galerkin's method would be his choice. As far as the present author knows, however, nobody other than Matsumoto(1986) has ever used Galerkin's method in 3D numerical crack analyses.

b) As has been pointed out, the C^1 base functions in 3.2 have been devised in order not to introduce non-physical singularities into the numerical solutions. Also, the method proposed 3.3 is viewed as a technique of eliminating singularities in ∇u at corners. In the present author's opinion, it is important to seek BIE formulations which do not introduce unfavourable singularities into the solution when one wishes to have an extremely accurate numerical method of analysis. This is true not only in crack problems but in any BIEM.

The usual direct BIE's for Laplace's equation, Helmholtz's

equation, elastostatics, etc., for example, necessarily bring about logarithmic singularity in the first derivatives of the solutions at nodal points unless the (tangential) derivatives of double layer densities are continuous. This is because these BIEs include the double layer potentials. One would therefore have to use C^1 base functions such as spline or Hermitian functions in order to calculate these derivatives accurately. Indeed, the logarithmic singularities would pollute the solution otherwise. From this point of view, piecewise linear elements are acceptable in the simple layer potential method for Laplace's equation (or Helmholtz's equation) provided that one uses a smooth boundary modeling except at corners. In this respect the method of Athanasiadis(1980) using quadratic shape function for density and Hermitian polynomials for boundary shapes is appropriate.

Finally, we remark that Chaudonneret's compatibility conditions (Chaudonneret(1978)) to be satisfied by displacements and tractions at a corner of elastic body can also be regarded as a special case of the condition of vanishing stress singularity in the direct BIE.

c) The idea of introducing auxiliary contours for the evaluation of singular integrals (see 3.3.2.) is due to Watson(1982). He used Hermitian boundary elements, and succeeded in obtaining highly accurate numerical results with small numbers of boundary elements in the problems of 2D linear elastostatics. It is, however, almost hopeless to extend his method to 3D.

d) Mixed boundary value problem is another typical case where the solution includes singularities. Indeed, the solution usually shows singularities at the boundary points where the types of boundary conditions change. For applications of BIEM to problems of this kind the reader is referred to the papers by Wendland et al.(1979) and Kawakami(1983), etc.

e) One may carry out the crack analysis presented in Part II in time domain also. Some attempts at crack analyses in time domain are found in Nishimura, Guo & Kobayashi(1987), in Nishimura, Kobayashi & Okada(1987) and in Das & Kostrov(1987).

f) The 1st, 2nd and the 3rd parts of this chapter are taken from Nishimura & Kobayashi(1984), Nishimura & Kobayashi(1987) and Kobayashi et al.(1984), respectively.

References

Arnold, D.N. & Wendland, W.L.(1982). Collocation versus Galerkin procedures for boundary integral methods, *Proc. 4th Int. Seminar BEM*, pp 18-33, Springer.

Athanasiadis, G.(1980). Torsion prismatischer Stäbe nach der Singularitäten Methode, *Ing. Arch.*, vol.49, pp 89-96.

Chaudonneret, M.(1978). On the discontinuity of the stress vector in the boundary integral equation method for elastic analysis, in:

Recent Advances in Boundary Element Methods (Ed. C.A..Brebbia), pp 185-94. Pentech Press.

Das, S. & Kostrov, B.V.(1987). On the numerical boundary integral equation method for three-dimensional dynamic shear crack problems, *J. Appl. Mech.*, vol.54, pp 99-104.

Hartmann, F.(1982). The physical nature of elastic layers, *J. Elasticity*, vol.12, pp 19-29.

Hult, J.A. & McClintock, F.A.(1956). Elastic-plastic stress and strain distributions around sharp notches under repeated shear, *Proc. 9th Int. Congr. Appl. Mech.*, Brussels, vol.8, pp 51-8.

Itou, S.(1980). Dynamic stress concentration around a rectangular crack in an infinite elastic medium, *ZAMM*, vol.60, pp 381-388.

Kaneko, M.(1987). A 3D dynamic crack analysis by the boundary integral equation method, M. Eng. thesis, Kyoto Univ. (in Japanese).

Kawakami, T.(1983). Considerations on the singularity in BIE for wave equations, B.Eng. thesis, Kyoto Univ.(in Japanese).

Kobayashi, S., Nishimura, N. & Kawakami, T.(1984). Simple layer potential method for domains having external corners, *Appl. Math. Modelling*, vol.8, pp 61-65.

Kupradze, V.D., Gegelia, T.G., Basheleishvili, M.O. & Burchuladze, T.V.(1979). *Three-Dimensional Problems of the Mathematical Theory of Elasticity and Thermoelasticity*, North-Holland.

Lachat, J.C. & Watson, J.O.(1976). Effective numerical treatment of boundary integral equations, *Int. J. Num. Meth. Eng.*, vol.10, pp 991-1005.

Mal, A.K.(1970). Interaction of elastic waves with a penny-shaped crack, *Int. J. Eng. Sci.*, vol.8, pp 381-388.

Matsumoto, K.(1986). A three-dimensional analysis of a cylindrical crack by BIEM, B. Eng. thesis, Kyoto Univ.(in Japanese)

Nedelec, J.C.(1986). The double layer potential for periodic elastic waves in R^3, *Proc. Int. Conf. on BEM, Beijing, China* (Ed. Du Q.), pp 439-448, Pergamon Pr.

Nishimura, N.(1979). Elastoplastic analysis by the integral equation method, M. Eng. thesis, Kyoto Univ.(in Japanese)

Nishimura, N., Guo, Q.C., & Kobayashi, S.(1987). Boundary integral equation methods in crack problems, *Proc. 9th Int. Conf. BEM, Vol. 2, Stress Analysis Applications* (Eds. C.A. Brebbia & W.L. Wendland), pp 279-291, Springer.

Nishimura, N. & Kobayashi, S.(1984). Elastoplastic analysis by indirect methods, In: *Developments in Boundary Element Methods - III* (Eds. P.K.Banerjee & S.Mukherjee), Appl. Sci. Publ.

Nishimura, N. & Kobayashi, S.(1987). An improved boundary integral equation method for crack problems, *Proc. IUTAM Symposium on Advanced Boundary Element Methods* (Ed. T.A. Cruse), to appear

Nishimura, N., Kobayashi, S. & Okada, M.(1987). A time domain BIE crack analysis, *Proc. 1st Japan China Symp. on Boundary Element Methods* (Eds. M. Tanaka & . Du), pp 85-94, Pergamon.

Polch, E.Z., Cruse, T.A. & Huang, C.-J.(1987). Traction BIE solutions for flat cracks, *Computational Mech.*, to appear.

Rice, J.R.(1968). Mathematical analysis in the mechanics of fracture, In: *Fracture* II (Ed. H.Liebowitz), pp 191-311, Academic Pr.

Sladek, V. & Sladek, J.(1984). Transient elastodynamic three dimensional problems in cracked bodies, *Appl. Math. Model*, vol.8, pp 2-10.

Takakuda, K.(1985). Stress singularities near crack front edges, *Bull. JSME*, vol.28, pp 225-231.
Takakuda, K., Koizumi, T. & Shibuya, T.(1985). On integral equation methods for crack problems, *Bull. JSME*, vol.28, pp 217-224.
Watson, J.O.(1982). Hermitian boundary elements for plane problems of fracture mechanics, *Res Mech.*, vol.4, pp 23-42.
Weaver, J.(1977). Three dimensional crack analysis, *Int. J. Solids Structures*, vol.13, pp 321-330.
Wendland, W.L., Stephan, E. & Hsiao, G.C.(1979). On the integral equation method for the plane mixed boundary value problem of the Laplacian, *Math. Meth. Appl. Sci.*, vol.1, pp 265-321.

Chapter 4 Elastodynamics

4 . 0 Introduction

In this chapter, we shall discuss some applications of the BIEM to elastodynamic boundary value problems ——— a special class of hyperbolic problems. As is very often claimed the applicability to problems for infinite domains is one of the most significant features of BIEM. This advantage makes BIEM particularly promising in applications relevant to wave propagations. This is because other conventional numerical methods, such as FEM, FDM, etc., cannot deal with infinite domains directly; these methods would require the introduction of fictitious boundaries, the reflection from which could pollute the solution. In addition the existing techniques to eliminate this unfavourable reflection are not necessarily reliable (e.g. Cohen & Jennings(1983)). It is therefore worthwhile to study BIEM for elastodynamics.

There are two approaches in formulating transient elastodynamic problems (for the related topics in acoustics, the reader is referred to the review by Shaw(1979)). One is the time-domain analysis and the other is the integral transform approach. Accordingly, we have two types of BIE formulations. The former approach yields hybrid integral equations (Volterra (Fredholm) type with respect to time (space)), while the latter leads to the Fredholm integral equations and the inversion of integral transformations. The integral transform approach is further classified into subgroups according as the type of integral transformation used. In practice Fourier or Laplace transforms are favoured because they have effective numerical means of inversion. Some early numerical investigations are found in Cruse & Rizzo(1968) and Cruse(1968), where these authors have tried a Laplace transform approach, and in Niwa et al.(1980) who used a time domain BIEM.

The Fourier transform approach, which we believe to be practical, uses the Fourier transform to reduce the original hyperbolic governing equations for elastodynamics into elliptic equations. The resulting equations are identical with the equations for time-harmonic elastodynamics. One then solves this transformed problem under the transformed boundary and radiation conditions by using BIEM. Finally, one carries out the inverse transformation by synthesising the time-harmonic BIEM solutions with the help of the FFT (Fast Fourier Transform) algorithm. A BIEM approach which follows the above steps in a vague manner was used earlier by Niwa et al.(1975). However, these authors did not recognise the possible non-uniqueness of the solutions of their integral equations. Nor is it clearly addressed how they deal with incident waves having an arbitrary time dependence. In view of this we shall spend this chapter for establishing a general BIEM in elastodynamics which uses the Fourier transform approach.

The first part of this chapter deals with interior and exterior problems. We investigate a BIE formulation for time-harmonic elastodynamics paying attention to the uniqueness of the solutions. As will be seen, the conventional BIE sometimes loses the uniqueness of the solution even in exterior problems, although the uniqueness of the solution to these boundary value problems (not the solutions of integral equations) is well established. This non-uniqueness is a

source of inaccuracy because the non-uniqueness of the original integral equation leads to an ill-conditioned numerical BIE matrix, if not to a singular one. We therefore seek some techniques to overcome this difficulty. We finally give some numerical examples. The second part of this chapter discusses the application of BIEM to half-plane problems. Since the half-plane boundary is of infinite length, we cannot apply directly the BIEM techniques developed so far. We here try to truncate the infinite boundary taking into consideration only the finite part of it. An approximation, as a rule, requires justification. We therefore test this method of truncation by comparing the obtained numerical results with more accurate results computed by a modified BIEM using Green's function. The second part of this chapter ends with the conclusion that the method of truncation is sufficiently accurate, economical, and therefore practical.

Part I

4 . 1 Interior and exterior problems

4 . 1 . 1 Formulation

Let D be a domain in R^N (N = 2 or 3), which may be interior or exterior to a piecewise smooth boundary ∂D. The equation of motion for isotropic elastic body is written as

$$\triangle^* \boldsymbol{u} + \rho \boldsymbol{b} := \mu \triangle \boldsymbol{u} + (\lambda+\mu) \nabla \mathrm{div}\ \boldsymbol{u} + \rho \boldsymbol{b} = \rho \ddot{\boldsymbol{u}} \quad , \tag{4.1.1.1}$$

where $\triangle$ is the Laplacian, $\dot{}$ is the time derivative $\partial / \partial t$ (t: time), λ and μ are Lamé's constants, ρ is density, and $\rho \boldsymbol{b} = \boldsymbol{f}$ is body force, respectively.

The elastodynamic initial- boundary value problem is formulated as follows :

To find a solution $\boldsymbol{u}(\boldsymbol{x}, t)$ of (4.1.1.1) in $D \times (t > 0)$, subject to the initial conditions

$$\boldsymbol{u}(\boldsymbol{x}, 0) = \acute{\boldsymbol{u}}(\boldsymbol{x}), \quad \dot{\boldsymbol{u}}(\boldsymbol{x}, 0) = \acute{\boldsymbol{v}}(\boldsymbol{x}) \quad \text{in } D, \tag{4.1.1.2a,b}$$

boundary conditions

$$\boldsymbol{u}(\boldsymbol{x}, t) = \boldsymbol{u}_0(\boldsymbol{x}, t), \quad \text{on } \partial D_u \times (t > 0),$$

$$\mathrm{T}\boldsymbol{u}(\boldsymbol{x}, t) := \lambda \boldsymbol{n} (\mathrm{div}\ \boldsymbol{u}(\boldsymbol{x}, t)) + \mu (\nabla \boldsymbol{u}(\boldsymbol{x}, t) + (\nabla \boldsymbol{u}(\boldsymbol{x}, t))^T) \boldsymbol{n}$$

$$= \boldsymbol{t}_0(\boldsymbol{x}, t) \quad \text{on } \partial D_s \times (t > 0), \quad (\partial D_s = \partial D \backslash \partial D_u) \tag{4.1.1.3a,b}$$

and, in addition, the radiation condition for the scattered field u_S defined by

$$u_S(x,t) = u(x,t) - u_I(x,t) \qquad (4.1.1.4)$$

if D is an exterior domain. The explicit form of this condition is given as

$$\frac{\partial u_{LS}}{\partial r} + \frac{1}{c_L}\frac{\partial u_{LS}}{\partial t} = o(r^{-(N-1)/2}), \quad u_{LS} = o(r^{-(N-3)/2}),$$

$$\frac{\partial u_{SS}}{\partial r} + \frac{1}{c_T}\frac{\partial u_{SS}}{\partial t} = o(r^{-(N-1)/2}), \quad u_{SS} = o(r^{-(N-3)/2}), \qquad (4.1.1.5a\text{-}d)$$

as $r := |x| \to \infty$ (Eringen & Suhubi(1975)).

In this statement, $\acute{u}(x), \acute{v}(x), u_0(x,t), t_0(x,t)$ and $u_I(x,t)$ denote the given initial displacement, initial velocity, boundary displacement, traction and the incident field, u_{LS} and u_{SS} indicate the lamellar and solenoidal parts of the scattered field, ∂D_u (∂D_s) stands for a portion of ∂D where the displacement (traction) is given, and c_L and c_T are the velocities of the longitudinal (P) and transverse (S) waves defined by

$$c_L = \sqrt{(\lambda+2\mu)/\rho}, \qquad c_T = \sqrt{\mu/\rho}, \qquad (4.1.1.6a,b)$$

respectively. Also, in part I of this chapter the unit normal vector n to ∂D is assumed to point into the infinite domain bounded by ∂D.

In order to solve the elastodynamic initial- boundary value problem, we use the method of Fourier transform. We first consider the interior problem assuming that the body force is absent and that the displacement field is with a quiescent past (see (4.1.1.2)), i.e.,

$$\acute{u}(x) = \acute{v}(x) = 0. \qquad (4.1.1.7)$$

The Fourier transform of (4.1.1.1) with respect to t is then written as

$$\triangle^* \hat{u}(x,\omega) + \rho\omega^2 \hat{u}(x,\omega) = 0, \qquad (4.1.1.8)$$

where the symbol ($\hat{}$) denotes the Fourier transform defined as

$$\hat{\cdot} = \frac{1}{2\pi}\int_{-\infty}^{\infty} \cdot\, e^{i\omega t} dt. \qquad (4.1.1.9)$$

Also, the boundary conditions are transformed into

$$\hat{u}(x,\omega) = \hat{u}_0(x,\omega), \quad x \in \partial D_u$$

$$T\hat{u}(x,\omega) = \hat{t}_0(x,\omega), \quad x \in \partial D_s \qquad (4.1.1.10a,b)$$

After solving this transformed problem the solution to the original problem is found in the form of the Fourier integral:

$$\boldsymbol{u}(\boldsymbol{x},t) = \int_{-\infty}^{\infty} \hat{\boldsymbol{u}}(\boldsymbol{x},\omega)e^{-i\omega t}d\omega. \qquad (4.1.1.11)$$

For the exterior problem, we apply the same method to u_S defined in (4.1.1.4). In other words, we solve (4.1.1.8) (with $\boldsymbol{u}$ replaced by u_S) subject to the boundary conditions

$$\hat{\boldsymbol{u}}_S(\boldsymbol{x},\omega) = \hat{\boldsymbol{u}}_0(\boldsymbol{x},\omega) - \hat{\boldsymbol{u}}_I(\boldsymbol{x},\omega) \ , \qquad \boldsymbol{x}\in\partial D_u$$

$$T\hat{\boldsymbol{u}}_S(\boldsymbol{x},\omega) = \hat{\boldsymbol{t}}_0(\boldsymbol{x},\omega) - T\hat{\boldsymbol{u}}_I(\boldsymbol{x},\omega) \ , \qquad \boldsymbol{x}\in\partial D_s \qquad (4.1.1.12a,b)$$

and the radiation conditions

$$\frac{\partial \hat{\boldsymbol{u}}_{LS}}{\partial r} - \frac{i\omega}{c_L}\hat{\boldsymbol{u}}_{LS} = o(r^{-(N-1)/2}), \ \hat{\boldsymbol{u}}_{LS} = o(r^{-(N-3)/2}),$$

$$\frac{\partial \hat{\boldsymbol{u}}_{SS}}{\partial r} - \frac{i\omega}{c_T}\hat{\boldsymbol{u}}_{SS} = o(r^{-(N-1)/2}), \ \hat{\boldsymbol{u}}_{SS} = o(r^{-(N-3)/2}), \qquad (4.1.1.13a\text{-}d)$$

as $r\to\infty$ (Kupradze et al.(1979)). Using the solution to this transformed boundary value problem, we find the solution to the original equation in the following form :

$$\boldsymbol{u}(\boldsymbol{x},t) = \int_{-\infty}^{\infty} \hat{\boldsymbol{u}}_S(\boldsymbol{x},\omega)e^{-i\omega t}d\omega + \boldsymbol{u}_I(\boldsymbol{x},t). \qquad (4.1.1.14)$$

We next examine the solution of (4.1.1.8), i.e., the equation for time-harmonic elastodynamics. We shall write $\boldsymbol{u}(\boldsymbol{x})$ instead of $\hat{\boldsymbol{u}}(\boldsymbol{x},\omega)$ in order to simplify the notation.

We first assume that D is interior to ∂D. The argument used in 1.1 yields the potential representation for the displacement field $\boldsymbol{u}(\boldsymbol{x})$ in the following form:

$$\tilde{\boldsymbol{u}}(\boldsymbol{x}) = \int_{\partial D}\Gamma(\boldsymbol{x},\boldsymbol{y})\,\boldsymbol{t}(\boldsymbol{y})dS_y - \int_{\partial D}\Gamma_I(\boldsymbol{x},\boldsymbol{y})\boldsymbol{u}(\boldsymbol{x})dS_y,$$

$$\boldsymbol{x}\in R^N\backslash\partial D \qquad (4.1.1.15)$$

where $\Gamma(\boldsymbol{x},\boldsymbol{y})$ is the fundamental solution of (4.1.1.8) which statisfies the radiation condition, $\Gamma_I(\boldsymbol{x},\boldsymbol{y})$ is the double layer kernel defined by (1.1.14) with the elastodynamic Γ, $\boldsymbol{t}$ is the traction defined by (4.1.1.3b), $\tilde{\boldsymbol{u}}$ is defined by

$$\tilde{u} = \begin{cases} u & \text{in } D, \\ 0 & \text{in } D^c \backslash \partial D, \end{cases} \qquad (4.1.1.16)$$

and D^c indicates the domain conjugate to D with respect to R^N, respectively. Letting $x \to x_0 \in \partial D$ from D^c side in (4.1.1.15), we obtain an integral equation

$$C^e u(x_0) = \int_{\partial D} \Gamma(x_0, y)\, t(y) dS_y - \text{v.p.} \int_{\partial D} \Gamma_1(x_0, y) u(y) dS_y,$$

$$x_0 \in \partial D \qquad (4.1.1.17)$$

where $C^e u(x_0)$ is the non-integral term of the exterior limit of the double layer potential ((1.3.3.6) tells $C^e u = u/2$ if the boundary is smooth near x_0), and v.p. stands for Cauchy's principal value, respectively.

Next let D be exterior to ∂D. Using the potential representation for the scattered field u_S, and assuming that the incident field u_I is regular (without singularity) in D^c, we see that the expression

$$\tilde{u}(x) = \int_{\partial D} \Gamma_1(x, y) u(y) dS_y - \int_{\partial D} \Gamma(x, y)\, t(y) dS_y + u_I(x)$$

$$x \in R^N \backslash \partial D \qquad (4.1.1.18)$$

holds true. The integral equation for the exterior problems is obtained by letting $x \to x_0 \in \partial D$ from D^c side in (4.1.1.18). The result is

$$-C^i u(x_0) = \text{v.p.} \int_{\partial D} \Gamma_1(x_0, y) u(y) dS_y - \int_{\partial D} \Gamma(x_0, y)\, t(y) dS_y + u_I(x_0),$$

$$x_0 \in \partial D \qquad (4.1.1.19)$$

where $C^i u$ is the non-integral term of the interior limit of the double layer potential ((1.3.3.6) says $C^i u = -u/2$ on the smooth portion of ∂D).

The fundamental solutions which fulfil the radiation conditions are well known to have the following forms (Kupradze et al.(1979)):

$$\Gamma(x, y) = \frac{1}{4\pi\mu} \left[\frac{e^{ik_T R}}{R} 1 + \frac{1}{k_T^2} \nabla \otimes \nabla \left(\frac{e^{k_T R}}{R} - \frac{e^{ik_L R}}{R} \right) \right], \quad (N=3)$$

$$\Gamma(x, y) = \frac{i}{4\mu} \left[H_0^{(1)}(k_T R) 1 + \frac{1}{k_T^2} \nabla \otimes \nabla \left(H_0^{(1)}(k_T R) - H_0^{(1)}(k_L R) \right) \right],$$

$$(N=2) \qquad (4.1.1.20a,b)$$

where $R = |x - y|$, $k_{L,T}$ are the wave numbers of the longitudinal and transverse waves defined by

$$k_{L,T} = \omega/c_{L,T} , \qquad (4.1.1.21)$$

1 is the identity tensor, and $H_0^{(1)}$ is the zeroth order Hankel function of the first kind.

4 . 1 . 2 Special classes of the problem

From now on we shall consider the two special classes of problems given below:

Problem A : Exterior boundary value problem for (4.1.1.8), in which ∂D may consist of several boundaries. The solution to this problem is known to be unique. We may use (4.1.1.18) and (4.1.1.19) to solve this problem.

Problem B : Let the bodies under consideration be as shown in Fig.4.1.2.1. Also, let the normals on S and S_0 be directed outward viewed form D_0. It is required to find a displacement field $\boldsymbol{u}$ which satisfies the field equations

$$(\triangle_i^* + \rho_i\omega^2)\boldsymbol{u} := \mu_i\triangle\boldsymbol{u} + (\lambda_i+\mu_i)\nabla\mathrm{div}\ \boldsymbol{u} + \rho_i\omega^2\boldsymbol{u} = 0 \quad \text{in } D_i ,$$

$$(\triangle_e^* + \rho_e\omega^2)\boldsymbol{u} := \mu_e\triangle\boldsymbol{u} + (\lambda_e+\mu_e)\nabla\mathrm{div}\ \boldsymbol{u} + \rho_e\omega^2\boldsymbol{u} = 0$$

$$\text{in } D_e , \qquad (4.1.2.1a,b)$$

boundary conditions on S_0 :

$$\boldsymbol{u}(\boldsymbol{x}) = \boldsymbol{u}_0(\boldsymbol{x}), \quad \boldsymbol{x}\in S_{0u}$$

$$\mathrm{T}_i\boldsymbol{u}(\boldsymbol{x}) := \lambda_i(\mathrm{div}\ \boldsymbol{u})\boldsymbol{n} + \mu_i(\nabla\boldsymbol{u} + (\nabla\boldsymbol{u})^{\mathrm{T}})\boldsymbol{n} = \boldsymbol{t}_0(\boldsymbol{x}),$$

$$\boldsymbol{x}\in S_{0s} \qquad (4.1.2.2a,b)$$

continuity conditions on S :

$$\boldsymbol{u}^-(\boldsymbol{x}) = \boldsymbol{u}^+(\boldsymbol{x}), \qquad \boldsymbol{x}\in S$$

$$\mathrm{T}_i\boldsymbol{u}^-(\boldsymbol{x}) = \mathrm{T}_e\boldsymbol{u}^+(\boldsymbol{x}), \quad \boldsymbol{x}\in S \qquad (4.1.2.3a,b)$$

and the radiation condition, given in (4.1.1.13), for the scattered

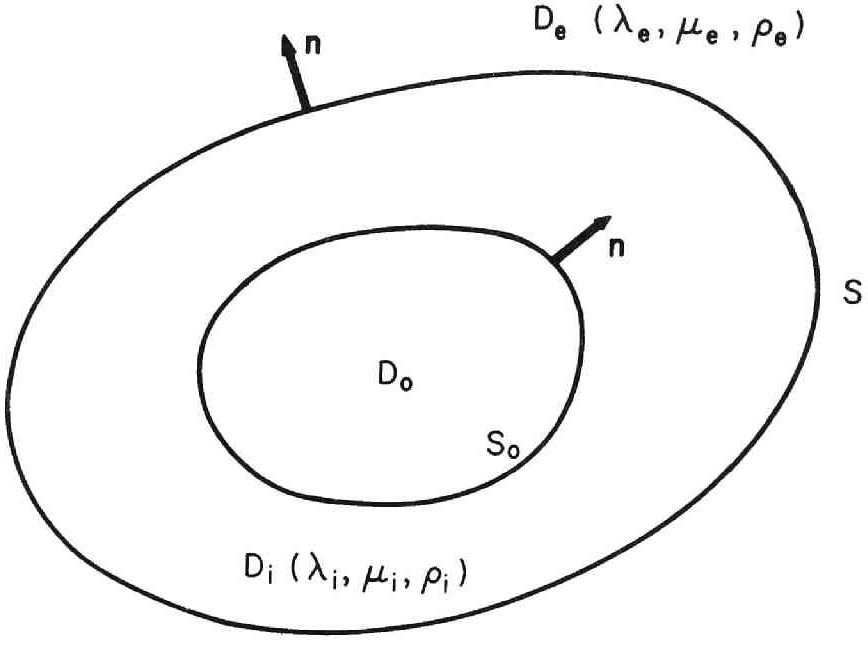

Fig.4.1.2.1 Domains and boundaries for problem B.

field $u_S = u - u_I$, where u_I is the given incident field which satisfies

$$\triangle_e^* u_I + \rho_e \omega^2 u_I = 0 \tag{4.1.2.4}$$

in the whole space except possibly at finite number of singular points in D_e , S_{0u} and S_{0s} stand for the disjoint portions of S_0 where the displacement and traction, respectively, are given, the superposed + indicates the limit on the boundary from the side into which n points, and - the limit from the opposite side, respectively. Also, the subscript e (i) indicates quantities relevant to D_e (D_i) . The solution to this problem is also unique.

The potential representations for the solutions to this problem are

$$u(x) = \int_S \Gamma_{Ie}(x,y)u(y)dS - \int_S \Gamma_e(x,y)t(y)dS + u_I(x),$$

$$x \in D_e \tag{4.1.2.5}$$

$$0 = \int_S \Gamma_{Ie}(x,y)u(y)dS - \int_S \Gamma_e(x,y)t(y)dS + u_I(x),$$

$$x \in D_e^c \backslash S \tag{4.1.2.6}$$

$$u(x) = \int_S \Gamma_i(x,y)t(y)dS - \int_S \Gamma_{Ii}(x,y)u(y)dS$$

$$+ \int_{S_0} \Gamma_{Ii}(x,y)v(y)dS - \int_{S_0} \Gamma_i(x,y)s(y)dS,$$

$$x \in D_i \tag{4.1.2.7}$$

$$0 = \int_S \Gamma_i(x,y)t(y)dS - \int_S \Gamma_{Ii}(x,y)u(y)dS$$

$$+ \int_{S_0} \Gamma_{Ii}(x,y)v(y)dS - \int_{S_0} \Gamma_i(x,y)s(y)dS,$$

$$x \in D_e \cup D_0 \tag{4.1.2.8}$$

where v and S are the displacement and the traction on S_0. Equations (4.1.2.5)-(4.1.2.8) follow trivially from (4.1.1.15) and (4.1.1.18). We then use (4.1.2.6) and (4.1.2.8) to have three integral equations given by

$$0 = C_e^i u(x) + \text{v.p.}\int_S \Gamma_{1e}(x,y)u(y)dS - \int_S \Gamma_e(x,y)t(y)dS + u_1(x),$$

$$x \in S$$

$$0 = \int_S \Gamma_i(x,y)t(y)dS - C_i^e u(x) - \text{v.p.}\int_S \Gamma_{1i}(x,y)u(y)dS$$

$$+ \int_{S_0} \Gamma_{1i}(x,y)v(y)dS - \int_{S_0} \Gamma_i(x,y)S(y)dS, \qquad x \in S$$

$$0 = \int_S \Gamma_i(x,y)t(y)dS - \int_S \Gamma_{1i}(x,y)u(y)dS + C_i^i v(x)$$

$$+ \text{v.p.}\int_{S_0} \Gamma_{1i}(x,y)v(y)dS - \int_{S_0} \Gamma_i(x,y)S(y)dS, \qquad x \in S_0 \qquad (4.1.2.9a\text{-}c)$$

which, after setting the specified values for v on S_{0u} and S on S_{0s} from (4.1.2.2), we expect to determine u, t and the unspecified halves of v and S.

4.1.3 Fictitious eigenfrequencies

We introduce the following notation in order to facilitate the description.

a) $D(\lambda,\mu,\rho)$: The body with the given material constants which occupies the domain D.
b) $\Omega(B)$: The set of all the eigenfrequencies of the displacement boundary value problems for the body B.
c) $[D(\lambda,\mu,\rho),\omega]$: The set of all the functions which satisfy the field equations

$$\Delta^* u + \rho\omega^2 u = 0 \qquad \text{in } D, \qquad (4.1.3.1)$$

and, in addition, the radiation condition provided that D is an exterior domain.
d) $[D(\lambda,\mu,\rho),\omega]_0$: The set of all the elements of $[D(\lambda,\mu,\rho),\omega]$ which vanish on ∂D.

We shall now explain the problem of fictitious eigenfrequencies. Consider Problem A for an exterior domain D. We may put $u_1 = 0$ without loss of generality (Otherwise replace u by u_S.). It is known (Kupradze

et al.(1979)) that the expression

$$W(\boldsymbol{x}) := \int_{\partial D} \Gamma_1(\boldsymbol{x},\boldsymbol{y})\boldsymbol{u}(\boldsymbol{y})\mathrm{d}S - \int_{\partial D} \Gamma(\boldsymbol{x},\boldsymbol{y})\boldsymbol{t}(\boldsymbol{y})\mathrm{d}S, \tag{4.1.3.2}$$

satisfies the conditions

$$W^+(\boldsymbol{x}) = \boldsymbol{u}(\boldsymbol{x}),\ TW^+(\boldsymbol{x}) = \boldsymbol{t}(\boldsymbol{x}), \qquad \boldsymbol{x}\in\partial D \tag{4.1.3.3a,b}$$

iff

$$W(\boldsymbol{x}) = 0 \tag{4.1.3.4}$$

identically in D^c. The boundary integral equation in (4.1.1.19), on the other hand, ensures

$$W(\boldsymbol{x}) \in [D^c(\lambda,\mu,\rho),\omega]_0, \tag{4.1.3.5}$$

from which (4.1.3.4) follows unless $\omega\in\Omega\left(D^c(\lambda,\mu,\rho)\right)$. However, if $\omega\in\Omega\left(D^c(\lambda,\mu,\rho)\right)$, it may happen that

$$W(\boldsymbol{x}) = \boldsymbol{u}^*(\boldsymbol{x}) \quad (\boldsymbol{x}\in D^c), \qquad \boldsymbol{u}^*(\boldsymbol{x})(\not\equiv 0)\in [D^c(\lambda,\mu,\rho),\omega]_0 \tag{4.1.3.6a,b}$$

hold. Actually, it is easy to see that the pair

$$\boldsymbol{t}(\boldsymbol{x}) = \begin{cases} T\boldsymbol{u}_E^+(\boldsymbol{x}) - T\boldsymbol{u}^{*-}(\boldsymbol{x}), & \boldsymbol{x}\in\partial D_u \\ 0, & \boldsymbol{x}\in\partial D_s \end{cases}$$

$$\boldsymbol{u}(\boldsymbol{x}) = \begin{cases} 0, & \boldsymbol{x}\in\partial D_u \\ \boldsymbol{u}_E^+(\boldsymbol{x}), & \boldsymbol{x}\in\partial D_s \end{cases} \tag{4.1.3.7a,b}$$

when introduced into (4.1.3.2), leads to (4.1.3.6), where $\boldsymbol{u}_E(\boldsymbol{x})\in[D(\lambda,\mu,\rho),\omega]$ stands for a function which satisfies the conditions

$$\boldsymbol{u}_E^+(\boldsymbol{x}) = 0, \qquad \boldsymbol{x}\in\partial D_u$$

$$T\boldsymbol{u}_E^+(\boldsymbol{x}) = T\boldsymbol{u}^{*-}(\boldsymbol{x}). \qquad \boldsymbol{x}\in\partial D_s \tag{4.1.3.8a,b}$$

Noting that $\boldsymbol{u}(\boldsymbol{x})$ ($\boldsymbol{t}(\boldsymbol{x})$) in (4.1.3.7) vanishes on ∂D_u (∂D_s), we see that (4.1.3.7) gives a non-trivial solution to the homogeneous integral equation associated with (4.1.1.19), and ω is, therefore, one of the fictitious eigenfrequencies. Hence we conclude that (4.1.1.19) does not render the solution unique for a particular set of frequencies, although the solution to the original boundary value problems is unique (Kupradze et al.(1979)). This difficulty may be termed the problem of fictitious eigenfrequencies.

An analogous phenomenon takes place in the integral equations for Problem B. Actually, we can state that the set of fictitious eigenfrequencies for this problem is

$$\Omega\left(D_e^c(\lambda_e,\mu_e,\rho_e)\right) \cup \Omega\left(D_0(\lambda_i,\mu_i,\rho_i)\right) . \qquad (4.1.3.9)$$

The corresponding eigendensities are

$$\boldsymbol{u} = \boldsymbol{u}_e^+ - \boldsymbol{F}_e^- = \boldsymbol{u}_i^- + \boldsymbol{F}_i \qquad \text{on } S,$$

$$\boldsymbol{t} = \mathrm{T}_e\boldsymbol{u}_e^+ - \mathrm{T}_e\boldsymbol{F}_e^- = \mathrm{T}_i\boldsymbol{u}_i^- + \mathrm{T}_i\boldsymbol{F}_i \qquad \text{on } S,$$

$$\boldsymbol{S} = \mathrm{T}_i\boldsymbol{u}_i^+ \qquad \text{on } S_{0u},$$

$$\boldsymbol{v} = \boldsymbol{u}_i^+ \qquad \text{on } S_{0s}, \qquad (4.1.3.10a\text{-}d)$$

where $\boldsymbol{u}_e \in [D_e(\lambda_e,\mu_e,\rho_e),\omega]$ and $\boldsymbol{u}_i \in [D_i(\lambda_i,\mu_i,\rho_i),\omega]$ are the functions which satisfy the jump conditions

$$\boldsymbol{u}_e^+ - \boldsymbol{u}_i^- = \boldsymbol{F}_e^- + \boldsymbol{F}_i = \boldsymbol{F}_i \qquad \text{on } S,$$

$$\mathrm{T}_e\boldsymbol{u}_e^+ - \mathrm{T}_i\boldsymbol{u}_i^- = \mathrm{T}_e\boldsymbol{F}_e^- + \mathrm{T}_i\boldsymbol{F}_i \qquad \text{on } S, \qquad (4.1.3.11a,b)$$

and the boundary conditions

$$\boldsymbol{u}_i^+ = 0 \qquad \text{on } S_{0u},$$

$$\mathrm{T}_i\boldsymbol{u}_i^+ = 0 \qquad \text{on } S_{0s}. \qquad (4.1.3.12a,b)$$

The functions $\boldsymbol{F}_i \in [D_0^c(\lambda_i,\mu_i,\rho_i),\omega]$ and $\boldsymbol{F}_e \in [D_e^c(\lambda_e,\mu_e,\rho_e),\omega]$ are chosen as follows :

a) If $\omega \in \Omega\left(D_e^c(\lambda_e,\mu_e,\rho_e)\right)$ but $\omega \notin \Omega\left(D_0(\lambda_i,\mu_i,\rho_i)\right)$ we set

$$\boldsymbol{F}_i = 0. \qquad (4.1.3.13)$$

For $\boldsymbol{F}_e$ we use an arbitrary nonzero element of $[D_e^c(\lambda_e,\mu_e,\rho_e),\omega]_0$.

b) If $\omega \in \Omega\left(D_0(\lambda_i,\mu_i,\rho_i)\right)$ but $\omega \notin \Omega\left(D_e^c(\lambda_e,\mu_e,\rho_e)\right)$ the appropriate choice for $\boldsymbol{F}_e$ is

$$\boldsymbol{F}_e = 0. \qquad (4.1.3.14)$$

Also we set $F_i \in [D_0^c(\lambda_i,\mu_i,\rho_i),\omega]$ to be a function which satisfies the boundary condition

$$F_i^+ = 0 \qquad \text{on } S_{0u},$$

$$T_i F_i^+ = T_i u^{*-} \qquad \text{on } S_{0s}, \qquad (4.1.3.15a,b)$$

and the radiation condition, where u^* is a non-zero element of $[D_0(\lambda_i,\mu_i,\rho_i),\omega]_0$.

c) If $\omega \in \Omega\big(D_0(\lambda_i,\mu_i,\rho_i)\big) \cap \Omega\big(D_e^c(\lambda_e,\mu_e,\rho_e)\big)$, we take F_i just as in b), and F_e as in a).

To prove this, we denote the RHSs in (4.1.2.5) and (4.1.2.6) by u_e and F_e, respectively. Also, we put the RHS in (4.1.2.8) in D_0 as u^*, noting, from (4.1.2.9b), that (4.1.2.8) is identically zero in D_e. Furthermore, we write the RHS of (4.1.2.7) as u_i+F_i, where F_i is defined in (4.1.3.15) with the u^* being just introduced. We may then put $u_I=0$ in (4.1.2.5) and (4.1.2.6) since we are interested in the homogeneous equations corresponding to (4.1.2.9). Equation (4.1.2.9c) tells that $u^* \in [D_0(\lambda_i,\mu_i,\rho_i),\omega]_0$, which implies $u^*=0$ if $\omega \notin \Omega\big(D_0(\lambda_i,\mu_i,\rho_i)\big)$. However, u^* may coincide with an appropriate eigenmode otherwise. Also (4.1.2.9a) says $F_e \in [D_e^c(\lambda_e,\mu_e,\rho_e),\omega]_0$, which means $F_e=0$ if $\omega \notin \Omega\big(D_e^c(\lambda_e,\mu_e,\rho_e)\big)$. However, F_e may coincide with a nonzero eigenmode otherwise.

We now use the jump properties of the double layer potential in (4.1.2.5)-(4.1.2.8) to have (4.1.3.10a,b) and

$$v = u_i^+ + F_i^+,$$

$$S = T_i u_i^+ + T_i F_i^+ - T_i u^{*-} \qquad \text{on } S_0. \qquad (4.1.3.16a,b)$$

Notice that the equalities in (4.1.3.10a,b) are consistent with each other if the conditions in (4.1.3.11) are satisfied. Also from (4.1.3.16) and (4.1.3.15) follow

$$v = 0 \qquad \text{on } S_{0u},$$

$$S = 0 \qquad \text{on } S_{0s} \qquad (4.1.3.17a,b)$$

if the conditions in (4.1.3.12) are fulfilled. In addition u_e satisfies the radiation condition by definition. Hence we may view u_e and u_i as displacement fields defined in $D_e \cup D_i$ which satisfy the connectivity conditions in (4.1.3.11) and the boundary conditions in (4.1.3.12). Such u_i and u_e are known to be determined uniquely for a given set of F_i and F_e (Kupradze et al.(1979)). Hence we have

$$u = t = 0 \qquad \text{on } S,$$

$$S = 0 \quad \text{on } S_{0u}, \qquad u = 0 \quad \text{on } S_{0s} \tag{4.1.3.18a-c}$$

if F_i=F_e=0. However, the definitions for F_i and F_e tell that these functions vanish identically unless ω belongs to the set in (4.1.3.9). In other words, the solutions to (4.1.2.9) are unique if ω does not belong to the set defined in (4.1.3.9). Moreover, we easily see that the RHSs in (4.1.3.10) and (4.1.3.11) are zero only if F_i=0 and F_e=0. Hence we conclude the fictitious eigenfrequencies for problem B to be as given in (4.1.3.9).

Specifically, when $(\lambda_i,\mu_i,\rho_i)=(\lambda_e,\mu_e,\rho_e)=(\lambda,\mu,\rho)$, Problem B reduces to Problem A for the domain $D = D_0^c$. Actually, we add (4.1.2.5) and (4.1.2.8), (4.1.2.6) and (4.1.2.7), and (4.1.2.6) and (4.1.2.8) to obtain (4.1.1.18). However, the integral equation for Problem B in (4.1.2.9) is not equivalent to that for Problem A given in (4.1.1.19). Indeed, (4.1.2.9) fails to give a unique solution at an additional set of fictitious eigenfrequencies, i.e., $\Omega\left(D_e^c(\lambda,\mu,\rho)\right)$.

In numerical calculations, one has to devise techniques to circumvent inconvenience caused by this non-uniqueness.

4 . 1 . 4 Methods of avoiding fictitious eigenfrequencies

This section presents some methods of avoiding the non-uniqueness of BIE solutions for the case of Problem A.

The non-uniqueness phenomenon in acoustics has long been known to mathematicians and some methods to avoid this difficulty are available. We now extend these methods to elastodynamics and classify them into the following (overlaping) categories:

a) Methods using interior constraints.

As has been discussed, the conventional BIE loses the uniqueness of the solution because the conventional BIE for Problem A given in (4.1.1.19) is not equivalent to (4.1.3.4). In view of this Schenck(1968) proposed to supplement the conventional BIE by the following N_c conditions:

$$W(x_i) = 0. \qquad x_i \in D^c \quad (i=1,2,\ldots..N_c) \tag{4.1.4.1}$$

where x_i's are points chosen arbitrarily in D^c, and W has been defined in (4.1.3.2). This method, however, fails when all the x_i's are on the nodal lines of the eigenmodes.

Jones's method in acoustics, which we shall discuss in depth later, can also be classified into this category (Jones(1974)).

b) Methods which use the uniqueness of the solution of certain boundary value problems.

As is clear from the discussion in 4.1.3, the conventional BIEM solves a homogeneous Dirichlet problem defined in D^c in order to have (4.1.3.4). This is why the conventional BIEM breaks down when the

solution of the Dirichlet problem for D^c is not unique. One may therefore think of obtaining new BIEs by utilising other boundary value problems for D^c having the uniqueness property. The following boundary value problems are easily seen to satisfy this requirement:

1) Let u be a solution of

$$(\triangle^* + \rho\omega^2)u = 0 \tag{4.1.4.2}$$

in D^c (interior domain) which satisfies the boundary condition

$$u^- = Tu^- = 0 \qquad \text{on } \partial D. \tag{4.1.4.3}$$

Then we have $u = 0$ identically in D^c. Actually (4.1.1.15) readily proves this.

2) Let u be a solution of (4.1.4.2) in D^c which satisfies

$$u^- = \alpha Tu^- \qquad \text{on } \partial D, \tag{4.1.4.4}$$

where α is a number whose imaginary part is non-zero. Again we have $u = 0$ identically in D^c. Indeed, a well-known argument shows

$$0 = \int_{\partial D} u^- \cdot \overline{Tu^-} dS - \int_{\partial D} \overline{u^-} \cdot Tu^- dS = 2i \ \mathrm{Im}\ \alpha \int_{\partial D} |Tu^-|^2 dS, \tag{4.1.4.5}$$

from which we have $u^- = Tu^- = 0$ on ∂D.

3) The solution to (4.1.4.2) in D_a subject to the boundary conditions

$$u^-(x) = 0, \qquad x \in \partial D$$

$$u^- - \alpha Tu^- = 0, \qquad x \in S \tag{4.1.4.6a,b}$$

vanishes identically, where D_a is an annular domain bounded externally by ∂D and internally by a surface S, and the unit normal vectors on ∂D and S are taken outward viewed from D_a.

We now discuss BIEs for exterior elastodynamics whose solutions are unique.

An elastodynamic counterpart of the method of Kleinman & Roach(1974) utilises 1) to avoid the fictitious eigenfrequency, or specifically they solve

$$W^-(x) = 0 \quad \text{and} \quad TW^-(x) = 0 \qquad x \in \partial D \tag{4.1.4.7a,b}$$

simultaneously using (4.1.3.2). Their method therefore yields an over determined system. The elastodynamic counterpart of the method of Burton & Miller(1971) makes use of 2) by solving the equation

$$W^-(x) - \alpha TW^-(x) = 0 \quad (\mathrm{Im}\ \alpha \neq 0) \qquad x \in \partial D \tag{4.1.4.8}$$

with (4.1.3.2). Finally, the method of Ursell(1973) uses 3) to obtain

a BIE which has a unique solution. His method can be written as

$$W'(x)^- = 0 , \qquad x \in \partial D \tag{4.1.4.9}$$

where

$$W' = \int_{\partial D} (T_y G(x,y))^T u(y) dS_y - \int_{\partial D} G(x,y) t(y) dS_y , \tag{4.1.4.10}$$

and $G(x,y)$ is a Green's function for $D \cup \partial D \cup D_a$ which satisfies

$$G(x,y)^- - \alpha T_x (G(x,y))^- = 0. \qquad (y \in (D \cup \partial D \cup D_a),\ x \in S) \tag{4.1.4.11}$$

Since (4.1.4.11) gives $W' - \alpha T W' = 0$ on S, we have $W' \equiv 0$ in D_a, thus ensuring the uniqueness of the integral equation obtained from (4.1.4.9) and (4.1.4.10).

c) Methods using modified kernels.

One may also obtain a BIE which has the aforementioned uniqueness by modifying the kernel functions Γ and Γ_1. For example, the method of Ursell uses G instead of Γ, as we have seen. Likewise, the method of Jones(1974) uses a modified kernel which allows an easier construction than that of Ursell.

In the next section we shall discuss the elastodynamic counterparts of Jones's methods, which are considered to be practical. We shall use the direct method for 2D exterior mixed problems (i.e. Problem A in the classification of the last section).

4 . 1 . 5 Some preliminaries

We prepare some formulae for later use. We first introduce a polar coordinate (r, θ) by which the cartesian coordinates of two points x and y are given as

$$\begin{bmatrix} x_1 \\ x_2 \end{bmatrix} = r \begin{bmatrix} \cos\theta \\ \sin\theta \end{bmatrix}, \quad \begin{bmatrix} y_1 \\ y_2 \end{bmatrix} = r_0 \begin{bmatrix} \cos\theta_0 \\ \sin\theta_0 \end{bmatrix} . \tag{4.1.5.1a,b}$$

We first expand the fundamental solution $\Gamma(x,y)$ into Fourier series on the circle defined by r = const. with the help of Fourier transform. To this end we use the fact that the Fourier transform of the fundamental solution $\Gamma(x,y)$ with respect to x is written as

$$- (\triangle^*(i\xi) + \rho\omega^2 1)^{-1} e^{-i\xi \cdot y}, \tag{4.1.5.2}$$

where ξ is the parameter of the Fourier transformation and $\triangle^*(i\xi)$ is the matrix obtained by replacing ∇ in $\triangle^*(\nabla)$ by $i\xi$ (See 1.1 and (4.1.1.1)). Using the polar coordinate $(|\xi|, \varphi)$ of ξ, we have

$$- \ (\triangle^*(i\boldsymbol{\xi})+\rho\omega^2\mathbf{1})^{-1}$$

$$= \frac{1}{4\mu}\{(\frac{1}{|\boldsymbol{\xi}|^2-k_T{}^2} + (\frac{k_L}{k_T})^2\frac{1}{|\boldsymbol{\xi}|^2-k_L{}^2})(\boldsymbol{v}\otimes\bar{\boldsymbol{v}} + \bar{\boldsymbol{v}}\otimes\boldsymbol{v})$$

$$- (\boldsymbol{v}\otimes\boldsymbol{v}e^{2i\varphi} + \bar{\boldsymbol{v}}\otimes\bar{\boldsymbol{v}}e^{-2i\varphi})(\frac{1}{|\boldsymbol{\xi}|^2-k_T{}^2} - (\frac{k_L}{k_T})^2\frac{1}{|\boldsymbol{\xi}|^2-k_L{}^2})\} \ , \qquad (4.1.5.3)$$

where k_L and k_T are the wave numbers of the longitudinal and transverse waves defined in (4.1.1.21), $\boldsymbol{v}$ and $\bar{\boldsymbol{v}}$ are vectors defined by $\boldsymbol{v}=\boldsymbol{i}_1-i\boldsymbol{i}_2$ and $\bar{\boldsymbol{v}}=\boldsymbol{i}_1+i\boldsymbol{i}_2$, and $\boldsymbol{i}_1$ and $\boldsymbol{i}_2$ are the base vectors, respectively. It is then easily seen that the Fourier coefficient of $e^{in\theta}$ in the Fourier expansion for $\Gamma(\boldsymbol{x},\boldsymbol{y})$ on the circle r = const. is given by

$$-\frac{1}{(2\pi)^2}\oint d\theta e^{-in\theta}\int_0^\infty d|\boldsymbol{\xi}|$$

$$\cdot\oint d\varphi \ |\boldsymbol{\xi}|e^{i|\boldsymbol{\xi}|r\cos(\varphi-\theta)}(\triangle^*(i\boldsymbol{\xi})+\rho\omega^2\mathbf{1})^{-1}e^{-i|\boldsymbol{\xi}|r_0\cos(\varphi-\theta_0)} . \qquad (4.1.5.4)$$

The well-known limiting absorption principle for $e^{-i\omega t}$ time-harmonic problem then says that we can calculate the integral in (4.1.5.4) assuming Im $k_{L,T}>0$. Indeed the use of some known formulae for the Bessel functions gives

$$\Gamma(\boldsymbol{x},\boldsymbol{y}) = -\frac{i}{16\mu}\sum_{n=-\infty}^{\infty}\sum_{i=1}^{2}(-1)^n\Psi_H^{ni}(\boldsymbol{x})\otimes\Psi_J^{ni}(\boldsymbol{y}) \qquad (4.1.5.5)$$

for $r_0<r$. For $r<r_0$ we must interchange the subscripts J and H in the above expression. The vectors $\Psi_J^{ni}(\boldsymbol{x})$ in (4.1.5.5) are defined by

$$\Psi_J^{n1}(\boldsymbol{x}) = e^{in\theta}(-J_{n+1}(k_Lr)V + J_{n-1}(k_Lr)\bar{V})\frac{k_L}{k_T}i ,$$

$$\Psi_J^{n2}(\boldsymbol{x}) = e^{in\theta}(J_{n+1}(k_Tr)V + J_{n-1}(k_Tr)\bar{V}) , \qquad (4.1.5.6a,b)$$

where J is the Bessel function, $V=\boldsymbol{i}_r-i\boldsymbol{i}_\theta$, $\bar{V}=\boldsymbol{i}_r+i\boldsymbol{i}_\theta$, and $\boldsymbol{i}_r$ and $\boldsymbol{i}_\theta$ are the unit vectors in the direction of r and θ coordinate at $\boldsymbol{x}$, respectively. $\Psi_H^{ni}(\boldsymbol{x})$ have the same expressions as $\Psi_J^{ni}(\boldsymbol{x})$ except that the Bessel functions in (4.1.5.6) are replaced by the Hankel functions of the first kind denoted by $H.^{(1)}$. In passing, we note that Kitahara(1985) reproduced the calculation leading to (4.1.5.5) in his book.

We next prove the identity

$$\int_{\partial D} T\Psi_J^{mi}(x)\cdot\Psi_H^{nj}(x)dS - \int_{\partial D}\Psi_J^{mi}(x)\cdot T\Psi_H^{nj}(x)dS$$

$$= 16\mu i(-1)^m\delta_{mn}\delta_{ij}, \quad -\infty<m,n<\infty, \quad 1\leqq i,j\leqq 2, \tag{4.1.5.7}$$

which holds for any boundary ∂D to which the origin is interior. To see this we assume that x (y) is exterior (interior) to ∂D. Equation (4.1.1.18) then gives

$$\Gamma(x,y) = \int_{\partial D}\Gamma_1(x,z)\Gamma(z,y)dS_z - \int_{\partial D}\Gamma(x,z)\ T_z\Gamma(z,y)dS_z. \tag{4.1.5.8}$$

Hence by substituting (4.1.5.5) into (4.1.5.8), followed by comparing the coefficients of the $\Psi_H^{mi}(x)\otimes\Psi_J^{nj}(y)$ term in (4.1.5.8), we obtain (4.1.5.7). Also, we see, from (4.1.5.6), that the relations

$$\Psi_H^{ni} = (-1)^n(\bar{\Psi}_H^{nj} - 2\bar{\Psi}_J^{nj}), \quad \Psi_J^{ni} = (-1)^{n+1}\bar{\Psi}_J^{nj} \tag{4.1.5.9a,b}$$

hold for $(-\infty<n<\infty\ , i=1,2)$. From (4.1.5.9) and (4.1.5.7) follow

$$\int_{\partial D}(T\Psi_H^{mi}\cdot\bar{\Psi}_H^{nj} - \Psi_H^{mi}\cdot\overline{T\Psi}_H^{nj})dS = 32\mu i\delta_{mn}\delta_{ij} \tag{4.1.5.10}$$

and

$$\int_{\partial D}(T\Psi_J^{mi}\cdot\bar{\Psi}_H^{nj} - \Psi_J^{mi}\cdot\overline{T\Psi}_H^{nj})dS = 16\mu i\delta_{mn}\delta_{ij} \tag{4.1.5.11}$$

for $-\infty<m,n<\infty$ and $i,j=1,2$.

These results could have been obtained by using the addition theorems and some identities for Wronskian of the Bessel functions (e.g. Shaw(1979) for acoustics). However, the present method is simpler.

4 . 1 . 6 Elastodynamic counterpart of Jones's methods

In this section we discuss the elastodynamic version of Jones's methods (Jones(1974)). We shall utilise the argument used by Ursell(1978) in the sequel.

Let the origin be in D^c. The elastodynamic counterpart of Jones's method is stated as follows: To solve (4.1.1.19) subject to the conditions

$$I^{ni} := \int_{\partial D} \Psi_H^{\beta i}(x) \cdot t(x) dS - \int_{\partial D} T\Psi_H^{\beta i}(x) \cdot u(x) dS = 0, \qquad (4.1.6.1)$$

for $-M \leqq n \leqq M$, $1 \leqq i \leqq 2$, where M is a certain integer. We shall call this method the first method. It is clear from Green's formula that the unique solution to (4.1.1.19) satisfies (4.1.6.1) when $\omega \notin \Omega(D^c, \lambda, \mu, \rho)$.

We next interpret (4.1.6.1) when $\omega \in \Omega(D^c, \lambda, \mu, \rho)$. Since the eigendensities for (4.1.1.19) are given by (4.1.3.7), we use Green's formula and (4.1.3.8) to rewrite (4.1.6.1) as

$$\int_{\partial D} \Psi_H^{\beta i}(x) \cdot Tu^*(x) dS - \int_{\partial D} T\Psi_H^{\beta i}(x) \cdot u^*(x) dS = 0, \qquad (4.1.6.2)$$

from which follows

$$\int_C \Psi_H^{\beta i}(x) \cdot Tu^*(x) dS - \int_C T\Psi_H^{\beta i}(x) \cdot u^*(x) dS = 0 \qquad (4.1.6.3)$$

for any circle C which is inside D^c and is centred at the origin. Indeed, we use Green's formula for a domain bounded by ∂D and C to show (4.1.6.3). Since the eigenmode u^* can be expanded in the interior of C as

$$u^*(x) = \sum_{n=-\infty}^{\infty} \sum_{i=1}^{2} C^{ni} \Psi^{\eta i}(x), \qquad (C^{ni} : \text{const.}) \qquad (4.1.6.4)$$

(4.1.6.3), together with (4.1.5.7), implies

$$C^{ni} = 0 \quad \text{for} \quad -M \leqq n \leqq M, \quad 1 \leqq i \leqq 2. \qquad (4.1.6.5)$$

Therefore, we conclude that $u^*(x) = 0$ in D^c unless we can find a nontrivial eigenmode u^* which satisfies (4.1.6.5). Since the lower eigenmodes generally contain terms having a small $|n|$ in (4.1.6.4), this method determines u and t for given ω uniquely if M is sufficiently large.

Jones also showed that an equivalent result can be achieved by using a modified kernel in a simple layer potential formulation for the Neumann problem for the Helmholtz equation. The elastodynamic counterpart of this second method, using direct method instead, may be stated as follows: Replace the kernels in (4.1.1.18) and (4.1.1.19) by the following expressions

$$\Gamma^*(x,y) := \Gamma(x,y) - \sum_{n=-M}^{M}\sum_{i=1}^{2}\varepsilon_{ni}(-1)^n\Psi_H^i(x)\otimes\Psi_H^{-ni}(y) ,$$

$$\Gamma_1^*(x,y) := \Gamma_1(x,y) - \sum_{n=-M}^{M}\sum_{i=1}^{2}\varepsilon_{ni}(-1)^n\Psi_H^i(x)\otimes T\Psi_H^{-ni}(y) , \qquad (4.1.6.6a,b)$$

respectively, and solve the modified version of (4.1.1.19), where ε_{ni}'s are constants such that the numbers

$$\mathrm{Im}\ \varepsilon_{ni} + 16\mu|\varepsilon_{ni}|^2 \quad (-\infty<n<\infty\ ,\ i=1,2) \qquad (4.1.6.7)$$

have the same sign for all n and i .

We shall now prove the equivalence of these formulations. Since we easily see that the first method implies the second, we show the converse.

Let $W^*(x)$ be defined by

$$W^*(x) = \int_{\partial D}\Gamma_1^*(x,y)u(y)dS - \int_{\partial D}\Gamma^*(x,y)t(y)dS\ ,\ x\in D^c\setminus\{0\} . \qquad (4.1.6.8)$$

The second method determines u and t on ∂D in a way that $W^{*-}(x) = 0$ is satisfied on ∂D. Since $W^*(x)$ solves the equation of elastodynamics in $D^c\setminus\{0\}$, we use Green's formula for a domain bounded by ∂D and C to have

$$0 = \int_{\partial D}(W^{*-}(x)\cdot\overline{TW^*(x)}^- - TW^*(x)^-\cdot\overline{W^*(x)}^-)dS$$

$$= \int_C(W^*(x)\cdot\overline{TW^*(x)} - TW^*(x)\cdot\overline{W^*(x)})dS , \qquad (4.1.6.9)$$

where C is a closed contour in D^c which does not touch ∂D and includes the origin in its interior. On the other hand (4.1.6.6), (4.1.6.8) and (4.1.6.1) yield

$$W^*(x) = \sum_{n=-\infty}^{\infty}\sum_{i=1}^{2}(-1)^n\Big(\frac{i}{16\mu}\Psi_J^{-ni}(x)+\varepsilon_{-ni}\Psi_H^{-ni}(x)\Big)I^{ni}\ ,\quad x\in C$$

$$\varepsilon_{ni} = 0. \quad (|n|>M) \qquad (4.1.6.10a,b)$$

Hence we can rewrite (4.1.6.9) into

$$0 = \sum_m\sum_i\sum_n\sum_j\Big[-\frac{i}{16\mu}\varepsilon_{-ni}\int_C\Big(\Psi_H^{-ni}\cdot\overline{T\Psi^{-mj}} - T\Psi_H^{-ni}\cdot\overline{\Psi^{-mj}}\Big)dS$$

$$+\frac{i}{16\mu}\bar{\varepsilon}_{-mj}\int_C\left(\Psi_j^{ni}\cdot\overline{T\Psi}^{mj}_H - T\Psi_j^{ni}\cdot\bar{\Psi}^{mj}_H\right)dS$$

$$+\varepsilon_{-ni}\bar{\varepsilon}_{-mj}\int_C\left(\Psi_H^{ni}\cdot\overline{T\Psi}^{mj}_H - T\Psi_H^{ni}\cdot\bar{\Psi}^{mj}_H\right)dS\Big]I^{ni}\ \bar{I}^{mj}\ , \quad (4.1.6.11)$$

where we have used (4.1.6.10) and Green's formula for $\Psi j^{\cdot}$. Equation (4.1.6.11) simplifies to

$$0=\sum_n\sum_i(-\varepsilon_{-ni}+\bar{\varepsilon}_{-ni} - 32\mu i\,|\,\varepsilon_{-ni}\,|^2)\,|\,I^{ni}\,|^2$$

$$=-2i\sum_{n=-N}^{N}\sum_{i=1}^{2}(\mathrm{Im}\ \varepsilon_{-ni}+16\mu\,|\,\varepsilon_{-ni}\,|^2)\,|\,I^{ni}\,|^2, \quad (4.1.6.12)$$

as we use (4.1.5.7), (4.1.5.10) and (4.1.5.11). Consequently (4.1.6.12), together with the assumption in (4.1.6.7), shows

$$I^{ni}=0,\quad n=-M,\ldots,0,\ldots M,\quad i=1,2\ , \quad (4.1.6.13)$$

thus proving the equivalence of the two methods.

4 . 1 . 7 Remarks concerning Jones's method

a) Kobayashi & Nishimura(1982b) proved the above result by using a different argument. The proof given there was quite involved in spite of more stringent restrictions imposed on ε_{ni} than those used here. Jones himself later extended his method to 3D displacement or traction boundary value problems of elastodynamics (Jones(1984)).

b) As is easily inferred, the methods of Jones can be extended to other problems whose fundamental solution allows a series expansion in terms of products of interior and exterior solutions. For examples, the fundamental solution for 3D time-harmonic elastodynamics given in (4.1.1.20) can be rewritten, after a formidable manipulation, as

$$\frac{i}{4\pi\mu k_T^2}\sum_{n=0}^{\infty}\sum_{m=-n}^{n}(-1)^m\left\{\Psi^{jL}_{n,m}(\boldsymbol{x})\otimes\Psi^{hL}_{n,-m}(\boldsymbol{y})\right.$$

$$\left.+\ \Psi^{jT_1}_{n,m}(\boldsymbol{x})\otimes\Psi^{hT_1}_{n,-m}(\boldsymbol{y})\ +\ \Psi^{jT_2}_{n,m}(\boldsymbol{x})\otimes\Psi^{hT_2}_{n,-m}(\boldsymbol{y})\right\} \quad (4.1.7.1)$$

for $|\boldsymbol{x}|<|\boldsymbol{y}|$, where

$$\Psi^{jL}_{n,m}(\boldsymbol{x})=\sqrt{(2n+1)}\,k_L\left(\frac{\partial}{\partial r}j_n(k_Lr)P_n^m(\cos\theta)\,i_r\right.$$

$$+ \frac{j_n(k_L r)}{r}\frac{\partial}{\partial\theta}P_n^m(\cos\theta)\,\boldsymbol{i}_\theta + i\,m\,\frac{j_n(k_L r)}{r}\frac{P_n^m(\cos\theta)}{\sin\theta}\boldsymbol{i}_\varphi\Big)e^{im\varphi},$$

$$\Psi^{j^T_1}_{n,m} = \sqrt{n(n+1)(2n+1)k_T}\Big(\frac{j_n(k_T r)}{r}P_n^m(\cos\theta)\,\boldsymbol{i}_r$$

$$+ \frac{1}{n(n+1)}\Big(\frac{\partial}{\partial r}j_n(k_T r) + \frac{j_n(k_T r)}{r}\Big)\frac{\partial}{\partial\theta}P_n^m(\cos\theta)\,\boldsymbol{i}_\theta$$

$$+ \frac{i\,m}{n(n+1)}\Big(\frac{\partial}{\partial r}j_n(k_T r) + \frac{j_n(k_T r)}{r}\Big)\frac{P_n^m(\cos\theta)}{\sin\theta}\boldsymbol{i}_\varphi\Big)e^{im\varphi},$$

$$\Psi^{j^T_2}_{n,m} = \sqrt{(2n+1)k_T/(n(n+1))}\ \Big(i\,m\,k_T\,j_n(k_T r)\frac{P_n^m(\cos\theta)}{\sin\theta}\boldsymbol{i}_\theta$$

$$- k_T\,j_n(k_T r)\frac{\partial}{\partial\theta}P_n^m(\cos\theta)\,\boldsymbol{i}_\varphi\Big)e^{im\varphi},$$

$$(n = 0,1,2,..,m = -n,...0,....-n)$$

$$\Psi^{j^T_0}_{0,0} = 0, \qquad \Psi^{j^T_0}_{0,0} = 0, \qquad (4.1.7.2a\text{-}e)$$

(r,θ,φ) are the spherical coordinates of x, $(\boldsymbol{i}_r,\boldsymbol{i}_\theta,\boldsymbol{i}_\varphi)$ are the unit base vectors, j_n is the spherical Bessel function, and P_n^m is the associated Legendre function, respectively. $\Psi^h_{\cdot\cdot}$ also has an obvious meaning. It is now clear how one should proceed in order to formulate a 3D version of Jones's methods in direct BIEM. We therefore omit the further detail.

4 . 1 . 8 Peripheral stress

The evaluation of the peripheral stress is one of the most important problems for engineers. The BIEM is well suited to this end because of its fine resolution for the boundary quantities. In this section we shall present one method of computing the peripheral stress.

In 3D case, we take a surface curvilinear coordinate system $\xi^K(1\leqq K\leqq 2)$ on the boundary ∂D of a body D. Also, the third axis is taken in the direction of the normal vector $\boldsymbol{n}$ to ∂D, with ξ^3 being the distance measured from ∂D (positive in the direction of $\boldsymbol{n}$). Then the peripheral stresses take the following forms:

$$\tau_{KL} = \lambda a_{KL}\frac{2\mu u_{I\,I\,J}a^{IJ} + t_3}{\lambda + 2\mu} + \mu(u_{K|L} + u_{L|K}),$$

$$\tau_{K3} = t_K \ , \quad \tau_{33} = t_3 \ , \tag{4.1.8.1a-c}$$

where $u_{K|L}$ * indicates the 3D covariant derivative defined as

$$u_{K|L} = \frac{\partial u_K}{\partial \xi^L} - u_M \Gamma^M_{KL} - u_3 b_{KL} , \tag{4.1.8.2}$$

and a_{KL}, b_{KL}, Γ^M_{KL} stand for the first and second fundamental forms of ∂D and the Christoffel symbol calculated from a_{KL}. All the quantities are referred to the specified curvilinear coordinates.

For the 2D problems, (4.1.8.1) is simplified considerably. Actually, we can write the result in physical components as

$$\tau_{\xi\xi} = \frac{4\mu(\lambda+\mu)}{(\lambda+2\mu)a} \frac{\partial u_\alpha}{\partial \xi} \frac{\partial x_\alpha}{\partial \xi} + \frac{\lambda n_\alpha t_\alpha}{\lambda+2\mu} \ ,$$

$$\tau_{\xi n} = \frac{1}{(a)^{1/2}} t_\alpha \frac{\partial x_\alpha}{\partial \xi} \ , \quad \tau_{nn} = n_\alpha t_\alpha \ , \tag{4.1.8.3a-c}$$

where ξ is the parameter which describes the boundary curve $x_\alpha(\xi)$, and

$$a = \frac{\partial x_\alpha}{\partial \xi} \frac{\partial x_\alpha}{\partial \xi} \ . \tag{4.1.8.4}$$

The vectors on the right-hand sides of (4.1.8.3) are referred to an arbitrary cartesian coordinate system.

Recently, Sladek & Sladek(1986) proposed formulae similar to (4.1.8.1).

4 . 1 . 9 Numerical procedures

We now describe the numerical procedures which we shall use in the next section. We restrict our attention to 2D cases in order to fix the idea. It is, however, not difficult to extend the present procedures to 3D cases.

a) Boundary elements

We use quadratic isoparametric boundary elements. The singular integrals and the non integral terms resulting from the double layer potential (see (4.1.1.17) and (4.1.1.19)) are evaluated with the help of the method of substitution proposed originally by Lachat & Watson(1976) in elastostatics. In elastodynamics, we use the following identities obtained from (4.1.1.17) and (4.1.1.19):

---

* The upper-case indices range from 1 to 2.

$$C^e u_p = \int_{\partial D} \Gamma t_p dS - \int_{\partial D} \Gamma_1 u_p dS \qquad (4.1.9.1)$$

for the interior problems and

$$-C^i u_p = \int_{\partial D} \Gamma_1 u_p dS - \int_{\partial D} \Gamma t_p dS + u_p \qquad (4.1.9.2)$$

for the exterior problems, where u_p and t_p are the displacement for a certain plane wave and the associated boundary traction, respectively. The plane S waves travelling, say, in x_1 and x_2 directions may be used to determine the singular terms completely.

For the calculation of the peripheral stresses we use (4.1.8.1) or (4.1.8.3) by identifying the parameters of the isoparametric element with the curvilinear coordinate system in (4.1.8.1) or (4.1.8.3).

The boundary modelling must be fine enough so as to be compatible with the wave number. We recommend the use of about four elements for one wavelength of an S wave.

b) Fundamental solution

The explicit form of the fundamental solution obtained from (4.1.1.20b), i.e.

$$\Gamma(x,y) = \frac{i}{4\mu}\left[1\left\{H_0^{(1)}(k_T R) + \frac{1}{k_T^2 R}\left(H_1^{(1)}(k_L R)k_L - H_1^{(1)}(k_T R)k_T\right)\right\}\right.$$

$$- \frac{\nabla R \otimes \nabla R}{k_T^2 R}\left\{R\left(k_T^2 H_0^{(1)}(k_T R) - k_L^2 H_0^{(1)}(k_L R)\right)\right.$$

$$\left.\left. - 2\left(k_T H_1^{(1)}(k_T R) - k_L H_1^{(1)}(k_L R)\right)\right\}\right] \qquad (4.1.9.3)$$

suggests that a cancellation may occur due to the three parenthesised terms, especially in the low frequency range, where $R = |x-y|$. Therefore, for small R, we should expand the Hankel functions in series and delete the unfavourable terms (terms of order $1/R^2$ in the first parentheses, and those of order $1/R^2$ and $\log R$ in the third), before numerical calculation. The use of standard subroutines for the Bessel functions available in most computer centres etc. should therefore be avoided. This applies to Γ_1 also.

c) FFT Algorithm

The use of an FFT algorithm is recommended for the numerical calculation of the Fourier transform, in order to cope with arbitrary boundary conditions and an arbitrary incident motion. However, we must remember that the finite Fourier transform approximates a non-periodic motion by a periodic motion. We therefore have to add sufficient number of 'additional zeros' to the incident field so that the solution actually has a quiescent past as we have assumed in

(4.1.1.7).

It is customary to use as many as 512 or more steady states for earthquake-response analysis. In such cases, we may carry out a smaller number of BIEM analyses, say 30, and then interpolate these results to complete the calculation.

d) Circumvention of the fictitious eigenfrequencies

As we have discussed in 4.1.4 ~ 4.1.6, we can prevent the occurence of the fictitious eigenfrequencies by several methods. These methods, however, may not always be very practical because some of them introduce very singular kernel functions while others involve evaluation of complicated series. For example, the elastodynamic version of the Burton-Miller method introduces hypersingular kernels, which are difficult to deal with numerically unless one regularises them. However, this regularisation is possible only with the use of C^1 boundary elements (see 3.2), thus making the computer code both inefficient and complicated. Although the methods discussed in 4.1.6 are considered to be practical, we still have to be careful in concluding that these methods are indispensable for <u>transient</u> wave analysis. Actually, our experience tells that the BIE formulations described in the previous section work well even for such values of ω that deviate from the unfavourable value ω^* by a small quantity, say 2-3% of ω^*. Therefore, we may use the following method: we use the conventional BIE formulations and check whether the ω is very close to one of the fictitious eigenfrequencies. If not, we accept the calculation. Otherwise, we give a small increment to ω, solve the new problem and check the validity of the results again. We repeat this process until we obtain accurate results. Some interpolation schemes are used thereafter to compute the results for the original frequency.

We then have to be able to tell if a certain frequency is a fictitious eigenfrequency or not for the abovementioned method to work. As we shall see, however, this is possible at least in traction boundary value problems. Consider Problem A. We arrange the obtained matrix in the following form:

$$\sum_{j=1}^{N} \boldsymbol{D}_{ij}\boldsymbol{u}(\boldsymbol{x}_j) = \sum_{j=1}^{N} \boldsymbol{S}_{ij}\boldsymbol{t}(\boldsymbol{x}_j) - \boldsymbol{u}_{\mathrm{I}}(\boldsymbol{x}_i), \tag{4.1.9.4}$$

where

$$\boldsymbol{D}_{jk} = \int_{\partial D} \Gamma_{\mathrm{I}}(\boldsymbol{x}_j, \boldsymbol{x})\Omega_k(\boldsymbol{x})\mathrm{d}S + \boldsymbol{C}^i(\boldsymbol{x}_j)\delta_{jk}, \qquad \text{(no sum on } j\text{)}$$

$$\boldsymbol{S}_{jk} = \int_{\partial D} \Gamma(\boldsymbol{x}_j, \boldsymbol{x})\Omega_k(\boldsymbol{x})\mathrm{d}S, \tag{4.1.9.5a,b}$$

$\Omega_j(\boldsymbol{x})$ is the shape function which satisfies

$$\Omega_j(\boldsymbol{x}_i) = \delta_{ij}, \tag{4.1.9.6}$$

for the nodal points $x_i \in \partial D$, and δ_{ij} is Kronecker's delta. According to our experience, one can $(L\text{-}U)$-decompose D_{ij} without using the partial pivoting algorithm whenever the frequency is not very close to one of the fictitious eigenfrequencies. Also, in this case, the minimum absolute value of the diagonal terms of the lower triangular matrix, denoted by L_{ij} and obtained with the help of the Crout method, is almost independent of the frequency. However, for the fictitious eigenfrequencies, the value of

$$\min_i |L_{ii}| \tag{4.1.9.7}$$

becomes very small. Therefore by checking if

$$\min_i |L_{ii}| < C \min_i |L_{ii}|_{\text{static}} , \tag{4.1.9.8}$$

we can distinguish a fictitious eigenfrequency from the ordinary ones, where $C < 1$ is a constant. Note that the RHS of (4.1.9.8) is obtained without additional computation because FFT usually requires a static analysis. For C we use 0.7 in the examples to follow. This simple algorithm works well as long as the fictitious eigenfrequencies are not very densely distributed. Therefore, this method is considered to be sufficient for our purpose because it is often unnecessary, as well as impractical, to take very high frequency contributions into consideration for transient analysis, and because it is the high frequency range where the fictitious eigenfrequencies are densely distributed. In the next section we shall compare the efficiency of this method and Jones's methods in transient elastodynamic analysis.

An analogous method is available in Problem B, provided that the boundary condition is of the second kind (i.e. $S_{0s}=S_0$). Actually, we arrange the discretised integral equation in the following form

$$\begin{cases} x_i \in S \\ x_k \in S_0 \\ x_m \in S \end{cases} \quad \begin{bmatrix} \underline{D}^e_{ij} & \underline{0} & -S^e_{in} \\ -\underline{D}^i_{kj} & \underline{D}^i_{kl} & S^i_{kn} \\ -D^i_{mj} & D^i_{ml} & S^i_{mn} \end{bmatrix} \begin{bmatrix} u(x_j) \\ v(x_l) \\ t(x_n) \end{bmatrix}$$

$$= \begin{bmatrix} 0 \\ S^i_{kp} \\ S^i_{mp} \end{bmatrix} [\, S(x_p) \,] + \begin{bmatrix} -u_l(x_i) \\ 0 \\ 0 \end{bmatrix} , \tag{4.1.9.9}$$

and then apply the same method as has been used with (4.1.9.4) to the underlined part of the matrix in (4.1.9.9). Note that we obtain the $L\text{-}U$ decomposition of the submatrix denoted by D^i_{kl} during the triangular decomposition process of the whole matrix because the upper right block of the underlined submatrix in (4.1.9.9) is identically zero. Since D^i_{kl} is the BIEM matrix for a traction boundary value problem for a domain exterior to D_0 we recall (4.1.3.9) to justify this method. Table 4.1.9.1 shows some numerical examples for a lined circular hole. For the notation, see 4.1.10.b.ii).

Table 4.1.9.1

$\min_i |L_{ii}|$ versus wave number. $E_i\rho_e/E_e\rho_i=E_i/E_e=2/3$, $\nu_i=1/6$, $\nu_e=1/4$ $a/b=1.2$

$k_{Te}a$	$\min_i \lvert L_{ii} \rvert$	Eigenfrequency
0	0.4427	×
3.204	0.5624×10^{-2}	○
3.250	0.3288	×
3.365	0.3677×10^{-2}	○
6.144	0.1340	○
6.400	0.3486	×
6.637	0.7511×10^{-1}	○

4 . 1 . 10 Examples

In this section we shall show some 2D examples. The following remarks are common to all the examples.

(1) Plane strain is assumed.
(2) 8-point Gaussian quadrature formula is used.
(3) FACOM M200 of Kyoto University Data Processing Centre is used.

The following remarks apply to all the examples of the transient analyses:

(4) The frequencies up to $k_{Te}a \sim 7$ are taken into consideration in the analyses, where a is the characteristic length of the problem (indicated for every problem).
(5) The incident field is assumed to be a plane step stress wave having a magnitude of τ_0 and the time dependence shown in Fig.4.1.10.1. We tried several values of t^0 in the range of $30a \leqq t^0 c_{Te} \leqq 120a$. The results, however, were essentially identical.
(6) The time is measured from the arrival time of the incident wave at the origin (indicated for every problem).

a) Steady-state solutions

First of all, we shall show some results of the time-harmonic analysis.

We calculated the stresses around a circular hole having a radius of a subject to the incident plane harmonic P and S waves. These problems were investigated analytically by Pao(1962) and Mow & Mente(1963), respectively. (For additional references, see the monograph by Pao & Mow(1971)) Fig.4.1.10.2 shows the hoop stress due to the incident P wave. The real (imaginary) part of the solution gives the stress at the moment when the peak (node) of the incident wave arrives at the centre of the hole. Our results show an excellent agreement with the analytical solution by Pao. Fig.4.1.10.3 shows the peripheral stress versus the wave numbers of the incident P and S waves. The results also agree well with the analytical solutions. All the analyses were carried out employing 24 boundary elements.

We next tested the methods of Jones by using the same example. We calculated the hoop stress around a circular hole having a radius of a subject to plane time-harmonic P wave. Poisson's ratio is 1/4. The fictitious eigenfrequencies for this problem are the zeros of the following expression (Vekua(1968)):

$$J_{n+1}(k_T a) J_{n-1}(k_L a) + J_{n+1}(k_L a) J_{n-1}(k_T a), \quad n = 0,1,\ldots. \tag{4.1.10.1}$$

Indeed, one readily sees this from the expressions for $\Psi_j^{\eta i}(x)$ given in (4.1.5.6). As can be easily checked, $k_L a = 3.906$ $(n = 3)$ is one of the zeros of (4.1.10.1).

The numerical analysis is carried out as follows:

(1) 24 quadratic isoparametric elements using 8-point Gaussian quadrature are employed.

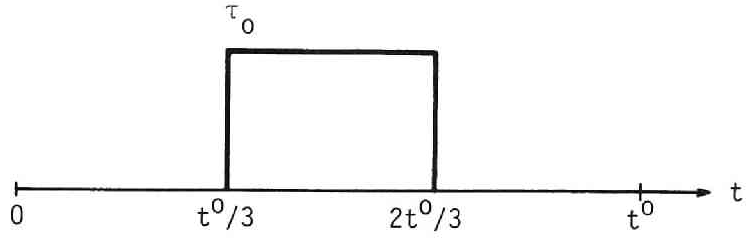

Fig.4.1.10.1 Incident stress history.

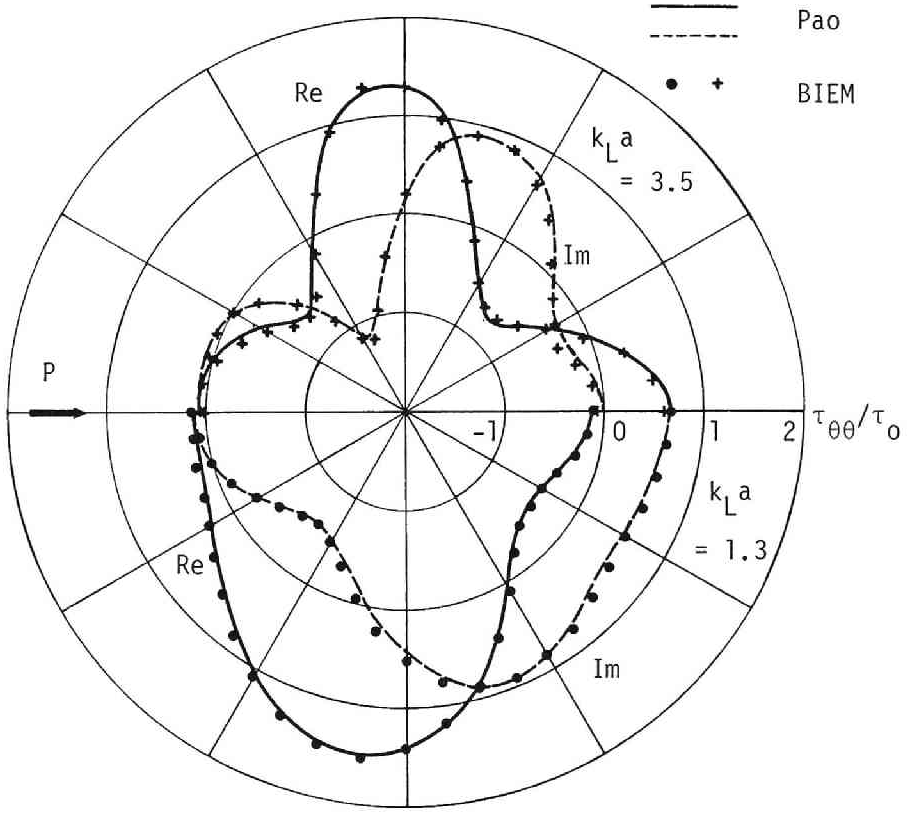

Fig.4.1.10.2 Steady state hoop stress distribution around a circular hole; incident P wave, ν = 0.26; lines: exact. symbols: BIE.

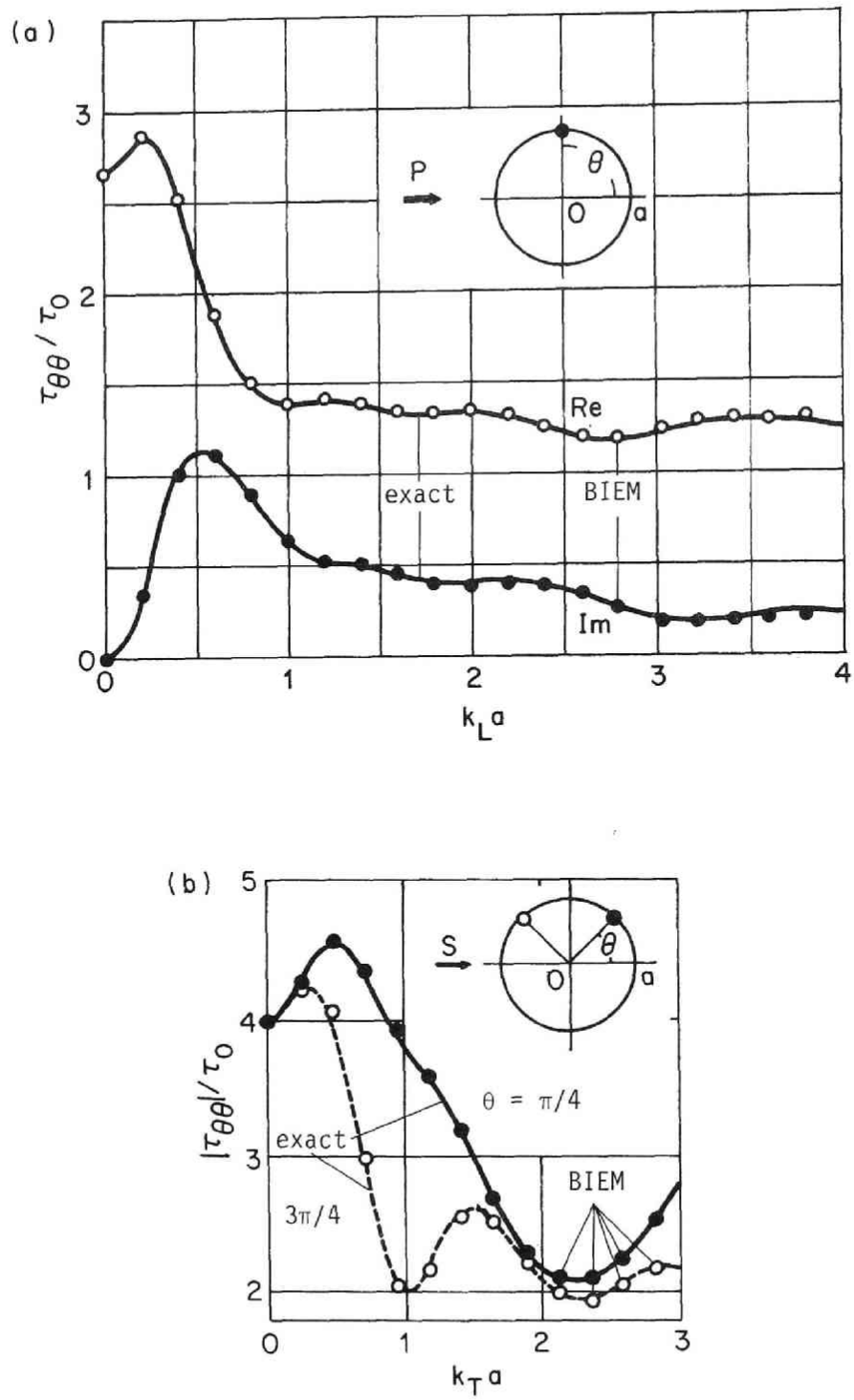

Fig.4.1.10.3 Steady state hoop stress. lines: exact. symbols: BIE. (a) Incident P wave, $\theta = \pi/2$. (b) Incident S wave, solid line: $\theta = \pi/4$. broken line: $\theta = 3\pi/4$.

(2) Boundary stress is calculated by differentiating boundary quantities directly with the help of (4.1.8.3).
(3) $M = 3$ for both first and second methods (See the lines below (4.1.6.1).).
(4) We set $\varepsilon_{ij} = -i/32\mu$.
(5) The first method requires the use of a least-square solver. We used the Householder transformations. For the second method, we used the Crout method.

Fig.4.1.10.4 shows the improvement of the result when $k_L a = 3.906$. The results of the both remedies have agreed completely. The imaginary parts of the conventional and modified BIE coincided by chance. This coincidence reflects the fact that the eigenmode is essentially real. Table 4.1.10.1 compares the CPU time of these methods. This result shows that the modified methods require about 30% more CPU time than the conventional method. The CPU time for the first and second methods are almost the same.

Table 4.1.10.1 CPU time (sec.)

	conventional BIE	first method	second method
make matrix	6.5	7.6	8.7
solver	0.5	1.7	0.5
total	7.0	9.3	9.2

Now, suppose that we attempt at a transient elastodynamic analysis by using m different frequencies with the conventional BIEM. The foregoing results tell that one should switch to Jones's methods if more than $m/3$ of these analyses yield inaccurate solutions due to the fictitious eigenfrequencies. In practical transient stress analysis, however, we are not likely to encounter this trouble of non-uniqueness that often. We shall therefore use the simple method of detecting fictitious eigenfrequencies described in 4.1.9.d) in the following analyses. It is to be remembered, however, that this conclusion is valid only in transient analysis, where one is not interested in a time-harmonic solution for a particular frequency. If one is, however, one should use the methods discussed in 4.1.3 ~ 4.1.6.

b) Transient stress and deformation states around a circular hole due to incident step waves

b.i) Transient response of a circular hole to the incident step waves

As the first example, we consider the transient response of a circular hole to the incident step tensile P wave. Poisson's ratio is 1/4. Fig.4.1.10.5 shows the peripheral stresses and deformations at the instant when the front of the incident wave reaches the indicated locations. Although a little tremor remains prior to the arrival of the incident wave, the amount is negligible from a practical point of view.

We compared the calculated stress and deformation histories at

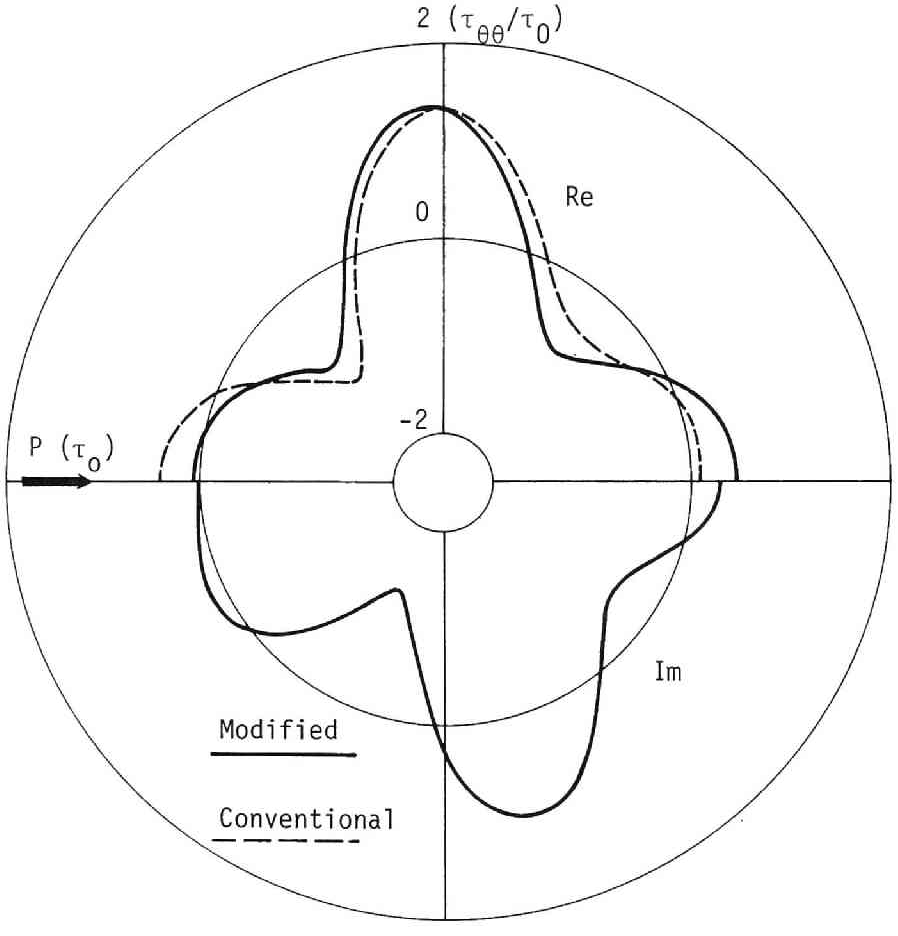

Fig.4.1.10.4 Hoop stress around a circular hole subject to plane time-harmonic P wave ($k_L a$ = 3.906, ν = 1/4).

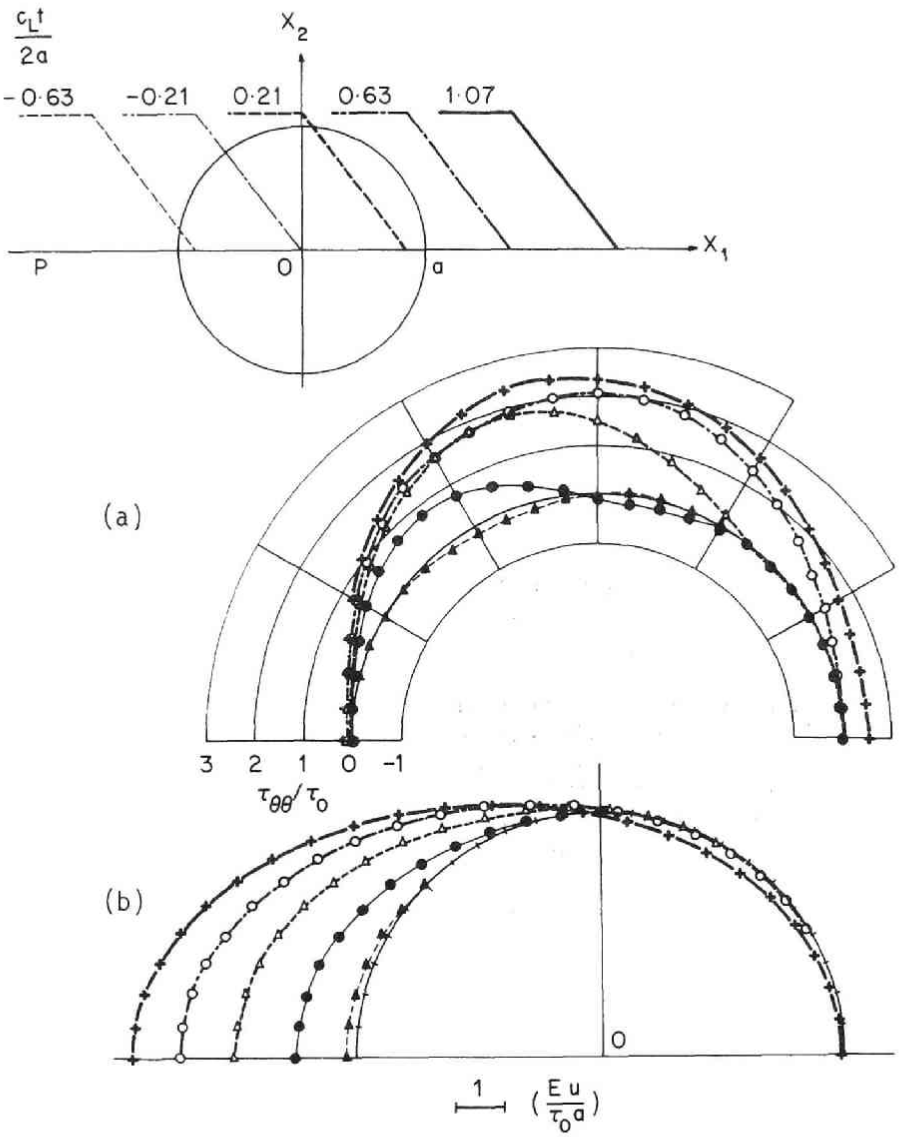

Fig.4.1.10.5 Transient stresses and deformations around a circular hole; incident P wave. (a) Hoop stress distribution. (b) Deformation of the boundary.

several boundary points with the approximate analytical results by Garnet & Crouzet-Pascal(1966) (Fig.4.1.10.6). Our results agree fairly well with theirs. We next calculated the transient response of a circular hole to the incident step S wave. Fig.4.1.10.7 shows the peripheral stresses and deformations at the moment when the incident wave front arrives at the specified positions. In Fig.4.1.10.8 we compared the stress histories obtained at several boundary points with the numerical results by Fujiki(1980), who used a time domain BIEM. Again these results agree quite well with each other.

All these analyses were carried out by using 24 boundary elements.

b.ii) Transient responses of a lined circular hole to the incident step waves

We consider the transient responses of a lined circular hole to the incident step waves. The following notation will be used:

a: outer radius of the lining, b: inner radius of the lining,
E: Young's modulus, ν, Poisson's ratio.

Also we shall put the subscript e (i) to the quantities relevant to the surrounding medium (lining).

Our calculations were carried out under the following conditions:

(1) 48 boundary elements are used.
(2) $\nu_e = 1/4$, $\nu_i = 1/6$, $\rho_e/\rho_i = 1$.
(3) $a/b = 1.2$.

As the first example, we show the responses to the step incident P wave. Fig.4.1.10.9 shows the peripheral stress ($\tau_{\theta\theta}$) histories at the indicated positions. The calculations were carried out for $E_i\rho_e/E_e\rho_i = E_i/E_e = 5/3$ and $2/3$.

We also analysed the responses to the incident S waves. The peripheral stress on the inner boundary of the lining at the indicated time is given in Fig.4.1.10.10. Also the tangential ($\tau_{\theta\theta}$) and shear ($\tau_{\theta r}$) stress histories at the indicated locations are plotted in Fig.4.1.10.11.

c) Transient responses of a lined horseshoe-shaped tunnel to the incident step S wave

We calculated the transient response of a lined horseshoe-shaped tunnel to the incident step S wave using the model depicted in Fig.4.1.10.12. The analysis was carried out under the same conditions as stated in 4.1.10.b). Also, we set $E_i/E_e = 5$.

Fig.4.1.10.12 shows the deformation during the passage of the wave front. The incident angle Θ is $\pi/4$ as shown in Fig.4.1.10.12. The tangential and shear stress histories at the indicated positions are given in Fig.4.1.10.13.

d) Transient responses of a pair of caverns to the incident step S wave

We calculated the transient responses of the pair of caverns, a typical shape of underground power stations, to the incident step S

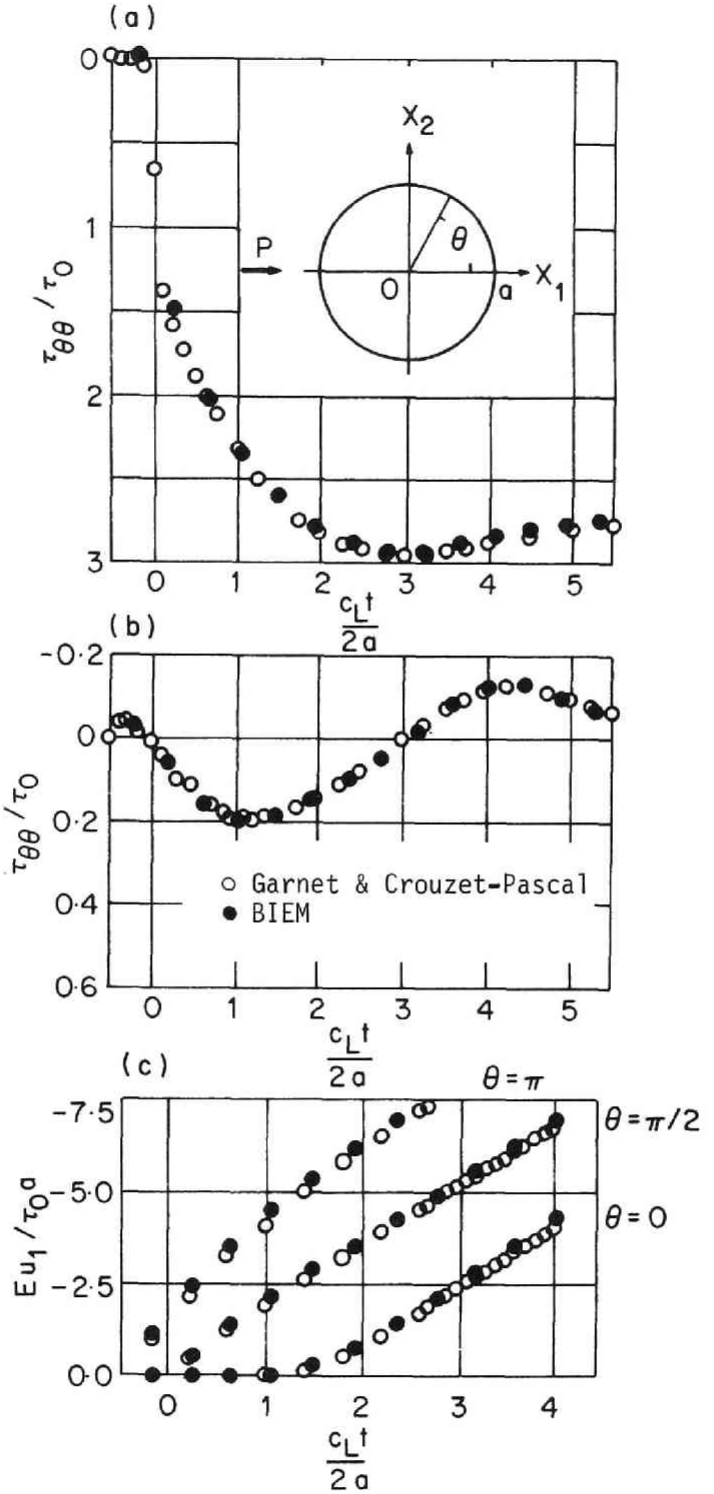

Fig.4.1.10.6 Transient stresses and deformations around a circular hole; incident P wave. (a) Hoop stress at $\theta = \pi/2$. (b) Hoop stress at $\theta = \pi$. (c) Displacement (u_1) at $\theta = 0$, $\pi/2$, and π.

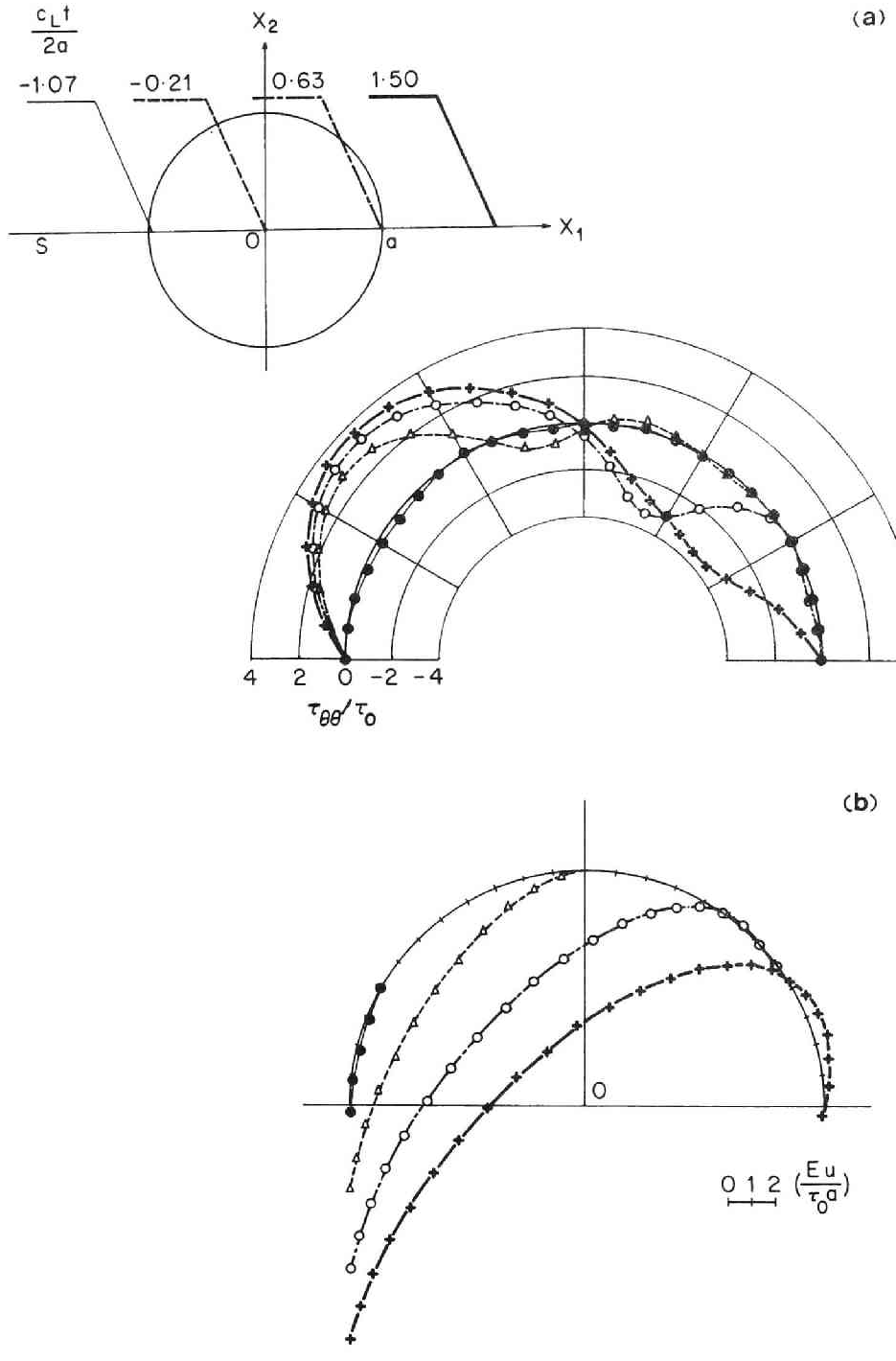

Fig.4.1.10.7 Transient stresses and deformations around a circular hole; incident S wave. (a) Hoop stress distribution. (b) Deformation of the boundary.

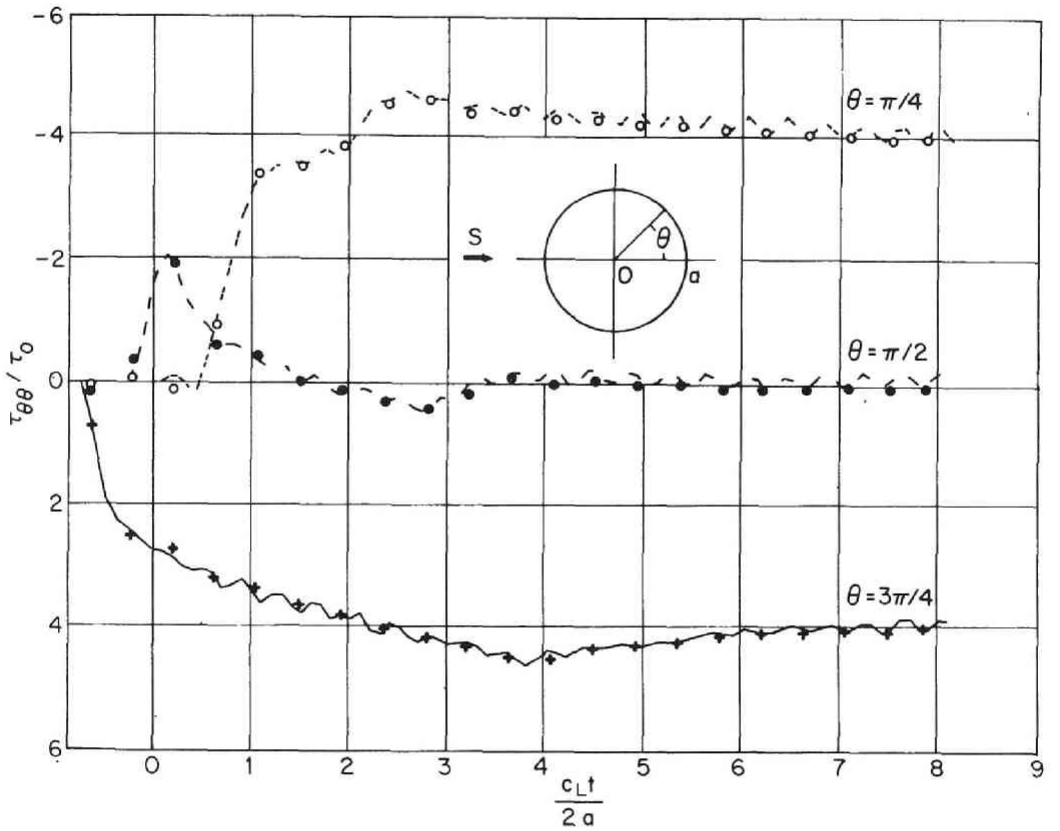

Fig.4.1.10.8 Transient hoop stresses around a circular hole; incident S wave. symbols: present method. lines: time domain BIEM.

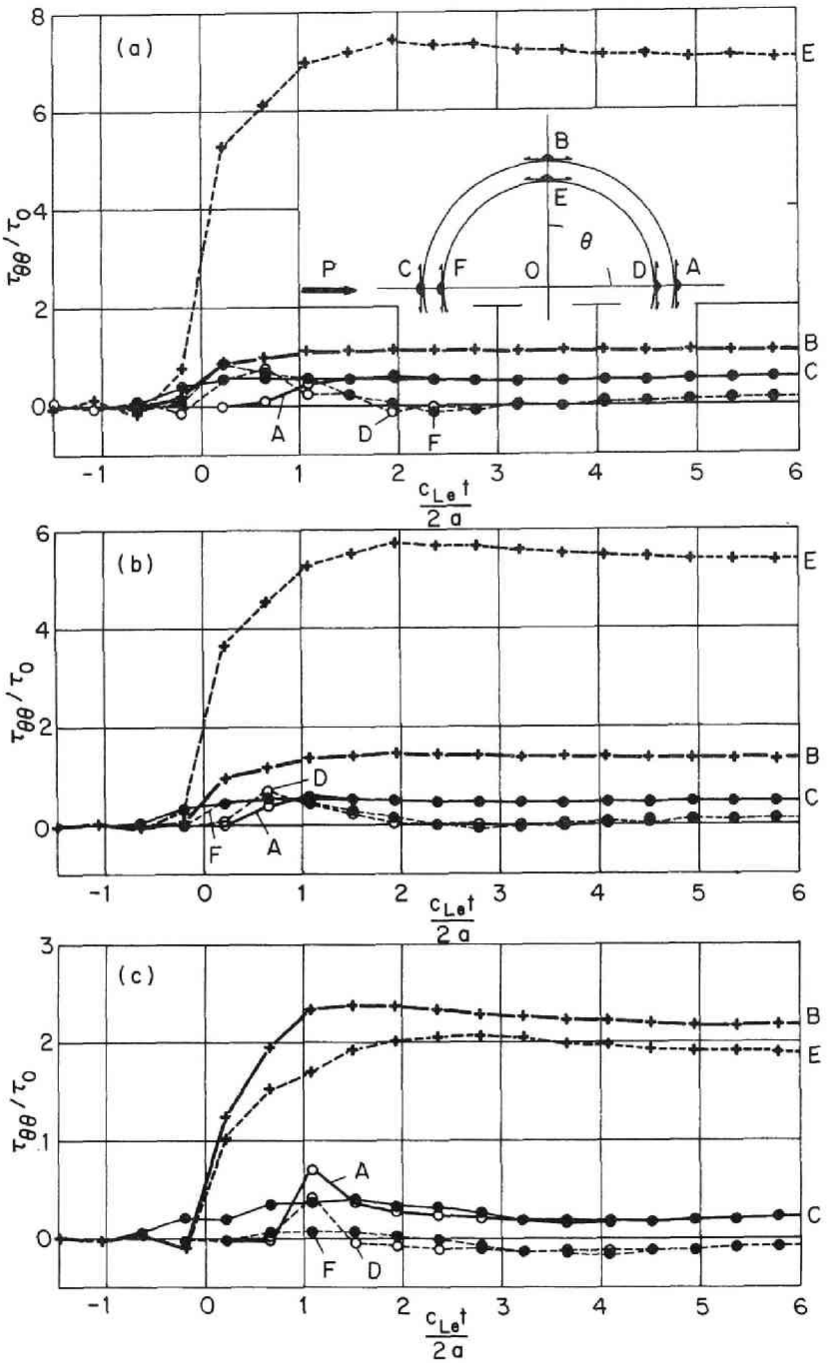

Fig.4.1.10.9 Transient tangential stresses around a lined circular hole; incident P wave. (a) E_i/E_e = 5. (b) E_i/E_e = 3. (c) E_i/E_e = 2/3.

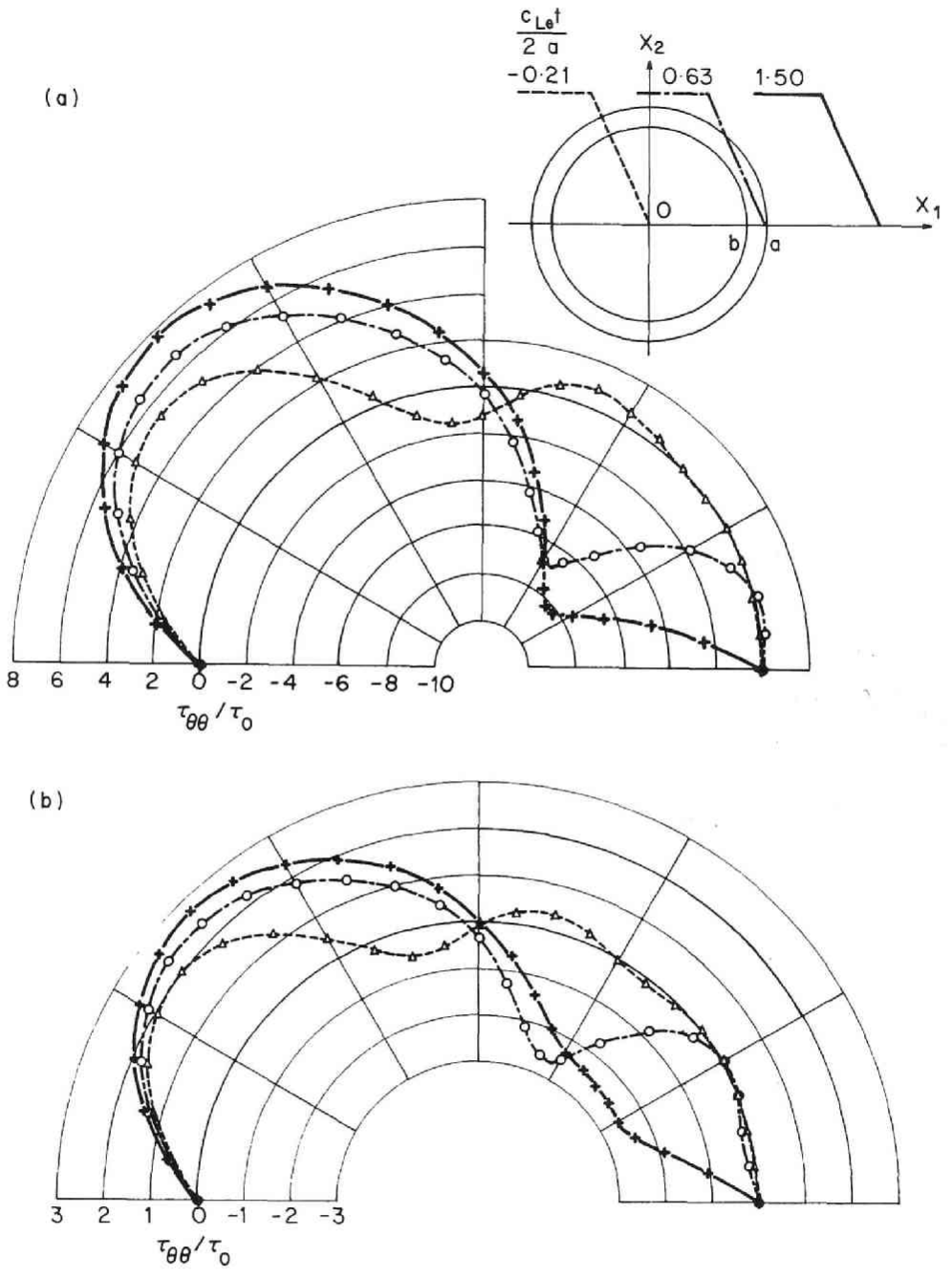

Fig.4.1.10.10 Transient stress distribution around a lined circular hole; incident S wave. $\tau_{\theta\theta}$ on the inner face of the lining. (a) E_i/E_e = 3. (b) E_i/E_e = 2/3.

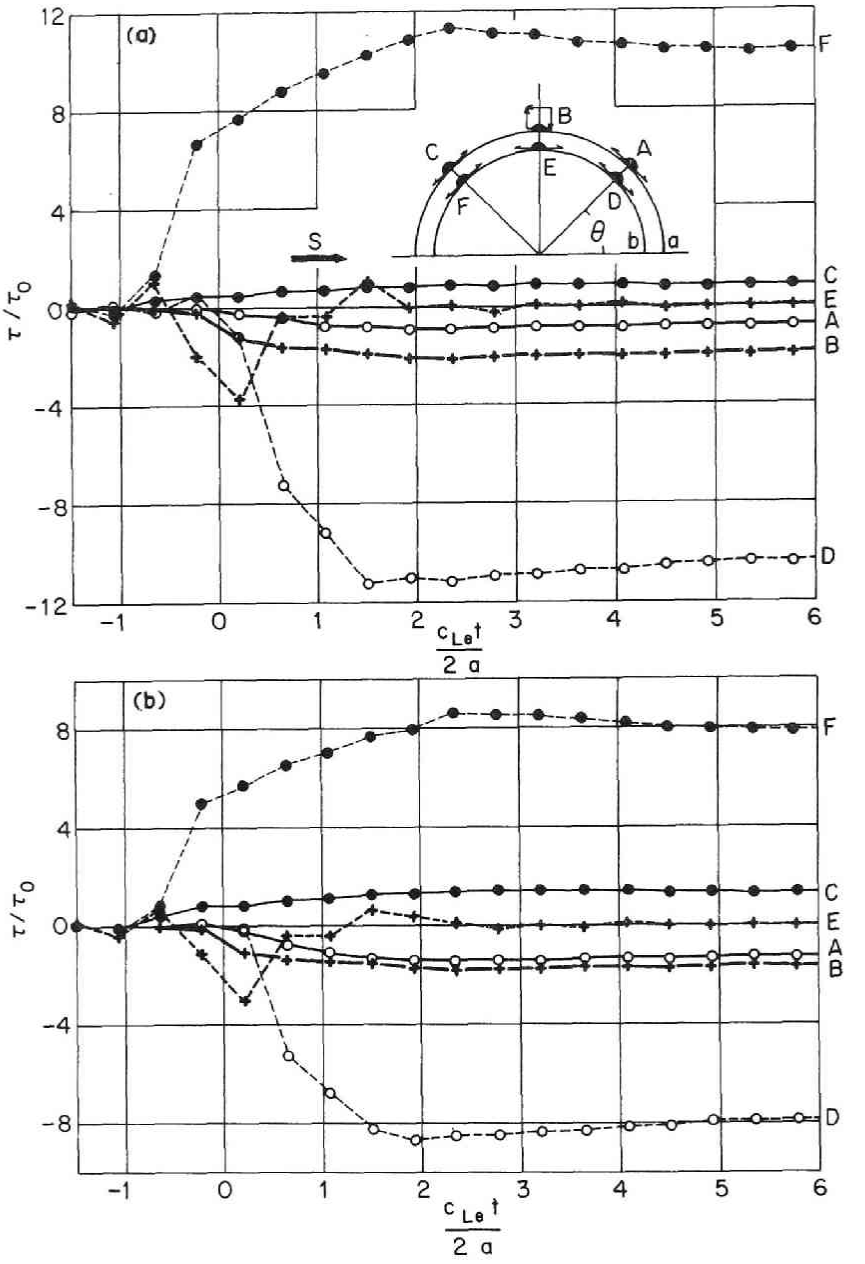

Fig.4.1.10.11 Transient stress around a lined circular hole; incident S wave. A,C-F: tangential stress. B: Shear stress. (a) E_i/E_e = 5. (b) E_i/E_e = 3. (c) E_i/E_e = 2/3.

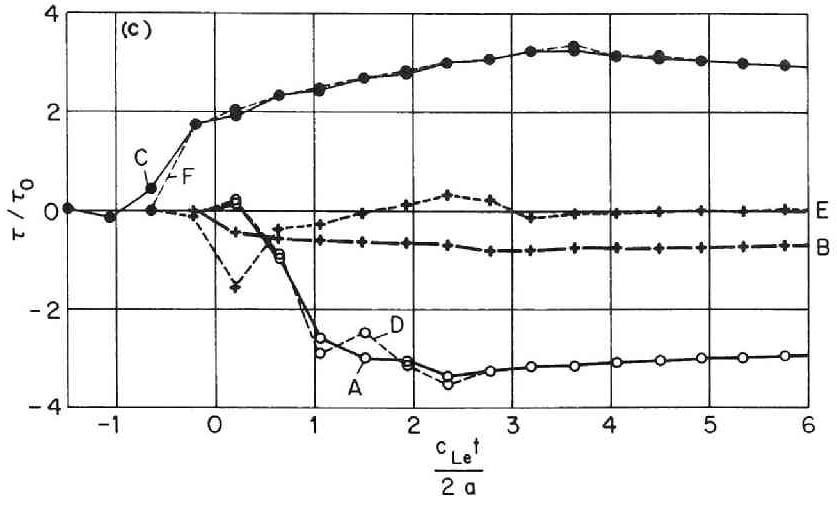

Fig.4.1.10.11 Continued.

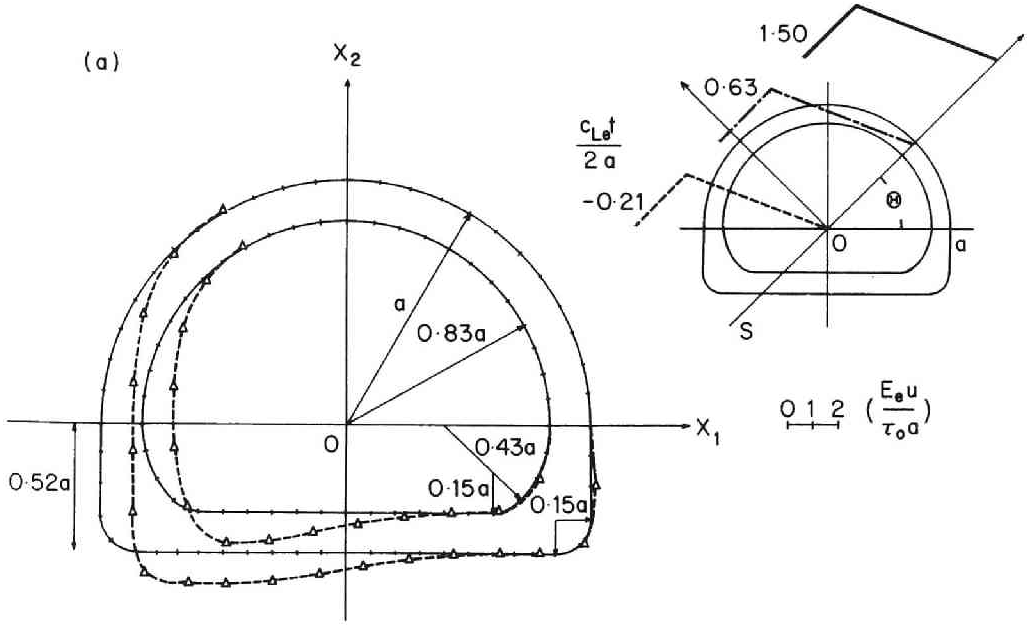

Fig.4.1.10.12 Transient deformation of a horseshoe-shaped tunnel; incident S wave.

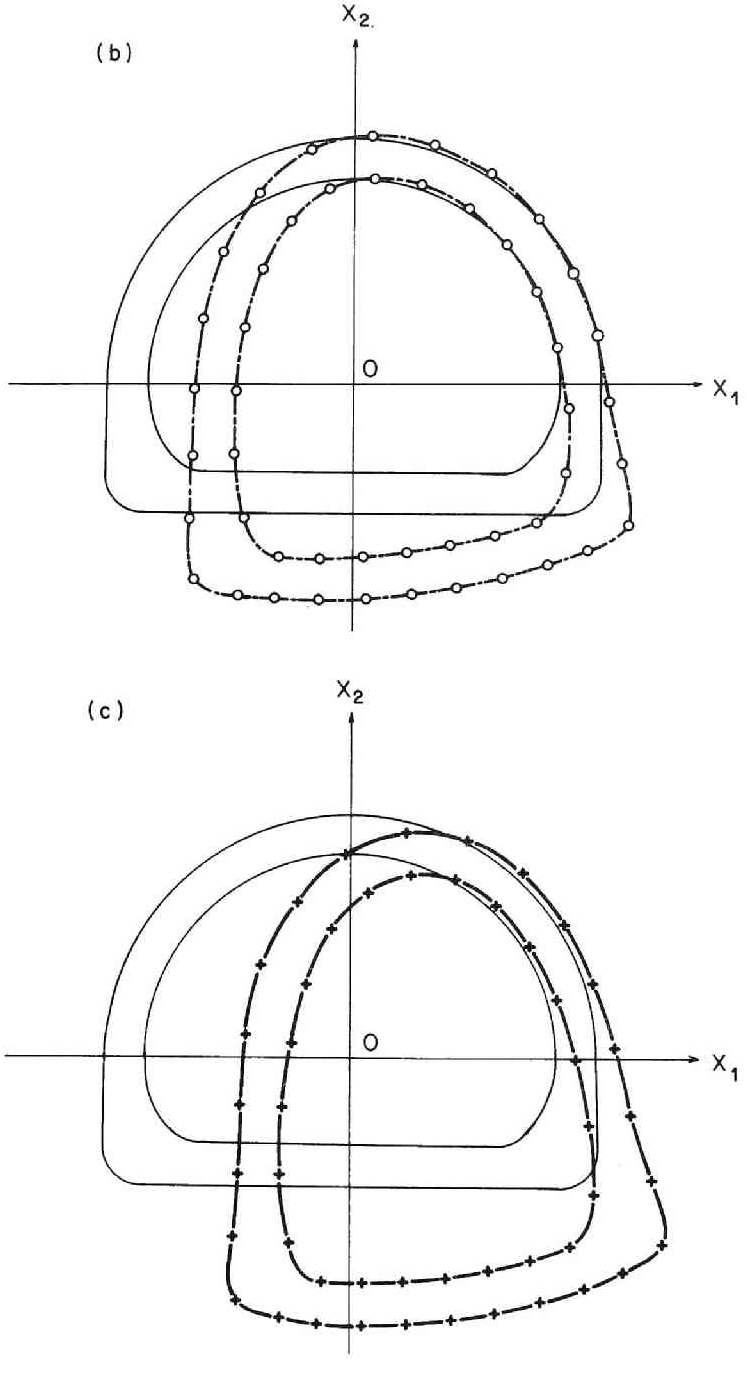

Fig.4.1.10.12 Continued.

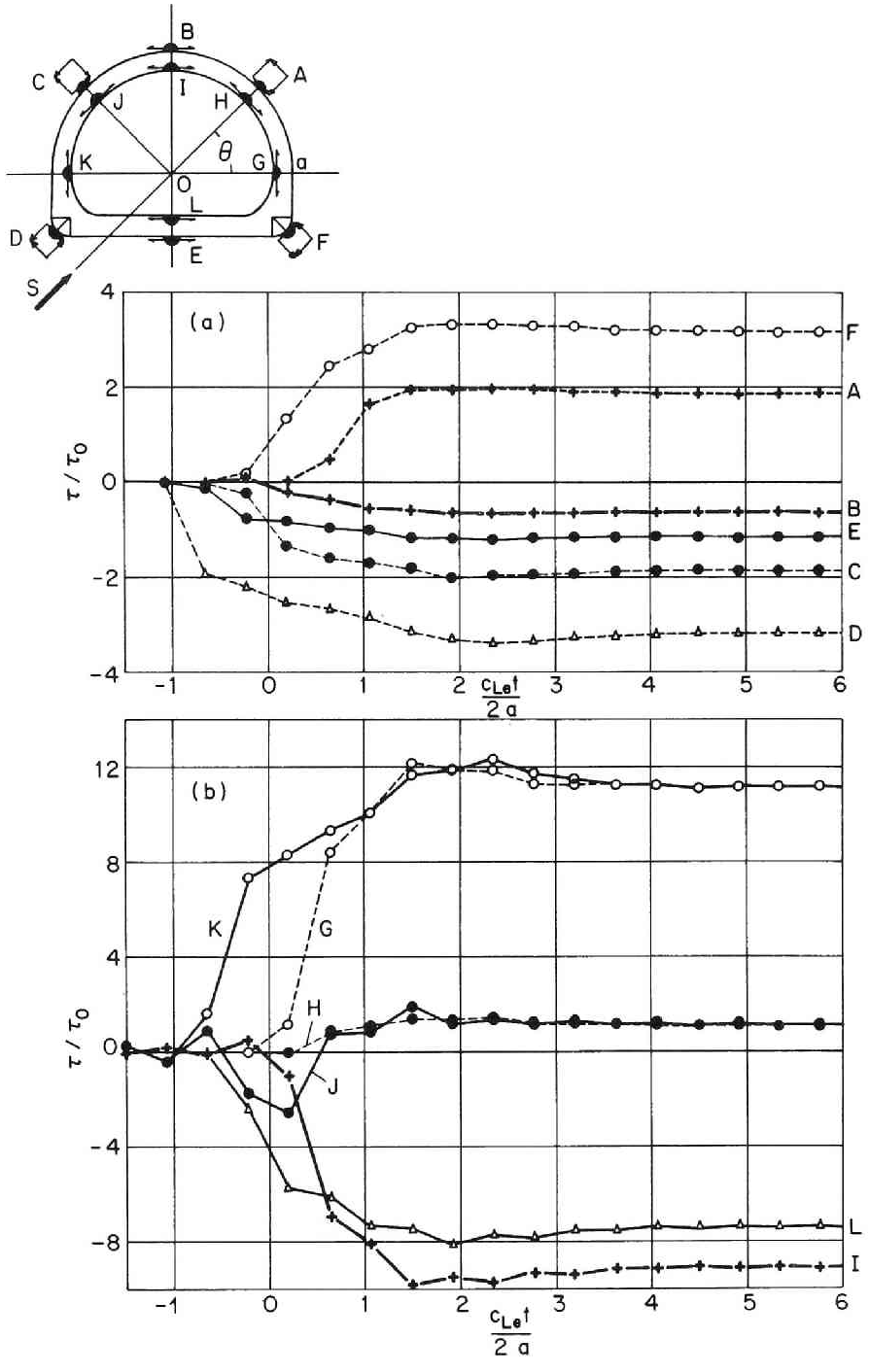

Fig.4.1.10.13 Transient stresses around a horseshoe-shaped tunnel; incident S wave. A,C,D,F: shear stress. B,G-L: tangential stress. (a) stresses in the surrounding medium. (b) stresses on the inner face of the lining.

wave. The incident angle Θ is $\pi/4$, and Poisson's ratio is 1/4.

Figs.4.1.10.14 and 4.1.10.15 show the deformation during the passage of the incident wave and the peripheral stress histories at the indicated points, respectively.

We employed 54 boundary elements for the analysis.

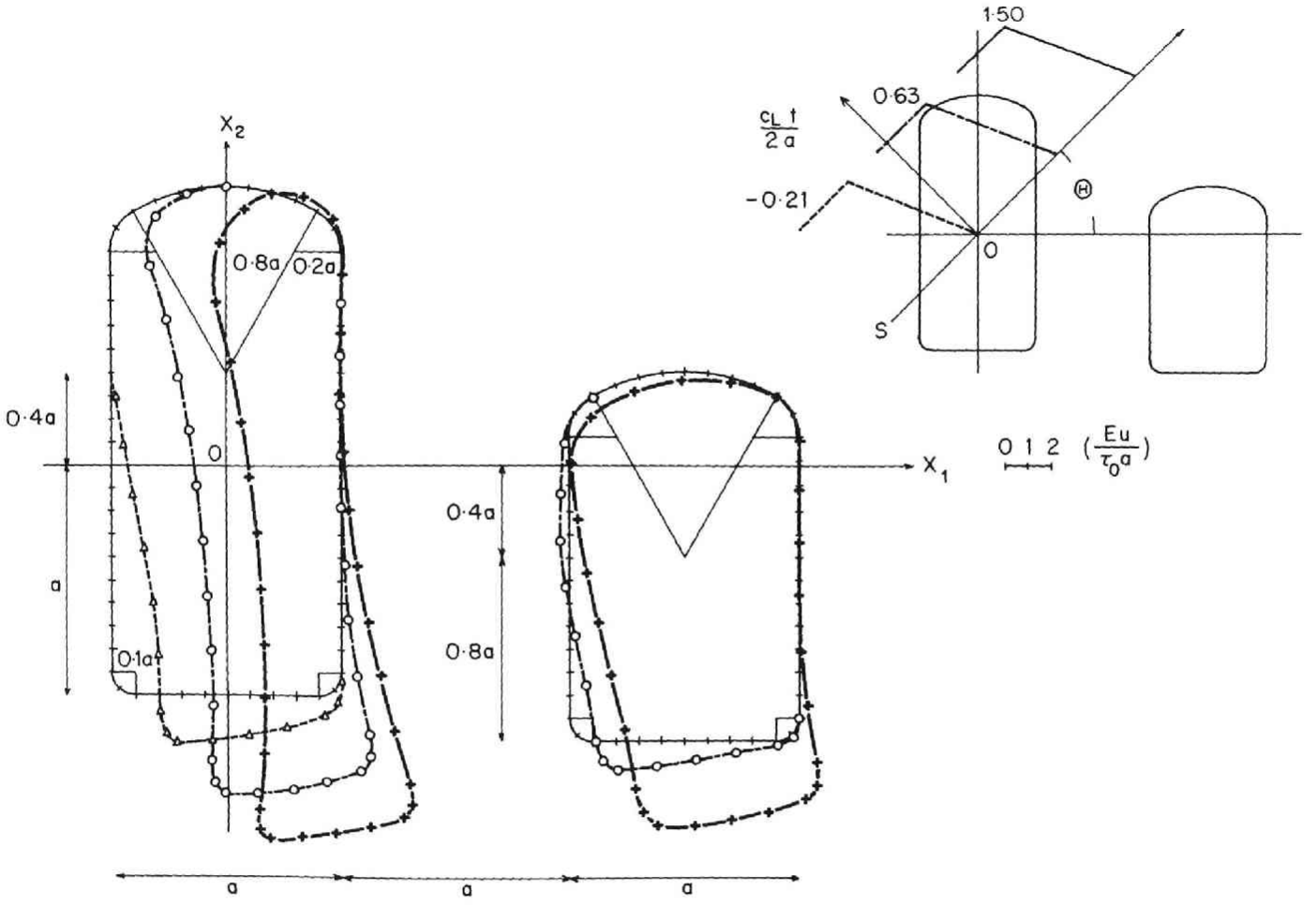

Fig.4.1.10.14 Transient deformation of a pair of caverns; incident S wave.

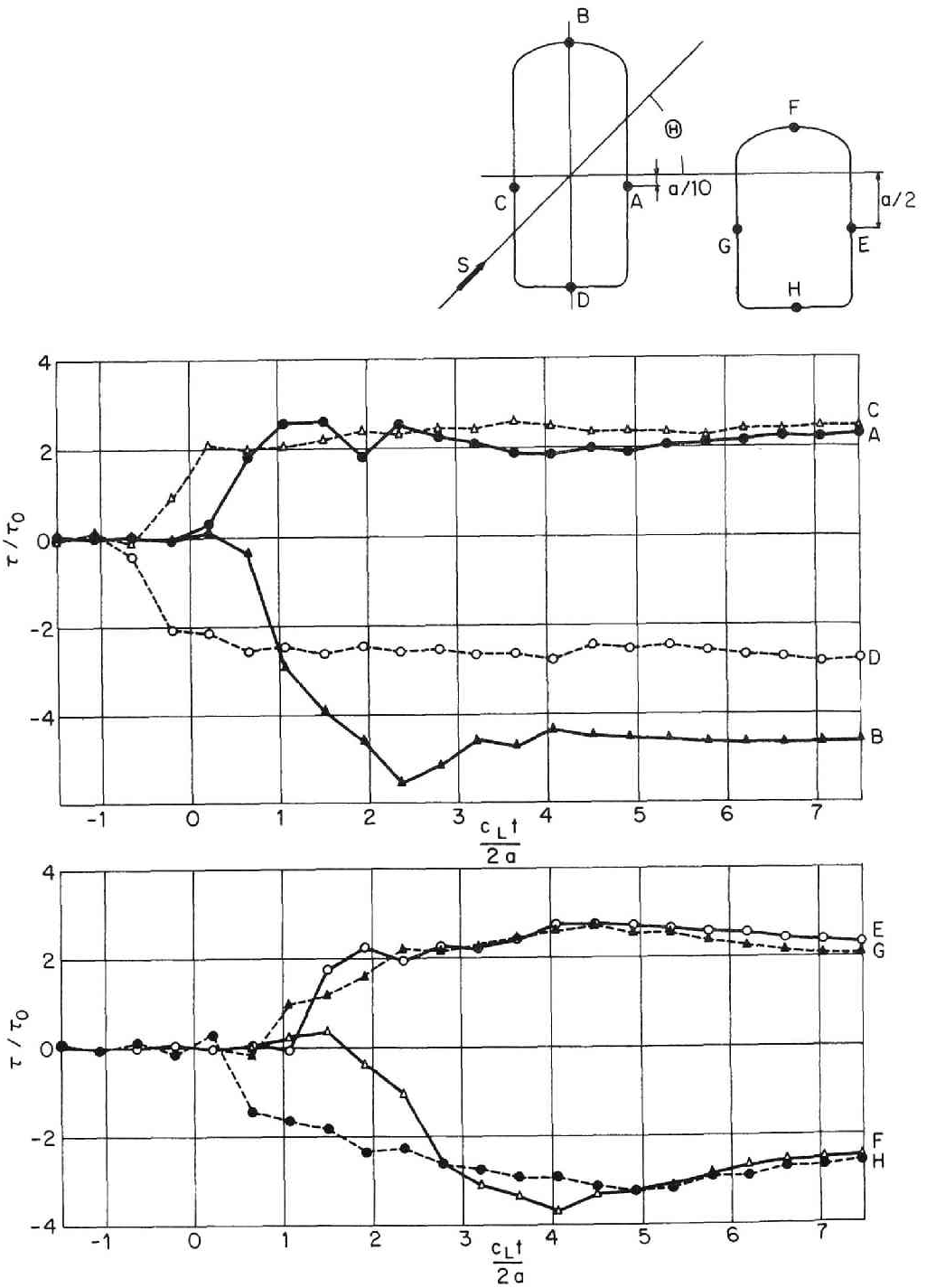

Fig.4.1.10.15 Transient hoop stresses around a pair of caverns; incident S wave.

4 . 2 Half-plane problems

In the rest of this chapter, we discuss the application of BIEM to half-plane problems.

Let $(x_1(\sigma),\ x_2(\sigma))$ $(-\infty<\sigma<\infty)$ be a smooth non-self-intersecting contour satisfying

$$\lim_{\sigma\to\infty}\begin{bmatrix} x_1(\sigma) \\ x_2(\sigma)\end{bmatrix} = [\ \infty\ 0\ ],\quad \lim_{\sigma\to-\infty}\begin{bmatrix} x_1(\sigma) \\ x_2(\sigma)\end{bmatrix} = \begin{bmatrix} -\infty \\ 0\end{bmatrix},$$

$$|\,x_2(\sigma)\,| < C,\quad (-\infty<\sigma<\infty). \tag{4.2.1a-c}$$

We denote by D the domain located above $(x_1(\sigma),\ x_2(\sigma))$ (Hence $(0,\infty)\in D$.) and having possibly finite number of holes of finite linear dimension. We also denote the union of $(x_1(\sigma),\ x_2(\sigma))$ and the hole boundaries by ∂D (See Fig.4.2.1).

We now consider the problem of determining the time-harmonic elastodynamic displacement field in D generated by an incident field $\boldsymbol{u}_I$ which satisfies (4.1.1.8), and by a traction $\boldsymbol{t}_0$ on ∂D :

$$\boldsymbol{t} := T\boldsymbol{u} = \boldsymbol{t}_0 \quad \text{on } \partial D. \tag{4.2.2}$$

For solving this problem we introduce the notion of a radiating field: A displacement field $\boldsymbol{u}$ which allows an integral representation

$$\tilde{\boldsymbol{u}}(\boldsymbol{x}) = \int_{\partial D}\Gamma(\boldsymbol{x},\boldsymbol{y})\,\boldsymbol{t}(\boldsymbol{y})\mathrm{d}S - \int_{\partial D}\Gamma_I(\boldsymbol{x},\boldsymbol{y})\boldsymbol{u}(\boldsymbol{y})\mathrm{d}S,\ \ \boldsymbol{x}\in R^2\backslash\partial D \tag{4.2.3}$$

is called a radiating field where $\tilde{\boldsymbol{u}}$ is defined in (4.1.1.16).

We now split the whole displacement field $\boldsymbol{u}$ into a sum of an incident field $\boldsymbol{u}_I$ and a radiating field $\acute{\boldsymbol{u}}_R$. By assumption $\acute{\boldsymbol{u}}_R$ satisfies the equation

$$\frac{\acute{\boldsymbol{u}}_R(\boldsymbol{x})}{2} = \int_{\partial D}\Gamma(\boldsymbol{x},\boldsymbol{y})\,\acute{\boldsymbol{t}}_R(\boldsymbol{y})\mathrm{d}S - \mathrm{v.p.}\int_{\partial D}\Gamma_I(\boldsymbol{x},\boldsymbol{y}))\acute{\boldsymbol{u}}_R(\boldsymbol{y})\mathrm{d}S_y\ ,$$

$$\boldsymbol{x}\in\partial D \tag{4.2.4}$$

where $\acute{\boldsymbol{t}}_R$ is the traction associated with $\acute{\boldsymbol{u}}_R$. One may think of computing the total field $\boldsymbol{u}$ by solving a BIE obtained form (4.2.4) and (4.2.2), followed by the use of

$$\boldsymbol{u}(\boldsymbol{x}) = \boldsymbol{u}_I(\boldsymbol{x}) + \int_{\partial D}\Gamma(\boldsymbol{x},\boldsymbol{y})\,\acute{\boldsymbol{t}}_R(\boldsymbol{y})\mathrm{d}S_y - \int_{\partial D}\Gamma_I(\boldsymbol{x},\boldsymbol{y})\acute{\boldsymbol{u}}_R(\boldsymbol{y})\mathrm{d}S_y.\quad \boldsymbol{x}\in D \tag{4.2.5}$$

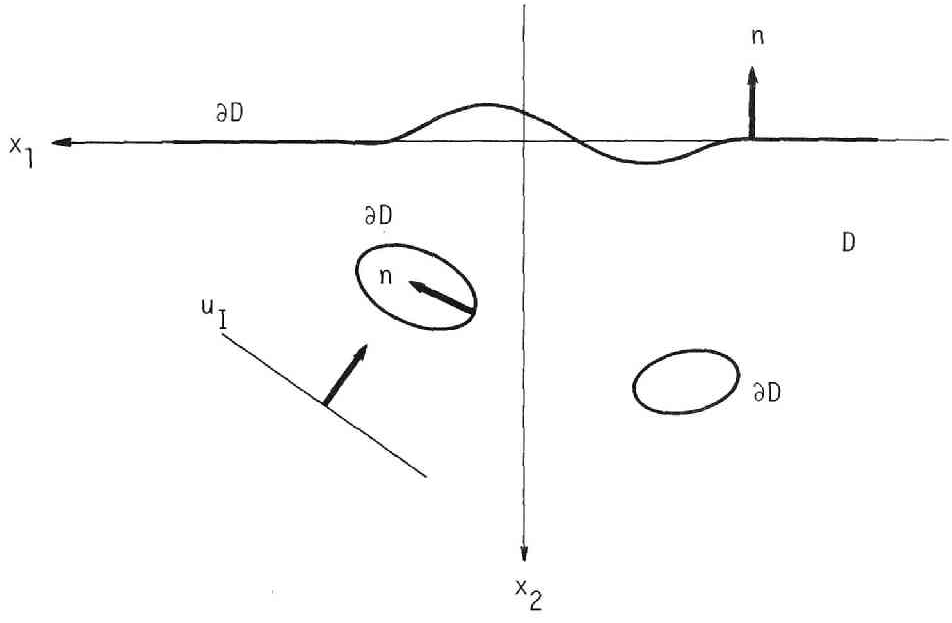

Fig.4.2.1 Half-planar domain.

This method, however, does not work, as we shall see. Consider, for example, the case where D is a half plane defined by $x_2>0$. Then the integral equation obtained from (4.2.4) and (4.2.2) is seen not to have a unique solution. Indeed, the surface displacement generated by Rayleigh waves satisfies the homogeneous version of (4.2.4).

This trouble, however, can be avoided if the displacement field u_H (sometimes called the free field) generated by u_I in a traction free half plane admits an analytical continuation into D. In this case, we replace (4.2.5) by

$$u(x) = u_H(x) + \int_{\partial D} \Gamma(x,y)\, t_R(y) dS_y - \int_{\partial D} \Gamma_I(x,y) u_R(y) dS_y \qquad x \in D \quad (4.2.6)$$

and solve

$$\frac{u_R(x)}{2} = \int_{\partial D} \Gamma(x,y)\, t_R(y) dS - \text{v.p.} \int_{\partial D} \Gamma_I(x,y)) u_R(y) dS_y \ ,$$

$$x \in \partial D \qquad (4.2.7)$$

subject to

$$\frac{\partial u_R}{\partial x_1} - \text{sgn}(x_1) i k_R u_R \to 0 \qquad \text{as } |x| \to \infty, \qquad (4.2.8)$$

where k_R is the wave number of Rayleigh waves. The condition in (4.2.8) is introduced so that the solution u_R of (4.2.7) includes only the outgoing Rayleigh waves. The next section introduces a numerical method based on (4.2.7) and (4.2.8).

4 . 2 . 1 Method of truncation

Equation (4.2.7) is a singular integral equation defined on a boundary having an infinite length. Hence the BIEMs developed so far cannot be used directly with (4.2.7) because these methods solve problems with boundaries of finite linear dimension only. We therefore have to devise a new numerical method.

A simple method of solution for (4.2.7) is to truncate the boundary and to take into consideration only a finite part of the original boundary. Namely, we solve (4.2.7) with ∂D replaced by a truncated boundary ∂D_t . Obviously, we may also view this approach as solving (4.2.7) and (4.2.2) on ∂D_t rather than on ∂D under a constraint given by

$$u_R = 0 \qquad \text{on} \quad \partial D \backslash \partial D_t \, . \qquad (4.2.1.1)$$

We may therefore expect that the method of truncation yields an approximate solution to the problem defined by (4,2,7), (4.2.2) and (4.2.8), since (4.2.1.1) loosely corresponds to (4.2.8).

In 4.2.3 we shall carry out a numerical experiment in order to test this truncation approach. Before doing this, however, we shall prepare a more reliable (but not necessarily practical) BIE formulation for half-plane problems which uses the Green's function for a traction free half plane. This Green's function approach will be used to obtain a 'reference' solution for assessing the applicability of the method of truncation.

4 . 2 . 2 Method of Green's function

Let D be an upper half-planner domain having possibly an indentation and/or holes. The boundary of infinite length $x_1(\sigma)$, $x_2(\sigma)$ is assumed to satisfy

$$x_1(\sigma) = \sigma, \ x_2(\sigma) = 0, \qquad (|\sigma| > {}^{\exists}a > 0)$$

$$x_2(\sigma) > 0. \qquad (|\sigma| < a) \tag{4.2.2.1a,b}$$

We consider a boundary value problem for (4.1.1.8) in D with boundary conditions given by

$$\boldsymbol{t} := T\boldsymbol{u} = \begin{cases} 0 & \text{on} \quad x_2 = 0, \ |x_1| > a, \\ t_0 & \text{for the rest of } \partial D. \end{cases} \tag{4.2.2.2}$$

By definition u_H satisfies

$$Tu_H = 0 \qquad \text{on} \quad x_2 = 0. \tag{4.2.2.3}$$

Also, u_R, defined by $u_R = u - u_H$, has a representation given by

$$u_R(x) = \int_S G(x,y)\, t_R(y)\, dS_y - \int_S (T_y G(x,y))^T u_R(y)\, dS_y, \quad x \in D \tag{4.2.2.4}$$

where $G(x,y)$ is the Green function for the upper half-plane which satisfies

$$T_y G(x,y) = 0, \ (y_2 = 0, \ x_2 > 0) \tag{4.2.2.5}$$

and S is a finite subset of ∂D defined by

$$S = \partial D \setminus \{ (x_1, 0) | \quad |x_1| \geqq a \}. \tag{4.2.2.6}$$

Equation (4.2.2.4) yields an integral equation on S, which can be solved with the help of the conventional BIE techniques since S is bounded.

In many problems of practical interest such as the cases of incident plane waves, we can write u_H explicitly. Hence we may now proceed to the determination of $G(x,y)$; a classical problem considered originally by Lamb(1904). The well established method of Fourier transform readily gives

$$G_{ij}(\boldsymbol{x},\boldsymbol{y}) = \Gamma_{ij}(\boldsymbol{x},\boldsymbol{y}) + \Gamma_{ij}(\boldsymbol{x},\boldsymbol{y}') - \mathfrak{F}^{-1}_{\xi\to(x_1-y_1)}\frac{1}{\mu k_T^2 F(\xi)}\begin{bmatrix} A & B \\ C & D \end{bmatrix}, \qquad (4.2.2.7)$$

where

$$A = \frac{\xi^2}{R_L}\left(2R_LR_Te^{-x_2R_T} - (2\xi^2-k_T^2)e^{-x_2R_L}\right)\left(2R_LR_Te^{-y_2R_T} - (2\xi^2-k_T^2)e^{-y_2R_L}\right),$$

$$B = -i\xi\left(2\xi^2e^{-x_2R_L} - (2\xi^2-k_T^2)e^{-x_2R_T}\right)\left(2R_TR_Le^{-y_2R_L} - (2\xi^2-k_T^2)e^{-y_2R_T}\right),$$

$$C = i\xi\left(2\xi^2e^{-x_2R_T} - (2\xi^2-k_T^2)e^{-x_2R_L}\right)\left(2R_LR_Te^{-y_2R_T} - (2\xi^2-k_T^2)e^{-y_2R_L}\right),$$

$$D = \frac{\xi^2}{R_T}\left(2R_TR_Le^{-x_2R_L} - (2\xi^2-k_T^2)e^{-x_2R_T}\right)\left(2R_LR_Te^{-y_2R_L} - (2\xi^2-k_T^2)e^{-y_2R_T}\right),$$

$$R_{L,T}=\sqrt{\xi^2-k_{L,T}^2}\,. \qquad (4.2.2.8a\text{-}e)$$

In (4.2.2.8) the branches for the radicals are taken as the limiting absorption principle ($\mathrm{Im}\ k_{L,T}\downarrow 0$) requires. Hence they are continuous and $R_{L,T}\sim|\xi|$ as $|\xi|\to\infty$ on the real axis. Also, $F(\xi)$ signifies the Rayleigh function defined by

$$F(\xi) = (2\xi^2-k_T^2)^2 - 4\xi^2R_LR_T, \qquad (4.2.2.9)$$

and y' indicates the mirror image of y with respect to $x_2 = 0$. The expression in (4.2.2.7) involves an inverse transform which can only be carried out numerically.

Our next step is to establish an effective numerical method of inverting the $\mathfrak{F}$ transform in (4.2.2.7). Since (4.2.2.7) is too complicated, however, we extract from (4.2.2.7) a typical term given by

$$\int_{-\infty}^{\infty}\frac{\xi^2R_T(2\xi^2-k_T^2)e^{-x_2R_T-y_2R_L+i\xi x}}{F(\xi)}d\xi, \qquad x = x_1 - y_1, \qquad (4.2.2.10a,b)$$

and discuss our method of inversion with (4.2.2.10a), where the path of integration in (4.2.2.10a) is as shown in Fig.4.2.2.1.

There are three reasons which make the evaluation of this integral difficult. The first is that the limits of the integration are $\pm\infty$. The second is that the integrand is oscillatory. The third is the

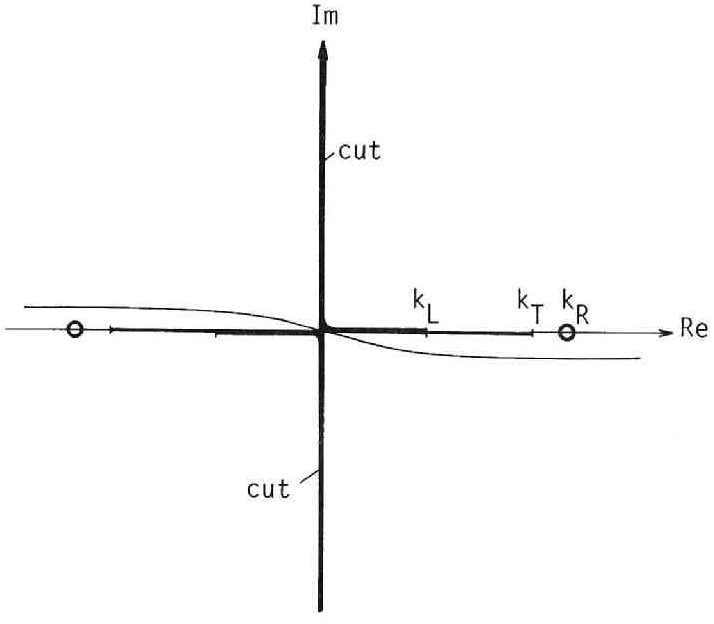

Fig.4.2.2.1 Path of integration and cuts.

singularity of the integrand at the Rayleigh poles. We here avoid these troubles by using a method of contour integration.

To begin with we observe that the exponent

$$-x_2R_T-y_2R_L+i\xi x \tag{4.2.2.11}$$

approaches on the complex plane to

$$(-x_2-y_2+ix)\xi \qquad \text{in the 1st and 4th quadrant}$$

$$(x_2+y_2+ix)\xi \qquad \text{in the 2nd and 3rd quadrant} \tag{4.2.2.12a,b}$$

asymptotically as $|\xi|\to\infty$, where we have made the radicals in (4.2.2.11) single valued by using the cuts shown in Fig.4.2.2.1. We therefore see that the exponent is asymptotically real negative on the paths defined by

$$\xi = \begin{cases} (x_2+y_2+ix)s/\overline{R}^2 \\ -(x_2+y_2)+ix)\,s/\overline{R}^2 \end{cases} \qquad (s\geqq 0) \tag{4.2.2.13}$$

where $\overline{R}^2=x^2+(x_2+y_2)^2$. This suggests that the change of the path of integration from the original path to the new one shown in Fig.4.2.2.2 would prevent the oscillation of the integrand. At the same time, this change of path eliminates the difficulty caused by the infinite integration limits because the Laguerre quadrature formulae for

$$\int_0^\infty f(t)e^{-t}dt \tag{4.2.2.14}$$

is applicable to our integral. This is because the integrand in the integral in (4.2.2.10) decays exponentially on the new path. Consequently, we perform the change of the path of integration in (4.2.2.10), followed by the addition of the residue contribution to (4.2.2.10) from the Rayleigh poles, to have

$$\int_{-\infty}^{\infty}\frac{\xi^2R_T(2\xi^2-k_T{}^2)e^{-x_2R_T-y_2R_L+i\xi x}}{F(\xi)}d\xi$$

$$=\int_0^\infty\left[\left(\frac{x_2+y_2+ix}{\overline{R}^2}\right)\frac{\xi_1^2\sqrt{\xi_1^2-k_T{}^2}\,(2\xi_1^2-k_T{}^2)e^{-x_2\sqrt{\xi_1^2-k_T^2}-y_2\sqrt{\xi_1^2-k_L^2}+i\xi_1x}}{F(\xi_1)}\right.$$

$$\left.+\left(\frac{x_2+y_2-ix}{\overline{R}^2}\right)\frac{\xi_2^2\sqrt{\xi_2^2-k_T{}^2}\,(2\xi_2^2-k_T{}^2)e^{-x_2\sqrt{\xi_2^2-k_T^2}-y_2\sqrt{\xi_2^2-k_L^2}+i\xi_2x}}{F(\xi_2)}\right]ds$$

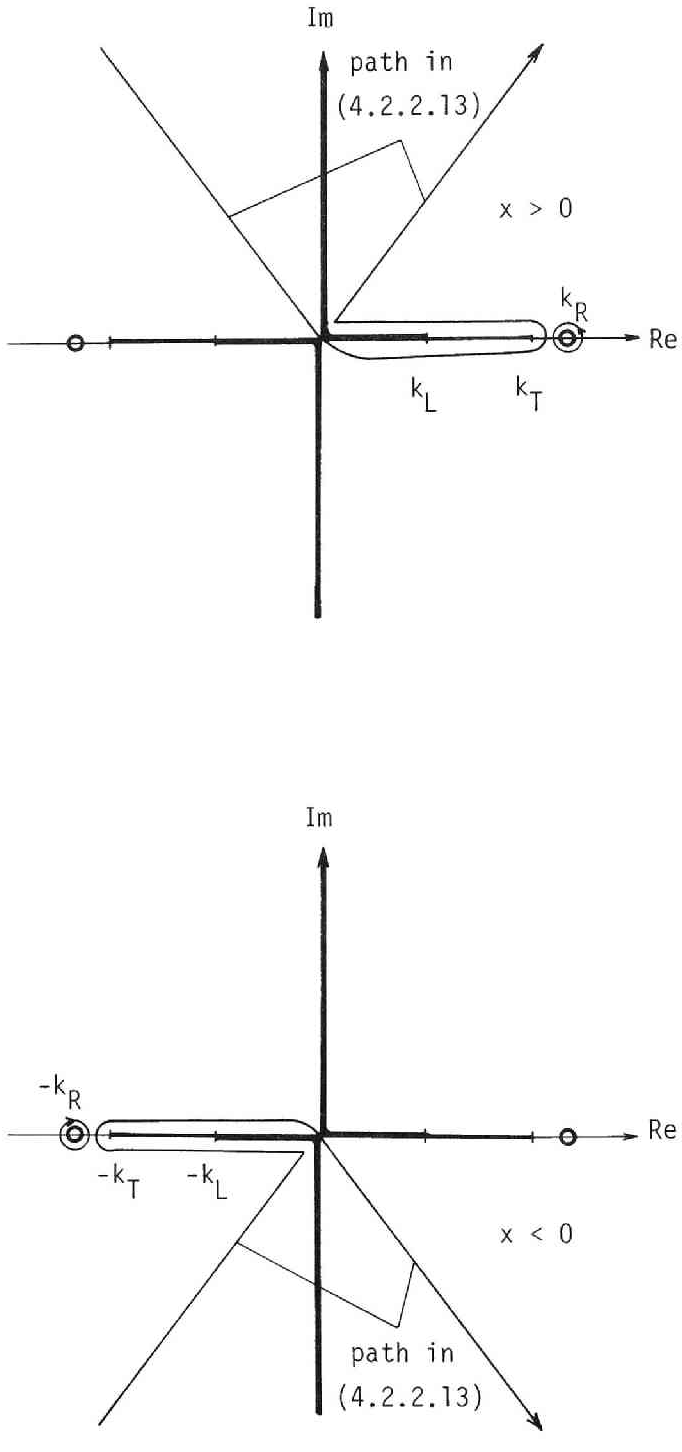

Fig.4.2.2.2 Modified path of integration.

$$-2i\int_{k_1}^{k_2}\frac{\xi^2(2\xi^2-k_T^2)e^{i\xi x}\sqrt{k_T^2-\xi^2}\cos(x_2\sqrt{k_T^2-\xi^2}+y_2\sqrt{k_L^2-\xi^2})}{(2\xi^2-k_T^2)^2+4\xi^2(k_L^2-\xi^2)^{1/2}(k_T^2-\xi^2)^{1/2}}d\xi$$

$$-2i\int_{k_3}^{k_4}\xi^2(2\xi^2-k_T^2)\sqrt{k_T^2-\xi^2}\,e^{i\xi x-y_2\sqrt{\xi^2-k_t^2}}$$

$$\cdot\mathrm{Re}\left(\frac{e^{ix_2\sqrt{k_T^2-\xi^2}}}{(2\xi^2-k_T^2)^2+4i\xi^2(k_T^2-\xi^2)^{1/2}(\xi^2-k_L^2)^{1/2}}\right)d\xi$$

$$+2\pi i\,\mathrm{sgn}(x)\frac{\xi^2R_T(2\xi^2-k_T^2)e^{-x_2R_T-y_2R_T+i\xi x}}{F'(\xi)}\Big|_{\xi=\mathrm{sgn}(x)k_R}, \qquad (4.2.2.15)$$

where

$$\xi_1=\frac{x_1+x_2+ix}{R^2}s\ ,\quad \xi_2=-\overline{\xi}_1,$$

$$k_1=\begin{cases}0\\-k_L\end{cases},\quad k_2=\begin{cases}k_L\\0\end{cases},\quad k_3=\begin{cases}k_L\\-k_T\end{cases},\quad k_4=\begin{cases}k_T\\-k_L\end{cases},$$

$$\text{for}\quad x\begin{cases}>0\\<0\end{cases}. \qquad (4.2.2.16a\text{-}f)$$

Equation (4.2.2.15) is suitable for numerical calculation since this equation consists of an integral which is evaluated by the Laguerre integration, integrals having finite limits of integration, and a residue term. We thus have established an accurate method of computing the Green's functions.

We finally remark that the modified BIEM using Green's function may lose the uniqueness of solutions in the half-plane problems. Indeed, we see that the fictitious eigenfrequencies for the present problems are either

a) Eigenfrequencies of displacement boundary value problems for the interiors of holes if any.

b) Eigenfrequencies of the domain enclosed by

$$x_2=0,\quad |x_1|<a\quad\text{and}\quad (x_1(\sigma),x_2(\sigma))\quad |\sigma|<a \qquad (4.2.2.17)$$

with the boundary conditions given by

$$\mathbf{T}\boldsymbol{u}=\mathbf{0}\quad\text{on}\quad x_2=0\ ,\quad |x_1|<a,$$

$$\boldsymbol{u}=\mathbf{0}\quad\text{on}\quad (x_1(\sigma),\ x_2(\sigma))\ ,\quad |\sigma|<a. \qquad (4.2.2.18a,b)$$

This trouble can be avoided in several ways as we have discussed in 4.1.3 ~ 4.1.6. Among them, the method by Schenck is the best choice, since this method does not make the algorithm too complicated.

We are now ready to apply the modified BIEM to half-plane problems.

4 . 2 . 3 Numerical example

We here compare the numerical results obtained by the method of truncation and the modified BIEM which uses Green's function. As we have stated, the objective of this study lies in assessing the applicability of the former approach. We here use, as an example, a column - half-plane system shown in Fig.4.2.3.1.

We carried out the analysis under the following conditions (see Fig.4.2.3.1 for notation):

Incident wave : Plane S wave, $l/a = 2$, $\theta = 30°$,
(l: incident wave length, θ: incident angle)

Material constants :
$\mu_2/\mu_1 = 10$, $\nu_1 = \nu_2 = 1/4$, $(\mu_2\rho_1)/(\rho_2\mu_1) = 10$,

where the subscript 1 (2) designates quantities relevant to the half-plane (column).

In the method of truncation we took into consideration the half-plane boundary of twice the incident wave length on both sides of the column. Also, we can show, by a numerical eigenvalue analysis, that the Green's function BIEM has a unique solution in the present case. Hence we did not use any measure against the fictitious eigenfrequencies. The boundary elements are piecewise constant.

Fig.4.2.3.2 shows the real and imaginary parts, respectively, of the displacement (normalised by the amplitude of the incident wave) obtained by the method of truncation. Here the real (imaginary) part of the solution indicates the displacement when the peak (node) of incident displacement field arrives at the origin shown in Fig.4.2.3.1. Fig.4.2.3.3 shows the same fields obtained for the reference purpose by the modified BIEM. We may conclude that there is no appreciable difference between these results. In addition, the thesis by Kinoshita(1983) reports more computations which support this conclusion. Consequently we state with confidence that the method of truncation is applicable for practical purpose provided we retain sufficient length of half-plane boundary.

The method of truncation is also economical in comparison with the Green's function BIEM. Indeed, our experience shows that the latter requires about 10 times the CPU time of the former. We thus conclude that the method of truncation is recommendable for engineering purpose.

We can now attempt to synthesise the solutions obtained by using the method of truncation to carry out a transient analysis. Fig.4.2.3.4 shows results of such an attempt. We calculated the deformation and stress around a circular hole having a radius of a near the surface of a half-plane, subject to plane S wave of critical

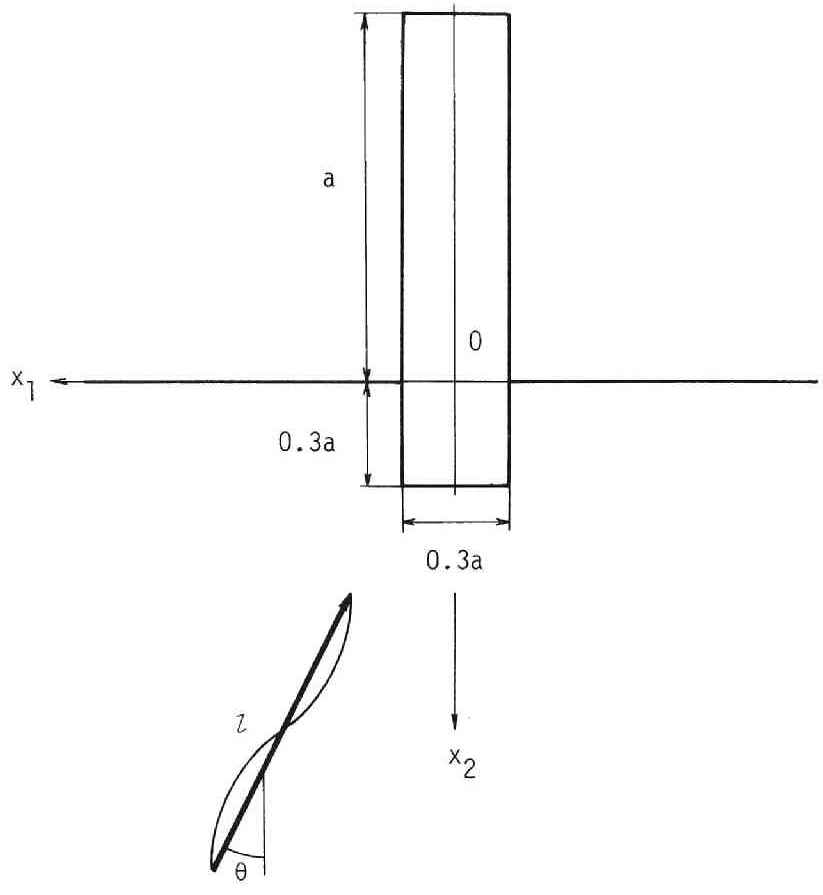

Fig.4.2.3.1 Column - half-plane system.

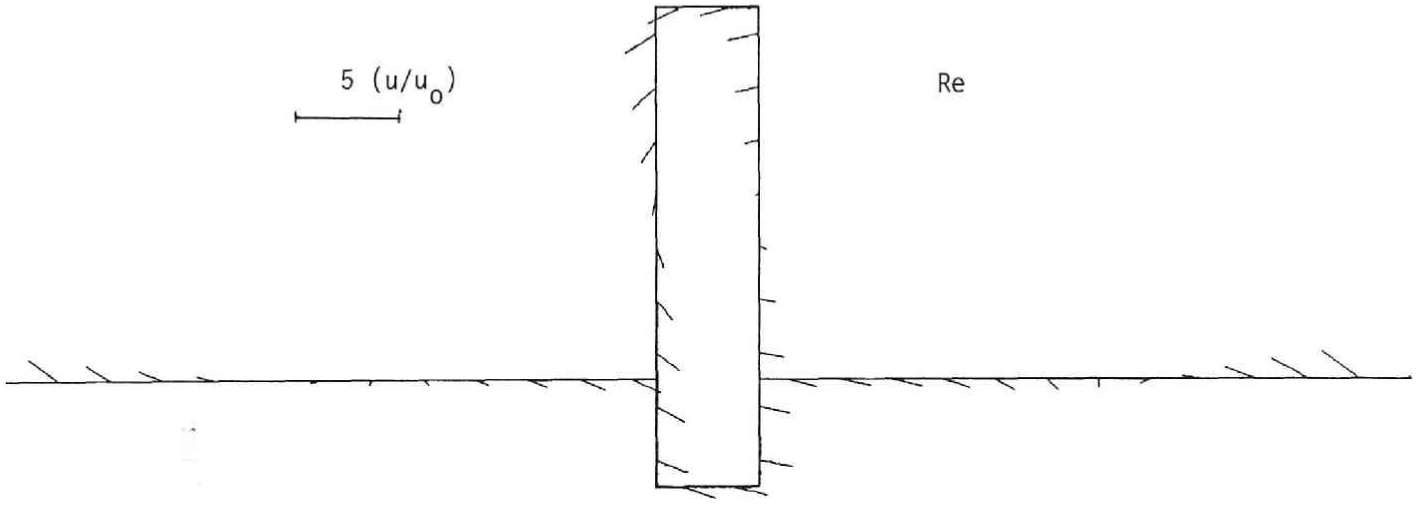

Fig.4.2.3.2 Displacements obtained by the method of truncation.

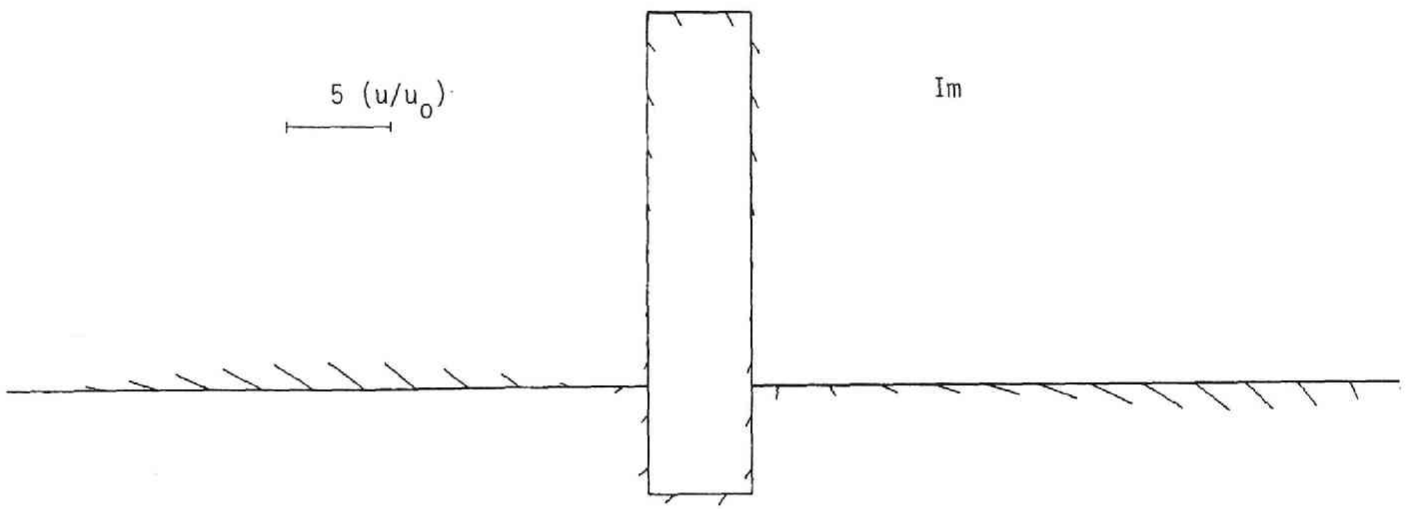

Fig.4.2.3.2 Continued.

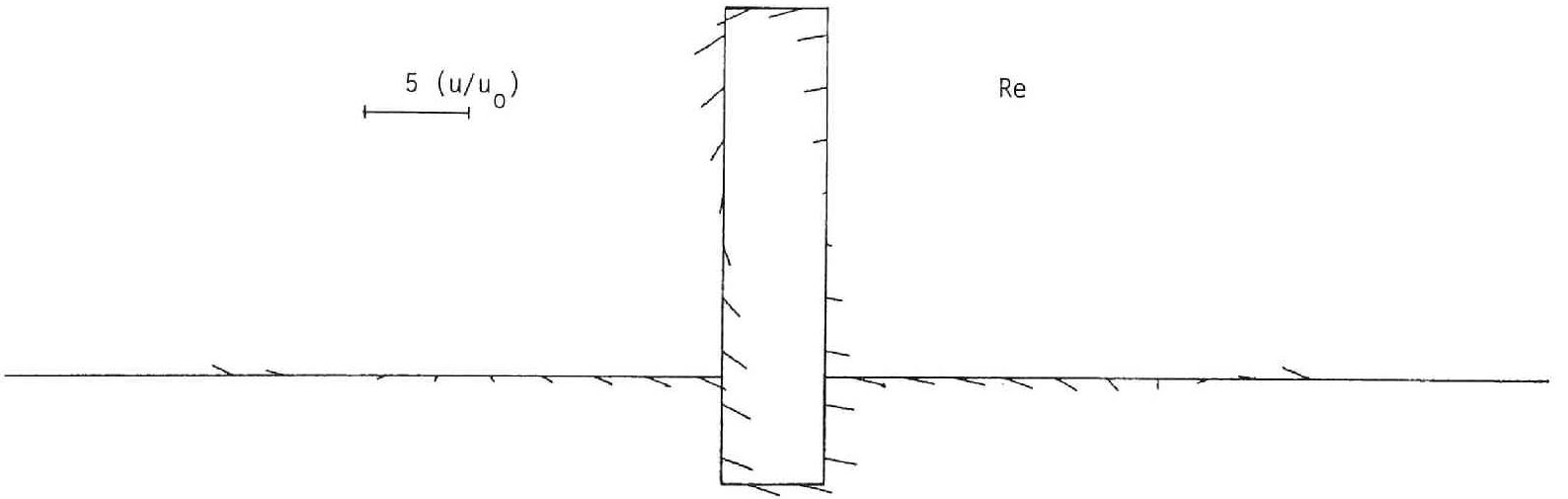

Fig.4.2.3.3 Displacements obtained by the Green's function BIEM.

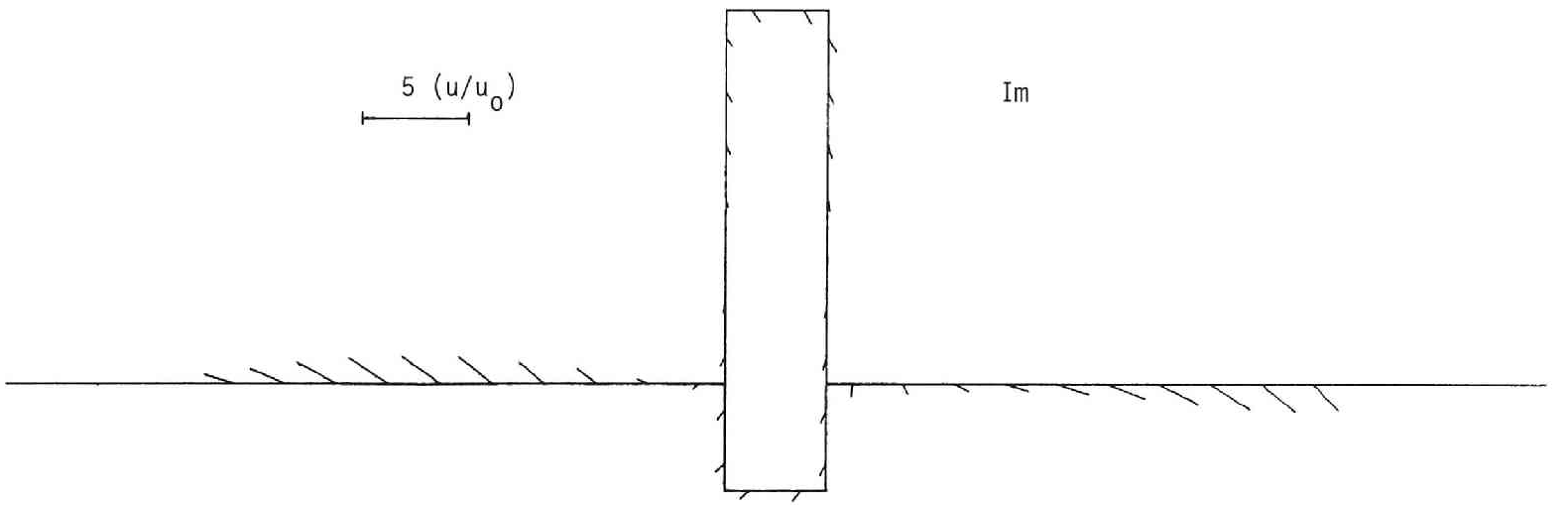

Fig.4.2.3.3 Continued.

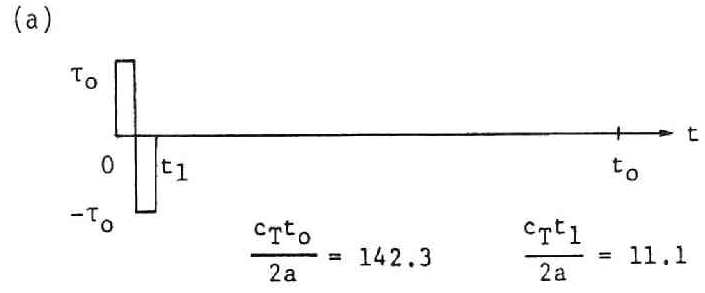

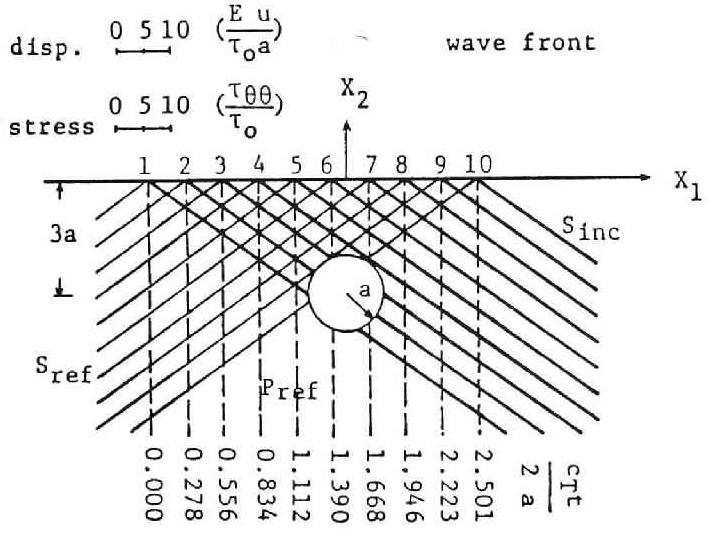

Fig.4.2.3.4 Transient displacement and stress around a circular hole in a half-plane. $\nu = 1/4$. (a) Incident and reflected fields. (b) Deformation of the boundary. (c) Hoop stress.

(b)

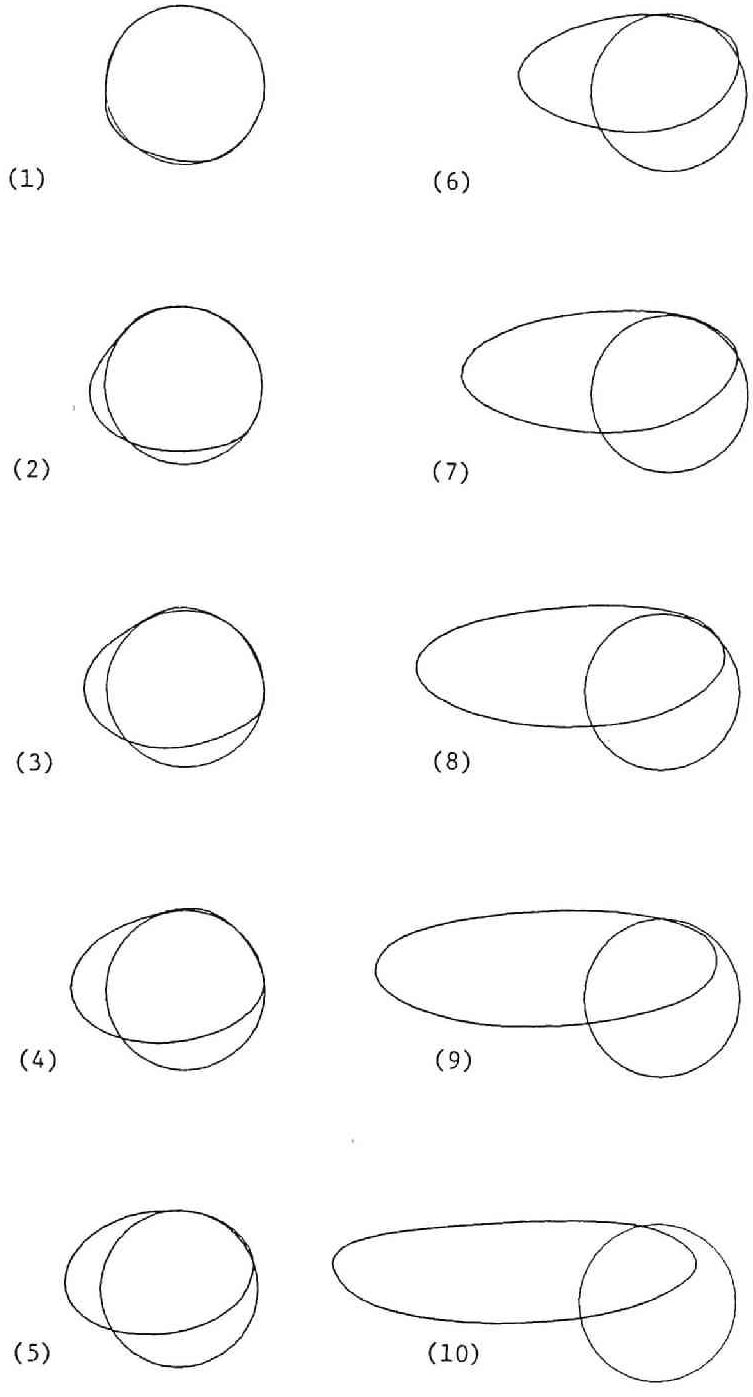

Fig.4.2.3.4 Continued.

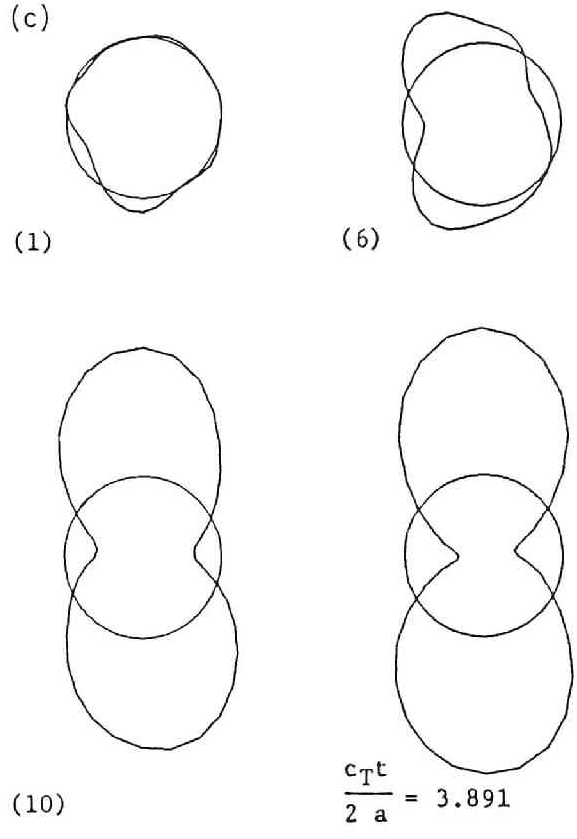

Fig.4.2.3.4 Continued.

incidence whose stress history is shown in Fig.4.2.3.4(a). Note that this stress history can be viewed as a step stress wave of a uniform magnitude in the time range shown in Figs.4.3.2.4(b) and (c). The depth of the centre of the hole is $3a$, the Poisson's ratio is 1/4, and we have used piecewise quadratic isoparametric boundary elements. Figs.4.2.3.4(b) and (c), respectively, show the displacement and stress around the hole when the wave fronts of incident (S) and reflected (P,S) waves arrive at the indicated location. These results confirm the applicability of the method of truncation to transient analysis.

4 . 3 Concluding Remarks

a) In this chapter we have discussed the integral transform formulation for transient elastodynamics using the BIE method. We also showed the efficiency and applicability of this method to many engineering problems.

The present method is especially advantageous for scattering problems because of its applicability to exterior domains. This method is also applicable to half plane problems with the help of the truncation technique. Although the non-uniqueness caused by the fictitious eigenfrequencies is a drawback, we can circumvent this either by using modified integral equations or by checking the resulting matrix numerically. From a numerical experiment we concluded that the former methods of avoiding fictitious eigenfrequencies are not indispensable for transient analyses. It goes without saying, however, that the use of the former methods are essential when one is interested in time-harmonic analysis for a certain frequency.

It is interesting, from various viewpoints, to compare the content of this chapter to the paper by Niwa et al.(1986a).

b) The extension of the content of this chapter to 3D cases is straightforward. Rizzo et al.(1985), for example, have investigated a 3D BIEM in time-harmonic elastodynamics. The method of integration for singular integrals presented in 4.1.9, however, seems to be much simpler than their counterpart which uses the elastostatic double layer kernel.

c) One of the attractive alternative numerical procedures in the transient elastodynamics is the time domain formulation. This approach seems to give finer early-time resolution than the present formulation, especially when the field contains some discontinuities. However, the time domain formulation as a numerical scheme is rather core consuming and susceptible to instability due to the accumulation of errors. In addition the time domain BIEM seems to have a different kind of instability than those in FDM or in FEM. Indeed, Fukui(1986) reports that a very small time increment is harmful for the stability of the BIEM algorithm. The Fourier transform approach, on the other hand, gives stable results for a long period of time. Manolis(1983) performed a comparative study of various formulations in elastodynamic BIEM, according to which the Laplace transform approach is the most efficient choice. This conclusion, however, is dubious because the

numerical procedures in Laplace and Fourier transform approaches differ only slightly.

We remark that Nishimura et al.(1986) extended the applicability of the time domain BIEMs to anisotropic cases. Also, Nishimura, Guo & Kobayashi(1987) and Nishimura, Kobayashi & Okada(1987) investigated a time domain BIEM in fracture mechanics.

d) Niwa's colleagues (Niwa & Hirose(1983), Kitahara et al.(1984) and Niwa et al.(1986b) for example) applied BIEM to problems in which a bounded part of a homogeneous domain has different (possibly non-constant) material properties. They either construct numerical Green's function by using BIEM including volume potentials, or use an explicit Green's function if possible, or use volume integrals with the help of fundamental solutions for a homogeneous material.

In the present author's opinion, however, a combination of BIEM (for homogeneous parts) and FEM (for inhomogeneities) could be an alternative for their problems; probably this alternative would be more practical than their methods. For such an attempt the reader is referred to Kobayashi et al.(1986) for example.

e) We did not discuss the method of determining various constants involved in Jones's methods. Kleinman & Roach(1982) claim to have established an 'optimum' choice for these constants in the context of acoustics. We may interpret their method as making the resultant numerical matrix most diagonally dominated. The practicability of their method, however, is dubious because it requires evaluation of an infinite series. Bencheikh(1986) proposed a modified BIEM using an arrangement of Ψ's different from the one in (4.1.6.6). His formulation includes the elastodynamic version of Jones's methods discussed in this chapter as special cases.

f) The method of computing Green's functions discussed in part II of this chapter uses a contour on which a function given in (4.2.2.11) becomes asymptotically real negative. We chose this contour inspired by the method of Cagniard(1962), as readers may probably infer. One may then think that the present numerical procedure can further be improved by using a contour on which (4.2.2.11) takes exactly a real negative value. This, however, would require a far more involved numerical calculation including a solution of quartic equations. This explains why we have decided to choose the linear path shown in (4.2.2.13).

The numerical method of calculating Green's function given in this chapter is applicable only when the new contour, given by (4.2.2.13), is sufficiently far from the Rayleigh pole. We therefore have to modify the procedure when the above condition is not met. Kinoshita(1983) describes one modification which splits the pertinent integrand into a sum of singular and non-singular terms, evaluating the integral of the former analytically, and that of the latter numerically. The samples shown in this chapter were obtained by using this modified method.

g) In the example shown in 4.2.3 we have truncated the half-plane boundary at points twice the incident wave length away from the structure. This 'twice the wave length' criterion, however, has been

set in an arbitrary manner. Indeed, Mori(1987) reported that a still shorter boundary modelling is sufficient in loaded half-plane problems. In general it is not very easy to establish a definite standard for an acceptable location of the truncation. Indeed, such location should depend not only on the wave length, but also on the size of the structure, hole location, etc. In practice it would be safe to try several truncations and check the agreement of the results.

Kinoshita(1981) and Mori(1987) tested the so called semi-infinite element devised by the present author (Kobayashi & Nishimura(1983)). This element uses a shape function having a spatial variation for an outgoing Rayleigh wave. These authors concluded, however, that the use of this element has only marginal effect on the solution. One may interpret this fact as another evidence of the validity of the method of truncation.

h) For additional existing BIEM researches the reader is referred to a review article by Kobayashi(1985).

i) The content of the first part of this chapter is taken from Kobayashi & Nishimura(1982a,b). The material in the second part has been published in Kobayashi & Nishimura(1982a) and Kobayashi & Nishimura(1983).

Appendix to chapter 4

BIEM in incompressible elastostatics

It can be shown that the same phenomenon as the fictitious eigenfrequencies takes place in BIE for the incompressible solids (or, what is the same thing, incompressible slow viscous fluid). The indeterminancy of the BIE solution to the exterior problem for Stokes's flow under the velocity boundary conditions is known in connection with the question of the existence of the solution (Odqvist(1930)). In this appendix we discuss the non-uniqueness problem in the incompressible elastostatics, and show that the methods described in 4.1.3 ~ 4.1.6 yield BIEs which have unique solutions. We consider 3D problems using the same notation for the domains as in problem A introduced in 4.1.2.

The governing equations of incompressible elastic solids are

$$-\mu\triangle \boldsymbol{u} + \nabla p = 0, \qquad \mathrm{div}\ \boldsymbol{u} = 0, \qquad (4.A.1a,b)$$

where we have neglected the body force. In (4.A.1) $\boldsymbol{u}$ stands for the displacement, p for the indeterminate pressure and μ for the modulus of rigidity, respectively.

The potential representations of the solutions in exterior problems are

$$\tilde{\boldsymbol{u}}(\boldsymbol{x}) = \int_{\partial D} \Gamma_1(\boldsymbol{x},\boldsymbol{y})\boldsymbol{u}(\boldsymbol{y})\mathrm{d}S - \int_{\partial D} \Gamma(\boldsymbol{x},\boldsymbol{y})\boldsymbol{t}(\boldsymbol{y})\mathrm{d}S,$$

$$\tilde{p}(x) = \int_{\partial D} \Pi_1(x,y) \cdot u(y) dS - \int_{\partial D} \Pi(x,y) \cdot t(y) dS, \qquad (4.A.2a,b)$$

where

$$\Gamma(x,y) = \frac{1}{8\pi\mu}(1\triangle - \nabla\otimes\nabla)\,|x-y|, \quad \Pi(x,y) = \nabla_y \frac{1}{4\pi}|x-y|^{-1},$$

$$\Gamma_1(x,y) = \left(S_y\Gamma(x,y)\right)^T + \nabla_y \frac{1}{4\pi}|x-y|^{-1}\otimes n_y,$$

$$\Pi_1(x,y) = S_y\Pi(x,y), \qquad S_y u = \mu\{\nabla_y u + (\nabla_y u)^T\} n_y,$$

$$t = Su - np, \qquad (4.A.3a\text{-}f)$$

respectively. We then let x approach ∂D from D^c in (4.A.2a) to obtain

$$0 = C^i(x)u(x) + \int_{\partial D} \Gamma_1(x,y)u(y) dS - \int_{\partial D} \Gamma(x,y)\, t(y) dS,$$

$$x \in \partial D \qquad (4.A.4)$$

where $C^i u$ is the non-integral term of the interior limit of the double layer potential. From the uniqueness theorems for the incompressible elastic solids and (4.A.4), we have

$$W(x) := \int_{\partial D} \Gamma_1(x,y)u(y) dS - \int_{\partial D} \Gamma(x,y)\, t(y) dS \equiv 0 \quad \text{in } D^c,$$

$$Q(x) := \int_{\partial D} \Pi_1(x,y) \cdot u(y) dS - \int_{\partial D} \Pi(x,y) \cdot t(y) dS \equiv \text{const}$$

$$\text{in } D^c. \qquad (4.A.5a,b)$$

Therefore the argument used in 4.1.3 shows that the solution to the homogeneous version of (4.A.4) is written as

$$u = u^e, \qquad t = t^e - nC \qquad \text{on } \partial D, \qquad (4.A.6a,b)$$

where u^e is an exterior displacement field, t^e is the corresponding traction on ∂D and C is a constant. The boundary condition for u^e is

$$u^e = 0 \quad \text{on } \partial D_u, \quad t^e = nC \quad \text{on } \partial D_s. \qquad (4.A.7a,b)$$

We thus conclude that the uniqueness of the solution does not hold in

this case.

We can apply the remedies analogous to those for elastodynamics to the BIE in (4.A.4) in order to assure the uniqueness of solutions. We here state the results without derivation.

1) The following method gives a unique solution; Solve (4.A.4) subject to a condition $Q(x) = 0$, where x is an arbitrary point in D^c.

2) The replacement of $\Gamma(x,y)$ and $\Gamma_1(x,y)$ by

$$\Gamma(x,y) + c_0\Phi(x)\otimes\Phi(y),$$

$$\Gamma_1(x,y) + c_0\Phi(x)\otimes\Psi(y) \qquad (4.A.8a,b)$$

in (4.A.4) renders the solution of (4.A.4) unique where c_0 is a nonzero constant,

$$\Phi(x) = \nabla\frac{1}{4\pi|x - x_0|}, \qquad \Psi(x) = 2\mu\frac{\partial}{\partial n}\Phi(x), \qquad (4.A.9a,b)$$

and x_0 is a point in D^c.

References

Bencheikh, L.(1986). Scattering of elastic waves by cylindrical cavities: integral equation methods and low-frequency matched asymptotic expansions, PhD thesis, Dept. Math., Univ. Manchester.

Burton A.J. & Miller, G.F.(1971). The application of integral equation methods to the numerical solution of some exterior boundary-value problems, *Proc. Roy. Soc. London*, Ser.A, vol.323, pp 201-210.

Cagniard, L.(1962). *Reflection and refraction of progressive seismic waves* (tr. E.A. Flinn & C.H. Dix), McGraw Hill.

Cohen, M. & Jennings, P.C.(1983). Silent boundary methods for transient analysis, In: *Computational Methods for Transient Analysis* (Eds. T. Belytschko & T.J.R. Hughes), pp 301-357, North Holland.

Cruse, T.A.(1968). A direct formulation and numerical solution of the general transient elastodynamic problem II, *J. Math. Anal. Appl.*, vol.22, pp 341-355.

Cruse, T.A. & Rizzo, F.J.(1968). A direct formulation and numerical solution of the general transient elastodynamic problem I, *J. Math. Anal. Appl.*, vol.22, pp 244-259.

Eringen, A.C. & Suhubi, E.S.(1975). *Elastodynamics, vol. 2, Linear Theory*, Academic Pr.

Fujiki, K.(1980). Analysis of the transient stresses around

underground cavities by the integral equation method, M. Eng. Thesis, Kyoto Univ. (in Japanese).
Fukui, T.(1986). Time marching analysis of boundary integral equations in two dimensional elastodynamics, *Proc. 4th Int. Symp. Num. Meth. Eng.* (Eds. R.P. Shaw et al.), pp 405-410, Springer.
Garnet, H & Crouzet-Pascal, J.(1966). Transient response of a circular cylinder of arbitrary thickness, in an elastic medium, to a plane dilatational wave, *J. Appl. Mech.*, vol.33, pp 521-531.
Jones, D.S.(1974). Integral equations for the exterior acoustic problem, *Q. J. Mech. Appl. Math.*, vol.27, pp 129-142.
Jones, D.S.(1984). An exterior problem in elastodynamics, *Math. Proc. Camb. Phil. Soc.*, vol.96, pp 173-182.
Kinoshita, M.(1981). Application of BIEM to dynamic analysis of a semiinfinite ground - structure system, B. Eng. thesis, Kyoto Univ. (in Japanese).
Kinoshita, M.(1983). Analysis of dynamic structure-ground systems by Green's function BIEM, M. Eng. Thesis, Kyoto Univ. (in Japanese).
Kitahara, M.(1985). *Boundary Integral Equation Methods in Eigenvalue Problems of Elastodynamics and Thin Plates*, Elsevier.
Kitahara, M., Niwa, Y., Hirose, S. & Yamazaki, M.(1984). Coupling of numerical Green's matrix and boundary integral equations for the elastodynamic analysis of inhomogeneous bodies on an elastic half-space, *Appl. Math. Model.*, vol.8, pp 397-407.
Kleinman, R.E. & Roach, G.F.(1974). Boundary integral equations for the three dimensional Helmholtz equation, *SIAM Review*, vol.16, pp 214-236.
Kleinman, R.E. & Roach, G.F.(1982). On modified Green functions in exterior problems for the Helmholtz equation, *Proc. Roy. Soc. London*, Ser.A, vol.383, pp 313-332.
Kobayashi, S.(1985). Fundamentals of boundary integral equation methods in elastodynamics, In: *Topics in Boundary Element Research, Vol. 2* (Ed. C.A. Brebbia), pp 1-54.
Kobayashi, S. & Nishimura, N.(1982a). Transient stress analysis of tunnels and cavities of arbitrary shape due to travelling waves, In: *Developments in Boundary Element Methods - 2* (Eds. P.K. Banerjee & R.P. Shaw), pp 177-210, Appl. Sci. Publ.
Kobayashi, S. & Nishimura, N.(1982b). On the indeterminancy of BIE solutions for the exterior problems of time-harmonic elastodynamics and incompressible elastostatics, *Proc. 4th Int. Conf. BEM* (Eds. C.A. Brebbia), pp 282-296, Springer.
Kobayashi, S. & Nishimura, N.(1983). Analysis of dynamic soil-structure interactions by boundary integral equation method. *Proc. 3rd Int. Symp. Num. Meth. Eng.* (Ed. P. Lascaux), pp 353-362, Pluralis.
Kobayashi, S., Nishimura, N. & Mori, K.(1986). Applications of boundary element - finite element combined method to three-dimensional viscoelastodynamic problems, *Proc. Int. Conf. BEM, Beijing* (Ed. Du Q.), pp 67-74. Pergamon.
Kupradze, V.D., Gegelia, T.G., Basheleishvili, M.O. & Burchuladze, T.V.(1979). *Three-Dimensional Problems of the Mathematical Theory of Elasticity and Thermoelasticity*, North Holland.
Lachat, J.C. & Watson, J.O.(1976). Effective numerical treatment of boundary integral equations, *Int. J. Num. Meth. Eng.*, vol.10, pp

991-1005.
Lamb, H.(1904). On the propagation of tremors over the surface of an elastic solid, *Phil. Trans. Roy. Soc. London*, Ser.A, vol.203, pp 1-42.
Manolis, G.D.(1983). A comparative study on three boundary element method approaches to problems in elastodynamics, *Int. J. Num. Meth. Eng.*, vol.19, pp 73-91.
Mori, K.(1987). Further considerations on elastodynamic BIEM for half-plane problems, M. Eng. thesis, Kyoto Univ. (in Japanese)
Mow, C.-C. & Mente, L.J.(1963). Dynamic stresses and displacements around cylindrical discontinuities due to plane harmonic shear waves, *J. Appl. Mech.*, vol.30, pp 598-604.
Nishimura, N., Kishima, T. & Kobayashi, S.(1986). A BIE analysis of wave propagation in anisotropic media, *Proc. 8th Int. Conf. BEM* (Eds. M. Tanaka & C.A. Brebbia), pp 425-434.
Nishimura, N., Kobayashi, S. & Okada, M.(1987). A time domain BIE crack analysis, *Proc. 1st Japan-China Symp. BEM* (Eds. M. Tanaka & Du Q.), pp 85-94, Pergamon.
Nishimura, N., Guo, Q.C. & Kobayashi, S.(1987). Boundary integral equation methods in elastodynamic crack problems, *Proc. 9th Int. Conf. BEM, Vol. 2, Stress Analysis Applications*, (Eds. C.A. Brebbia & W.L. Wendland), pp 279-291, Springer.
Niwa, Y., Fukui,T., Kato, S. & Fujiki, K.(1980). An application of the integral equation method to two-dimensional elastodynamics, *Proc. 28th Japan Nat. Congr. Appl. Mech. 1978*, pp 281-290.
Niwa, Y. & Hirose, S.(1983). An analysis of wave propagation in a inhomogeneous ground, Preprint for JSCE Kansai convention, I-78. (in Japanese).
Niwa, Y., Hirose, S. & Kitahara, M.(1986a). Application of the boundary integral equation (bie) method to transient response analysis of inclusions in a half space, *Wave Motion*, vol.8, pp 77-91.
Niwa, Y., Hirose, S. & Kitahara, M.(1986b). Elastodynamic analysis of inhomogeneous anisotropic bodies, *Int. J. Solids Structures*, vol.22, pp 1541-1548.
Niwa, Y., Kobayashi, S. & Azuma, N.(1975). An analysis of transient stresses produced around cavities of arbitrary shape, *Trans. JSCE*, vol.195, pp 27-35 (in Japanese).
Odqvist, F.K.G.(1930). Über die Randwertaufgaben der Hydrodynamik zäher Flüssigkeiten, *Math. Zeit.*, vol.32, pp 329-375.
Pao, Y.-H.(1962). Dynamic stress concentration in an elastic plate, *J. Appl. Mech.*, vol.29, pp 299-305.
Pao, Y.-H. & Mow, C.-C.(1971). *Diffractions of elastic waves and dynamic stress concentrations*, Rand Corporation.
Rizzo, F.J., Shippy, D.J. & Rezayat, M.(1985). A boundary integral equation method for radiation and scattering of elastic waves in three dimensions, *Int. J. Num. Meth. Eng.*, vol.21, pp 115-129.
Schenck, H.A.(1968). Improved integral formulation for acoustic radiation problems, *J. Acoust. Soc. Am.*, vol.44, pp 745-748.
Shaw, R.P.(1979). Boundary integral equation methods applied to wave problems, In: *Developments in Boundary Element Methods - 1* (Eds. P.K. Banerjee & R. Butterfield), pp 121-153, Appl. Sci. Publ.
Sladek, V. & Sladek, D.(1986). Improved computation of stresses using the boundary element method, *Appl. Math. Model*, vol.10, pp

249-255.
Ursell, F.(1973). On the exterior problems of acoustics, *Proc. Camb. Phil. Soc.*, vol.74, pp 117-125.
Ursell, F.(1978). On the exterior problems of acoustics - II, *Proc. Camb. Phil. Soc.*, vol.84, pp 545-548.
Vekua, I.N.(1968). *New Methods of Solving Elliptic Equations* (tr. D.E. Brown & A.B. Taylor), North Holland.

Chapter 5 Consolidation Problems

5 . 0 Introduction

This chapter presents some applications of BIEM to Biot's theory of consolidation (Biot(1941))——— a special case of parabolic problems.

As in elastodynamics we can carry out the analysis either in the time domain or in a certain transformed domain. We here choose the former approach because of two reasons. The first reason is concerned with our intention of showing the usefulness of potential methods for applied mathematical purposes. Indeed, we shall emphasise in the first part of this chapter that the present formulation provides an effective tool of investigating the behaviour of the solution. It is preferable, to this end, that all the field quantities are given in terms of physical variables including time. The second reason is related to the jump properties of the solution. We know that the most outstanding difference between the solution of Biot's theory and that of heat equation is that the former solution often jumps (as a function of time) while that of the latter does not. It is therefore conceivable that the time domain method will give better numerical results than the other since most transformation methods tend to blur discontinuities.

In the first part of this chapter we present some results concerning the behaviour of the solution. We maintain the description as general as possible; the obtained results are valid for fully anisotropic cases. This generality is achieved by using the method of Fourier transform used in Chapter 1. This method enables us to discuss problems whose fundamental solutions cannot be written explicitly. Specifically, we discuss the initial behaviour and jump properties of the solutions. We also determine the structure of the singularities of fluid velocity on the boundary at the instant of sudden loading.

The second part describes a method of numerical analysis using the present formulation. We discuss the method of space and time integration in detail. We finally show sample analyses which show the applicability of our formulation.

Part I

5 . 1 Initial- boundary value problems for Biot's equations

The well-known equations of Biot in forms familiar to soil engineers can be written as

$$\triangle^* \boldsymbol{u} - \nabla p = -\boldsymbol{f}, \tag{5.1.1}$$

$$\mathrm{div}\ \dot{\boldsymbol{u}} + m\dot{p} - \boldsymbol{K}\cdot\nabla\nabla p = g\ , \tag{5.1.2}$$

where $\boldsymbol{u}$, p, $\boldsymbol{f}$, g and $\boldsymbol{K}$, m (>0) stand for the displacement, pressure, body force, $(i - f_f\ \boldsymbol{K}\cdot\nabla\boldsymbol{f})$ (f_f : fraction of fluid which is assumed to

be a constant, i : rate of fluid injection per unit volume), permeability tensor and the compressibility of the fluid. The symbol $\triangle^*$ stands for the Navier operator defined by

$$\triangle^* \boldsymbol{u} := \operatorname{div} C[\nabla \boldsymbol{u}] \ , \qquad (\boldsymbol{u}: \text{vector}) \tag{5.1.3*}$$

where C is the elasticity tensor (4th order) which is assumed to be constant. We also assume the usual symmetry and positive definiteness for both C and K, and use $\dot{}$ for the time derivative ($\dot{} = \mathrm{d}/\mathrm{d}t$, t:time**).

It is plain to see that the following identity holds for any sufficiently smooth vectors $\boldsymbol{u}$, $\boldsymbol{u}^*$ and scalars p, p^*:

$$\int_{t_1}^{t_2} \int_{\partial D} \left\{ \dot{\boldsymbol{u}}^* \cdot \boldsymbol{S} - \dot{\boldsymbol{S}}^* \cdot \boldsymbol{u} - p^* \boldsymbol{n} \cdot K \nabla p + \boldsymbol{n} \cdot K(\nabla p^*) p \right\} \mathrm{d}S \mathrm{d}t$$

$$= \int_{t_1}^{t_2} \int_D \{ \dot{\boldsymbol{u}}^* \cdot (\triangle^* \boldsymbol{u} - \nabla p) - (\triangle^* \dot{\boldsymbol{u}}^* + \nabla \dot{p}^*) \cdot \boldsymbol{u}$$

$$+ p^* (\operatorname{div} \dot{\boldsymbol{u}} + m\dot{p} - K \cdot \nabla \nabla p) - (\operatorname{div} \dot{\boldsymbol{u}}^* - m\dot{p}^* - K \cdot \nabla \nabla p^*) p \} \mathrm{d}V \mathrm{d}t$$

$$- \int_D [\, p^* (\operatorname{div} \boldsymbol{u} + mp) \,]_{t_1}^{t_2} \, \mathrm{d}V \tag{5.1.4}$$

where D is a bounded (open) domain with smooth boundary ∂D, $[\ \cdot\ ]_{t_1}^{t_2} = \cdot(t_2) - \cdot(t_1)$, and $\boldsymbol{S}$ and $\boldsymbol{S}^*$ are the traction and 'adjoint' surface traction defined by

$$\boldsymbol{S} = (C[\nabla \boldsymbol{u}] - 1p)\boldsymbol{n}, \qquad \boldsymbol{S}^* = (C[\nabla \boldsymbol{u}^*] + 1p^*)\boldsymbol{n} \ . \tag{5.1.5a,b}$$

Note that $\boldsymbol{S}$ has the same physical meaning as $\boldsymbol{t}$ in other chapters (e.g. (1.1.11)). However, we here use this notation in order to emphasise the dependence of $\boldsymbol{S}$ on p. Also, the quantity $\boldsymbol{S}^*$ does not have any particular physical meaning.

Suggested by (5.1.4) we seek a solution of the following initial boundary value problem.

Find a regular solution $(\boldsymbol{u}, p)$ of (5.1.1) and (5.1.2) in D and $t>0$, subject to an initial condition

$$(\operatorname{div} \boldsymbol{u} + mp)\big|_{t=0} = \theta \qquad \text{in } D \tag{5.1.6}$$

and boundary conditions for $t>0$

$$\boldsymbol{u} = \boldsymbol{u}_0 \qquad \text{on } \partial D_u \ ,$$

---

* $C[\varepsilon]_{ij} := C_{ijkl}\varepsilon_{kl}$

** s is also used for time.

$$\boldsymbol{S} = \boldsymbol{S}_0 \qquad \text{on } \partial D_s \ , \ (\partial D_u \cup \partial D_s = \partial D, \quad \partial D_u \cap \partial D_s = \phi)$$

$$p = p_0 \qquad \text{on } \partial D_p \ ,$$

$$r := -\boldsymbol{n} \cdot K \nabla p = r_0 \quad \text{on } \partial D_r \ ,$$

$$(\partial D_p \cup \partial D_r = \partial D, \quad \partial D_p \cap \partial D_r = \phi) \tag{5.1.7a-d}$$

where θ, $\boldsymbol{u}_0$, $\boldsymbol{S}_0$, p_0 and r_0 are given functions.
By the word "regular" we mean

1) $\boldsymbol{u}$ and p in $D \times R^+$ are piecewise smooth in t for a fixed $\boldsymbol{x}$ (analytical backward, to be precise) and the limits $\boldsymbol{u}(\boldsymbol{x}, t^{\pm})$, $p(\boldsymbol{x}, t^{\pm})$ $(t>0)$, $\boldsymbol{u}(\boldsymbol{x}, 0^+)$ and $p(\boldsymbol{x}, 0^+)$ are sufficiently smooth in $\boldsymbol{x}$ $(\boldsymbol{x} \in D)$ so that the following arguments are justified

2) For points $\boldsymbol{x} \in (\partial D_u \cup \partial D_s) \cap (\partial D_p \cup \partial D_r) = \partial D_R$, $\boldsymbol{u}$, $\boldsymbol{S}$ and p satisfy the same condition as in 1) (except that "$\boldsymbol{x} \in D$" is replaced by "$\boldsymbol{x} \in \partial D_R$"). As to $\partial p / \partial n$ (or r) we allow it to have singularities of the following forms

$$\sum_{i=0}^{M} C_i(\boldsymbol{x}) H(t - s_i)(t - s_i)^{\beta_i} \qquad (s_0 = 0), \tag{5.1.8}$$

where $C_i(\boldsymbol{x})$ is a function sufficiently smooth on ∂D_R , $s_i (0 \leqq i \leqq M)$ are the values of t where the solution suffers discontinuity, $H(\cdot)$ is the step function and β_i are constants such that

$$\beta_i > -1 \ . \tag{5.1.9}$$

Equation (5.1.9) implies that the amount of the fluid flow through ∂D in a infinitesimal time interval must be infinitesimal.

3) $\boldsymbol{u}$, $\boldsymbol{S}$, p, $\partial p / \partial n$ on ∂D may have singularities near points in $\partial D \backslash \partial D_R$, but the order of the singularity is sufficiently small that the following arguments are justified.

Accordingly, we specify the data $\boldsymbol{u}_0$, $\boldsymbol{S}_0$, p_0, r_0 and θ keeping consistency with the conditions 1) ~ 3). As to $\boldsymbol{f}$ and g, we assume piecewise continuity in t for a fixed $\boldsymbol{x} \in \bar{D} = D + \partial D$ and smoothness in $\boldsymbol{x}$.

The uniqueness of the solution to this problem is easily established by using the standard argument, together with an identity

$$\int_0^s \int_{\partial D} (\dot{\boldsymbol{u}} \cdot \boldsymbol{S} + p \boldsymbol{n} \cdot K \nabla p) \mathrm{d}S \mathrm{d}t + \int_0^s \int_D (\dot{\boldsymbol{u}} \cdot \boldsymbol{f} + pg) \mathrm{d}V \mathrm{d}t$$

$$+\frac{1}{2}\left\{\int_{\partial D}\boldsymbol{u}\cdot\boldsymbol{S}\,dS+\int_D(\mathrm{div}\,\boldsymbol{u}+m\dot{p})p\,dV+\int_D\boldsymbol{u}\cdot\boldsymbol{f}\,dV\right\}\Big|_{t=0}$$

$$=\int_0^s\int_D\dot{\boldsymbol{u}}\cdot(\triangle^*\boldsymbol{u}-\nabla p+\boldsymbol{f})dVdt$$

$$+\int_0^s\int_D p(-\mathrm{div}\,\dot{\boldsymbol{u}}-m\dot{p}+\boldsymbol{K}\cdot\nabla\nabla p+g)dVdt$$

$$+\frac{1}{2}\int_D\boldsymbol{u}\cdot(\triangle^*\boldsymbol{u}-\nabla p+\boldsymbol{f})\,|_{t=0}dV+\frac{1}{2}\int_D\nabla\boldsymbol{u}\cdot\boldsymbol{C}[\nabla\boldsymbol{u}]\,|_{t=s}dV$$

$$+\int_D\frac{1}{2}mp^2|_{t=s}dV+\int_0^s\int_D\nabla p\cdot\boldsymbol{K}\nabla p\,dVdt, \qquad (5.1.10)$$

which holds for any smooth vector fields $(\boldsymbol{u}, \boldsymbol{f})$, scalar fields (p, g) and a scalar s (time) > 0. Indeed, (5.1.10) shows the uniqueness of the solution within a rigid body motion if $\partial D_u = \phi$. If $m = 0$ and $\partial D_p = \partial D_s = \phi$, we see that the pressure is determined to within a constant. For other cases the solution is totally unique. The boundary and field data cannot always be given arbitrarily. Actually, substituting $\boldsymbol{u}^*(\boldsymbol{x}, t) = H(s-t)\boldsymbol{u}_R(\boldsymbol{x})$ ($\boldsymbol{u}_R$: rigid displacement), $p^* = 0$ in (5.2.4) we have

$$\int_{\partial D}\boldsymbol{S}(\boldsymbol{x},s)dS+\int_D\boldsymbol{f}(\boldsymbol{x},s)dV=0, \qquad s>0 \qquad (5.1.11)$$

and

$$\int_{\partial D}\boldsymbol{x}\times\boldsymbol{S}(\boldsymbol{x},s)dS+\int_D\boldsymbol{x}\times\boldsymbol{f}(\boldsymbol{x},s)dV=0. \qquad s>0 \qquad (5.1.12)$$

If $m = 0$, introduction of $p^*(\boldsymbol{x}, t) = H(s - t)$ and $\boldsymbol{u}^*(\boldsymbol{x}, t) = 0$ in (5.1.4) yields

$$\int_{\partial D}\boldsymbol{n}\cdot\boldsymbol{u}|_{t=s}dS+\int_0^s\int_{\partial D}r\,dSdt=\int_0^s\int_D g\,dVdt+\int_D\theta\,dV\,.$$

$$s>0 \qquad (5.1.13)$$

Equations (5.1.11) and (5.2.12) are necessary conditions for the solvability of the present problem when $\partial D_u = \phi$. Equation (5.1.13) is necessary for the solvability when $\partial D_s = \partial D_p = \phi$ and $m = 0$. It is highly plausible that these conditions are also sufficient, but the present author does not have the proof at present.

Before closing this section we shall make a comment on the physical interpretation of the initial condition. Assume that there was a certain consolidation process going on before $t = 0$. For example we have $u = 0$, $p = 0$ for $t < 0$ if the soil was at rest under no load before the loading begins. We then integrate (5.1.2) with respect to time from $-\triangle t$ to $\triangle t$ $(\triangle t > 0)$ to obtain

$$(\mathrm{div}\ u + mp)\,|_{t=\triangle t}$$

$$= (\mathrm{div}\ u + mp)\,|_{t=-\triangle t} + \int_{-\triangle t}^{\triangle t} (K \cdot \nabla\nabla p + g)dt. \tag{5.1.14}$$

Since the integral on the RHS of (5.1.14) tends to zero as $\triangle t \downarrow 0$, we get

$$(\mathrm{div}\ u + mp)\,|_{t=0^+} = (\mathrm{div}\ u + mp)\,|_{t=0^-}. \tag{5.1.15}$$

Consequently we are led to interpret θ in (5.1.6) as

$$\theta = (\mathrm{div}\ u + mp)\,|_{t=0^-}. \tag{5.1.16}$$

In particular, we have $\theta = 0$ if the soil is with a quiescent past.

5.2 Green's formula, fundamental solution and integral representation of the solution

Let $\dot{U}$, $\dot{V}$, P and Q be functions which satisfy the 'causality' (i.e. $\dot{U}$ etc. vanish for $t < 0$) and the equation

$$\begin{bmatrix} \triangle^* & -\nabla\partial/\partial t \\ -\nabla & -m\partial/\partial t + K \cdot \nabla\nabla \end{bmatrix} \begin{bmatrix} \dot{U} & \dot{V} \\ P & Q \end{bmatrix}$$

$$= -\begin{bmatrix} 1\delta(t)\delta(x) & 0 \\ 0 & \delta(t)\delta(x) \end{bmatrix}, \tag{5.2.1}$$

where $\delta(\cdot)$ is the Dirac delta. $\dot{U}$, $\dot{V}$, P and Q are called the fundamental solutions for (5.1.1) and (5.1.2). These fundamental solutions can easily be obtained by using the Fourier transform. Namely, we have

$$\dot{U} = \delta(t)U_0 + \dot{\mathrm{u}},$$

$$\dot{V} = \delta(t)V_0 + \dot{\mathrm{U}},$$

$$P = -iH(t)\mathcal{F}_\xi^{-1}\left(\frac{\triangle^{*-1}(\xi)\xi}{m + \xi\cdot\triangle^{*-1}(\xi)\xi}\mathrm{ex}(\xi,t)\right),$$

$$Q = H(t)\mathcal{F}_\xi^{-1}\left(\frac{1}{m + \xi\cdot\triangle^{*-1}(\xi)\xi}\mathrm{ex}(\xi,t)\right), \qquad (5.2.2a\text{-}d)$$

where

$$U_0 = \mathcal{F}_\xi^{-1}\left\{\left(\triangle^{*-1}(\xi) - \frac{\triangle^{*-1}(\xi)\xi\otimes\triangle^{*-1}(\xi)\xi}{m + \xi\cdot\triangle^{*-1}(\xi)\xi}\right)\right\},$$

$$V_0 = \mathcal{F}_\xi^{-1}\left(\frac{-i\triangle^{*-1}(\xi)\xi}{m + \xi\cdot\triangle^{*-1}(\xi)\xi}\right),$$

$$\dot{U} = \mathcal{F}_\xi^{-1}\left\{H(t)\triangle^{*-1}(\xi)\xi\otimes\triangle^{*-1}(\xi)\xi\frac{\xi\cdot K\xi}{(m + \xi\cdot\triangle^{*-1}(\xi)\xi)^2}\ \mathrm{ex}(\xi,t)\right\},$$

$$\dot{V} = \mathcal{F}_\xi^{-1}\left(H(t)i\triangle^{*-1}(\xi)\xi\frac{\xi\cdot K\xi}{(m + \xi\cdot\triangle^{*-1}(\xi)\xi)^2}\mathrm{ex}(\xi,t)\right). \qquad (5.2.3a\text{-}d^*)$$

Also, $\mathcal{F}_\xi^{-1}$ indicates the Fourier inverse transform ($\xi \to x$), $\triangle^{*-1}(\xi)$ the inverse of the matrix obtained by replacing ∇ in $\triangle^*$ by ξ, and

$$\mathrm{ex}(\xi,t) = e^{-\xi\cdot K\xi/(m + \xi\cdot\triangle^{*-1}(\xi)\xi)t}\ . \qquad (5.2.4)$$

Note that $\dot{P}$ and $\dot{Q}$ can be expressed as

$$\dot{P}(x,t) = P_0(x)\delta(t) + \dot{\mathcal{P}}(x,t),$$

$$\dot{Q}(x,t) = Q_0(x)\delta(t) + \dot{\mathcal{Q}}(x,t), \qquad (5.2.5a,b)$$

where

$$P_0 = V_0, \qquad \dot{\mathcal{P}} = \dot{V},$$

$$Q_0 = \mathcal{F}_\xi^{-1}\left(\frac{1}{m + \xi\cdot\triangle^{*-1}(\xi)\xi}\right),$$

---

* For $N = 2$ one would either have to interpret the non-integrable integral included in the Fourier inversion of (5.2.3a) as p.f. or an integral performed on a path in a complex plane which circumvents the singular point of the integrand (origin).

$$\mathcal{Q} = -H(t)\mathcal{F}_\xi^{-1}\left(\frac{\xi \cdot K\xi}{(m + \xi \cdot \triangle^{*-1}(\xi)\xi)^2}\mathrm{ex}(\xi, t)\right). \qquad (5.2.6a\text{-}d)$$

The Fourier transforms of U_0, V_0, P_0 and Q_0 are homogeneous functions of order (-2,0), (-1,0), (-1,0), (0,0), respectively (see 1.3 for the definition). For the case of N spatial dimension (N = 2 or 3) this observation, together with the theory of Fourier transforms of homogeneous functions (see Mizohata(1963) or 1.3 of this thesis), shows

i) U_0 is a (2,-3)-homogeneous function when N = 3. When N = 2, U_0 is a $C^\infty(R^2 \setminus \{0\})$ function having an estimate

$$|U_0(x)| \leqq C_1 + C_2 \log|x| \qquad (C_1, C_2 \text{ constants}) \qquad (5.2.7)$$

near the origin.

ii) V_0, P_0 and ∇U_0 are (1,-N)-homogeneous functions.

iii) Q_0 can be expressed as

$$Q_0(x) = C_Q\delta(x) + \mathrm{v.p.}\grave{Q}_0(x), \qquad (5.2.8)$$

where

$$C_Q = \frac{1}{|S_N|}\int_{S_N} \mathcal{F}_x Q_0(\xi)\,dS,$$

$$\mathrm{v.p.}\grave{Q}_0(x) = \mathcal{F}_\xi^{-1}\{\mathcal{F}_x Q_0(\xi) - C_Q\}, \qquad (5.2.9a,b)$$

S_N is the N-dimensional unit sphere, and $|S_N|$ is its surface area, respectively. Also, $\grave{Q}_0(x)$ is a (0,-N)-homogeneous function whose mean value over S_N vanishes. We may sometimes write Q_0 for $\grave{Q}_0$ since they are identical except at the origin. ∇V_0 also has an expression analogous to (5.2.8).

We next consider the time dependent kernels ($\grave{\mathcal{U}}$ etc.) in (5.2.2) and (5.2.3). A useful observation is that these kernels are written as

$$\mathcal{F}_\xi^{-1}\,\hat{F}(\xi)\mathrm{ex}(\xi, t) = \frac{1}{(2\pi)^N}\int_{R^N}\hat{F}(\xi)\mathrm{ex}(\xi, t)e^{i\xi\cdot x}d\xi \qquad t > 0, \qquad (5.2.10)$$

where $\hat{F}(\xi)$ is a certain $(n,0)$-homogeneous function ($-1 \leqq n \leqq 2$) (n = -1 for P, 2 for $\nabla\grave{U}$, etc.). Writing this integral as $I(x,t)$ we readily establish

$$I(x,t) = \frac{1}{(t^{N+n})^{1/2}} I\left(\frac{x}{t^{1/2}},1\right) . \tag{5.2.11}$$

$I(x,1)$ is a C^∞ function in x. Since $(\partial/\partial\xi)^\alpha \hat{F}(\xi)\mathrm{ex}(\xi,t)$ is integrable (near the origin, and therefore in R^N) for $n - |\alpha| \geqq -N + 1$, we have

$$|I\left(\frac{x}{t^{1/2}},1\right)| \leqq \mathrm{Const} \left(\frac{t^{1/2}}{|x|}\right)^{n+N-1} , \quad (n + N - 1 \geqq 0), \tag{5.2.12}$$

and

$$|I(x,t)| \leqq \mathrm{Const} \frac{1}{t^{1/2}|x|^{n+N-1}} \tag{5.2.13}$$

for $|x| \neq 0$. This proves that $\dot{u}$, $\nabla\dot{u}$, $\dot{U}$, $\nabla\dot{U}$, P, $\dot{\mathcal{P}}$, ∇P, Q, $\dot{\mathcal{Q}}$ and ∇Q are C^∞ functions for a non-zero t and are integrable in t for a fixed $|x| \neq 0$. We also note that from (5.2.2c-d) and (5.2.6a,c) follows

$$(P(x,t),Q(x,t)) \to (P_0(x),Q_0(x)) \quad \text{as} \quad t \downarrow 0. \tag{5.2.14}$$

We now proceed to the construction of the potential representations for u and p. To this end, we introduce functions $\dot{U}^*$, $\dot{V}^*$, P^* and Q^* defined as

$$\begin{bmatrix} \dot{U}^*(x,t) & \dot{V}^*(x,t) \\ P^*(x,t) & Q^*(x,t) \end{bmatrix} = \begin{bmatrix} -\dot{U}(-x,-t) & -\dot{V}(-x,-t) \\ P(-x,-t) & Q(-x,-t) \end{bmatrix}. \tag{5.2.15}$$

These functions are easily seen to satisfy the 'anti-causality' (i.e. $\dot{U}^*$ etc. vanish for $t > 0$) and the equation

$$\begin{bmatrix} \triangle^* & \nabla\partial/\partial t \\ \nabla & -m\partial/\partial t - K\cdot\nabla\nabla \end{bmatrix} \begin{bmatrix} \dot{U}^* & \dot{V}^* \\ P^* & Q^* \end{bmatrix}$$

$$= \begin{bmatrix} 1\delta(t)\delta(x) & 0 \\ 0 & \delta(t)\delta(x) \end{bmatrix}. \tag{5.2.16}$$

We then substitute $\dot{U}^*$ etc. into $\dot{u}^*$ etc. in (5.1.4) with the help of (5.2.15). This process yields potential representations of the solution to (5.1.1) and (5.1.2) in the following forms:

$$\tilde{u}(x,s) = \int_{\partial D} U_0(x-y)S(y,s)dS - \int_{\partial D} S_0(x,y)u(y,s)dS$$

$$+\int_D U_0(\boldsymbol{x}-\boldsymbol{y})\boldsymbol{f}(\boldsymbol{y},s)\mathrm{d}V+\int_{\partial D}\int_0^s \dot{\mathfrak{U}}(\boldsymbol{x}-\boldsymbol{y},s-t)\boldsymbol{S}(\boldsymbol{y},t)\mathrm{d}t\mathrm{d}S$$

$$-\int_{\partial D}\int_0^s \dot{\mathfrak{s}}(\boldsymbol{x},\boldsymbol{y},s-t)\boldsymbol{u}(\boldsymbol{y},t)\mathrm{d}t\mathrm{d}S-\int_{\partial D}\int_0^s P(\boldsymbol{x}-\boldsymbol{y},s-t)r(\boldsymbol{y},t)\mathrm{d}t\mathrm{d}S$$

$$+\int_{\partial D}\int_0^s Z(\boldsymbol{x},\boldsymbol{y},s-t)p(\boldsymbol{y},t)\mathrm{d}t\mathrm{d}S+\int_D\int_0^s \dot{\mathfrak{U}}(\boldsymbol{x}-\boldsymbol{y},s-t)\boldsymbol{f}(\boldsymbol{y},t)\mathrm{d}t\mathrm{d}V$$

$$+\int_D\int_0^s P(\boldsymbol{x}-\boldsymbol{y},s-t)g(\boldsymbol{y},t)\mathrm{d}t\mathrm{d}V+\int_D P(\boldsymbol{x}-\boldsymbol{y},s)\theta(\boldsymbol{y})\mathrm{d}V\ , \qquad (5.2.17)$$

and

$$\tilde{\boldsymbol{p}}(\boldsymbol{x},s)=\int_{\partial D}V_0(\boldsymbol{x}-\boldsymbol{y})\cdot\boldsymbol{S}(\boldsymbol{y},s)\mathrm{d}S-\int_{\partial D}T_0(\boldsymbol{x},\boldsymbol{y})\cdot\boldsymbol{u}(\boldsymbol{y},s)\mathrm{d}S$$

$$+\int_D V_0(\boldsymbol{x}-\boldsymbol{y})\cdot\boldsymbol{f}(\boldsymbol{y},s)\mathrm{d}V+\int_{\partial D}\int_0^s \dot{\mathfrak{V}}(\boldsymbol{x}-\boldsymbol{y},s-t)\cdot\boldsymbol{S}(\boldsymbol{y},t)\mathrm{d}t\mathrm{d}S$$

$$-\int_{\partial D}\int_0^s \dot{\mathfrak{T}}(\boldsymbol{x},\boldsymbol{y},s-t)\cdot\boldsymbol{u}(\boldsymbol{y},t)\mathrm{d}t\mathrm{d}S-\int_{\partial D}\int_0^s Q(\boldsymbol{x}-\boldsymbol{y},s-t)r(\boldsymbol{y},t)\mathrm{d}t\mathrm{d}S$$

$$+\int_{\partial D}\int_0^s W(\boldsymbol{x},\boldsymbol{y},s-t)p(\boldsymbol{y},t)\mathrm{d}t\mathrm{d}S+\int_D\int_0^s \dot{\mathfrak{V}}(\boldsymbol{x}-\boldsymbol{y},s-t)\cdot\boldsymbol{f}(\boldsymbol{y},t)\mathrm{d}t\mathrm{d}V$$

$$+\int_D\int_0^s Q(\boldsymbol{x}-\boldsymbol{y},s-t)g(\boldsymbol{y},t)\mathrm{d}t\mathrm{d}V+\int_D Q(\boldsymbol{x}-\boldsymbol{y},s)\theta(\boldsymbol{y})\mathrm{d}V,$$

$$\boldsymbol{x}\notin\partial D \qquad (5.2.18)$$

where S_0, $\dot{\mathfrak{s}}$, T_0, $\dot{\mathfrak{T}}$, Z and W are kernels defined by

$$\begin{bmatrix} S_{0ij}(\boldsymbol{x},\boldsymbol{y},s) \\ T_{0j}(\boldsymbol{x},\boldsymbol{y},s)\end{bmatrix}=\frac{\partial}{\partial y_l}\begin{bmatrix} U_{0ik}(\boldsymbol{x}-\boldsymbol{y},s) \\ V_{0k}(\boldsymbol{x}-\boldsymbol{y},s)\end{bmatrix}C_{jmkl}n_m(\boldsymbol{y})$$

$$+\begin{bmatrix} P_{0i}(\boldsymbol{x}-\boldsymbol{y},s) \\ Q_0(\boldsymbol{x}-\boldsymbol{y},s)\end{bmatrix}n_j(\boldsymbol{y}),$$

$$\begin{bmatrix} \dot{\mathfrak{s}}_{ij}(\boldsymbol{x},\boldsymbol{y},s) \\ \dot{\mathfrak{T}}_j(\boldsymbol{x},\boldsymbol{y},s)\end{bmatrix}=\frac{\partial}{\partial y_l}\begin{bmatrix} \dot{\mathfrak{U}}_{ik}(\boldsymbol{x}-\boldsymbol{y},s) \\ \dot{\mathfrak{V}}_k(\boldsymbol{x}-\boldsymbol{y},s)\end{bmatrix}C_{jmkl}n_m(\boldsymbol{y})$$

$$+ \begin{bmatrix} \mathring{\Phi}_i(\boldsymbol{x}-\boldsymbol{y},s) \\ \mathring{\mathcal{Q}}(\boldsymbol{x}-\boldsymbol{y},s) \end{bmatrix} n_j(\boldsymbol{y}).$$

$$\begin{bmatrix} Z_i(\boldsymbol{x},\boldsymbol{y},s) \\ W(\boldsymbol{x},\boldsymbol{y},s) \end{bmatrix} = -\frac{\partial}{\partial y_j} \begin{bmatrix} P_i(\boldsymbol{x}-\boldsymbol{y},s) \\ Q(\boldsymbol{x}-\boldsymbol{y},s) \end{bmatrix} K_{jk} n_k(\boldsymbol{y}) \qquad (5.2.19a\text{-}c)$$

and

$$(\tilde{\boldsymbol{u}},p) = \begin{cases} \boldsymbol{u},p & \boldsymbol{x} \in D \\ 0,0 & \boldsymbol{x} \in D^e = R^N \backslash \overline{D}. \end{cases} \qquad (5.2.20)$$

To be precise, (5.2.7-9) and (5.2.13) are not enough to clarify the meaning of the time-volume integral involving $\mathring{U}$. We shall return to this problem later in 5.6, where this integral will be seen to converge in the ordinary sense.

5 . 3 Initial fields

In sections 5.3-5.5 we shall discuss the initial behaviour of the solution to our initial- boundary value problem. The result of this investigation will be used in Part II of this chapter to implement an accurate BIEM. Our discussion takes for granted the existence of the unique solution to our initial- boundary value problem, which satisfies (5.2.17) and (5.2.18). We may therefore use these potential representations to examine the property of the solution.

In the first place we have to introduce some definitions. By 'initial field' we mean

$$\lim_{s \downarrow 0} \boldsymbol{u}(\boldsymbol{x},s) \qquad \boldsymbol{x} \in D \qquad (5.3.1)$$

etc. A limit of this form for a certain fixed point in R^N is called the initial value. The initial condition is what we 'prescribe', but the initial field is what we 'compute'. In other words, the initial field is a part of the unknowns. The 'boundary value' of a certain field, say $\boldsymbol{u}(\boldsymbol{x},s)$, indicates the limit

$$\lim_{x(\in D \text{ or } D^e) \to x_0} \boldsymbol{u}(\boldsymbol{x},s) \qquad (5.3.2)$$

where x_0 is a point on the boundary, and D^e is the domain exterior to D as defined in (5.2.20), respectively. Hence the boundary value of the initial field of $\boldsymbol{u}(\boldsymbol{x},s)$ is

$$\lim_{x(\in D) \to x_0} \lim_{s \downarrow 0} \boldsymbol{u}(\boldsymbol{x},s) \qquad (5.3.3)$$

while the initial value of the boundary value of $\boldsymbol{u}(\boldsymbol{x},s)$ is

$$\lim_{s\downarrow 0}\ \lim_{x(\in D)\to x_0}\ u(x,s) \tag{5.3.4}$$

In the sequel we shall write

$$u(x,0) := \lim_{s\downarrow 0} u(x,s), \quad (x\in R^N)$$

$$u(x_0,s) := \lim_{x(\in D)\to x_0} u(x,s). \quad (x_0\in \partial D,\ s>0) \tag{5.3.5a,b}$$

Our tools for the investigation of the initial fields are the equations

$$\tilde{u}(x,0) = \int_{\partial D} U_0(x-y)S(y,0)\mathrm{d}S - \int_{\partial D} S_0(x,y)u(y,0)\mathrm{d}S$$

$$+ \int_D U_0(x-y)f(y,0)\mathrm{d}V + \int_D P_0(x-y)\theta(y)\mathrm{d}V \tag{5.3.6}$$

and

$$\tilde{p}(x,0) = \int_{\partial D} V_0(x-y)\cdot S(y,0)\mathrm{d}S - \int_{\partial D} T_0(x-y)\cdot u(y,0)\mathrm{d}S$$

$$+ \int_D V_0(x-y)\cdot f(y,0)\mathrm{d}V + \int_D Q_0(x-y)\theta(y)\mathrm{d}V, \qquad x\notin\partial D \tag{5.3.7}$$

which we obtain by letting $s \downarrow 0$ in (5.2.17) and (5.2.18) with the help of (5.2.13) and (5.2.14). The last integral in (5.3.7) is short for

$$C_Q\tilde{\theta}(x) + \mathrm{v.p.}\int_D \dot{Q}_0(x-y)\theta(y)\mathrm{d}V \tag{5.3.8}$$

(see (5.2.8) and (5.2.9)).

Equations (5.3.6) and (5.3.7) are the representations of the initial fields in terms of the initial values of the boundary values of u and S. It is important to notice that there is no a priori reason to assume

$$\lim_{x(\in D)\to x_0} u(x,0) = u(x_0,0),$$

$$\lim_{x(\in D)\to x_0} p(x,0) = p(x_0,0) \quad (x_0\in\partial D) \tag{5.3.9a,b}$$

at this moment. Actually, we shall see that (5.3.9a) is correct, but (5.3.9b) is not.

We now prepare formulae for the boundary values of the potentials in (5.3.6) and (5.3.7). This is in order to relate the boundary values of $u(x,0)$ and $p(x,0)$ $(x \notin \partial D)$ to $u(x_0,0)$ and $p(x_0,0)$ $(x_0 \in \partial D)$. We first note from (5.2.2),(5.2.3) and (5.2.19) that these potentials are of the type discussed in 1.3. Hence we may utilise (1.3.1.4), (1.3.1.13), (1.3.1.24), (1.3.2.2) and (1.3.2.16) to obtain

$$\lim_{x \to x_0} \int_{\partial D} U_0(x-y) S(y,s) dS = \int_{\partial D} U_0(x_0-y) S(y,s) dS \ , \tag{5.3.10}$$

$$\lim_{x \to x_0} \int_{\partial D} S_0(x,y) u(y,s) dS$$

$$= \pm \frac{1}{2} u(x_0,s) + \text{v.p.} \int_{\partial D} S_0(x_0-y) u(y,s) dS \ , \tag{5.3.11}$$

$$\lim_{x \to x_0} \int_D U_0(x-y) f(y,s) dV = \int_D U_0(x_0-y) f(y,s) dV \ , \tag{5.3.12}$$

$$\lim_{x \to x_0} \int_D P_0(x-y) \theta(y) dV = \int_D P_0(x_0-y) \theta(y) dV \ , \tag{5.3.13}$$

$$\lim_{x \to x_0} \int_{\partial D} V_0(x-y) \cdot S(y,s) dS = \pm \frac{1}{2} \frac{\triangle^{*-1}(n)n}{m + n \cdot \triangle^{*-1}(n)n} \cdot S(x_0,s)$$

$$+ \text{v.p.} \int_{\partial D} V_0(x_0-y) \cdot S(y,s) dS \ , \tag{5.3.14}$$

$$\lim_{x \to x_0} \int_{\partial D} T_0(x,y) \cdot u(y,s) dS$$

$$= \mp \frac{1}{2} \frac{\partial}{\partial \xi_\alpha} \left(\frac{C[\triangle^{*-1}(\xi)\xi \otimes \xi]n - n}{m + \xi \cdot \triangle^{*-1}(\xi)\xi} \right)_j \Bigg|_{\xi=n} \frac{\partial u_j}{\partial x_\alpha}(x_0,s)$$

$$+ \text{p.f.} \int_{\partial D} T_0(x,y) \cdot u(y,s) dS$$

$$= \mp\frac{1}{2}\left(\frac{\operatorname{div} \boldsymbol{u}(x_0,s) - \triangle^{*-1}(\boldsymbol{n})\boldsymbol{n}\cdot\boldsymbol{C}[\nabla\boldsymbol{u}(x_0,s)]\boldsymbol{n}}{m + \boldsymbol{n}\cdot\triangle^{*-1}(\boldsymbol{n})\boldsymbol{n}}\right)$$

$$+ \text{p.f.}\int_{\partial D} T_0(\boldsymbol{x},\boldsymbol{y})\cdot\boldsymbol{u}(\boldsymbol{y},s)\mathrm{d}S, \tag{5.3.15*}$$

$$\lim_{x\to x_0}\int_D V_0(\boldsymbol{x}-\boldsymbol{y})\cdot\boldsymbol{f}(\boldsymbol{y},s)\mathrm{d}V = \int_D V_0(\boldsymbol{x}_0-\boldsymbol{y})\cdot\boldsymbol{f}(\boldsymbol{y},s)\mathrm{d}V\ , \tag{5.3.16}$$

$$\lim_{x\to x_0}\int_D Q_0(\boldsymbol{x}-\boldsymbol{y})\theta(\boldsymbol{y})\mathrm{d}V = \frac{1}{2}\left(C_Q \mp \frac{1}{m + \boldsymbol{n}\cdot\triangle^{*-1}(\boldsymbol{n})\boldsymbol{n}}\right)\theta(\boldsymbol{x}_0)$$

$$+ \text{v.p.}^{-}\int_D Q_0(\boldsymbol{x}_0-\boldsymbol{y})\theta(\boldsymbol{y})\mathrm{d}V\ , \tag{5.3.17}$$

where the upper (lower) sign indicates the approach from the exterior (interior) of D, C_Q is defined in (5.2.9a), and the cartesian frame used in (5.3.15) is the same as the one in 1.3. The apparent dependence of the non-integral term in (5.3.15) on $\partial\boldsymbol{u}/\partial n$ is resolved by substituting $\nabla\boldsymbol{u} - \boldsymbol{n}\otimes(\partial\boldsymbol{u}/\partial n)$ for $\nabla\boldsymbol{u}$ in (5.3.15). The limiting values of these integrals as $s\downarrow 0$ are obtained by putting $s = 0$ on the RHS's of (5.3.10-17).

We are now ready to compute the boundary values of the expressions (5.3.6) and (5.3.7) with the help of (5.3.10-17). Actually, we easily obtain

$$\lim_{x\to x_0}\tilde{\boldsymbol{u}}(\boldsymbol{x},0) = \mp\frac{1}{2}\boldsymbol{u}(\boldsymbol{x}_0,0) + \int_{\partial D} U_0(\boldsymbol{x}_0-\boldsymbol{y})\boldsymbol{S}(\boldsymbol{y},0)\mathrm{d}S$$

$$- \text{v.p.}\int_{\partial D} S_0(\boldsymbol{x}_0,\boldsymbol{y})\boldsymbol{u}(\boldsymbol{y},0)\mathrm{d}S + \int_D U_0(\boldsymbol{x}_0-\boldsymbol{y})\boldsymbol{f}(\boldsymbol{y},0)\mathrm{d}V$$

$$+ \int_D P_0(\boldsymbol{x}_0-\boldsymbol{y})\theta(\boldsymbol{y})\mathrm{d}V, \qquad \boldsymbol{x}_0 \in \partial D_R \tag{5.3.18}$$

$$\lim_{x\to x_0}\tilde{p}(\boldsymbol{x},0) = \pm\frac{1}{2}\frac{\triangle^{*-1}(\boldsymbol{n})\boldsymbol{n}}{m + \boldsymbol{n}\cdot\triangle^{*-1}(\boldsymbol{n})\boldsymbol{n}}\cdot\boldsymbol{S}(\boldsymbol{x}_0,0)$$

---

* Greek index runs from 1 to N-1.

$$\pm\frac{1}{2}\left(\frac{\operatorname{div} u(x_0,s) - \triangle^{*-1}(n)n\cdot C[\nabla u(x_0,s)]n}{m + n\cdot\triangle^{*-1}(n)n}\right)$$

$$+\left(\frac{C_Q}{2} \mp \frac{1}{2}\frac{1}{m + n\cdot\triangle^{*-1}(n)n}\right)\theta(x_0)$$

$$+ \text{v.p.}\int_{\partial D} V_0(x_0-y)\cdot S(y,0)dS - \text{p.f.}\int_{\partial D} T_0(x_0,y)\cdot u(y,0)dS$$

$$+ \int_D V_0(x_0-y)\cdot f(y,0)dV + \text{v.p.}^{-}\int_D Q_0(x_0-y)\theta(y)dV \ .$$

$$x_0 \in \partial D_R \qquad (5.3.19)$$

From (5.3.18) follows

$$\lim_{x(\in D)\to x_0} u(x,0) = \lim_{x(\in D)\to x_0} \tilde{u}(x,0) - \lim_{x(\in D^e)\to x_0} \tilde{u}(x,0)$$

$$= u(x_0,0), \qquad x_0 \in \partial D_R \qquad (5.3.20)$$

where we have used (5.2.20). In the same manner we use (5.3.19) to obtain

$$\lim_{x(\in D)\to x_0} p(x,0) = \lim_{x(\in D)\to x_0} \tilde{p}(x,0) - \lim_{x(\in D^e)\to x_0} \tilde{p}(x,0)$$

$$= -\frac{\triangle^{*-1}(n)n}{m + n\cdot\triangle^{*-1}(n)n}\cdot S(x_0,0)$$

$$- \frac{\operatorname{div} u(x_0,s) - \triangle^{*-1}(n)n\cdot C[\nabla u(x_0,s)]n}{m + n\cdot\triangle^{*-1}(n)n}$$

$$+ \frac{\theta(x_0)}{m + n\cdot\triangle^{*-1}(n)n}. \qquad (5.3.21)$$

Also, we can write these limits as

$$\lim_{x(\in D)\to x_0} u(x,0) = \lim_{x(\in D)\to x_0} \tilde{u}(x,0) + \lim_{x(\in D^e)\to x_0} \tilde{u}(x,0)$$

$$= 2\Big(\int_{\partial D} U_0(x-y)S(y,0)dS - \text{v.p.}\int_{\partial D} S_0(x_0,y)u(y,0)dS$$

$$+ \int_D U_0(\boldsymbol{x}_0-\boldsymbol{y})\boldsymbol{f}(\boldsymbol{y},0)\mathrm{d}V + \int_D P_0(\boldsymbol{x}_0-\boldsymbol{y})\theta(\boldsymbol{y})\mathrm{d}V\Big),$$

$$\boldsymbol{x}_0 \in \partial D_R \tag{5.3.22}$$

and

$$\lim_{x(\in D)\to x_0} p(\boldsymbol{x},0) = \lim_{x(\in D)\to x_0} \tilde{p}(\boldsymbol{x},0) + \lim_{x(\in D^e)\to x_0} \tilde{p}(\boldsymbol{x},0)$$

$$= 2\Big(\frac{C_0}{2}\theta(\boldsymbol{x}_0) + \mathrm{v.p.}\int_{\partial D} V_0(\boldsymbol{x}_0-\boldsymbol{y})\cdot\boldsymbol{S}(\boldsymbol{y},0)\mathrm{d}S$$

$$- \mathrm{p.f.}\int_{\partial D} \boldsymbol{T}_0(\boldsymbol{x}_0,\boldsymbol{y})\cdot\boldsymbol{u}(\boldsymbol{y},0)\mathrm{d}S + \int_D V_0(\boldsymbol{x}_0-\boldsymbol{y})\cdot\boldsymbol{f}(\boldsymbol{y},0)\mathrm{d}V$$

$$+ \mathrm{v.p.}^{-}\int_D Q_0(\boldsymbol{x}_0-\boldsymbol{y})\theta(\boldsymbol{y})\mathrm{d}V\Big). \qquad \boldsymbol{x}_0 \in \partial D_R \tag{5.3.23}$$

Equations (5.3.20) and (5.3.21) are useful for computing the boundary values of the initial field, whereas (5.3.23) will be used later to find a relation between the limit in (5.3.23) and $p(\boldsymbol{x}_0,0)$ $(\boldsymbol{x}_0\in\partial D)$.

It is also interesting to establish a relation between the boundary values of the initial field $\boldsymbol{u}(\boldsymbol{x},0)$, $p(\boldsymbol{x},0)$ and $\boldsymbol{S}(\boldsymbol{x}_0,0)$ $(\boldsymbol{x}_0\in\partial D)$. One may do this by differentiating (5.3.6), followed by the use of the formulae analogous to (5.3.14-17). We here take another approach, which considers the physical meaning of the initial field. To this purpose an equation

$$\begin{bmatrix} \triangle^* & -\nabla \\ -\nabla & -m \end{bmatrix}\begin{bmatrix} U_0 & V_0 \\ P_0 & Q_0 \end{bmatrix} = -\begin{bmatrix} 1\delta(\boldsymbol{x}) & 0 \\ 0 & \delta(\boldsymbol{x}) \end{bmatrix}, \tag{5.3.24}$$

which readily follows from (5.2.3a,b) and (5.2.6a,c), turns out to be useful.

Assume $m\neq 0$ first. Equation (5.3.24) readily gives

$$\Big(\triangle^* + \frac{1}{m}\nabla\mathrm{div}\Big)U_0 = -1\delta(\boldsymbol{x}). \tag{5.3.25}$$

Obviously, (5.3.25) means that U_0 is a fundamental solution of elastostatics with $\boldsymbol{C} + (1\otimes 1)/m$ as the elasticity tensor. Also (5.2.9a) gives

$$\begin{bmatrix} S_{0ij}(\boldsymbol{x},\boldsymbol{y}) \\ T_{0j}(\boldsymbol{x},\boldsymbol{y}) \end{bmatrix} = \partial_{y_l}\begin{bmatrix} U_{0ik}(\boldsymbol{x}-\boldsymbol{y}) \\ V_{0k}(\boldsymbol{x}-\boldsymbol{y}) \end{bmatrix}\Big(C_{jpkl} + \frac{\delta_{jp}\delta_{kl}}{m}\Big)n_p$$

$$|x-y| \neq 0 \qquad (5.3.26)$$

because we have

$$\begin{bmatrix} P_0(x-y) \\ Q_0(x-y) \end{bmatrix} = \frac{1}{m}\,\mathrm{div}_y \begin{bmatrix} U_0(x-y) \\ V_0(x-y) \end{bmatrix} + \begin{bmatrix} 0 \\ \delta(x-y)/m \end{bmatrix} \qquad (5.3.27)$$

from (5.3.24). Equation (5.3.26) says that S_0 is the double layer kernel associated with U_0 and the modified elasticity tensor. In addition, the use of (5.3.27) transforms the volume integrals in (5.3.6) and (5.3.7) into

$$\int_D P_0(x-y)\theta(y)dV = \frac{1}{m}\int_D \mathrm{div}_y U_0(x-y)\theta(y)dV$$

$$= \frac{1}{m}\int_{\partial D} U_0(x-y)n\theta(y)dS - \frac{1}{m}\int_D U_0(x-y)\nabla\theta(y)dV \qquad (5.3.28)$$

and

$$\int_D Q_0(x-y)\theta(y)dV = \frac{1}{m}\int_D \mathrm{div}_y V_0(x-y)\theta(y)dV + \frac{1}{m}\tilde{\theta}(x)$$

$$= \frac{1}{m}\int_{\partial D} V_0(x-y)\cdot n\theta(y)dS - \frac{1}{m}\int_D V_0(x-y)\cdot\nabla\theta(y)dV$$

$$+ \frac{1}{m}\tilde{\theta}(x). \qquad (5.3.29)$$

Hence we substitute (5.3.28) and (5.3.29) into (5.3.6) and (5.3.7), respectively, to obtain

$$\tilde{u}(x,0) = \int_{\partial D} U_0(x-y)\left(S(y,0) + \frac{1}{m}n\theta(y)\right)dS - \int_{\partial D} S_0(x,y)u(y,0)dS$$

$$+ \int_D U_0(x-y)\left(f(y,0) - \frac{1}{m}\nabla\theta(y)\right)dV \qquad (5.3.30)$$

and

$$\tilde{p}(x,0) = \int_{\partial D} V_0(x-y)\cdot\left(S(y,0) + \frac{1}{m}n\theta(y)\right)dS - \int_{\partial D} T_0(x,y)\cdot u(y,0)dS$$

$$+ \int_D V_0(x-y) \cdot \left(f(y,0) - \frac{1}{m} \nabla\theta(y) \right) dV + \frac{1}{m} \tilde{\theta}(x)$$

$$= \frac{1}{m} \left(-\mathrm{div}\, \tilde{u}(x) + \tilde{\theta}(x) \right), \qquad x \in \partial D, \tag{5.3.31}$$

where we have used (5.3.26), (5.3.27) and (5.2.6a). We thus conclude from (1.1.7), (5.3.25), (5.3.30) and (5.3.31) that: "When $m \neq 0$, the initial values of u and p coincide with the displacement and $-1/m \times$ (volume strain) $+ \theta/m$ of the elastostatic solution whose elasticity tensor is $C + (1 \otimes 1)/m$, and whose given data are $u_0(\cdot,0)$ for the surface displacement on ∂D_u, $S_0(\cdot,0) + n\theta(\cdot)/m$ for the traction on ∂D_s and $f(\cdot,0) - \nabla\theta(\cdot)/m$ for the body force, respectively." In particular we have

$$S(x_0,0) = \lim_{x(\in D) \to x_0} \left\{ C[\nabla u(x,0)]n + \frac{n}{m} \mathrm{div}\, u(x,0) \right\} - \frac{n}{m} \theta(x_0)$$

$$= \lim_{x(\in D) \to x_0} \left\{ C[\nabla u(x,0)]n - p(x,0)n \right\} = \lim_{x(\in D) \to x_0} S(x,0). \tag{5.3.32}$$

When $m = 0$ we see from (5.3.24) that U_0, V_0, P_0 and Q_0 are the fundamental solutions of elastostatics with prescribed volumetric strain (see the appendix to chapter 4 or Kobayashi & Nishimura(1982)) Bearing this in mind we conclude from (5.3.6) and (5.3.7) that "When $m = 0$ the initial values of u and p coincide with the displacement and indeterminate pressure of the elastostatic solution whose elasticity tensor, volumetric strain, surface displacement on ∂D_u, surface traction on ∂D_s and body force are C, θ, $u_0(\cdot,0)$, $S_0(\cdot,0)$, and $f(\cdot,0)$, respectively." Hence we obtain (5.3.32) again.

One may think that these results are trivial. For example when $m = 0$, one may 'use' (5.1.1) and (5.1.6) to obtain

$$\triangle^* u - \nabla p + f = 0,$$

$$\mathrm{div}\, u = \theta \qquad \text{in } D \ (t = 0) \tag{5.3.33a,b}$$

and

$$u = u_0(\cdot,0) \qquad \text{on } \partial D_u,$$

$$\{C[\nabla u] - p\} n = S_0(\cdot,0) \qquad \text{on } \partial D_s \tag{5.3.34a,b}$$

for $t = 0$. This is exactly the result which we have just proved. However, this argument is ambiguous. Indeed, the same argument might have concluded that

$$C[\nabla \boldsymbol{u}]\boldsymbol{n} = \boldsymbol{S}_0(\cdot,0) + p_0(\cdot,0)\boldsymbol{n} \qquad \text{on} \quad \partial D_s \cap \partial D_p \tag{5.3.35}$$

were the boundary condition for the initial field, which is obviously wrong. This explains why the above lengthy calculation is necessary. Also, it is seen from the foregoing argument that (5.3.6) and (5.3.7) are not independent.

Finally, we consider how one can compute the initial field. As can be easily seen, one just has to determine $\boldsymbol{u}(x_0,0)$ and $\boldsymbol{S}(x_0,0)$ $(x_0 \in \partial D)$ and use (5.3.6) and (5.3.7) to compute the initial field. Hence we are led to the following question: How can we determine $\boldsymbol{u}(x_0,0)$ and $\boldsymbol{S}(x_0,0)$ for $x_0 \in \partial D$? Equations (5.1.7a,b) show that half of these quantities are given as the boundary data, but the unknown halves of $\boldsymbol{u}(x_0,0)$ and $\boldsymbol{S}(x_0,0)$ are still to be determined. We can, however, easily obtain an integral equation to determine these quantities. Namely, we use the exterior limit in (5.3.18) to have

$$\begin{aligned} 0 = -\frac{1}{2}\boldsymbol{u}(x_0,0) &+ \int_{\partial D} U_0(x_0-y)\boldsymbol{S}(y,0)\,dS \\ &- \text{v.p.}\int_{\partial D} \boldsymbol{S}_0(x_0,y)\boldsymbol{u}(y,0)\,dS + \int_D U_0(x_0-y)\boldsymbol{f}(y,0)\,dV \\ &+ \int_D P_0(x_0-y)\theta(y)\,dV. \qquad x_0 \in \partial D_R \end{aligned} \tag{5.3.36}$$

If $m \neq 0$ one may alternatively use a BIE obtained from (5.3.30). As could be inferred from the dependence of (5.3.7) on (5.3.6), one does not have to consider a BIE obtained from (5.3.7) for determining the initial field. This is in contrast to the subsequent analysis to be discussed in 5.6 where one has to solve 2 integral equations simultaneously. As a cost for this saving, however, (5.3.36) loses the uniqueness of the solution when $m = 0$ and D has holes, although the solution to the original boundary value problem is unique. This purely mathematical phenomenon could be eliminated by using remedies discussed in Kobayashi & Nishimura(1982) and in the appendix to chapter 4. After solving (5.3.36) for $\boldsymbol{u}(x_0,0)$ and $\boldsymbol{S}(x_0,0)$ $(x_0 \in \partial D)$, one may determine the boundary values of the initial fields through (5.3.20) and (5.3.21).

Before closing this section we remark, as another consequence of (5.2.17) and (5.2.18), that the possible jumps of $\boldsymbol{u}$ and p at $s_0 > 0$ satisfy

$$\begin{aligned} [\tilde{\boldsymbol{u}}(x,s_0)] = &\int_{\partial D} U_0(x-y)\,[\boldsymbol{S}(y,s_0)]\,dS - \int_{\partial D} \boldsymbol{S}_0(x,y)\,[\boldsymbol{u}(y,s_0)]\,dS \\ &+ \int_D U_0(x-y)\,[\boldsymbol{f}(y,s_0)]\,dV, \end{aligned} \tag{5.3.37}$$

and

$$[\tilde{p}(x,s_0)] = \int_{\partial D} V_0(x-y)\cdot[S(y,s_0)]\,dS - \int_{\partial D} T_0(x,y)\cdot[u(y,s_0)]\,dS$$

$$+ \int_D V_0(x-y)\cdot[f(y,s_0)]\,dV\ , \qquad x \notin \partial D \qquad (5.3.38)$$

where $[\tilde{u}(x,s_0)]$ indicates $\tilde{u}(x,s_0^+) - \tilde{u}(x,s_0^-)$ and so on. Therefore, we can interpret $[u(x,s_0)]$ and $[p(x,s_0)]$ in almost the same manner as we did the initial values by utilising the obvious correspondence such as $u(x,0) \sim [u(x,s_0)]$, $\theta \sim 0$ etc. between (5.3.6-7) and (5.3.37-38).

5 . 4 Initial behaviour of time dependent potentials on the boundary

In this section and the next we shall continue the effort of relating

$$p(x_0,0) \tag{5.4.1}$$

and

$$\lim_{x(\in D)\to x_0} p(x,0). \quad x_0 \in \partial D \tag{5.4.2}$$

We first remember that the analysis in 5.3 has yielded expressions for the limit in (5.4.2). Obviously, one needs an analogous expression for (5.4.1) to discuss relations between (5.4.1) and (5.4.2). With this in mind we shall attempt to carry out the limit calculation of letting x $(\in D)$ tend to x_0 followed by letting $s \downarrow 0$ in (5.2.18). A part of this work, however, has been done in the previous section where we have considered time independent potentials. Actually, we put $s = 0$ in (5.3.10-17) to obtain what we need. We are thus led to the computation of the aforementioned limit for the potentials in (5.2.18) having time dependent kernels. In the sequel we shall do this with the help of the method of Fourier transform used in 1.3. Specifically, we generalise the problem a little and consider the limits

$$\lim_{s\downarrow 0}\lim_{x\to x_0}\int_0^s\int_{\partial D} F(x-y,s-t)\ \psi(y,t)\ dS_y\ dt, \tag{5.4.3}$$

$$\lim_{s\downarrow 0}\lim_{x\to x_0}\int_0^s\int_{D} F(x-y,s-t)\ \psi(y,t)\ dV_y\ dt, \tag{5.4.4}$$

$$\lim_{s\downarrow 0}\lim_{x\to x_0}\int_{D} F(x-y,s)\ \psi(y,0)\ dV_y, \tag{5.4.5}$$

where $\psi(y,t)$ is a density function having an asymptotic expansion

$$\psi(x,t) \sim \sum_i \varphi_i(x)\, t^{\beta_i} \qquad \text{as } t \downarrow 0, \tag{5.4.6}$$

with exponents $-1 < \beta_1 < \beta_2 < \cdots\cdots$, and F is a kernel which has a (partial) Fourier transform

$$\int_{\mathbb{R}^N} F(x,t)e^{-i\xi\cdot x}\ dx = \hat{F}(\xi)e^{-G(\xi)t}. \tag{5.4.7*}$$

For the purpose of completeness we shall also consider potentials in

(5.2.17) since this can be done without additional effort. Equations (5.2.2-4) and (5.2.19) then suggest an assumption that $\hat{F}$ is $(n, 0)$ homogeneous with $-1 \leqq n \leqq 2$ and smooth except at the origin. Also, we require G to be (2, 0) homogeneous (see 1.3) and 'differentiable and positive' except at the origin. It is then sufficient to set the parameters n and β_1 as in the following table:

	n	β_1	kernels (n)
surface-time integral (5.4.3)	-1,0	$\beta_1 > -1$	P (-1) $\dot{U}, Q, Z$ (0)
	1,2	$\beta_1 = 0$	$\dot{V}, \dot{\Sigma}, W$ (1) $\dot{T}$ (2)
volume-time integral (5.4.4)	-1,0,1	$\beta_1 = 0$	$P(-1)$ $\dot{U}, Q(0), \dot{V}(1)$
volume integral (5.4.5)	-1,0	$\beta_1 = 0$	$P(-1)$ $Q(0)$

Indeed, one readily shows that the above combinations cover all the possibilities one may encounter in the investigation of the integrals in (5.2.17) and (5.2.18). For example, one has to consider a negative β only in surface-time integrals involving r in (5.2.17) and (5.2.18). Since these integrals have either P or Q as kernel functions, one may keep his/her attention only to the cases with $n = -1, 0$.

5 . 4 . 1 Surface-time integrals

We now consider the limit shown in (5.4.3) assuming, as in 1.3, that ∂D is locally plane. Again, as in 1.3, only the effect of the singularity of the kernel function F on (5.4.3) is of interest. Since this singularity is localised at a boundary point x_0, we may pay attention only to the contribution to (5.4.3) from the immediate vicinity of x_0. This justifies us to assume that the domain of integration is R^{N-1}. Actually, we may approximate ψ by a function defined on a small planer disc S centred at x_0 and tangent to ∂D, followed by putting $\psi = 0$ in $R^{N-1} \backslash S$. It is then convenient to use a cartesian frame whose origin is at x_0 and whose x_N axis is in the direction of the normal vector $\boldsymbol{n}$ to S (see Fig.5.4.1.1). With these tools thus introduced, we are now ready to investigate the limit in (5.4.3) by considering the following partial Fourier transform with respect to x_α $(1 \leqq \alpha \leqq N-1)$:

$$\lim_{s \downarrow 0} \lim_{x_N \to 0} \hat{E}(\xi_\alpha | x_N, s)$$

---

* One may take $G(\xi)$ to be short for $\exp(\xi, 1)$ in (5.2.4).

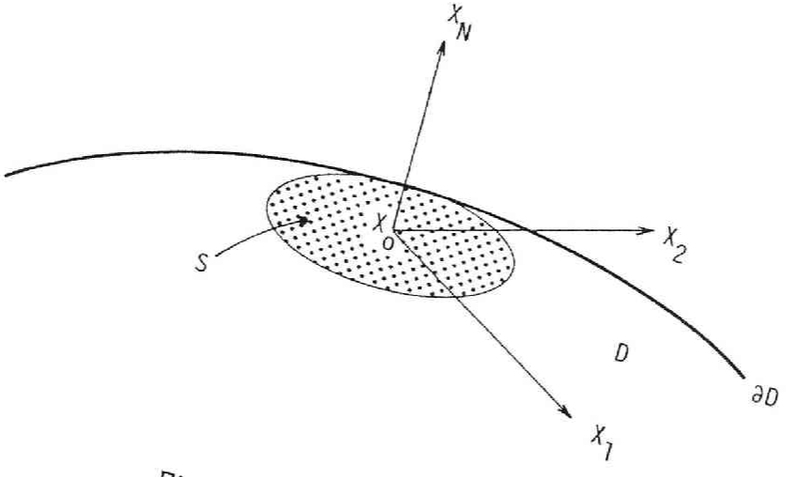

Fig.5.4.1.1 Notation.

$$= \lim_{s\downarrow 0} \lim_{x_N\to 0} \frac{1}{2\pi} \lim_{\varepsilon\downarrow 0} \int_0^s t^\beta dt \int_{-\infty}^{\infty} e^{i\xi_N x_N - \varepsilon\xi_N^2} \hat{F}(\xi_\alpha, \xi_N) e^{-G(\xi_\alpha,\xi_N)(s-t)} d\xi_N, \quad (5.4.1.1)$$

where β is one of β_i's in (5.4.6) (β_1 in most cases). The limit in (5.4.3) is then obtained by multiplying (5.4.1.1) by the N-1 dimensional Fourier transform of ψ, followed by a Fourier inversion.

To begin with we prepare a

Proposition. Let $\hat{F}$ be $(n,0)$ homogeneous, with either n=-1, or 'n=0 and $\hat{F}(0,1) = 0$.' Also, let G be a positive $(2,0)$ homogeneous function. Furthermore, $\hat{F}$ and G are assumed to be continuously differentiable except at the origin. We then have

$$\lim_{\varepsilon\downarrow 0}\int_{-\infty}^{\infty} \hat{F}(\xi_\alpha, \xi_N) e^{-G(\xi_\alpha,\xi_N)\varepsilon} d\xi_N$$

$$= \text{v.p.} \int_{-\infty}^{\infty} \left(\hat{F}(\xi_\alpha, \xi_N) - \frac{1}{\xi_N} H(\xi_\alpha)\right) d\xi_N, \quad (5.4.1.2)$$

where H is a certain function independent of G. Hence this limit is independent of the form of G. In particular,

$$\lim_{\varepsilon\downarrow 0}\int_{-\infty}^{\infty} \hat{F}(\xi_\alpha, \xi_N) e^{-G(\xi_\alpha,\xi_N)\varepsilon} d\xi_N = \lim_{\varepsilon\downarrow 0}\int_{-\infty}^{\infty} \hat{F}(\xi_\alpha, \xi_N) e^{-\varepsilon\xi_N^2} d\xi_N. \quad (5.4.1.3)$$

Proof. We have

$$\int_{-\infty}^{\infty} \hat{F}(\xi_\alpha, \xi_N) e^{-G(\xi_\alpha,\xi_N)\varepsilon} d\xi_N$$

$$= \text{v.p.} \int_{-\infty}^{\infty} \left(\hat{F}(\xi_\alpha, \xi_N) - \frac{1}{\xi_N} H(\xi_\alpha)\right) e^{-G(\xi_\alpha,\xi_N)\varepsilon} d\xi_N$$

$$+ H(\xi_\alpha) \text{ v.p.} \int_{-\infty}^{\infty} \frac{e^{-G(\xi_\alpha,\xi_N)\varepsilon}}{\xi_N} d\xi_N, \quad (5.4.1.4)$$

where v.p. stands for Cauchy's principal value, and

$$H(\xi_\alpha) = \begin{cases} \hat{F}(0,1), & (n=-1) \\ \xi_\beta \, \partial/\partial\xi_\beta \, \hat{F}(\xi)\,|_{(\xi_\alpha,\xi_N)=(0,1)}. & (n=0) \end{cases} \quad (5.4.1.5)$$

The first integral on the RHS of (5.4.1.4) tends to the RHS of (5.4.1.2) as $\varepsilon\downarrow 0$ because the expression in the parentheses in (5.4.1.4) is $O(1/\xi_N^2)$ as $|\xi_N| \to \infty$. The integral in the second term on the RHS of (5.4.1.4) is rewritten as

$$\text{v.p.}\int_{-\infty}^{\infty}\frac{e^{-G(\xi_\alpha,\xi_N)\varepsilon}}{\eta}\,d\eta = \int_0^{\infty}\frac{e^{-G(\sqrt{\varepsilon}\xi_\alpha,\eta)} - e^{-G(-\sqrt{\varepsilon}\xi_\alpha,\eta)}}{\eta}d\eta, \qquad (5.4.1.6)$$

which tends to zero as $\varepsilon \downarrow 0$ due to the assumption on G. This concludes the proof.

We now compute (5.4.3) for various combinations of n and β:

i) $n = -1,0$, $\beta > -1$. We first rewrite the time integral in (5.4.1.1) into

$$\int_0^s e^{-G(\xi)(s-t)}t^\beta dt = e^{-G(\xi)s}s^{1+\beta}\int_0^1 e^{G(\xi)su}u^\beta du. \qquad (\beta > -1) \qquad (5.4.1.7)$$

The asymptotic expansion for incomplete gamma function then shows that the last integral in (5.4.1.7) is of the order of $s^\beta/G(\xi)$ for a large $|\xi|$. We are thus justified (by Lebesgue's theorem) to write (5.4.1.1) as

$$\lim_{s\downarrow 0}\lim_{x_N\to 0}\hat{E}(\xi_\alpha|x_N,s)$$

$$= \frac{1}{2\pi}\lim_{s\downarrow 0}\int_{-\infty}^{\infty}d\xi_N\int_0^s\hat{F}(\xi_\alpha,\xi_N)e^{-G(\xi_\alpha,\xi_N)(s-t)}t^\beta dt\ , \qquad (5.4.1.8)$$

because the integrand (as a function of ξ_N) is of order $n-2$ ($\leqq -2$) at infinity. In passing we present two other forms for the integral in (5.4.1.8), i.e.

$$s^{1+\beta}\int_0^1 u^\beta du\int_{-\infty}^{\infty}\hat{F}(\xi)e^{-G(\xi)s(1-u)}\,d\xi_N \qquad (5.4.1.9)$$

and

$$s^{1/2+\beta-n/2}\int_{-\infty}^{\infty}d\eta\int_0^1\hat{F}(\sqrt{s}\xi_\alpha,\eta)e^{-G(\sqrt{s}\xi_\alpha,\eta)(1-u)}u^\beta du, \qquad (5.4.1.10)$$

for later use.

When $n = -1$ the proposition and (5.4.1.9) give

$$|\hat{E}(\xi_\alpha|0,s)| \leqq s^{1+\beta}C(\xi_\alpha), \qquad (5.4.1.11)$$

where $C(\xi_\alpha)$ is a constant dependent on ξ_α but not on s. This means $\lim_{s\downarrow 0}\hat{E}(\xi_\alpha|0,s) = 0$ for $n = -1$ since $\beta > -1$. Hence we conclude

$$\lim_{s\downarrow 0}\lim_{x\to x_0}\int_0^s\int_S F(x-y,s-t)\varphi(y)\,t^{\beta}dS_y\,dt = 0 \qquad (5.4.1.12)$$

for $n = -1$ and $\beta > -1$ (see (5.4.7) and (5.4.1.1)), where φ indicates φ_1 in (5.4.6).

For $n = 0$, (5.4.1.10) yields

$$\lim_{s\downarrow 0} s^{-(1/2+\beta)}\hat{E}(\xi_\alpha|0,s) = \frac{1}{2\pi}\int_{-\infty}^{\infty}d\eta\int_0^1\hat{F}(0,\eta)e^{-G(0,\eta)(1-u)}u^{\beta}du$$

$$= \frac{1}{2(\pi)^{1/2}}\,\frac{\hat{F}(0,1)}{(G(0,1))^{1/2}}\,B(\beta+1,\frac{1}{2}), \qquad (5.4.1.13)$$

where $B(\cdot,\cdot)$ is the Beta function. This equation then shows that

$$\lim_{s\downarrow 0}\hat{E}(\xi_\alpha|0,s) \qquad (5.4.1.14)$$

is finite only if $\beta \geqq -1/2$ for a non-zero $\hat{F}(0,1)$. Moreover this limit is nonzero only if $\beta = -1/2$, in which case we have

$$\lim_{s\downarrow 0}\hat{E}(\xi_\alpha|0,s) = \frac{\sqrt{\pi}}{2}\,\frac{\hat{F}(0,1)}{(G(0,1))^{1/2}}. \qquad (n = 0,\ \beta = -\frac{1}{2}) \quad (5.4.1.15)$$

Hence we have the following result:

$$\lim_{s\downarrow 0}\lim_{x\to x_0}\int_0^s\int_S F(x-y,s-t)\varphi(y)\,t^{\beta}dS_y\,dt$$

$$= \begin{cases} (\pi)^{1/2}\,\hat{F}(n)\ \varphi(x_0)/2(G(n))^{1/2}, & (\beta = -1/2) \\ 0. & (\beta > -1/2) \end{cases} \qquad (5.4.1.16)$$

The limit in (5.4.1.16) cannot be finite for $\beta < -1/2$ in general.

ii) $n = 1,2$, $\beta = 0$. We first perform the time integration in (5.4.1.1) to obtain

$$\hat{E}(\xi_\alpha|x_N,s)$$

$$= \frac{1}{2(\pi)^{1/2}}\lim_{\varepsilon\downarrow 0}\int_{-\infty}^{\infty}e^{i\xi_N x_N-\varepsilon\xi_N^2}\left(\frac{\hat{F}(\xi)}{G(\xi)} - \frac{\hat{F}(\xi)e^{-G(\xi)s}}{G(\xi)}\right)d\xi_N. \qquad (5.4.1.17)$$

An additional assumption $\hat{F}(0,1) = 0$ for $n=2$, which our particular potentials of interest will be seen to satisfy, then transforms the first term on the RHS of (5.4.1.17) into

$$\lim_{x_N \to 0} \lim_{\varepsilon \downarrow 0} \int_{-\infty}^{\infty} e^{i\xi_N x_N - \varepsilon \xi_N^2} \frac{\hat{F}(\xi)}{G(\xi)} \, d\xi_N$$

$$= \pm \hat{H}(\xi_\alpha) + \lim_{\varepsilon \downarrow 0} \int_{-\infty}^{\infty} e^{-\varepsilon \xi_N^2} \frac{\hat{F}(\xi)}{G(\xi)} d\xi_N, \qquad (5.4.1.18)$$

where

$$\hat{H}(\xi_\alpha) = \begin{cases} i(\hat{F}(\xi)/2G(\xi))\,|_{(\xi_\alpha, \xi_N)=(0,1)}, & (n=1) \\ i\ \xi_\alpha(\partial/\partial\xi_\alpha)(\hat{F}(\xi)/2G(\xi))\,|_{(\xi_\alpha, \xi_N)=(0,1)}, & (n=2) \end{cases} \qquad (5.4.1.19)$$

and the $\pm$ is for the approach from $x_N > 0$ (upper) and $x_N < 0$ (lower) *. Equations (5.4.1.18) and (5.4.1.19) follow from (1.3.1.10) and (1.3.1.16). We next apply Lebesgue's theorem to the second term on the RHS of (5.4.1.17) to show

$$\lim_{x_N \to 0} \lim_{\varepsilon \downarrow o} \int_{-\infty}^{\infty} e^{i\xi_N x_N - \varepsilon \xi_N^2} \frac{\hat{F}(\xi)}{G(\xi)} e^{-G(\xi)s} d\xi_N = \int_{-\infty}^{\infty} \frac{\hat{F}(\xi)}{G(\xi)} e^{-G(\xi)s} d\xi_N. \qquad (5.4.1.20)$$

This result and the proposition then prove

$$\lim_{s \downarrow 0} \lim_{x_N \to 0} \lim_{\varepsilon \downarrow 0} \int_{-\infty}^{\infty} e^{i\xi_N x_N - \varepsilon \xi_N^2} \frac{\hat{F}(\xi)}{G(\xi)} e^{-G(\xi)s} d\xi_N$$

$$= \lim_{s \downarrow 0} \int_{-\infty}^{\infty} \frac{\hat{F}(\xi)}{G(\xi)} e^{-G(\xi)s} d\xi_N = \lim_{\varepsilon \downarrow 0} \int_{-\infty}^{\infty} \frac{\hat{F}(\xi)}{G(\xi)} e^{-\varepsilon \xi_N^2} d\xi_N. \qquad (5.4.1.21)$$

Hence by combining (5.4.1.17), (5.4.1.18) and (5.4.1.21) we obtain

$$\lim_{s \downarrow 0} \lim_{x_N \to 0} \hat{E}(\xi_\alpha | x_N, s) = \pm \hat{H}(\xi_\alpha). \qquad (5.4.1.22)$$

Consequently we have

$$\lim_{s \downarrow 0} \lim_{x_N \to 0} \int_0^s \int_S F(x-y, s-t)\varphi(y) dS_y dt$$

$$= \begin{cases} \pm (i/2)(\hat{F}(n)/G(n))\ \varphi(x_0), & n = 1 \\ \pm\ (1/2)(\partial/\partial\xi_\alpha)(\hat{F}/G)\,|_{\xi=n}\ (\partial/\partial\xi_\alpha)\varphi(x_0), & n = 2 \end{cases} \qquad (5.4.1.23)$$

if a condition

$$\hat{F}(n) = 0 \qquad (5.4.1.24)$$

---

* This convention is consistent with the sign convention in 5.3.

is satisfied for n=2, where we have used (5.4.1.19) and (5.4.1.22). We remark that the condition in (5.4.1.24) is essential in the present application because of e^{-Gt} term in (5.4.7). This is in contrast to the elastostatics case (see (1.3.1.14)) where we did not have to assume (5.4.1.24).

One may wonder if terms with $\beta > 0$ might give rise to any additional nonzero terms to (5.4.3). That this is impossible is seen by using

$$\hat{E}(\xi_\alpha | x_N, s)$$

$$= \lim_{\varepsilon \downarrow 0} \int_{-\infty}^{\infty} e^{i\xi_N x_N - \varepsilon \xi_N^2} \left(s^\beta \frac{\hat{F}(\boldsymbol{\xi})}{G(\boldsymbol{\xi})} - \beta \frac{\hat{F}(\boldsymbol{\xi})}{G(\boldsymbol{\xi})} \int_0^s \frac{e^{-G(\xi)(s-t)}}{t^{1-\beta}} \, dt \right), \qquad (5.4.1.25)$$

which one obtains from (5.4.1.1) and

$$\int_0^s e^{-G(\xi)(s-t)} t^\beta dt = \frac{s^\beta}{G(\boldsymbol{\xi})} - \frac{\beta}{G(\boldsymbol{\xi})} \int_0^s \frac{e^{-G(\xi)(s-t)}}{t^{1-\beta}} \, dt. \qquad (5.4.1.26)$$

The first term in the integral in (5.4.1.25) is evaluated by using (5.4.1.18). Since $\beta > 0$, however, this term vanishes as $s \downarrow 0$. For the second term we use the proposition and (5.4.1.9) (with β replaced by $\beta - 1$) to see that this also vanishes as $s \downarrow 0$ ($\hat{F}(0,1) = 0$ for $n = 2$ by assumption). This completes the proof.

5 . 4 . 2 Volume-time integrals

The method used in 5.4.1 yields

$$\lim_{s \downarrow 0} \lim_{x \to x_0} \int_0^s \int_D F(x-y, s-t) \varphi(y) t^\beta dy dt = 0.$$

$$\beta \geqq 0, \quad -1 \leqq n \leqq 1, \quad x_0 \in \partial D \qquad (5.4.2.1)$$

We shall, however, omit the proof in order to avoid repetition.

5 . 4 . 3 Volume integrals

In this section we shall use P and Q (see (5.2.2) and (5.2.6)) for arbitrary (1,0) and (0,0) homogeneous kernels, respectively, in order to save symbols.

Again the same argument as has been used in 5.4.1 gives

$$\lim_{s \downarrow 0} \lim_{x \to x_0} \int_D P(x-y, s) \theta(y) dV = \int_D P_0(x_0 - y) \theta(y) dV, \qquad (5.4.3.1)$$

$$\lim_{s\downarrow 0}\lim_{x\to x_0}\int_D Q(x-y,s)\theta(y)dV = \frac{C_Q}{2}\theta(x_0) + \text{v.p.}\int_D Q_0(x_0-y)\theta(y)dV,$$

$$x_0 \in \partial D \qquad (5.4.3.2)$$

where C_Q is defined in (5.2.9) and v.p. indicates a principal value integral defined in (1.3.2.17).

5 . 4 . 4 Potentials in consolidation

Using the results given in (5.4.1.12),(5.4.1.16),(5.4.1.23) and (5.4.2.1) we obtain the following formulae in addition to (5.4.3.1-2):

$$\lim_{s\downarrow 0}\lim_{x\to x_0}\int_{\partial D}\int_0^s \dot{U}(x-y,s-t)S(y,t)dtdS = 0, \qquad (5.4.4.1)$$

$$\lim_{s\downarrow 0}\lim_{x\to x_0}\int_{\partial D}\int_0^s \dot{S}(x,y,s-t)u(y,t)dtdS = 0, \qquad (5.4.4.2)$$

$$\lim_{s\downarrow 0}\lim_{x\to x_0}\int_{\partial D}\int_0^s P(x-y,s-t)r(y,t)dtdS = 0, \qquad (5.4.4.3)$$

$$\lim_{s\downarrow 0}\lim_{x\to x_0}\int_{\partial D}\int_0^s Z(x,y,s-t)p(y,t)dtdS = 0, \qquad (5.4.4.4)$$

$$\lim_{s\downarrow 0}\lim_{x\to x_0}\int_{D}\int_0^s \dot{U}(x-y,s-t)f(y,t)dtdV = 0, \qquad (5.4.4.5)$$

$$\lim_{s\downarrow 0}\lim_{x\to x_0}\int_{D}\int_0^s P(x-y,s-t)g(y,t)dtdV = 0, \qquad (5.4.4.6)$$

$$\lim_{s\downarrow 0}\lim_{x\to x_0}\int_{\partial D}\int_0^s \dot{U}(x-y,s-t)\cdot S(y,t)dtdS$$

$$= \mp\frac{1}{2}\left(\frac{\triangle^{*-1}(\boldsymbol{n})\boldsymbol{n}}{m + \boldsymbol{n}\cdot\triangle^{*-1}(\boldsymbol{n})\boldsymbol{n}}\right)\cdot S(\boldsymbol{x}_0,0)\,, \tag{5.4.4.7}$$

$$\lim_{s\downarrow 0}\lim_{x\to x_0}\int_{\partial D}\int_0^s \dot{T}(\boldsymbol{x},\boldsymbol{y},s-t)\cdot u(\boldsymbol{y},t)\,dt\,dS$$

$$= \pm\frac{1}{2}\left(\frac{\operatorname{div} \boldsymbol{u}(\boldsymbol{x}_0,s) - \triangle^{*-1}(\boldsymbol{n})\boldsymbol{n}\cdot C[\nabla \boldsymbol{u}(\boldsymbol{x}_0,s)]\boldsymbol{n}}{m + \boldsymbol{n}\cdot\triangle^{*-1}(\boldsymbol{n})\boldsymbol{n}}\right), \tag{5.4.4.8}$$

(Equation (5.4.1.24) is satisfied.)

$$\lim_{s\downarrow 0}\lim_{x\to x_0}\int_{\partial D}\int_0^s Q(\boldsymbol{x}-\boldsymbol{y},s-t)r(\boldsymbol{y},t)\,dt\,dS$$

$$= \begin{cases} \text{divergent}, & -1 < \beta < -1/2 \\ -(\pi\ \boldsymbol{n}\cdot K\boldsymbol{n})^{1/2}\ \gamma(\boldsymbol{x}_0)/2\left(m + \boldsymbol{n}\cdot\triangle^{*-1}(\boldsymbol{n})\boldsymbol{n}\right)^{1/2}, & \beta = 1/2 \\ 0 & -1/2 < \beta, \end{cases} \tag{5.4.4.9}$$

where β and $\gamma(\boldsymbol{x}_0)$ are the exponent of the lowest power and the corresponding coefficient of the asymptotic expansion of $(\partial p/\partial n)(\boldsymbol{x}_0,t)$ near $t = 0$, i.e.,

$$\frac{\partial p}{\partial n}(\boldsymbol{x}_0,t) = t^{\beta}\gamma(\boldsymbol{x}_0) + o(t^{\beta}) \quad \text{as } t \downarrow 0, \tag{5.4.4.10}$$

$$\lim_{s\downarrow 0}\lim_{x\to x_0}\int_{\partial D}\int_0^s W(\boldsymbol{x},\boldsymbol{y},s-t)p(\boldsymbol{y},t)\,dt\,dS = \mp\frac{1}{2}p(\boldsymbol{x}_0,0)\ , \tag{5.4.4.11}$$

$$\lim_{s\downarrow 0}\lim_{x\to x_0}\int_{D}\int_0^s \dot{U}(\boldsymbol{x}-\boldsymbol{y},s-t)\cdot \boldsymbol{f}(\boldsymbol{y},t)\,dt\,dV = 0, \tag{5.4.4.12}$$

$$\lim_{s\downarrow 0}\lim_{x\to x_0}\int_{D}\int_0^s Q(\boldsymbol{x}-\boldsymbol{y},s-t)g(\boldsymbol{y},t)\,dt\,dV = 0. \tag{5.4.4.13}$$

5 . 5 Initial behaviour of pressure and fluid velocity on the boundary

In this section we discuss the initial behaviour of p and r on the

boundary. Specifically we shall consider the relation between the limits in (5.4.1) and (5.4.2). The result of this section will be used in part II of this chapter to set the initial conditions for p and r on ∂D.

It is now a simple matter to compute the limit in (5.4.1) from (5.2.18) with the help of the results in 5.4. Indeed, we use (5.2.18), (5.4.4.7-13) and (5.4.3.2) to obtain

$$p(x_0,0) := \lim_{s\downarrow 0} p(x_0,s)$$

$$= 2\Big(\text{v.p.}\int_{\partial D} V_0(x_0-y)\cdot S(y,0)dS - \text{p.f.}\int_{\partial D} T_0(x_0,y)\cdot u(y,0)dS$$

$$+ \int_D V_0(x_0-y)\cdot f(y,0)dV + \frac{C_0}{2}\theta(x_0) + \text{v.p.}\int_D Q_0(x_0-y)\theta(y)dV$$

$$- \lim_{s\downarrow 0}\lim_{x\to x_0}\int_{\partial D}\int_0^s Q(x-y,s-t)r(y,t)dtdS\Big). \quad x_0 \in \partial D_R \tag{5.5.1}$$

Hence by comparing (5.5.1) and (5.3.23) we obtain

$$\lim_{x(\in D)\to x_0} p(x,0) = p(x_0,0) + 2\lim_{s\downarrow 0}\lim_{x\to x_0}\int_{\partial D}\int_0^s Q(x-y,s-t)r(y,t)dtdS.$$

$$x_0 \in \partial D_R \tag{5.5.2}$$

In contrast to (5.3.20) which says that the boundary value of the initial displacement coincides with the limit to $t = 0$ of the boundary displacement, the implication of (5.5.2) is not trivial. Actually, (5.5.2), together with (5.4.4.9), rules out the possibility of $-1 < \beta < -1/2$ (see (5.4.4.10)), because p has to be finite by assumption. Also we see that (5.5.2) reduces to

$$\lim_{x(\in D)\to x_0} p(x,0) = p(x_0,0) - \left(\frac{\pi n\cdot Kn}{m + n\cdot\triangle^{*-1}(n)n}\right)^{1/2}\gamma(x_0), \tag{5.5.3}$$

with the help of (5.4.4.9), where

$$\gamma(x_0) = \lim_{s\downarrow 0}\frac{\partial p}{\partial n}(x_0,s)\sqrt{s}. \tag{5.5.4}$$

Hence, we conclude

$$\beta = -\frac{1}{2} \tag{5.5.5}$$

as far as the limits in (5.4.1) and (5.4.2) are both finite and different. In this case the coefficient γ of the $s^{-1/2}$ singularity in $\partial p/\partial n$ (see (5.5.4)) is obtained from (5.5.3). If $\beta > -1/2$ holds, or, in particular, if $x_0 \in \partial D_r$ and the data $r_0(x_0,t)$ is bounded as a function of t (see (5.1.7.d)), we necessarily have

$$\lim_{x(\in D)\to x_0} p(x,0) = p(x_0,0), \qquad x_0 \in \partial D_R \tag{5.5.6}$$

because $\gamma(x_0)=0$ in (5.5.3) and (5.5.4).

Finally, we shall make two remarks. The first remark is concerned with the relation

$$\lim_{x(\in D)\to x_0} p(x,0) \neq p(x_0,0) \tag{5.5.7}$$

which might look queer at first. As a matter of fact, it is not. Indeed, the process of determining (5.4.2) discussed in 5.3 tells that (5.4.2) is independent of p_0 or r_0 (see (5.1.7)). Actually, (5.4.2) is determined only by u_0, S_0, f and θ because one obtains (5.4.2) by solving (5.3.36) followed by the use of (5.3.21). On the other hand we are supposed to specify $p(x_0,0) = p_0$ on ∂D_p arbitrarily. Therefore $p(x_0,0)$ on ∂D_p is independent of the data in (5.1.6)-(5.1.7) and, hence, independent of (5.3.21). Therefore we generally have (5.5.7).

The second remark is concerned with (5.3.20). In deriving this formula we have utilised expressions for initial fields (see 5.3). One may wonder if the method of this section yields a result consistent with (5.3.20) when applied to u. To answer this question in the affirmative, we use a potential representation for the limit in (5.3.4) obtained from (5.2.17), (5.4.4.1-6) and (5.4.3.1). The result of this manipulation is seen to be identical with (5.3.22), thus concluding (5.3.20) once again.

Example

In the case of isotropy we have

$$C_{ijkl} = \lambda\delta_{ij}\delta_{kl}+\mu(\delta_{ik}\delta_{jl}+\delta_{il}\delta_{jk}), \qquad K_{ij} = k\delta_{ij}, \tag{5.5.8a,b}$$

where (λ, μ) and k are Lame's constants and the permeability constant, respectively. Furthermore, we assume the fluid to be incompressible by putting $m = 0$. The one dimensional motion

$$u_1 = u_1(x_1,t), \quad u_{2,3} = 0, \quad p = p(x_1,t) \tag{5.5.9a-c}$$

with initial and boundary conditions (see (5.1.6) and (5.1.7))

$$\left.\frac{du_1}{dx_1}\right|_{t=0} = 0,$$

$$s_1 = p^0 \text{ (constant)}, \quad p = 0 \quad \text{on } x_1 = 0$$

$$u_1 = 0, \quad \frac{\partial p}{\partial n} = 0 \quad \text{on } x_1 = h \quad (h > 0\text{:constant}) \tag{5.5.10a-e}$$

produces p given by (Terzaghi(1943))

$$p(x_1) = \sum_{m=0}^{\infty} \frac{2p^0}{M} \sin\frac{Mx_1}{h} \exp(-M^2 T_v) \ , \tag{5.5.11}$$

where $M = (2m + 1)\pi/2$, $T_v = c_v t/h^2$ and

$$c_v = k(\lambda + 2\mu) . \tag{5.5.12}$$

At $x_1 = 0$, we have

$$\frac{\partial p}{\partial n} = - \sum_{m=0}^{\infty} \frac{2p^0}{h} \exp(-M^2 T_v) \ , \tag{5.5.13}$$

which approaches asymptotically to

$$- \frac{2p^0}{h\pi} T_v^{-1/2} \int_0^{\infty} e^{-t^2} dt = - \frac{2p^0}{\pi (c_v t)^{1/2}} \cdot \frac{\sqrt{\pi}}{2} = -p^0 (\pi c_v t)^{-1/2} \tag{5.5.14}$$

as $t \downarrow 0$. Therefore (5.5.4) gives $\gamma(0) = -p^0/\sqrt{\pi c_v}$. Also, (5.5.11) yields $p(x_1,0) = p^0$ $(0 < x_1 < h)$. On the other hand the boundary condition at $x_1 = 0$ says $p(0,0) = 0$. Hence by using

$$\left(\frac{n \cdot \triangle^{*-1}(n) n}{n \cdot Kn} \right)^{1/2} = \sqrt{k(\lambda + 2\mu)} \ , \tag{5.5.15}$$

which follows from (1.2.3), we conclude that (5.5.3) is satisfied.

5 . 6 Boundary integral equations

This section considers the limits of (5.2.17) and (5.2.18) for $s > 0$ as the observation point x tends to a point x_0 on the boundary. This calculation determines the boundary integral equations for consolidation problems. Hence this section is intended as a preparation for the numerical BIEM to be discussed in Part II.

As a matter of fact a part of this work has already been done in 5.3, where we have considered potentials whose kernels do not include time. In addition we have already considered a more difficult problem of letting $s \downarrow 0$ in the limits which we shall compute here. Hence in this section we shall deal with the limits of the forms

$$\lim_{x\to x_0}\int_{\partial D}\int_0^s F(x-y,s-t)\psi(y,t)dtdS,$$

$$\lim_{x\to x_0}\int_D\int_0^s F(x-y,s-t)\psi(y,t)dtdV,\quad (x\in\partial D,\ x_0\in\partial D) \tag{5.6.1a,b}$$

without going into the detail of the derivation, where F is a kernel function whose spatial Fourier transform is written as in (5.4.7) and ψ is a density function which appears in (5.4.3-5).

As in 1.3 we start by replacing ∂D and D by a circular disc S and a half ball B. We then compute the Fourier transform of (5.6.1a) by using the backward analyticity of ψ assumed in 1) and 2) in 5.1 to have

$$\mathfrak{F}\{\int_S\int_0^s F\ \psi\ dtdS\}$$

$$=\hat{F}(\xi)\left\{\int_0^s e^{-G(\xi)(s-t)}\ dt\hat{\psi}(\xi_\alpha,s)\ +\ \cdots\cdots\right\}$$

$$=\frac{\hat{F}(\xi)}{G(\xi)}\hat{\psi}(\xi_\alpha,s)\ +\ \cdots\cdots \tag{5.6.2}$$

and a similar result for (5.6.1b), where $\hat{\psi}(\xi_\alpha,s)$ stands for the Fourier transform of $\psi(\cdot,s)$ on S, and the suppressed terms in the series include functions of order $O(|\xi|^{n-4})$ as $|\xi|\to\infty$. The cartesian axes which we have used here are the same as those used in 1.3 and 5.4. Since $\hat{F}/G$ is an $(n-2,0)$ homogeneous function, we can apply the the results in 1.3 to this leading term. Therefore we do not have to assume (5.4.1.24) even when $n=2$. This is in contrast to the case discussed in 5.4.1. In addition the remaining terms in (5.6.2) are seen to give rise only to an integrable contribution to (5.6.1) because $-1\leqq n\leqq 2$ (see (1.3.1.2) and (1.3.1.3)). Therefore the boundary behaviour of the potentials in question is completely the same as that of a time-independent potential having $\mathfrak{F}^{-1}(\hat{F}/G)$ as the kernel and $\psi(\cdot,s)$ as the density function. We thus obtain

$$\lim_{x\to x_0}\int_{\partial D}\int_0^s \mathfrak{U}(x-y,s-t)\mathcal{S}(y,t)\mathrm{d}t\mathrm{d}S$$

$$=\int_{\partial D}\int_0^s \mathfrak{U}(x_0-y,s-t)\mathcal{S}(y,t)\mathrm{d}t\mathrm{d}S, \tag{5.6.3}$$

$$\lim_{x\to x_0}\int_{\partial D}\int_0^s \dot{\mathcal{S}}(x,y,s-t)u(y,t)dtdS$$

$$= \text{v.p.}\int_{\partial D}\int_0^s \dot{\mathcal{S}}(x_0,y,s-t)u(y,t)dtdS, \tag{5.6.4}$$

$$\lim_{s\downarrow 0}\lim_{x\to x_0}\int_{\partial D}\int_0^s \dot{U}(x-y,s-t)\cdot S(y,t)dtdS = \mp\frac{1}{2}\left(\frac{\triangle^{*-1}(n)n}{m+n\cdot\triangle^{*-1}(n)n}\right)\cdot S(x_0,s)$$

$$+\ \text{v.p.}\int_{\partial D}\int_0^s \dot{U}(x_0-y,s-t)\cdot S(y,t)dtdS, \tag{5.6.5}$$

$$\lim_{x\to x_0}\int_{\partial D}\int_0^s \dot{T}(x,y,s-t)\cdot u(y,t)dtdS$$

$$= \pm\frac{1}{2}\left(\frac{\text{div } u(x_0,s) - \triangle^{*-1}(n)n\cdot C[\nabla u(x_0,s)]n}{m+n\cdot\triangle^{*-1}(n)n}\right)$$

$$+\ \text{p.f.}\int_{\partial D}\int_0^s \dot{T}(x_0,y,s-t)\cdot u(y,t)dtdS, \tag{5.6.6}$$

$$\lim_{x\to x_0}\int_{\partial D}\int_0^s W(x,y,s-t)p(y,t)dtdS = \mp\frac{1}{2}p(x_0,s)$$

$$+\ \text{v.p.}\int_{\partial D}\int_0^s W(x_0,y,s-t)p(y,t)dtdS. \qquad x_0\in\partial D \tag{5.6.7}$$

Other potentials satisfy relations similar to (5.6.3).

From these results, (5.2.17) and (5.2.18) we obtain the following integral equations for consolidation problems:

$$\frac{1}{2}u(x,s) = \int_{\partial D}U_0(x-y)S(y,s)dS - \text{v.p.}\int_{\partial D}S_0(x,y)u(y,s)dS$$

$$+\int_D U_0(x-y)f(y,s)dV + \int_{\partial D}\int_0^s \dot{U}(x-y,s-t)S(y,t)dtdS$$

$$-\ \text{v.p.}\int_{\partial D}\int_0^s \dot{\mathcal{S}}(x,y,s-t)u(y,t)dtdS - \int_{\partial D}\int_0^s P(x-y,s-t)r(y,t)dtdS$$

$$+ \int_{\partial D}\int_0^s Z(x,y,s-t)p(y,t)dtdS + \int_D\int_0^s \dot{U}(x-y,s-t)f(y,t)dtdV$$

$$+ \int_D\int_0^s P(x-y,s-t)g(y,t)dtdV + \int_D P(x-y,s)\theta(y)dV\ , \qquad (5.6.8)$$

and

$$\frac{1}{2}p(x,s) = \text{v.p.}\int_{\partial D} V_0(x-y)\cdot S(y,s)dS - \text{p.f.}\int_{\partial D} T_0(x,y)\cdot u(y,s)dS$$

$$+ \int_D V_0(x-y)\cdot f(y,s)dV + \text{v.p.}\int_{\partial D}\int_0^s \dot{U}(x-y,s-t)\cdot S(y,t)dtdS$$

$$- \text{p.f.}\int_{\partial D}\int_0^s \dot{T}(x,y,s-t)\cdot u(y,t)dtdS - \int_{\partial D}\int_0^s Q(x-y,s-t)r(y,t)dtdS$$

$$+ \text{v.p.}\int_{\partial D}\int_0^s W(x,y,s-t)p(y,t)dtdS + \int_D\int_0^s \dot{U}(x-y,s-t)\cdot f(y,t)dtdV$$

$$+ \int_D\int_0^s Q(x-y,s-t)g(y,t)dtdV + \int_D Q(x-y,s)\theta(y)dV.$$

$$x \in \partial D \qquad (5.6.9)$$

For $s > 0$ we solve (5.6.8) and (5.6.9) simultaneously to determine boundary quantities completely.

It is noteworthy that (5.6.8), viewed as an integral operator on $u(\cdot,s)$ and $s(\cdot,s)$, has the same singularity as that of the direct integral equation for elastostatics. This is seen from (5.6.2) and

$$\mathfrak{F}\, U_0 + \frac{\mathfrak{F}\,\dot{U}|_{t=0}}{\mathrm{ex}(\cdot,1)} = \triangle^{*-1}, \qquad (5.6.10)$$

which follows from (5.2.3a,c). As to (5.6.9) the apparent singularities of the kernels in the integrals involving $u(\cdot,s)$ and $S(\cdot,s)$ cancel with each other to reduce themselves to integrable singularities. This result is read off from (5.6.2) and

$$\mathfrak{F}\, V_0 + \frac{\mathfrak{F}\,\dot{U}|_{t=0}}{\mathrm{ex}(\cdot,1)} = 0, \qquad (5.6.11)$$

which follows from (5.2.3b,d). Also, we see form (5.6.8) and (5.6.9) that the strongest possible singularities of kernels which operate on

p and r are v.p. singularities.

Finally we note that the argument used in this section proves that the volume-time integrals in (5.2.17) and (5.2.18) are actually integrable.

5 . 7 Numerical procedure

In the sequel we shall discuss a numerical method of analysis using the formulation developed so far. We shall restrict our attention to the isotropic case characterised by (5.5.8a,b), where the fundamental solution is available. Also, we shall neglect the compressibility of fluid ($m = 0$) following a common practice among soil engineers.

5 . 7 . 1 Fundamental solutions

In the first place we have to determine the fundamental solutions. The calculation of these solutions, however, does not introduce any difficulty. Indeed, the Fourier inversion based on (5.2.3) leads to

$$\dot{U} = \frac{\delta(t)}{\pi}\left(-\frac{1}{4\mu}\log R + \frac{\nabla R\otimes\nabla R}{4\mu}\right) + \frac{kH(t)}{\pi}\left[\mathbf{1}\left(\frac{1 - e^{-R^2/4c_v t}}{2R^2}\right)\right.$$

$$\left. - \nabla R\otimes\nabla R\left\{\frac{1 - e^{-R^2/4c_v t}}{R^2} - \frac{e^{-R^2/4c_v t}}{4c_v t}\right\}\right],$$

$$\dot{V} = \delta(t)\frac{\nabla R}{2\pi\rho} - \frac{H(t)Re^{-R^2/4c_v t}}{8\pi c_v t^2}\nabla R,$$

$$P = H(t)\left(\frac{1 - e^{-R^2/4c_v t}}{2\pi\rho}\right)\nabla R,$$

$$Q = H(t)\frac{e^{-R^2/4c_v t}}{4\pi k t}, \qquad (N = 2) \qquad (5.7.1.1a\text{-}d)$$

and

$$\dot{U} = \frac{1}{8\pi\mu}(\mathbf{1}\triangle - \nabla\otimes\nabla)R\delta(t)$$

$$- \frac{kH(t)}{2\pi^{3/2}}\left[\left\{\frac{e^{-R^2/4c_v t}}{R^2(4c_v t)^{1/2}} - \frac{1}{R^3}\mathrm{Erf}\left(\frac{R}{(4c_v t)^{1/2}}\right)\right\}\mathbf{1}\right.$$

$$\left. - \nabla R\otimes\nabla R\left\{\frac{2e^{-R^2/4c_v t}}{(4c_v t)^{3/2}} + \frac{3e^{-R^2/4c_v t}}{R^2(4c_v t)^{1/2}} - \frac{3}{R^3}\mathrm{Erf}\left(\frac{R}{(4c_v t)^{1/2}}\right)\right\}\right],$$

$$\dot{V} = \frac{\delta(t)}{4\pi R^2}\nabla R - H(t)\frac{2Rc_v}{\pi^{3/2}}\frac{e^{-R^2/4c_v t}}{(4c_v t)^{5/2}}\nabla R,$$

$$P = \frac{H(t)}{2\pi^{3/2}}\left(\frac{1}{R^2}\mathrm{Erf}\left(\frac{R}{(4c_v t)^{1/2}}\right) - \frac{e^{-R^2/4c_v t}}{R(4c_v t)^{1/2}}\right)\nabla R,$$

$$Q = \frac{c_v H(t) e^{-R^2/4c_v t}}{(4\pi c_v t)^{3/2} k}, \qquad (N = 3) \qquad (5.7.1.2a\text{-}d)$$

where c_v is a constant defined in (5.5.12), $R = |x - y|$, $\delta(t)$ is Dirac's delta, $H(t)$ is the step function and Erf is the error function defined by

$$\mathrm{Erf}(z) = \int_0^z e^{-t^2} dt \ , \qquad (5.7.1.3)$$

respectively. ∇ 's in (5.7.1.1) and (5.7.1.2) are with respect to x.

5 . 7 . 2 Integral equations

In the sequel, we shall restrict our attention to 2 dimensional case for the purpose of simplicity.

The integral representations investigated so far convert the original initial- boundary value problems to a system of integral equations (5.6.8) and (5.6.9). For the special case of 2D isotropy, these integral equations reduce to

$$\frac{u(x,s)}{2} = \int_{\partial D} U_0(x-y)S(y,s)dS - \int_{\partial D} S_0(x,y)u(y,s)dS$$

$$- \text{v.p.}\int_{\partial D} P_0(y-x)q(x,s)dS - \int_D U_0(y-x)f(y,s)dV$$

$$+ \int_{\partial D}\int_0^s \dot{U}(x-y,s-t)S(y,t)dtdS - \text{v.p.}\int_{\partial D}\int_0^s \dot{S}(x,y,s-t)u(y,t)dtdS$$

$$- \text{v.p.}\int_{\partial D}\int_0^t \dot{\Phi}(y-x,s-t)q(y,t)dtdS + \int_{\partial D}\int_0^s Z(x,y,s-t)p(y,t)dtdS$$

$$+ \int_D\int_0^s \dot{U}(x-y,s-t)f(y,t)dtdV + \int_D\int_0^s P(x-y,s-t)g(y,t)dtdV$$

$$+ \int_D P(\boldsymbol{x}-\boldsymbol{y},s)\theta(\boldsymbol{y})dV \ , \qquad (5.7.2.1)$$

and

$$\frac{p(\boldsymbol{x},s)}{2} = \text{v.p.}\int_{\partial D} V_0(\boldsymbol{x}-\boldsymbol{y})\cdot S(\boldsymbol{y},s)dS - \text{p.f.}\int_{\partial D} T_0(\boldsymbol{x},\boldsymbol{y})\cdot \boldsymbol{u}(\boldsymbol{y},s)dS$$

$$- \int_D V_0(\boldsymbol{y}-\boldsymbol{x})\cdot \boldsymbol{f}(\boldsymbol{y},s)dV + \text{v.p.}\int_{\partial D}\int_0^s \hat{U}(\boldsymbol{x}-\boldsymbol{y},s-t)\cdot S(\boldsymbol{y},t)dtdS$$

$$- \text{p.f.}\int_{\partial D}\int_0^s \hat{T}(\boldsymbol{x},\boldsymbol{y},s-t)\cdot \boldsymbol{u}(\boldsymbol{y},t)dtdS - \int_{\partial D}\int_0^s \hat{Q}(\boldsymbol{x}-\boldsymbol{y},s-t)q(\boldsymbol{y},t)dtdS$$

$$- \int_{\partial D}\int_0^s W(\boldsymbol{y},\boldsymbol{x},s-t)p(\boldsymbol{y},t)dtdS + \int_D\int_0^s \hat{U}(\boldsymbol{x}-\boldsymbol{y},s-t)\cdot \boldsymbol{f}(\boldsymbol{y},t)dtdS$$

$$+ \int_D\int_0^s Q(\boldsymbol{x}-\boldsymbol{y},s-t)g(\boldsymbol{y},t)dtdV + \int_D Q(\boldsymbol{x}-\boldsymbol{y},s)\theta(\boldsymbol{y})dV, \qquad (5.7.2.2)$$

where

$$q(\boldsymbol{x},s) = \int_0^s r(\boldsymbol{x},t)dt \ ,$$

$$\hat{P}(\boldsymbol{x},s) = -\frac{H(s)Re^{-R^2/4c_v s}}{8\pi c_v s^2}\nabla R \qquad (5.7.2.3a,b)$$

and

$$\hat{Q}(\boldsymbol{x},s) = \frac{H(s)}{4\pi k}\left\{\frac{R^2 e^{-R^2/4c_v s}}{4c_v s^3} - \frac{e^{-R^2/4c_v s}}{s^2}\right\}. \qquad (5.7.2.4)$$

In deriving (5.7.2.1) and (5.7.2.2) from (5.6.8) and (5.6.9), we have used integration by part with respect to t, along with (5.2.5a,b) in integrals including r (q). This is in order to eliminate the possible $1/\sqrt{s}$ singularity of $r(\cdot,s)$ discussed in 5.5. The apparent non-symmetry of (5.7.2.1) and (5.7.2.2) is due to the assumption of isotropy, with which Q_0 is seen to vanish*. Also the absence of v.p. symbols in front of integrals involving S_0 and W is due to the assumed isotropy and incompressibility of fluid.

One may doubt the effectiveness of (5.7.2.2) for numerical applications because of the apparently very strong singularity of the

---

* $C\,\delta(\boldsymbol{x})$ to be precise, where C is a constant.

kernels. As one may gather from the discussion in 5.6, however, this is not to be the case. Indeed, the singularities in the integrands in (5.7.2.2) are expected to cancel with each other to reduce themselves to integrable singularities. A direct calculation to be shown in the next section confirms this.

5 . 7 . 3 Numerical methods of integration

In this section we shall implement a numerical method of solution of Biot's equations using the formulation investigated so far.
Our method consists of the following steps

1) We first compute the initial field. A direct BIEM discussed in 1.5. is used to this end. Namely, we discretise (5.3.36) by using boundary conditions (5.1.7a,b) and certain shape functions, solve the resulting algebraic equations for discretised $u(x_0,0)$ and $s(x_0,0)$, and then use (5.3.6) and (5.3.7) to obtain the initial fields.

We next compute the initial values of the boundary quantities u, s, p and q as a preparation for the subsequent analysis. The first two, however, have been obtained as solutions of (5.3.36), and the initial value of q is zero by definition. As to p on ∂D_p the boundary condition (5.1.7c) provides the answer. Finally, one uses (5.5.3) and (5.1.7d) to set the initial value of p on ∂D_r after computing (5.4.2) from (5.3.21) and the solution of (5.3.36). In the present context (5.3.21) simplifies to

$$\lim_{y(\in D)\to x(\in \partial D)} p(y,0) = 2\mu\Big(\theta(x) - c\cdot\frac{\partial u}{\partial c}(x,0)\Big) - S\cdot n, \qquad (5.7.3.1)$$

where c is a unit tangent vector to ∂D at x. As can be inferred from (5.7.3.1) it is convenient to use a sufficiently smooth shape function for u since (5.7.3.1) includes tangential differentiation.

As has been pointed out in 5.3 the integral equation for the initial field loses the uniqueness of solution when D has holes. Correspondingly, the associated numerical equation yields inaccurate results. We therefore avoid this inaccuracy by using one of the remedies discussed in Kobayashi & Nishimura(1982) or in the appendix to chapter 4.

2) Let the solution be known up to a certain time $s - \triangle t \geqq 0$ where $\triangle t > 0$ is a constant. We now wish to obtain the solution at $s = s(> 0)$. To this end, we introduce time interpolation functions $\Omega_1(t)$ and $\Omega_2(t)$ in the interval $[s-\triangle t, s]$ in a way that

$$\Omega_1(s) = 1, \quad \Omega_1(s-\triangle t) = 0,$$

$$\Omega_2(s) = 0, \quad \Omega_2(s-\triangle t) = 1 \qquad (5.7.3.2a\text{-}d)$$

are satisfied. One may then interpolate a function of t, say

$\boldsymbol{u}(\cdot,t)$, by

$$\boldsymbol{u}(\cdot,t) \sim \boldsymbol{u}(\cdot,s)\Omega_1(t) + \boldsymbol{u}(\cdot,s-\triangle t)\Omega_2(t) \qquad (5.7.3.3)$$

in $[s-\triangle t, s]$, where $\boldsymbol{u}(\cdot,s-\triangle t)$ is known, but $\boldsymbol{u}(\cdot,s)$ may not be. It may then be clear that the integral equations (5.7.2.1) and (5.7.2.2), with approximations of the forms in (5.7.3.3) applied to boundary quantities such as $\boldsymbol{u}$, reduce themselves to integral equations of the following form:

$$\int_{\partial D} (\text{kernels}) \cdot (\text{quantities at } t = s) dS = \text{known functions}. \qquad (5.7.3.4)$$

We shall henceforth call the transformation of this type as 'time-discretisation'. After time-discretising (5.7.2.1) and (5.7.2.2), we apply the conventional BIE techniques using spatial shape functions. The solution to the resulting simultaneous algebraic equations determines the boundary quantities at $t = s$.

3) Repeat step 2) by setting $s + \triangle t$ for the new s

We next discuss our specific choice of the time interpolation function and the method of integration. In principle we may use any time interpolation function. We here choose linear time variation so as to keep the method simple. This time variation also allows us to calculate all the pertinent time integrals analytically. Indeed, the following glossary is useful to this end:

$$\int (s-t)e^{-A/(s-t)} dt$$

$$= -\frac{(s-t)^2}{2} e^{-A/(s-t)} + \frac{A(s-t)}{2} e^{-A/(s-t)} + \frac{A^2}{2} \mathrm{Ei}(-A/(s-t)),$$

$$\int e^{-A/(s-t)} dt = -(s-t)e^{-A/(s-t)} - A\,\mathrm{Ei}(-A/(s-t)),$$

$$\int \frac{e^{-A/(s-t)}}{s-t} dt = \mathrm{Ei}(-A/(s-t)),$$

$$\int \frac{e^{-A/(s-t)}}{(s-t)^2} dt = -\frac{1}{A} e^{-A/(s-t)},$$

$$\int \frac{e^{-A/(s-t)}}{(s-t)^3} dt = -\frac{e^{-A/(s-t)}}{A(s-t)} - \frac{1}{A^2} e^{-A/(s-t)},$$

$$(A := R^2/4c_v) \qquad (5.7.3.5a\text{-}e)$$

where Ei denotes the exponential integral function.

We now use the formulae in (5.7.3.5) to compute the kernel functions in the time-discretised versions of (5.7.2.1) and (5.7.2.2). Only the kernels which operate on $\boldsymbol{u}(\cdot,s)$ are considered because the other kernels can also be determined in the same manner. To begin with we shall list the explicit forms of the relevant kernels in (5.7.2.1) and (5.7.2.2):

$$S_0(\boldsymbol{x},\boldsymbol{y}) = \frac{1}{\pi R}\,(\nabla R\cdot\boldsymbol{n})\;\nabla R\otimes\nabla R,$$

$$\dot{\boldsymbol{s}}(\boldsymbol{x},\boldsymbol{y},s) = -\frac{2\mu kH(s)}{\pi R}\Big[\{(1-4\nabla R\otimes\nabla R)(\nabla R\cdot\boldsymbol{n})+\boldsymbol{n}\otimes\nabla R+\nabla R\otimes\boldsymbol{n}\}$$

$$\cdot\left\{\frac{e^{-R^2/4c_vs}}{4c_vs}-\frac{1-e^{-R^2/4c_vs}}{R^2}\right\}$$

$$+\{\nabla R\otimes\boldsymbol{n}-\nabla R\otimes\nabla R(\nabla R\cdot\boldsymbol{n})\}\;\frac{R^2e^{-R^2/4c_vs}}{8c_v{}^2s^2}\Big],$$

$$T_0(\boldsymbol{x},\boldsymbol{y}) = -\mu(\boldsymbol{n}-2\nabla R(\nabla R\cdot\boldsymbol{n}))/\pi R^2,$$

$$\dot{\boldsymbol{t}}(\boldsymbol{x},\boldsymbol{y},s) = \frac{\mu H(s)}{8\pi c_v}\Big[\frac{R^2e^{-R^2/4c_vs}}{c_vs^3}(\boldsymbol{n}-\nabla R(\nabla R\cdot\boldsymbol{n}))$$

$$-\frac{2e^{-R^2/4c_vs}}{s^2}\,\boldsymbol{n}\Big]. \qquad (5.7.3.6a\text{-}d)$$

In the derivation of (5.7.3.6) we have used (5.7.1.1) and (5.2.19). The kernel $K_1(\boldsymbol{x},\boldsymbol{y})$ which operates on $\boldsymbol{u}(\cdot,s)$ in the time-discretised version of (5.7.2.1) is written as

$$K_1(\boldsymbol{x},\boldsymbol{y}) := S_0(\boldsymbol{x},\boldsymbol{y}) + \int_{s-\triangle t}^{s}\dot{\boldsymbol{s}}(\boldsymbol{x},\boldsymbol{y},s-t)\Big(1-\frac{s-t}{\triangle t}\Big)dt\ , \qquad (5.7.3.7)$$

where we have used a linear time interpolation. Use of (5.7.3.5) and (5.7.3.6) then transforms (5.7.3.7) into

$$K_1(\boldsymbol{x},\boldsymbol{y})$$

$$=\frac{1}{2\pi(\lambda+2\mu)R}\{(\mu 1+2(\lambda+\mu)\nabla R\otimes\nabla R)(\nabla R\cdot\boldsymbol{n})+\mu(\boldsymbol{n}\otimes\nabla R-\nabla R\otimes\boldsymbol{n})\}$$

$$- \frac{\mu}{4\pi(\lambda+2\mu)R}\left(\frac{A}{\triangle t}\right)\Big[\{(1 - 4\nabla R\otimes\nabla R)(\nabla R\cdot n) + n\otimes\nabla R + \nabla R\otimes n\}$$

$$\cdot\left(E_2(\frac{A}{\triangle t}) - E_1(\frac{A}{\triangle t})\right) + 4\{\nabla R\otimes n - \nabla R\otimes\nabla R(\nabla R\cdot n)\}E_1(\frac{A}{\triangle t})$$

$$- \{1(\nabla R\cdot n) + n\otimes\nabla R - 3\nabla R\otimes n\}\ \mathrm{Ei}(-\frac{A}{\triangle t})\Big], \qquad (5.7.3.8)$$

where

$$E_1(x) = \frac{e^{-x} - 1}{x}, \quad E_2(x) = \frac{e^{-x} - 1 + x}{x^2}. \qquad (5.7.3.9a,b)$$

In the same manner we obtain a similar kernel (denoted by K_2) in the time-discretised version of (5.7.2.2) as

$$K_2(x,y) := T_0(x,y) + \int_{s-\triangle t}^{s} \dot{T}(x,y,s-t)(1 - \frac{s-t}{\triangle t})dt$$

$$= \frac{\mu}{8\pi c_v}\Big[(4n - (\nabla R\cdot n)\nabla R)\ \frac{A}{(\triangle t)^2}(E_1(\frac{A}{\triangle t}) + E_2(\frac{A}{\triangle t}))$$

$$- \frac{1}{\triangle t}\Big\{4e^{-A/\triangle t}(n - (\nabla R\cdot n)\nabla R)$$

$$- 2n\ \{\mathrm{Ei}(-\frac{A}{\triangle t}) - E_1(\frac{A}{\triangle t})\}\Big\}\Big]. \qquad (5.7.3.10)$$

These forms will be used in the numerical calculations to be presented in 5.8.

As a check of the general theory in 5.6.concerning the behaviour of the kernels we shall compute the singularities in K_1 and K_2. A direct calculation shows that (5.7.3.8) has an asymptotic form

$$K_1(x,y) = \frac{1}{2\pi(\lambda+2\mu)R}\{(\mu 1 + 2(\lambda+\mu)\nabla R\otimes\nabla R)(\nabla R\cdot n)$$

$$+ \mu(n\otimes\nabla R - \nabla R\otimes n)\} + O(R\log R) \qquad \text{as } R\downarrow 0. \qquad (5.7.3.11)$$

The singular term in this expression is seen to coincide with the elastostatic double layer kernel (see Chapter 1). Similarly, we see that (5.7.3.10) behaves as

$$K_2(x,y) = -\frac{\mu}{2\pi c_v \triangle t} n \log R + 0(1) \qquad (5.7.3.12)$$

for a small R. This shows that $K_2(x,y)$ has an integrable singularity at $R = 0$. These results conform to the prediction of the general theory in 5.6.

Now that we have shown the singularities of our kernels to be the same as those of elasticity, we may apply the techniques for evaluating the elastostatic singular integrals to our integral equations. Namely, we may compute such integrals in (5.7.2.1) and (5.7.2.2) so that the discretised versions of (5.7.2.1) and (5.7.2.2) are satisfied by some known solutions of (5.1.1) and (5.1.2). In elastodynamics plane waves have turned out to be a convenient choice for the 'known solutions' (see Chapter 4). In consolidation, we may use

1. Rigid translation

$$u = u_R \cdot f(t), \quad p = 0, \qquad (5.7.3.13a,b)$$

where u_R is a constant vector, and $f(t)$ is an arbitrary function of time.

2. Uniform shear

$$u = (\text{uniform simple shear}) \cdot f(t), \quad p = 0. \qquad (5.7.3.14a,b)$$

This satisfies (5.1.1) and (5.1.2) because div $u = 0$.

3. Uniform pressure

$$u = 0, \quad p = \text{constant}. \qquad (5.7.3.15a,b)$$

p may be an arbitrary function of time if m vanishes.

4. Radial expansion

$$u = \frac{x}{|x|^2} f(t), \quad p = 0. \qquad (5.7.3.16a,b)$$

This is a solution of (5.1.1) and (5.1.2) when the material is isotropic.

1 ~ 3 are interior solutions while 4 is an exterior solution of (5.1.1) and (5.1.2). In using the method of substitution one has to remember that an interior (exterior) solution satisfies integral equations for interior (exterior) problems. One may, however, use an exterior solution for computing singular integrals in interior problems and vice versa. Indeed, one first adds u (p) to the RHS of (5.7.2.1) ((5.7.2.2)) to obtain the BIE for exterior problems, which will be satisfied by an exterior solution. The method of substitution

then computes some singular integrals in the BIE for exterior problems. This process determines singular integrals in the BIE for interior problems at the same time because the exterior BIE and the interior BIE differ only by non-integral terms. Note that we now have more known solutions that the number of singular integrals (2 in 2D) in (5.7.2.1) and (5.7.2.2). As it turned out, however, use of this technique to some of logarithmically singular integrals increases the accuracy of the numerical solution considerably. Hence we shall try to use as many of the above 4 solutions as possible in the numerical examples to follow.

5 . 8 Numerical examples

In this section we shall test the performance of the present method by applying it to some sample problems. We shall use p^0 for a constant having a dimension of stress.

5 . 8 . 1 Circular disc

We solved the following initial- boundary value problem for a circular domain D having a radius of a.

Initial condition

$$\theta = 0, \tag{5.8.1.1}$$

Boundary conditions

$$S = -p^0 n, \quad p = 0 \quad \text{on} \quad \partial D, \tag{5.8.1.2a,b}$$

Poisson's ratio

$$\nu = 0, \quad 1/3. \tag{5.8.1.3}$$

For this analysis we used 32 linear isoparametric boundary elements. The time shape function is also linear. All the time integrations are carried out analytically, whereas the spatial integrals are evaluated by use of the Gaussian integration together with the method of substitution with (5.7.3.13). The time increment $\triangle t$ is kept constant ($\triangle t c_v/a^2 = 1/100$) during the analysis.

Fig.5.8.1.1 shows the obtained boundary displacement as a function of time factor tc_v/a^2. The BIE results shown by symbols agree well with the analytical solution given by curves(Tamura(1981)). The CPU time was about 3 sec. per step by using VP100 of the Data Processing Centre of Kyoto University.

5 . 8 . 2 Circular hole in an infinite plane

We next consider a circular hole (radius = a) in an infinite plane. We assume that this infinite plane has an initial stress τ^0 and a

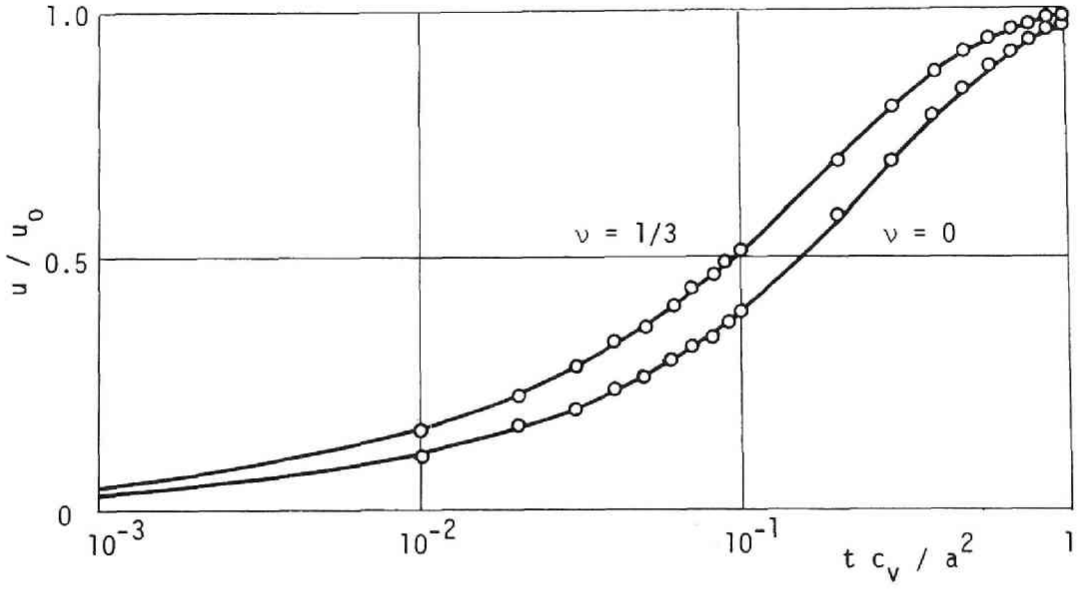

Fig.5.8.1.1 Boundary displacement of a circular disc. symbols: BIE, lines: exact, u_0: final displacement.

vanishing initial pressure. We then 'excavate' a hole in a way that it satisfies the following conditions:

Initial condition

$$\theta = 0, \tag{5.8.2.1}$$

Boundary conditions

$$S = 0, \quad p = 0 \quad \text{on } \partial D. \tag{5.8.2.2a,b}$$

In the present analysis we set $\tau_{11}^0 = -0.4p^0$, $\tau_{22}^0 = -0.8p^0$, $\tau_{12}^0 = 0$, and $\nu = 0$. Also, we have used 32 piecewise linear boundary elements of equal length. Fig.5.8.2.1 shows the deformation of the boundary calculated by using the present formulation. The out-most circle represents the undeformed shape of the boundary and the least flat (flattest) curve shows the initial (final) shape. In this figure we have plotted two series of numerical results together, i.e., the displacements on ∂D for $0 < c_v t/a^2 < 1$ obtained with $c_v \triangle t/a^2 = 1/100$ and those for $1 < c_v t/a^2 < 10$ obtained with $c_v \triangle t/a^2 = 1/10$. As it turned out, this problem is particularly sensitive to the accuracy of numerical integration. Therefore we have used the method of substitution with (5.7.3.13), (5.7.3.14) and (5.7.3.16) in order to obtain not only v.p. integrals, but also some of logarithmically singular integrals.

5 . 8 . 3 Loaded half-plane

As the third example we consider a loaded half-plane. The conditions are

Initial condition

$$\theta = 0, \tag{5.8.3.1}$$

Boundary conditions

$$S = \text{as given in the inset of Fig.5.8.3.1,}$$

$$p = 0 \qquad \text{on } \partial D, \tag{5.8.3.2a,b}$$

Poisson's ratio

$$\nu = 0. \tag{5.8.3.3}$$

From a physical point of view the displacement field for this problem is rather pathological because it behaves logarithmically at the point of infinity. In addition the solution is not unique in the sense that one may superpose a rigid motion on one solution of this problem to obtain another. In civil engineering practice, however, one usually sets vertical displacements at certain points (usually taken away from the loaded zone) equal to zero by superposing a rigid

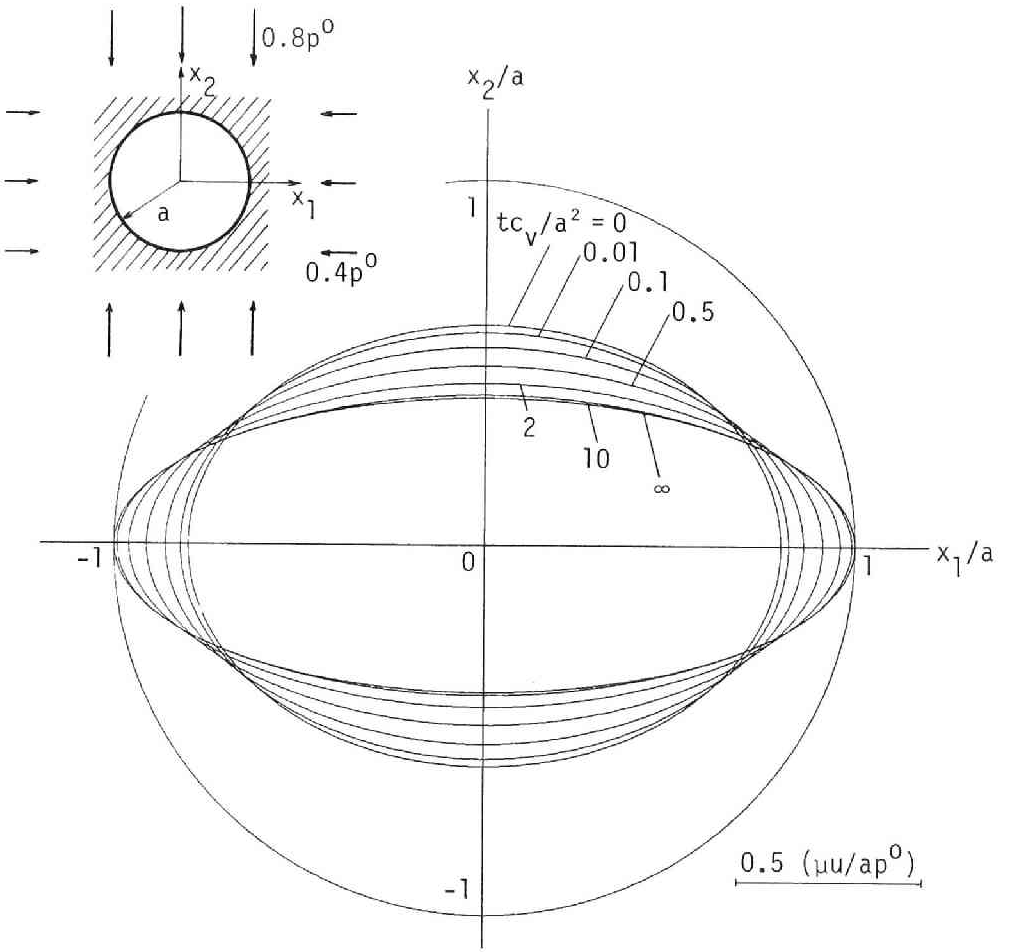

Fig.5.8.2.1 Deformation of a circular hole subject to biaxial compression. Poisson's ratio = 0.

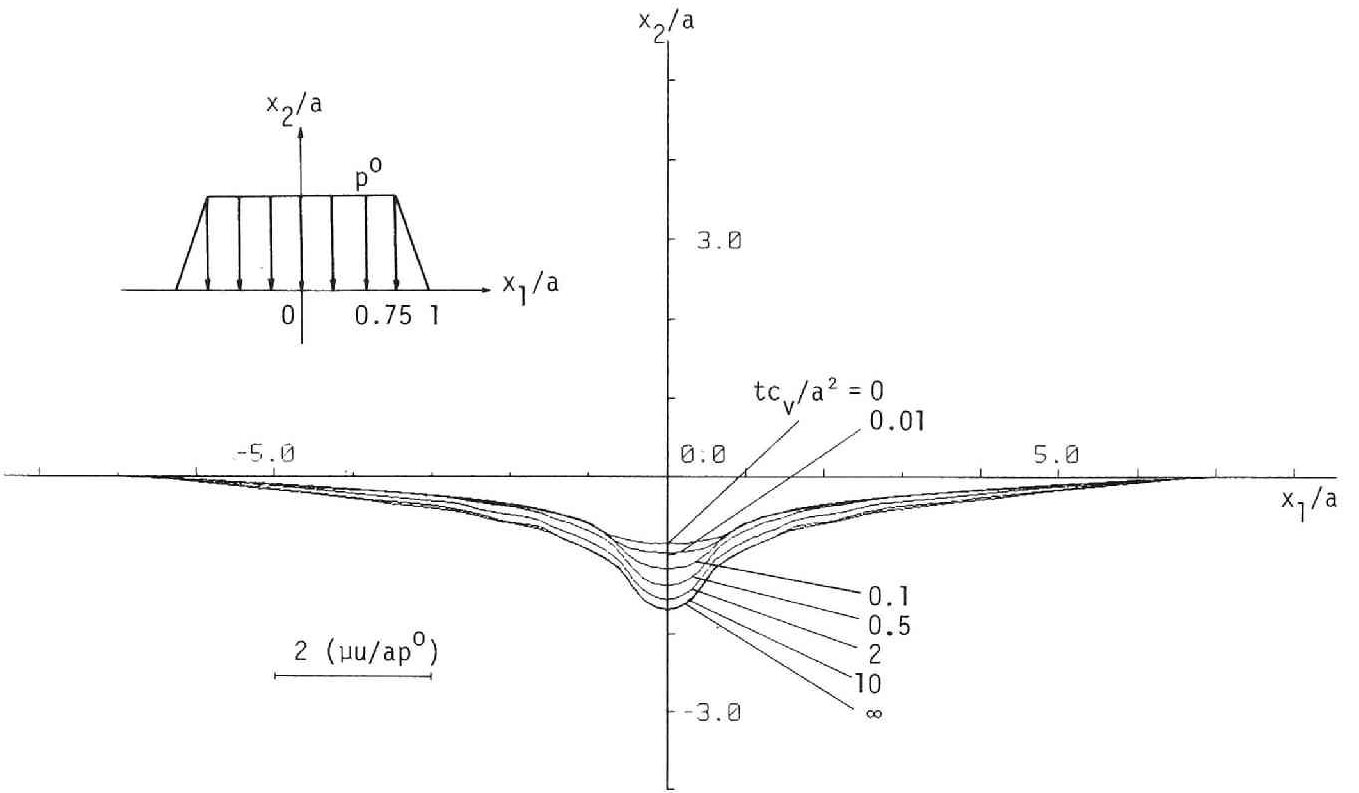

Fig.5.8.3.1 Deformation of a loaded halfplane. Poisson's ratio = 0.

motion. We here follow this practice by setting $u_2 = 0$ at $x_1 = \pm 7a$, $x_2 = 0$. It should therefore be remembered that the pattern of the displacement, rather than its absolute value, bears physical meaning. Another peculiarity of this problem arises from the fact that the length of the boundary is infinite. Since our method cannot deal with such a boundary, we truncate it and take only the finite part of it into account. In order to see the effect of this truncation we have carried out two numerical analyses, one with the truncation at $x_1 = \pm 9a$ and the other at $x_1 = \pm 20a$. This comparison has shown practically no difference between these two computations, thus justifying the method of truncation. The deformation pattern shown in Fig.5.8.3.1 is obtained by using $c_v \triangle t/a^2 = 1/10$ and $1/100$ ($1/100$ for $c_v t/a^2 < 1$ and $1/10$ for $c_v t/a^2 > 1$. The number of (linear) boundary elements is 45 and the boundary is truncated at $x_1 = \pm 20a$. In this example it is inadmissible to use the method of substitution because ∂D does not form a closed contour. Hence we used a standard Gaussian integration even for computing singular integrals, but only after reducing them to ordinary integrals by using the geometrical symmetry of the element. For example we use formulae such as

$$\text{v.p.}\int_{-a}^{a+b} \frac{1}{x}\, dx = \int_{a}^{b} \frac{1}{x}\, dx \qquad (a,b > 0) \tag{5.8.3.4}$$

to reduce singular integrals to ordinary integrals. The upper-most curve in Fig.5.8.3.1 shows the initial deformation. As the time proceeds the deformation at the mid point of the boundary increases apparently.

5 . 9 Concluding remarks

a) Some authors have developed different BIE formulations for the same problem. Predeleanu(1981) used a potential representation for $\dot{u}$ rather than u as a basis of his method. This is, however, not very convenient for consolidation problems since u sometimes jumps as a function of time, and, hence, $\dot{u}$ may behave like Dirac's delta $\delta(s)$. In addition, Predeleanu's formulation uses p as the initial condition, which is not only awkward physically but also inconvenient numerically. Actually this means that his method almost always requires volume integration since the initial pressure p is seldom zero in practical problems. Hence his method is possible only after sacrificing the boundary only nature of BIEM. Banerjee & Butterfield(1981) proposed a BIEM using BIE's for elastostatics and heat equation. Kuroki et al.(1982) also proposed essentially the same method independently. Their method is not of 'boundary' type, in the strict sense of the word, since their formulation involves volume integrals. Besides, their approach seems to reflect the mathematical structure of the problem only in an awkward manner. For example, their exponential factor in their fundamental solution is different from the natural one given in (5.7.1.1) and (5.7.1.2). However, their method is superior to the present formulation as far as the core saving is concerned. Aramaki et al.(1982) extended the Banerjee Butterfield Kuroki formulation to the case where the soil has a thin layer of permeable material.

Garcia-Suarez & Alarcon (1982) also proposed a method going along a similar line as that of Banerjee Butterfield Kuroki formulation except that they used a finite difference formula to reduce heat equation to a Helmholtz type equation. Their method, at its best, is an approximation to Banerjee Butterfield Kuroki formulation which is another. In addition, their treatment of initial field is inadequate. Cheng and Liggett(1984) proposed a BIEM using Laplace transform with respect to time. Their approach is expected to provide a practical alternative to the present formulation. It appears to the present author, however, that their argument could have been simplified by the use of $\boldsymbol{u}$ and p as unknowns. Recently, Cheng & Predeleanu(1987) obtained a formulation similar to the present one.

b) The author emphasised the effectiveness of the present formulation for applied mathematical applications. In particular, we could determine the structure of singularity of fluid eflux on the boundary at $s = 0$. We may further improve the accuracy of the numerical solution by taking the exact singular behaviour of the solution into account. The analysis in chapter 3 may help the reader understand what kind of numerical techniques one will require for such refinements.

c) Soil engineers often use a quantity called 'degree of consolidation' defined by

$$U(s) = 1 - \int_D p(\boldsymbol{x},s)dV / \int_D p(\boldsymbol{x},0)dV \tag{5.9.1}$$

It is easy to see that this quantity is also a 'boundary' quantity when the skeleton is linearly elastic. Indeed, assuming that the body force vanishes, we have

$$0 = \int_D \boldsymbol{x} \cdot (\mathrm{div}\, \boldsymbol{\tau}' - \nabla p)dV$$

$$= \int_{\partial D} \boldsymbol{x} \cdot \boldsymbol{S}dS - \int_D (\mathrm{tr}\boldsymbol{\tau}' - Np)dV \ , \tag{5.9.2}$$

for the N dimensional case, where $\boldsymbol{\tau}'$ stands for the effective stress. From (5.9.2) we conclude

$$\int_D p(\boldsymbol{x},s)dV = -\frac{1}{N}\int_{\partial D}\left[\boldsymbol{x}\cdot\boldsymbol{S}(\boldsymbol{x},s) - \mathrm{tr}\{\boldsymbol{C}[\boldsymbol{u}(\boldsymbol{x},s)\otimes\boldsymbol{n}]\}\right]dS \ . \tag{5.9.3}$$

In particular, we have

$$\int_D p(\boldsymbol{x},s)dV = -\frac{1}{N}\int_{\partial D}\left[\boldsymbol{x}\cdot\boldsymbol{S}(\boldsymbol{x},s) - (N\lambda + 2\mu)\boldsymbol{u}(\boldsymbol{x},s)\cdot\boldsymbol{n}\right]dS \tag{5.9.4}$$

for isotropic cases. We can therefore calculate this quantity directly

from the boundary traction and displacement obtained as BIE solutions.

d) Biot's theory of consolidation is closely related to coupled thermoelasticity in that these theories are based on similar equations. Sladek & Sladek(1983) investigated several BIEM's in various theories of linear thermoelasticity.

e) The material in this chapter is taken from Nishimura(1984), Nishimura & Kobayashi(1987), Nishimura, Umeda & Kobayashi(1986) and Nishimura(1987).

References

Aramaki, G., Kuroki, T. & Onishi, K.(1982). Consolidation analysis by boundary element method, *Proc. 4th Int. Conf. BEM* (Ed. C.A. Brebbia), pp 363-376, Springer.

Banerjee, P.K. & Butterfield, R.(1981). *Boundary Element Methods in Engineering Science*, McGraw Hill.

Biot, M.(1941). General theory of three-dimensional consolidation, *J. Appl. Phys.*, vol.12, pp 155-164.

Cheng, A.H.-D. & Liggett, J.A.(1984). Boundary integral equation method for linear porous-elasticity with applications to soil consolidation, *Int. J. Num. Meth. Eng.*, vol.20, pp 255-278.

Cheng, A.H.-D. & Predeleanu, M.(1987). Transient boundary element formulation for linear poroelasticity, *Appl. Math. Model.*, vol. 11, pp 285-290.

Garcia-Suarez, C. & Alarcon, E.(1982). Consolidation problems, *Proc. 4th Int. Conf. BEM* (Ed. C.A. Brebbia), pp 377-390, Springer.

Kobayashi, S. & Nishimura, N.(1982). On the indeterminancy of BIE solutions for the exterior problems of time-harmonic elastodynamics and incompressible elastostatics, *Proc. 4th Int. Conf. BEM* (Ed. C.A. Brebbia), pp 282-296, Springer.

Kuroki, T., Ito, T. & Onishi, K.(1982). Boundary element method in Biot's linear consolidation, *Appl. Math. Model.*, vol.6, pp 105-110.

Mizohata, S.(1963). *Theory of Partial Differential Equations*, Iwanami.

Nishimura, N.(1984). A BIE formulation for consolidation problems, *Proc. 7th Int. Conf. BEM* (Eds. C.A. Brebbia & G. Maier), pp 10/47-10/55, Springer.

Nishimura, N.(1987). Boundary integral equation methods for consolidation problems, *Topics in Boundary Element Research-4*, (Ed. C.A. Brebbia), pp 76-95, Springer.

Nishimura, N. & Kobayashi, S.(1987). On the behaviour of potentials in consolidation and thermoelasticity, *Mem. Fac. Eng. Kyoto Univ.*, vol.49, pp 308-325.

Nishimura, N., Umeda, A. & Kobayashi, S.(1986). Analysis of consolidation by boundary integral equation method, *Proc. Int. Conf. BEM, Beijing* (Ed. Q. Du), pp 119-126, Pergamon.

Predeleanu, M.(1981). Boundary integral method for porous media, *Proc. 3rd Int. Conf. BEM* (Ed. C.A. Brebbia), pp 325-334, Springer.

Sladek, V. & Sladek, J.(1983). Boundary integral equation method in thermoelasticity, Part I: general analysis, *Appl. Math. Model.*, vol.7, pp 241-253.
Tamura, T.(1981). Eigenvalue problem of consolidation, *Mem. Fac. Eng. Kyoto Univ.*, vol.42, pp 35-52.
Terzaghi, K.(1943). *Theoretical Soil Mechanics*, Chapman & Hall.